uOttawa

L'Université canadienne
Canada's university

FACULTÉ DES ÉTUDES SUPÉRIEURES ET POSTOCTORALES

uOttawa

L'Université canadienne
Canada's university

FACULTY OF GRADUATE AND POSDOCTORAL STUDIES

Lawton James Stubbert
AUTEUR DE LA THÈSE / AUTHOR OF THESIS

Ph.D. (Cellular and Molecular Medicine)
GRADE / DEGREE

Department of Cellular and Molecular Medicine
FACULTÉ, ÉCOLE, DÉPARTEMENT / FACULTY, SCHOOL, DEPARTMENT

Determining the Response of Tumor Cells to UV Light Cisplatin
TITRE DE LA THÈSE / TITLE OF THESIS

Bruce McKay
DIRECTEUR (DIRECTRICE) DE LA THÈSE / THESIS SUPERVISOR

CO-DIRECTEUR (CO-DIRECTRICE) DE LA THÈSE / THESIS CO-SUPERVISOR

Ian Lorimer

Luc Sabourin

Rebecca Laposa (University of Toronto)

David Picketts

Gary W. Slater
Le Doyen de la Faculté des études supérieures et postdoctorales / Dean of the Faculty of Graduate and Postdoctoral Studies

Determining the Response of Tumour Cells to UV Light and Cisplatin

Lawton James Stubbert

This thesis is submitted as a partial fulfillment of the PhD degree in Cellular and Molecular Medicine

December 16, 2009

Ottawa, ON

Your file Votre référence
ISBN: 978-0-494-61391-7
Our file Notre référence
ISBN: 978-0-494-61391-7

Authorizations for the Use of Published Figures.

1. Figure 1 was reproduced from: D'Errico M, Lemma T, Calcagnile A, Proietti De Santis L, Dogliotti E. Cell type and DNA damage specific response of human skin cells to environmental agents. *Mutation research* 2007; 614:37-47.

Licensee: Lawton J Stubbert

License Date: August 24, 2009

License Number: 2255390625648

Publication: Mutation Research/Fundamental and Molecular Mechanisms of Mutagenesis

Title: Cell type and DNA damage specific response of human skin cells to environmental agents

Type of Use: Thesis / Dissertation

2. Figure 2 was reproduced from: Matsumura Y, Ananthaswamy HN. Toxic effects of ultraviolet radiation on the skin. *Toxicol Appl Pharmacol* 2004; 195:298-308.

Licensee: Lawton J Stubbert

License Date: September 20, 2009

License Number: 2273340989810

Publication: Toxicology and Applied Pharmacology

Title: Toxic effects of ultraviolet radiation on the skin

Type of Use: Thesis / Dissertation

3. Figures 3 and 5 were reproduced from: Batista LF, Kaina B, Meneghini R, Menck CF. How DNA lesions are turned into powerful killing structures: insights from UV-induced apoptosis. *Mutation research* 2009; 681:197-208.

Licensee: Lawton J Stubbert

License Date: August 24, 2009

License Number: 2255390248602

Publication: Mutation Research/Reviews in Mutation Research

Title: How DNA lesions are turned into powerful killing structures: insights from UV-induced apoptosis

Type of Use: Thesis / Dissertation

4. Figures 4A and 4B were reproduced from: Hanawalt PC, Spivak G. Transcription-coupled DNA repair: two decades of progress and surprises. *Nat Rev Mol Cell Biol* 2008; 9:958-70.

Licensee: Lawton J Stubbert

License Date: August 24, 2009

License Number: 2255390941242

Publication: Nature Reviews Molecular Cell Biology

Title: Transcription-coupled DNA repair: two decades of progress and surprises

Type of Use: Thesis / Dissertation

5. Chapter 2 text and figures have been previously published in:

Stubbert LJ, Smith JM, Hamill JD, Arcand TL, McKay BC. The anti-apoptotic role for p53 following exposure to ultraviolet light does not involve DDB2. *Mutation research* 2009; 663:69-76.

Licensee: Lawton J Stubbert

License Date: August 24, 2009

License Number: 2255400776758

Publication: Mutation Research/Fundamental and Molecular Mechanisms of Mutagenesis

Title: The anti-apoptotic role for p53 following exposure to ultraviolet light does not involve DDB2

Type of Use: Thesis / Dissertation

Acknowledgements

I would like to sincerely thank Dr. Bruce McKay for his consistent support and for allowing me opportunities to work independently and creatively on a number of projects in the study of DNA repair.

Thanks to my graduate committee composed of Drs. Barbara Vanderhyden, Robin Parks and David Stodjl who were consistently helpful with constructive criticism and thoughtful suggestions.

This work was supported during 2008 by an Ontario Graduate Scholarship in Science and Technology. This project was funded through an IDEA grant from the Prostate Cancer Research Initiative and later from the National Canadian Institute of Cancer with funds from the Terry Fox Run, funds from an Ontario Premier's Research Excellence Award to Dr. Bruce McKay, The Ottawa Regional Cancer Foundation and The Cancer Research Society. I would also like to thank the Ottawa Regional Cancer Center and Ottawa Health Research Institute for providing the space and equipment for this project.

I thank my colleagues, Jeff Hamill, Dr. Jennifer Spronck, Tanya Arcand, Cecilia Becceril, Ghadi Antoun, Christine McKinnon-Roy and Brian Melanson for their research assistance and support and for making the lab an enjoyable place to work.

Thanks to my family, both here in Canada and the USA, for their unwavering support during this work. Special thanks to my parents Enis and Beth for encouragement, meals and rent-free living when I needed it most. To my bothers Tim and Chris – thanks for listening to rants and giving me a place to crash. To my grandparents Joy, Maurice, Jesse and Hollis – your life-stories, values and work ethic have been a constant motivating factor and inspiration.

A special thanks to Jennifer Smith, great friend and colleague from the beginning, for the patience to endure our many collaborative efforts and for insisting that I pursue graduate studies.

Thanks to Daisy the dog who's sure she's human.

Finally, Alisha – you are my sunshine.

Abstract

Nucleotide excision repair (NER) recognizes and repairs sunlight-induced DNA damage as well as cisplatin induced intrastrand DNA cross-links. When treated with cisplatin, NER capacity of a tumour has been shown to be predictive of outcome in some human cancers. Similarly, *in vitro*, the response of tumours cells to cisplatin is dependent on NER, where polymorphisms in some NER components alter the outcome. NER consists of two sub-pathways, transcription-coupled (TC-) NER and global-genomic (GG-) NER, differing only in their recognition of DNA lesions. While GG-NER deficiency, resulting in xeroderma pigmentosum (XP), increases rates of cancer in man, TC-NER deficiency, resulting in Cockayne syndrome (CS) does not. Both these syndromes have multiple genetic causes whose study has allowed a more complete understanding of NER. In primary human fibroblasts, keratinocytes and mouse embryonic fibroblasts TC-NER and not GG-NER is important in the avoidance of apoptosis after UV and cisplatin. However, mouse embryonic stem cells do not require TC-NER to recover from this type of DNA damage and so it may be difficult to predict the role of this repair pathway in all cellular contexts.

We assessed the importance of TC-NER in the cisplatin response of tumour cells by manipulating TC-NER and measuring DNA repair and sensitivity to DNA damaging agents UV-C and cisplatin. Targeting TC-NER by transient transfection of siRNA against Cockayne syndrome B (CSB), xeroderma pigmentosum A (XPA) and XPA-binding protein 2 (XAB2) sensitized tumour cells to cisplatin. This sensitization was largely independent of p53 tumour suppressor and mismatch repair status of these cells. As a preliminary *in vivo* test, we generated a colon cancer cell line in which CSB expression was stably reduced and used this cell line in a tumour xenograft model. Treating the animals with a single-week regimen of cisplatin resulted in a decrease in tumour volume initially and delayed tumour re-growth compared to control tumours. Taken together, these results indicate that TC-NER is a potential target in combined cisplatin tumour therapy. This work also suggests that TC-NER capacity may be clinically predictive.

List of Tables **Page**

List of Figures

Chapter 1 General Introduction

List of Figures

Chapter 2 The Anti-apoptotic Role for p53 Following Exposure to Ultraviolet Light does not Involve DDB2

List of Figures

Chapter 3 Targeting Cockayne Syndrome Group B Protein Sensitizes Tumour Cells to Ultraviolet Light and Cisplatin Independent of p53 and MLH1

List of Figures

Chapter 4 Targeting TC-NER Sensitizes Human Tumour Cells in an *In Vivo* Xenograft Model

List of Figures

Appendix 1 Supplementary Figures

List of Abbreviations

6-4-PP	6, 4 pyrimidine-pyrimidone photoproducts
Ad	replication deficient adenovirus
AdlacZ	Ad-expressing β-galactosidase
APAF-1	apoptotic protease-activating factor-1
ATM	ataxia telangiectasia-mutated
ATPase	adenosine triphosphate catalase
ATR	ataxia telangiectasia-radiation
BAX	BCL2-associated X protein
Bcl-2	B-cell CLL/lymphoma 2
BER	base excision repair
BH3	Bcl-2-homology domain 3
bp	base pair
BRCA	breast cancer protein
caspase	cysteine-aspartic acid protease
cDNA	complementary DNA
CEN2	centrin-2
Chk1	checkpoint kinase 1
Chk2	checkpoint kinase 2
cisplatin	cis-diamminedichloroplatinum(II)
COP9	constitutive photomorphogenic protein 9
CPD	cis, syn cyclobutane pyrimidine dimers
CS	Cockayne syndrome
CSA, -B	CS group A, -B protein

DDB1	damaged DNA binding protein 1
DDB2	damaged DNA binding protein 2
DISC	death-inducing signalling complex
DMEM	Dulbecco's modified Eagle medium
DNA	deoxyribonucleic acid
DNA-PK	DNA-protein kinase
DSB	double strand breaks
E6	human papillomavirus type 16 E6 transforming protein
ERCC1	excision repair cross-complementary protein 1
FADD	Fas associated protein with death domain
FANC	Fanconi anemia complementing
Fas	TNF family member 6 receptor
FasL	Fas ligand
GG-NER	global-genomic nucleotide excision repair
HCR	host cell reactivation
HDAC	histone deacetylase
hDM2	human double minute 2 p53 binding protein homolog
HEK293	human embryonic kidney 293 cell line
hHR23B	human homolog of Rad23B
HPV	human papillomavirus
HRP	horseradish peroxidase
IgG	immunoglobulin G
IR	ionizing radiation
ku70	lupus Ku autoantigen protein p70

ku80	lupus Ku autoantigen protein p80
Lig1	DNA ligase I
MMP	mitochondrial membrane permeabilization
MMR	mismatch repair
MOI	multiplicity of infection
mRNA	messenger RNA
NER	nucleotide excision repair
NHEJ	non-homologous end-joining
p300	binding protein p300
PBS	phosphate-buffered saline
PCNA	proliferating cell nuclear antigen
PCR	polymerase chain reaction
pfu	plaque forming units
POLH	polymerase (DNA directed), eta
PUMA	p53-upregulated modulator of apoptosis
Pt	platinum
RNA	ribonucleic acid
RNAi	RNA interference
RNAPII	RNA polymerase II complex
ROS	reactive oxygen species
RPA	replication protein A
RRS	Recovery of RNA synthesis
RT-PCR	reverse transcriptase-polymerase chain reaction
SAM	S-adenosylmethionine

SDS	sodium dodecyl sulfate
SDS-PAGE	SDS-polyacrylamide gel electrophoresis
SEM	Standard error of the mean value
shRNA	short-hairpin RNA
siRNA	short-interfering RNA
SNF2	sucrose non-fermentable protein 2
SV40	simian virus 40
TBST	tris-buffered saline with Tween-20
TC-NER	transcription-coupled nucleotide excision repair
TFIIH	transcription factor IIH
TLS	translesion synthesis
TNF	tumour necrosis factor
TP53	tumour suppressor protein 53 (53kDa)
TTD	tricothiodystrophy
UDS	unscheduled DNA synthesis
UV	ultraviolet
UV-A	UV light from 320-400 nm
UV-B	UV light from 280-320 nm
UV-C	UV light < 280 nm
UV-DDB	UV-DNA damage-binding complex
$UV^{S}S$	UV sensitivity syndrome
WAF1	wild-type p53 activated fragment 1 (p21)
XAB2	XPA-binding protein 2
XP	xeroderma pigmentosum

XP-A–G, -V	XP group A–G, -V cells
XPA-G,-V	XP complementation group A
XRCC	X-ray repair cross-complementing
Z-VAD-fmk	carbobenzoxy-valyl-alanyl-aspartyl-[O-methyl]- fluoromethylketone
β-gal	β-galactosidase
γ-H2AX	phosphorylated histone 2AX

1.0 General Introduction

1.1 Cancer

Cancer is a group of diseases associated with uncontrolled growth that invade and damage adjacent tissues, and in the case of solid tumours sometimes metastasize.[1] Pre-cancerous cells progressively acquire six generalized traits on the path to tumourigenesis, including: self-sufficiency in growth signals, insensitivity to inhibitory growth signals, evasion of programmed cell death (apoptosis), limitless replicative potential, sustained angiogenesis and metastasis.[2-4] This process also coincides with a progressive accumulation of aberrant genetic traits and accumulation of DNA damage. A mutator phenotype, characterized by progressive loss of DNA maintenance mechanisms, accelerates mutagenesis and genomic instability.[2, 5-9]

Early accounts of tumour biology describe the gross anatomy of tumours, the physiological effects of cancer and the experimental, often unsuccessful surgical interventions that initially contributed more to understanding of aetiology than to curative outcomes.[10-13] Almost 150 years later, the continued presence and societal impact of cancer is reflected by the world-wide efforts to understanding and treating this multi-faceted disease.[1]

Currently almost 40% of Canadian women and almost 45% of men will develop cancer during their lifetime while 24% of women and almost 29% of men (approximately 1 in 4 Canadians) will die from cancer.[1] These sobering statistics underline the crucial importance of understanding the contributing factors, genesis and aetiology of cancer and developing more effective, life-extending therapies for those afflicted. Although there

exists healthy debate on the molecular origins of some malignancies (i.e. the role of exogenous hormones in reproductive cancers; or the roles of some environmental and lifestyle factors) it is clear that parameters such as germ-line mutations, exposure to mutagens, deficient immune systems, dietary and exercise deficiencies, as well as viral and bacterial infections, are all legitimate risk factors for neoplastic disease.[14-24]

1.2 Cancer and DNA Damage

All cells, from simple bacteria to specialized mammalian lineages, are equipped with mechanisms that maintain genetic fidelity. Chromosomal abnormalities that arise due to mutations in genes encoding proteins involved in these protective mechanisms are a universal feature of cancer.[25-29] Sources of endogenous DNA damage include reactive oxygen species (ROS), arising as a consequence of oxidative metabolism[30, 31] and alkylation of DNA bases [*S*-adenosylmethionine (SAM)].[32] Endogenous DNA damage is repaired predominantly by base excision repair (BER) and related endonucleases that recognize and excise specific types of damage on DNA bases.[30]

Sources of exogenous DNA damage also represent a serious threat to DNA, causing a wide array of lesions, including base damage (i.e. oxidative lesions), base-base cross links and DNA strand breaks.[19, 33] Extrinsic DNA damaging agents include products of combustion [polycyclic aromatic hydrocarbons (PAH)][34] and sunlight [ultraviolet light (UV)].[35] This DNA damage is repaired in a lesion-specific manner by a number of repair mechanisms, including: BER (UV-light induced ROS); translesion synthesis (TLS) (replica-

tion blocking lesions); homologous recombination (HR) and non-homologous end-joining (NHEJ) (double strand break repair); nucleotide excision repair (NER) (UV damage).

1.3 Ultraviolet Light as a Model DNA Damaging Agent

The study of UV-induced DNA damage is in large part due to the importance of UV as the principle human mutagen. Skin malignancies, although the least likely to result in mortality, are the most prevalent in Canada.[1] These rates are strongly correlated with polar ozone layer degradation due to increased UV light penetrance.[19, 36] Human skin is composed of two layers, the upper epidermis and lower dermis. The epidermis has several layers, the uppermost being cornified (stratum corneum) followed by granular, spinous and basal layers of keratinocytes and melanocytes, at decreasing rates of terminal differentiation and increasing states of proliferation, respectively. The dermis, found on the upper side of the basement membrane, consists of dermal fibroblasts, often established *ex vivo* in cell culture due to their relatively high growth potential compared to cells from the upper layers (Figure 1).[37]

UV-induced DNA lesions result from high-energy photons in the ultraviolet spectrum of light that penetrate the stratum corneum, irradiate keratinocytes and act directly on bonds between DNA base pairs. This can result in two predominant lesion types: cis, syn cyclobutane pyrimidine dimers (CPD) (66-75% of UV lesions) and less common 6,4 pyrimidine-pyrimidone photoproducts (6-4-PP) (25-33% of UV lesions).[37-42] The DNA damaging components of sunlight consist of UV-A (320-400 nm), UV-B (280-320 nm) and UV-C (< 280 nm) making up 40, 5 and 0 percent of light reaching the earth's surface, re-

Figure 1. Human Skin Components.

Human skin diagram shows the five layers of the epidermis and underlying dermis. Re-produced with permission.

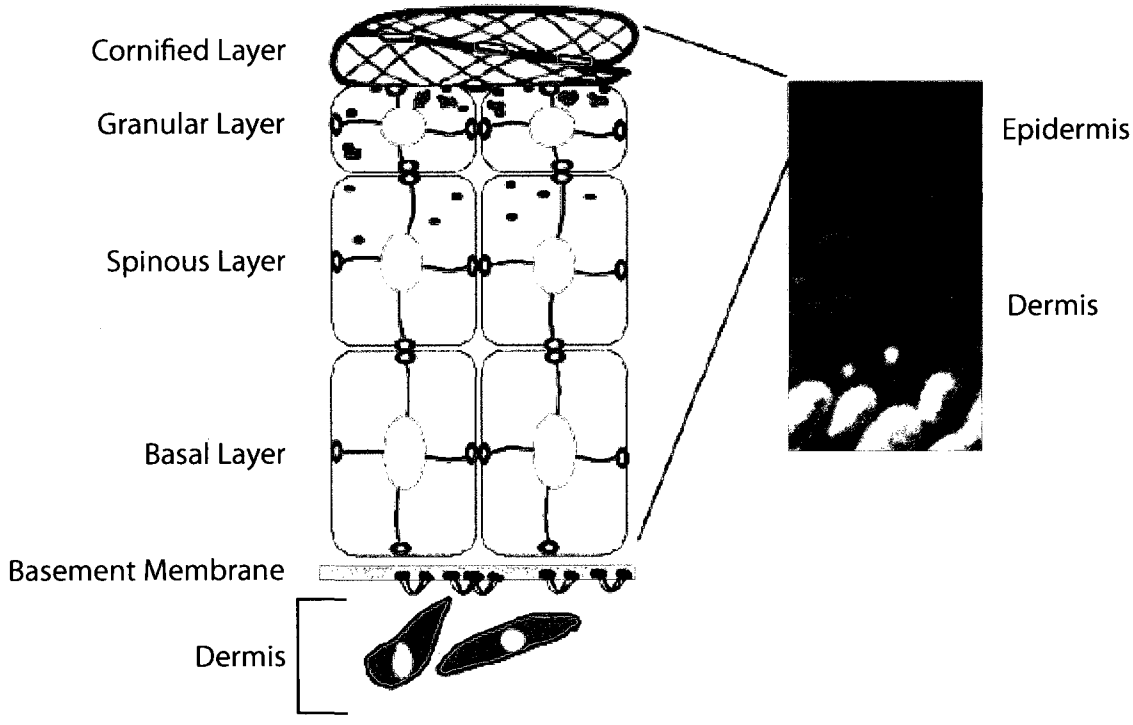
Cornified Layer
Granular Layer
Spinous Layer
Basal Layer
Basement Membrane
Dermis
Epidermis
Dermis

spectively[20, 38, 39, 42-44] (Figure 2). UV-C and most of UV-B (up to ~310 nm) are absorbed by atmospheric oxygen and ozone.[38, 42] CPD are a result of covalent linkages between adjacent pyrimidines with formation of a single-bonded four-member ring from the 5,6 double bonds of adjacent bases [42] (Figure 3). 6-4-PP occur in adjacent pyrimidines by linkage of the C6 position of the 5'-pyrimidine, to the C4 position of the 3'-pyrimidine.[42] 6-4-PP are formed at 5'-T–C-3', 5'-C–C-3', 5'-T–T-3' but not at 5'-C–T-3' sites in DNA[38] (Figure 3). It has been observed that TT and TC sequences are more photosensitive than CT and CC sequences.[42] UV-A and UV-B, in addition to causing DNA damage, described above, also generate reactive oxygen species (ROS) upon absorption by cellular components. ROS also cause DNA damage, ranging from relatively innocuous base modification to highly genotoxic double strand breaks (DSB).[45] More recently it was discovered that UV-A could directly create CPD lesions in DNA[46] instead of requiring an as yet unknown photosensitizing cellular molecule.[20, 38, 43, 44, 47] This is particularly relevant to skin cancer research as UV-A is the predominant UV component of sunlight that reaches the Earth's surface[44] and is also the majority constituent of the UV spectrum used in tanning beds.[48]

6-4-PP are repaired at a faster rate than CPD and this is thought to result from the greater geometric strain and distortion seen with 6-4-PP, therefore causing these lesions to be more 'visible' to DNA repair mechanisms.[39, 41, 49] Regardless of UV spectrum used, CPD are more prevalent and more slowly repaired compared to 6-4-PP[39] however, the balance of 6-4-PP increases somewhat after exclusive UV-A compared to exclusive UV-B exposure.[42]

Figure 2. UV spectrum.

Spectrum of UV radiation showing wavelengths and physiological effects. Reproduced with permission.

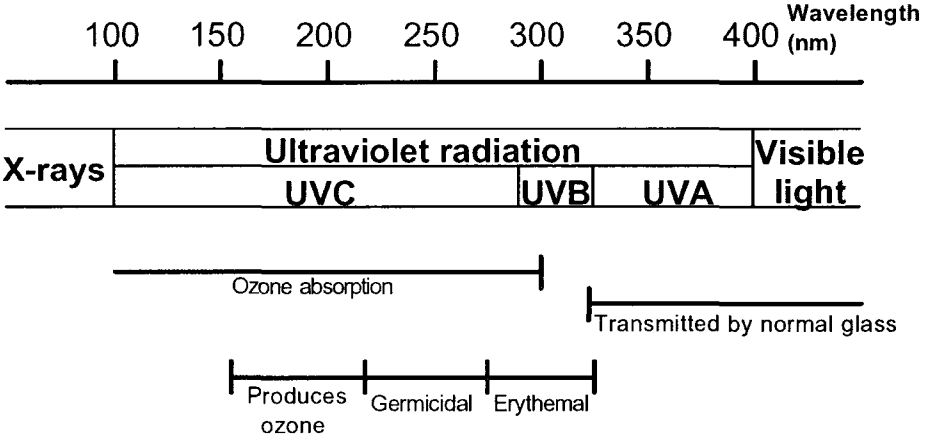
100
150
200
250
300
350
400
Wavelength (nm)
X-rays
Ultraviolet radiation
UVC
UVB
UVA
Visible light
Ozone absorption
Transmitted by normal glass
Produces ozone
Germicidal
Erythemal

Figure 3. UV-induced DNA Damage.

Lesions formed by UV-induced DNA damage. Reproduced with permission.

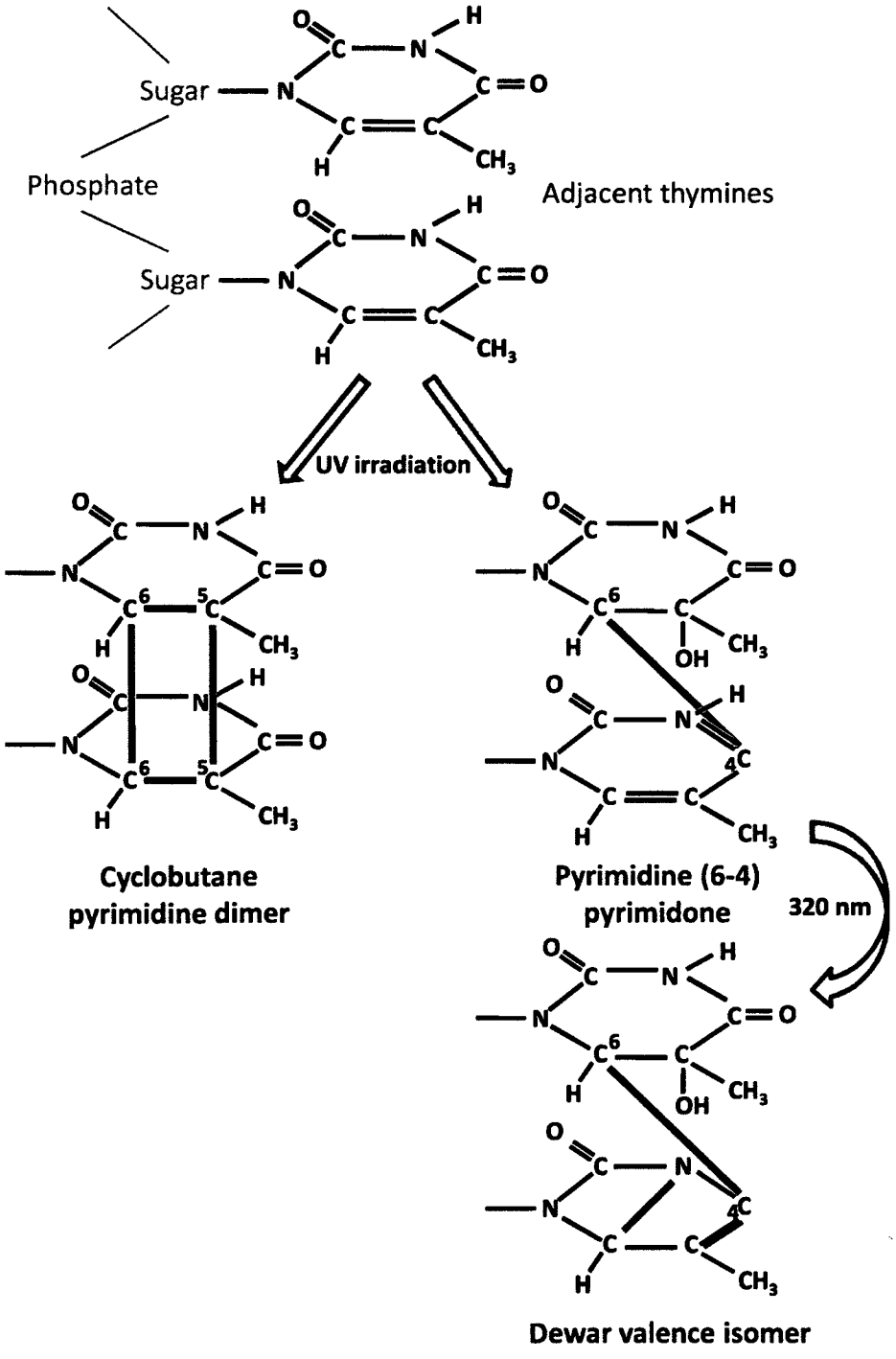
Sugar
Phosphate
Sugar
Adjacent thymines
UV irradiation
Cyclobutane
pyrimidine dimer
Pyrimidine (6-4)
pyrimidone
320 nm
Dewar valence isomer

1.3.1 Cell Culture Models for Studying the UV Response

By virtue of their physiological role in skin tissue and thus persistent exposure to UV, keratinocytes are more efficient at NER compared to any other human cell type[37] and this holds true in similar comparisons of mouse tissue.[50] In fact, derived from the same individual, human keratinocytes repair CPD 2-fold quicker than skin fibroblasts and are almost 2-fold more resistant to apoptosis after ultraviolet light exposure.[51-54] Interestingly, there is no difference between cell types in their repair of the less common 6-4-PP.[51, 52] Despite the important differences in DNA repair characteristics between keratinocytes and fibroblasts, the laboratory culture of keratinocytes is fraught with technical difficulties. *In vivo*, keratinocytes are the most superficial of the cellular layers in the stratified epidermal growth environment (Figure 1). Therefore, successful *in vitro* growth of keratinocytes requires a feeder layer of irradiated cells that mimic the presence of basal dermal fibroblasts. Despite the ability to force keratinocytes to terminally differentiate into cells resembling those of the upper spinous and granular layers, these cells will stop dividing after a few passages after isolation from human tissue.[37] The limited number of cell divisions before cellular senescence, a phenomenon common to all normal human cells in culture conditions,[55] can be subverted using any number of immortalization techniques (reviewed in Hahn 2002[56]). However, extending replicative potential results in gene expression profile changes (reviewed in Fridman and Tainsky 2008[57]) whose implications may cloud interpretations of many cellular responses. The field of DNA repair has therefore almost universally adopted the use of dermal fibroblasts for *in vitro* study of DNA repair except where specific models of skin cancer study require use of keratino-

cytes. Established dermal fibroblast cell lines are widely available from normal or DNA repair deficient human patients and persist in culture for up to 30 passages without the need for immortalization.

1.4 UV Sensitive Syndromes

UV sensitive human syndromes were first documented by Dr. Moritz Kaposi, a European dermatologist, in the 19th century.[58] These autosomal recessive disorders include a wide spectrum of sun-sensitivity syndromes with a vast array of additional specific clinical manifestations and include Xeroderma pigmentosum (XP), Cockayne syndrome (CS), UV-sensitivity syndrome ($UV^{S}S$) and trichothiodystrophy (TTD). Commonalities to all these diseases are inherent defects in DNA repair due to mutated components of nucleotide excision repair (NER). Initially, patients were identified and sub-categorized phenotypically (reviewed in Cleaver 1999[59]) and then by complementation analysis[60] of their dermal fibroblasts. Affected patient cells regained UV-resistance after fusion with a cell line carrying the missing protein.[60] In the case of XP, groups A-G and V were identified. While for CS, groups A and B were identified.[59] In each group, mutations in a single gene are associated with the disease. NER can be sub-divided into two mechanistic pathways that differ only in their modes of detection of lesions: global-genomic (GG-) NER and transcription-coupled (TC-) NER. A summary of known genetic defects for each, categorized by clinical syndrome and involvement of either of the NER sub-pathways, can be found in Table 1.

1.4.1 Xeroderma Pigmentosum

Patients affected with Xeroderma pigmentosum (XP) are found at nearly 1 : 500 000 within the European population, while for yet unknown reasons some regional populations have higher rates (i.e. Mediterranean and Japanese).[61, 62] XP appeared in medical literature in the 1870s, described by Kaposi, who noted a striking pigmentation disorder only on sun-exposed skin and in a heritable manner (reviewed in Clarkson 2003[58]). This human condition was later described as having dense speckled pigmentation, accompanied by skin and eye lesions, increasing in severity with age.[63-65] Patients suffer a broad range of symptoms but are most uniformly characterized by hypersensitivity to sunlight exhibited by freckling and ocular dysmorphias, pre-malignant lesions of sun-exposed skin, high incidence of skin cancer (up to 2000-fold increased risk compared to general population), tumours in other organs, progressive hearing loss and neurodegeneration.[61, 63, 64, 66-68] All of these symptoms are suspected to result from DNA repair defects.[49, 69-76] In a subset of rare cases, developmental deficits include telangiectasia (small dilated blood vessels at the surface of the skin), bird-like facies (sunken eyes, beaked nose and projecting jaws), mental retardation and abnormal gait further characterize the most severe forms of XP.[58]

1.4.2 Cockayne Syndrome

More often seen clinically than XP, Cockayne syndrome (CS) was first characterized by Dr. E.A. Cockayne in 1936 as a developmental deficiency involving dwarfism and deafness.[77] Cockayne syndrome is found at approximately 1 : 300 000 live births in the European population.[62] Compared to children of the same age, those afflicted are short in

stature (dwarfism), exhibit bird-like facies with neuro-malformation and neurodegeneration (retinopathy, microcephaly, deafness) and fail to thrive beyond early teenage years (retardation of growth and development shortly after birth).[77-83] In contrast to XP patients, CS patients exhibit sun sensitivity but do not develop cancer.[78, 79, 82] However, since these patients live to a median age of 13 years,[78] they may simply lack the longevity needed to develop neoplasms.

1.4.3 UV Sensitivity Syndrome

UV sensitivity syndrome ($UV^{S}S$) is an extremely rare disorder characterized by photosensitivity and mild freckling but no neurological disorders and no increased risk of photocarcinogenesis.[84, 85] These patients were initially designated by medically observable symptoms as having a mild form of Cockayne syndrome.[86] Subsequently, the genetic heterogeneity of patients as well as disparate phenotypes have confounded its true cause. Although $UV^{S}S$ is separable from Cockayne syndrome symptomatically,[87, 88] it is still considered by some as the mildest presentation of CS.[85]

1.4.4 Tricothiodystrophy

Tricothiodystrophy (TTD) broadly describes a series of syndromes (Pollitt, Tay, Amish brittle hair, Marinesco–Sjögren and Sabinas syndromes) that exhibit: 1) various developmental abnormalities of the skin, hair and teeth; 2) neurological, immune and ocular abnormalities; and 3) skeletal and neurological dysmorphias.[59] A common feature of these syndromes is brittle hair and finger nails, due to improper keratinocyte differentia-

tion.[59, 89] Graded from mild to severe, TTD patients show ranges of severity of symptoms, including: failure to thrive, dwarfism and mental retardation. UV and photosensitivity occurs in approximately 50% of patients while all succumb to the disease early in life.[89] TTD is characterized by increased rates of cancer and is associated with defects in genes classically attributed to XP.[84, 85]

1.4.5 Cerebro-oculo-facio-skeletal and De Sanctis–Cacchione Syndromes

Cerebro-oculo-facio-skeletal syndrome (COFS) and De Sanctis–Cacchione syndrome (DSC) are both extremely rare clinical manifestations of various NER defects[79, 90] and represent the most severe developmental defects and sun-sensitivity of the UV sensitivity syndromes. COFS, as the name suggests, is most often associated with widespread developmental defects of brain, eyes, face and skeleton[91] while DSC patients exhibit microcepahly, growth and mental retardation, ataxia and deafness.[92] Clinically, there is currently no consensus on whether these patients should be considered as having separable diseases or if their symptoms should be characterized as the most severe forms of XP or CS.[84, 85] These rare DNA repair diseases, with often severe clinical phenotypes underline the crucial importance of NER to normal development and maintenance of genomic stability.

1.5 Nucleotide Excision Repair

The presence of DNA lesions, from simple base damage to double strand breaks, presents a critical issue that can have diverse negative impacts in eukaryotic cells. The

ability of a cell to repair DNA damage often determines how effectively it will avoid apoptosis, maintain genomic stability and avoid neoplastic development.[66, 76, 82, 93-96]

The notion that DNA could be damaged in some manner by UV light, leading to loss of viability was first recognized in early research of bacteria starting in the 1940s (reviewed in Sancar 2008[97]). It was first noticed that bacteria, survived UV irradiation more readily if allowed to recover in visible light instead of darkness.[98, 99] This led to the discovery of photolyase, an enzyme responsible for the light-assisted repair of UV-induced CPD in bacteria, or photoreactivation[99] that was later isolated from baker's yeast extracts[100] and characterized in a number of other prokaryotes and simple eukaryotes, but not mammalian cells[101-103] (reviewed in Carell 2001[104]). The observation that DNA could be repaired was further characterized in bacteria,[105, 106] seen using phage transfer of DNA[107-110] and in mammalian cells.[111]

The NER pathway was first associated with human disease in the late 1960s after ground-breaking work done by James Cleaver. In a collaborative effort comprising a variation on a previous replication repair assay,[112] combined with his own technique to measure unscheduled DNA synthesis,[111] Cleaver made a ground-breaking connection between sun-sensitivity, cancer and DNA repair. Cleaver suggested the sun-sensitivity and high rates of skin cancer seen in Xeroderma pigmentosum (XP) patients was due to a deficit in DNA repair of UV-induced DNA lesions.[113-115] The following year, Setlow *et al.* (1969) showed that XP was in fact due to improper excision of pyrimidine dimers after UV exposure and postulated that this could explain the oncogenicity of UV radiation.[65] These ex-

periments were crucial in elucidating the importance of NER in cell survival and jump-started the molecular search that would characterize this DNA repair pathway.

1.5.1 Cloning Proteins Involved in NER

Using tissue isolated from XP patients described by Kramer and colleagues, cell lines were established and in some cases immortalized using the SV40 large T antigen.[116] These XP cell lines were found to exhibit UV sensitivity and displayed impaired DNA repair capacities compared to normal cells, as measured by unscheduled DNA synthesis (UDS) assays (repair synthesis)[60, 117-120] or host cell reactivation of introduced damaged DNA.[121] An important conclusion from this work is that cell survival is determined by DNA repair capacity and early on, differences between isolated cell lines were noted.[69, 121] These resources were useful for cloning DNA repair genes.

A creative strategy was used to identify the individual repair defects in cell lines derived from UV-sensitive patients. Fibroblasts from different isolated cell lines were fused by polyethylene glycol, resulting in polynucleated cells. From this complementation analysis it was clear that missing factors from DNA repair deficient cells could be complemented from repair proficient nuclei or other complementation groups.[60, 120, 121] Eight complementation groups, XP-A through XP-G and XP-V were identified.[95, 122-124] XPV patients exhibit dermal sun sensitivity, but while NER competent, their cells are unable to perform translesion synthesis, the successful replication of DNA in the presence of a bulky DNA lesion encountered by DNA polymerases at the replication fork.[125-127] XPV is the ma-

jor translesion synthesis bypass polymerase eta (Pol η) that accommodates error-free bypass of CPD (among other lesions) (reviewed in Gratchev 2003[128]).

As indicated previously, cells from various XP patients were found to be sensitive to UV exposure.[69, 121] Correction of UV-sensitivity through the expression of cDNAs permitted identification of repair gene proteins.

The nomenclature of NER proteins reflects this history. For example, the XPA-XPG and CSA and CSB proteins are named because DNA from their cells complemented the repair defect in the corresponding complementary group of XP or CS. Excision repair cross-complementary proteins (ERCC1 and ERCC4) are human proteins named because their respective DNA corrected UV-sensitivity of UV-sensitive CHO mutants in complementary groups 1 and 4. There is also historical overlap in names for the following: (CSB = ERCC6; CSA = ERCC6; XPB = ERCC2; XPD = ERCC3; etc.) (reviewed in Kraemer *et al.* 2007[129]) (Table 2).

1.6 Global Genomic NER

GG-NER is a stepwise mechanism that can be sub-divided into: **1) lesion recognition; 2) verification of the presence of a lesion; 3) removal of DNA containing the damaged bases**; and **4) DNA synthesis**. The sub-mechanisms of NER (GG-NER and TC-NER) differ only in the **lesion recognition step** (Figures 4A and 4B).

Lesion recognition by GG-NER is initiated by the UV damage binding complex (UV-DDB) comprising DNA binding protein 1 (DDB1) and 2 (DDB2 - also known as XPE/p48).[130-138] UV-DDB binds CPDs and 6-4-PPs[139-141] as well as a number of other bulky lesions

Figure 4A. Nucleotide Excision Repair.

A simplified outline of NER. Lesions (A) are initially recognized, either by a translocating RNA polymerase (RNAPII) or through the binding of lesion sensor DNA damage-binding-2 (DDB2) (B) — which forms a heterodimer with DDB1 to make up the DDB complex. XPC in a multimeric complex provides a site of nucleation for ensuing repair factors. The sub-pathways converge on common steps to both pathways (C). TFIIH is recruited and stabilized by XPG, joined by subunits XPD and XPB. Helicase activity stimulates opening of the DNA. RPA and XPA serve lesion-verification roles, protect the single-stranded DNA in the denatured bubble and stabilize the pre-incision complex (D). The XPF–ERCC1 endonuclease complex is recruited and incises the damaged DNA strand at the 5′ side of the bubble, whereas XPG incises on the 3′ side (E). RFC loads PCNA to accommodate DNA polymerases δ or ε. The final ligation step can be carried out by DNA ligase-I (F). Reproduced with permission.

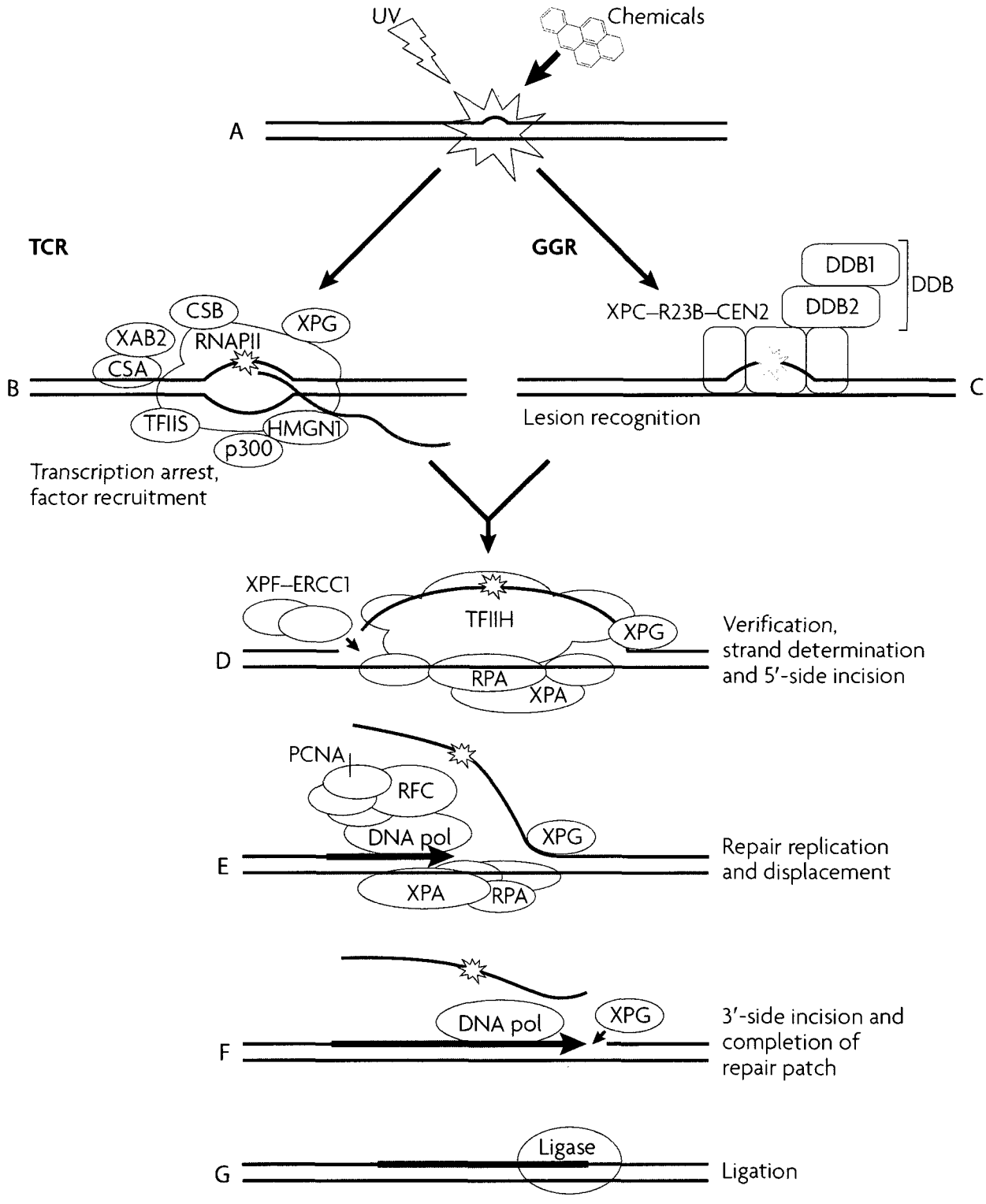
UV
Chemicals
A
TCR
GGR
DDB1
DDB
DDB2
XPC–R23B–CEN2
CSB
XPG
XAB2
RNAPII
CSA
B
C
TFIIS
HMGN1
p300
Transcription arrest,
factor recruitment
Lesion recognition
XPF–ERCC1
TFIIH
XPG
D
RPA
XPA
Verification,
strand determination
and 5′-side incision
PCNA
RFC
DNA pol
XPG
E
XPA
RPA
Repair replication
and displacement
DNA pol
XPG
F
3′-side incision and
completion of
repair patch
Ligase
G
Ligation

that are known to be repaired by NER, such as cisplatin[121, 130, 131, 142-144] and other chemically-induced lesions.[135, 145] The UV-DDB complex and specifically DDB2 is required for efficient removal of lesions from DNA during NER. DDB2 may act directly at the lesion site by binding and displaying the lesion for subsequent repair steps, while the DDB1 protein stabilizes this interaction[146] and later regulates molecular turn-over of the complex. DDB1 and Cullin 4 combine to form an E3-ubiquitin ligase that ubiquitinates DDB2, XPC and histones.[141, 147-152] This is thought to initiate future steps in the repair process.[150] The lesion-bound UV-DDB is then hypothesized to dissociate from the DNA damage as another dimeric complex, XPC bound to the human homolog of Rad23B (XPC/hHRad23),[153, 154] locates and binds the lesion site.[155] Upon ubiquitination, XPC interacts with transcription factor TFIIH through its carboxy terminus, likely recruiting it as a member of the subsequent repair machinery,[156] thus fulfilling its hypothesized role of providing a nucleation site for the subsequent steps in the NER process.[150]

A ***lesion verification*** step confirms the presence of a DNA lesion by high-specificity binding of XPA to the DNA lesion.[139, 157-162] The XPA protein is considered to be a major limiting factor of NER.[163] It is thought to aid in recruiting other repair factors including excision repair cross-complementing protein 1 (ERCC1), replication protein A (RPA) and the TFIIH general transcription factor to the lesion.[164-170]

The TFIIH transcription factor contains two helicases, XPB and XPD and this is thought to unwind DNA at the repair site.[171-178] ERCC1/XPF and XPG are structure-specific endonucleases that incise the unwound DNA on the 5' and 3' sides of the lesion, respectively.[179] XPG incises six nucleotides to the 3' side of a photodimer and ERCC1/XPF incises

22 nucleotides to the 5' side of the lesion,[58, 142, 179-181] releasing a thirty base pair contiguous stretch of single stranded DNA containing the lesion site.[182] The resulting gap is filled using the intact complementary strand as the template. DNA repair synthesis requires replicative DNA polymerases epsilon (ε) and delta (δ) in the presence of RPA, RFC and the proliferating cell nuclear antigen protein (PCNA). Here DNA ligase I (Lig1) seals the nick in the DNA along with a DNA polymerase (δ or ε).[183, 184]

1.7 Evidence that NER can be Coupled to Transcription

Early in the study of DNA repair defective cells from UV sensitive syndromes it was realized that human fibroblast cells isolated from Cockayne syndrome patients lack the ability to recover nascent RNA synthesis after UV-exposure, suggesting that CS cells have a defect in repairing expressed genes.[185, 186] In fact, CS cells are unable to transcribe mRNA from damaged templates and are significantly delayed or transcription-deficient even after extended periods of recovery time.[87, 185, 187-189]

It was found that CPD were repaired at a greater rate in the transcriptionally active template strand versus transcriptionally inactive or coding regions of genes.[190-194] This was confirmed with the observation that UV lesions in matrix-associated DNA are preferentially repaired, a phenomenon absent in CS cells.[195] Additionally, this transcription-dependent DNA repair requires on-going transcription but not translation,[196] so measurements of nascent mRNA synthesis will correlate with the capacity of this type of DNA repair.[87, 185, 187-189] Further linking repair to transcription, Tu *et al.* (1997) showed that strand preference for repair is detected in areas of genes where RNAPII is elongating.[197]

Importantly though, it was recognized that CS cells retain the ability to repair UV-damage at the 'genome overall' rate (reviewed in Kantor *et al.* 1995[198]) and this was considered reflective of their retained ability to perform GG-NER. Indeed, transcription-dependent repair, defective in CS cells but still intact in XP-C cells,[195, 199, 200] is thus genetically separable from GG-NER. This heterogeneity of DNA repair, referring to the differences between NER capacity of XP and CS cells, justified the delineation of NER into two distinct sub-pathways, GG-NER and TC-NER (reviewed in Hanawalt 1991[201]).

1.7.1 Mechanism of TC-NER

Unlike GG-NER, TC-NER is poorly understood. It is thought that the processivity of RNAPII is required to locate lesions that block transcription elongation as a single UV- or cisplatin-induced DNA lesion can persistently stall transcription in the absence of TC-NER[202-206] (Figure 4B). Persistently stalled transcription results in an acute stress response potentially leading to apoptosis (reviewed in van den Boom *et al.* 2002[207]). It is thought that TC-NER allows for temporary displacement of the stalled RNAPII (or conformational changes allowing access to the lesion), repair of the lesion (by mechanisms common to GG-NER) and resumption of the transcription of the stalled transcript (reviewed in Fousteri and Mullenders 2008[83] and Hanawalt and Spivak 2008[85]). When fluorescently-tagged, CSB can be observed to intermittently interact with an elongating RNA polymerase complex but will associate more tightly when DNA damage is present.[208] Cells deficient in CSB do not ubiquitinate the large subunit of RNAPII in a normal fashion,[209] an event that may be required for efficient TC-NER.[210] CSB is known to associate with RNAPII

Figure 4B. Transcription-coupled Nucleotide Excision Repair.

Simplified model of TC-NER. RNAPII translocates along the DNA (A). Transcription is arrested when RNAPII encounters a lesion (B). CSB becomes tightly bound to the arrested RNAPII and recruits factors that are needed to accomplish transcription-coupled repair. TFIIH localizes to the arrested elongation complex with xeroderma pigmentosum (XP) complementation group G (XPG) and XPA along with XAB2 and RPA (C). The chromatin remodelling factors containing HMGN1 and p300 loosen the nucleosome structure behind the polymerase and RNAPII reverses direction, backtracking from the obstacle and degrading the nascent RNA product. TFIIH with associated XPG, XPA and RPA remain at the site of the obstacle. XPA and RPA bind the single-stranded DNA in the vicinity of the obstruction, providing lesion verification and strand specificity (D). Once RNAPII has backtracked, TFIIH extends the denatured region around the lesion to approximately 30 nucleotides allowing DNA nicking by XPG and the XPF–ERRC1 complex. CSA, as a component of a cullin-containing ubiquitylation E3 ligase complex, might facilitate resumption of transcription by removing or deactivating factors (E). Reproduced with permission.

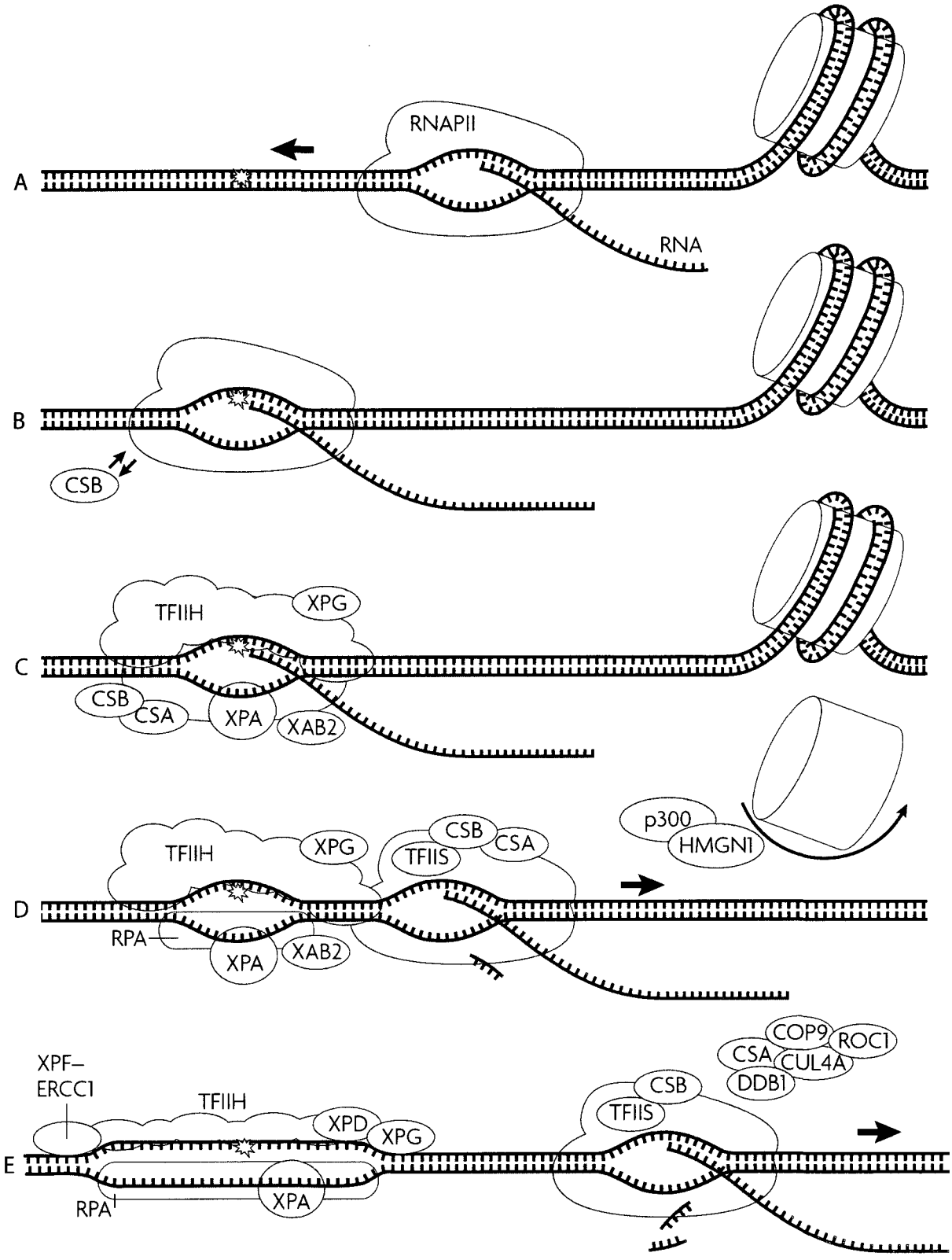
A
RNAPII
RNA
B
CSB
C
TFIIH
XPG
CSB
CSA
XPA
XAB2
D
p300
HMGN1
TFIIH
XPG
CSB
CSA
TFIIS
RPA
XPA
XAB2
E
XPF–
ERCC1
TFIIH
XPD
XPG
RPA
XPA
COP9
ROC1
CSA
CUL4A
DDB1
CSB
TFIIS

both dynamically during transcription itself[206, 211] and in a DNA damage dependent manner where the interaction becomes stabilized,[208] while CSA does not interact with the transcription complex[206] prior to DNA damage.[212, 213] CSB is thought to accomplish a transcription-repair coupling role by restraining RNAPII while recruiting pre-incision TC-NER proteins and subsequently the core NER endonuclease complex.[214] CSA is found in a ubiquitin-ligase complex and although required for TC-NER, is not required for recruitment of NER incision factors.[214] Based on a recent study, CSA appears to be required for chromatin remodelling by recruiting XPA binding protein 2 (XAB2) and transcription factor IIS (TFIIS) as well as perhaps a role in signalling.[214] Although phenotypically CS-A and -B cells and patients exhibit no difference in repair capacity and sensitivity to DNA damage, the CSA protein is not involved in assembling the core NER complex.[83, 214] CSB is also suspected to possess chromatin remodelling activity[215] though it may instead be through its association and recruitment of histone acetyltransferase p300. [214]

Like CSB, the XPG protein has also been shown to interact dynamically with RNAPII during normal transcription[216] but also may play an important role in assembly of the TC-NER repair complex downstream of CSB interactions with repair components.[214] These interactions fit well with phenotypic observations that some XP-G patients, with a truncated XPG protein, can exhibit CS-like characteristics without increased cancer risk.[58]

XAB2 was identified as a binding protein of XPA in a yeast two hybrid screen[217] and appeared to associate with CSA, CSB and RNAPII.[217, 218] XAB2 has since been shown to be an enigmatic component of several pathways, including pre-mRNA splicing, TC-NER and transcription itself.[83, 214, 218, 219] XAB2 deletion in mice results in embryonic lethality[217] and

XAB2 is not known to be mutated in humans. When antiserum generated against XAB2 was microinjected into cells, TC-NER function and not GG-NER function was severely impaired.[217] XAB2 may associate with CSB and RNAPII and may also bind with XPA in a stabilizing manner during DNA damage verification. Interestingly, its association with XPA is independent of XPA function in GG-NER since blocking XAB2 with antiserum does not interfere with GG-NER capability. It has also been suggested that XAB2 plays an accessory role in transcription,[218] an observation which may explain consequential embryonic lethality associated with loss of expression of XAB2.

1.7.2 Detailed Characterization of CS proteins

CSB is a key protein involved in TC-NER. It encodes a 1493 amino acid protein from chromosome 10 with seven sequential helicase domains and shares much homology with proteins involved in regulation of transcription, chromosome stability and DNA repair.[220] The CSB protein is encoded by 21 exons[221] on chromosome 10 (q11-q21)[222] forming an mRNA transcript of approximately 4.7kb[221] encoding a 1493 amino acid protein[220] that results in a 168kDa protein detectable by immunoblot analysis.[223] A second transcript, of approximately 6.7kb encodes a differentially polyadenylated form that is thought to encode the same CSB protein as the 4.7kb transcript but containing approximately 2kb more 3' untranslated sequence.[221] Structurally, the most striking aspect of the coding sequence is the presence of a long repeat region encompassing exons 7-15 that resembles a helicase domain.[220, 221] CSB was characterized as a member of the SNF2 family of chromatin remodelling factors[224] containing ATPase and helicase domains but no

helicase activity.[225] In fact it is the ATPase domain that is important for functionality in TC-NER[226] and when deleted, promotes UV-induced apoptosis, a hallmark of defective TC-NER.[227] CSB is responsible for chromatin remodelling by modulating the position of nucleosomes in an ATP-dependent manner[215] by physically wrapping and unwrapping DNA.[228] Its interaction with transcription machinery is stabilized by UV-induced DNA damage.[208] Additionally, RNAPII, stalled at a cisplatin lesion, acts as a nucleation site for repair factors and is able to proceed with transcription only in the presence of CSB.[229] In fact CSB does this by recruitment of several key players involved in chromatin remodelling, namely histone acetyltransferase p300, NER repair proteins (involved in lesion verification) and CSA-DDB1 E3-ubiquitin ligase complex with the COP9 signalosome.[214] A model emerged that described CSB as the main player in TC-NER, in a transcriptional regulatory role, not as a transcription factor, but in physically interacting directly with the RNA polymerase II (RNAPII) machinery in a UV-dependent manner.[205, 206, 211, 225, 230]

CSA, also key to TC-NER was identified in a similar manner to CSB.[231, 232] Subsequent to its cloning, CSA was found to bind CSB and a subunit of the TFIIH transcription factor, the first clear evidence that the CS proteins had some role in transcription regulation.[233] This concept became widely supported by work linking transcriptional defects to CS cells.[177, 204, 209, 234] Fousteri *et al.* (2006) show elegantly that CSA is dispensable for recruiting core NER factors but does associate with XAB2 and the TFIIS transcription component (detailed below).[214]

1.7.3 Role of TC-NER in the acute response to UV light and cisplatin

The precise manner by which stalled transcription is made known to repair machinery is unknown, however RNAPII remains a very sensitive detector of cisplatin and UV-lesions.[235-237] These transcriptional blocks occur by two different processes that have been recently shown for the first time by x-ray crystallography.[238] In the presence of a CPD, the 5'-thymine of the lesion is brought into contact with the active site of RNAPII but due to the altered DNA base bond angles set up by the dimer (DNA kink), uracil monophosphate (UMP) is mis-incorporated opposite the 5'-thymine, previously shown to be a very slow step and rate limiting.[239] This results in a persistent stall as the mis-incorporated UMP that does not form favourable bonds with any of the other dNTPs. Brueckner *et al.* (2009)[238] argue that it is not the bulky CPD lesion but CPD-directed mis-incorporation of UMP that causes stalling, as they show in an artificial template, RNAPII will bypass other monophosphates or 5'-dTTP:UMP replaced with 5'-dTTP:dATP.[238, 239] Therefore, it is hypothesized that stalled RNAPII blocks access to the lesion by shielding repair proteins from DNA lesions.[239] This is supported by previous observations using foot-printing techniques that illustrate lesion-blocking characteristics of stalled RNAPII.[230, 240]

In partial contrast, cisplatin induces bulkier lesions as the Pt atom binds the N7 atoms of two adjacent guanines. Due to steric hindrance, the approaching RNAPII is physically impeded from receiving the lesion into its active site, thereby stalling transcription.[238] Nonetheless, both lesions are repaired with similar efficiency by TC-NER, demonstrating the highly plastic nature of this repair process.[241]

Primary human cells cultured from CS and XP patients as well as UV-sensitive rodent cells have been useful tools in deciphering the relative sub-pathway contributions to NER. Cells deficient in GG-NER are no more sensitive to UV- or cisplatin-induced apoptosis than wild type cells, while in contrast, TC-NER deficient cells are exquisitely sensitive to these agents.[187, 188, 210, 242-245] There is a strong inverse correlation between recovery of mRNA synthesis and apoptosis in cells treated with cisplatin.[243] As observed following UV exposure, Andera and Wasylyk (1997) showed that TC-NER deficient fibroblasts were sensitive to cisplatin, unlike the GG-NER deficient cells tested.[246] This was confirmed by McKay *et al.* (2001) who also showed sensitivity of TC-NER deficient fibroblasts to cisplatin-induced apoptosis was independent of p53.[187] Similarly Furuta *et al.* (2002) and Bulmer *et al.* (2005) illustrated the same hypersensitivity of TC-NER deficient fibroblasts to cisplatin treatment, but their GG-NER deficient counterparts were unaffected.[188, 247]

Based on the acute apoptotic response of TC-NER deficient fibroblasts, TC-NER could be considered a relevant target in combined cisplatin therapy. Particularly CSB, whose interaction with RNAPII is thought to be the rate limiting step in TC-NER, could be an attractive candidate in tumour therapy.

1.8 Programmed Cell Death as a Result of DNA Damage

Apoptosis is orderly, programmed cell death, that occurs strategically during developmental processes of multi-cellular organisms as well as after cells are exposed to xenobiotics such as UV light or cisplatin (reviewed in Wyllie and Golstein 2001[248]). Cells undergoing apoptosis contract their membranes and nuclear envelopes (pyknosis) and

thus retract from their neighbours, bleb their membranes and disintegrate into contained vesicles known as apoptotic bodies.[29, 249] These apoptotic bodies are consumed by phagocytes so the process does not leak cell contents, a process that can cause an inflammatory response associated instead with necrosis.[249, 250] During apoptosis, the cell's infrastructure fragments, while Golgi, endoplasmic reticulum and mitochondria disintegrate, followed by hydrolysis of DNA into internucleosomal fragments of approximates 200 base pairs (karyorrhexis).[29, 251]

1.8.1 Initiation of Apoptosis

Apoptosis is initiated through two main pathways, involving both extracellular signalling through death receptors (i.e. Fas) and their ligands (i.e. FasL) or internally, through activation of pro-apoptotic factors linked to mitochondria (i.e. BH3-only proteins) (reviewed in Zhivotovsky and Kroemer (2004)[29]). Both these pathways ultimately result in the activation of intracellular caspases, a group of cysteine proteases with aspartate-directed cleavage activity, that coordinate apoptosis (reviewed in Earnshaw *et al.* 1999[252]). The extrinsic pathway activates caspases directly, utilizing adapter proteins, while the intrinsic pathway involves mitochondrial membrane permeability (MMP). These two cascades are historically designated the intrinsic and extrinsic apoptosis pathways but there is significant crosstalk between them. For example, both can rely on mitochondrial membrane permeabilization (MMP) to generate the apoptotic end point. Interestingly, UV exposure prompts apoptotic responses through the extrinsic[253, 254] and also intrinsic

pathways[255, 256] depending on cell-type, the wavelength, dose and retention of function of JNK signalling cascades.[257]

1.8.2 Intrinsic Apoptosis Pathway

B-cell lymphoma-2 (BCL-2) protein is an anti-apoptotic protein that was found to rescue lymphoid cells from certain death after removal of necessary growth factors.[258] BCL-2 is the prototype of a family of proteins that have either pro- or anti-apoptotic properties that work together to regulate MMP. The three sub-families of BCL-2 proteins all contain loosely similar BCL-2 homology (BH) domains (BH1-BH4). The BH3-only sub-family are all pro-apoptotic and respond to different stress stimuli to promote the MMP process and release of cytochrome C from the mitochondria.[249] The release of cytochrome C stimulates formation of a death promoting structure, the apoptosome, that is an assembly of 7 molecules of apoptotic protease-activating factor-1 (APAF1) and the same number of caspase-9 homodimers.[29] The assembled apoptosome activates caspases 3 and 7.[29] An ensuing cascade of caspase activation results in cleavage of hundreds of cellular substrates, causing structural fragmentation of the cell (described above).[29, 249, 259, 260]

1.8.3 Extrinsic Apoptosis Pathway

Cells may receive death signals from their neighbours or from immune cells via the tumour necrosis factor receptor family. For example, Fas ligand from an external source can bind Fas receptor on the target cell surface resulting in intracellular association of Fas with Fas associated protein with death domain (FADD). This association recruits inactive

monomeric caspase 8 and subsequently the formation of the oligomeric death-inducing signalling complex (DISC). Assembled DISC activates its component caspase 8 molecules, leading to a potent apoptotic caspase cascade (reviewed in Riedl and Shi 2004[261]). Caspase 8 is considered the activator caspase and can initiate the MMP process or directly activate effector caspases 3 and 7, both potent activators of apoptosis (as described above).[29, 249, 262]

1.8.4 DNA Damage Sensors

The first responders to DNA damage are phosphoinositide 3-kinase-related kinases (PIKKs) acting primarily as sensors (reviewed in Roos and Kaina 2006[263]), that allow transduction of the initial stress response. In earlier models, ataxia telangiectasia mutated protein (ATM) readily binds ionizing radiation-induced DSBs while the ATM and Rad3-related protein (ATR) senses single stranded DNA generated at stalled replication forks and bulky DNA cross links (reviewed in Zhivotovsky and Kroemer 2004[29]). Additionally, DNA dependent protein kinase (DNA-PK) is thought to be required for mediating NHEJ (reviewed in Durocher and Jackson 2001[264]). Interestingly, these PIKK family members all seem to require similar activation, through similar amino acid motifs, that result in similar signalling cascades, which suggests an evolutionary conservation of structure and function. Specifically, conserved motifs on NBS1, ATRIP and Ku80 are required for ATM, ATR and DNA-PK sensory activity respectively, including activation, binding to damage and subsequent signalling.[265] During initial characterization, ATM appeared important for the stress response following ionizing radiation while ATR seemed important for response to UV ex-

posure. However recent work suggests significant sharing of roles with each responding to a broadly overlapping complement of DNA damage, with equivalent outcome: generation of a DNA damage signal.[266] ATR-dependent phosphorylation of ATM can be detected independent of DSB, after UV treatment.[266] ATM-dependent activation of ATR can be seen after ionizing radiation[267] and ATR is regulated by ATM in response to DSB.[268] In the presence of DSB both Ku70 and Ku80, components of the DNA-PK complex, regulate an ATM and ATR response, further linking all three members of the PIKK family[269](as described above). Additionally, a cooperative stress response was seen by Colton *et al.* (2006)[270] where ATM is required for NER of cisplatin lesions. While cisplatin cross-links are ATR-sensed, ATR is not required for removal of cisplatin lesions.[271] After autophosphorylation in the presence of DNA damage, ATM and ATR both activate cell cycle checkpoints (through Chk1 and Chk2 checkpoint kinases) and subsequent cell cycle arrest that may allow for either DNA repair or apoptosis (reviewed in Roos and Kaina 2006[263]). An additional substrate of ATM/ATR and of particular importance here is the activation of the p53 tumour suppressor that then exerts its effect on cell cycle regulation, DNA repair and apoptosis. Damage response described herein can be seen further simplified in Figure 5.

1.8.5 Cancer Therapy by Induction of DNA Damage

Cancer therapy often involves one or several of surgery, ionizing radiation (IR), conventional chemotherapeutics in sequential mono-therapy or in combinatorial cocktails, monoclonal antibodies or oncolytic viruses (as yet solely experimental). The choice of treatment regimen is governed by consideration of parameters such as the histopatho-

Figure 5. DNA Damage Response.

Summary of the main cellular responses after UV irradiation (further explained in text). DNA is the main target of UV irradiation forming CPDs and 6-4-PPs that block replication and transcription machineries. Activation of tumour suppressor proteins such as p53 can lead to cell death. UV light (mainly UVA and UVB) can directly activate membrane death receptors that may trigger apoptosis independently of DNA damage. Reproduced with permission.

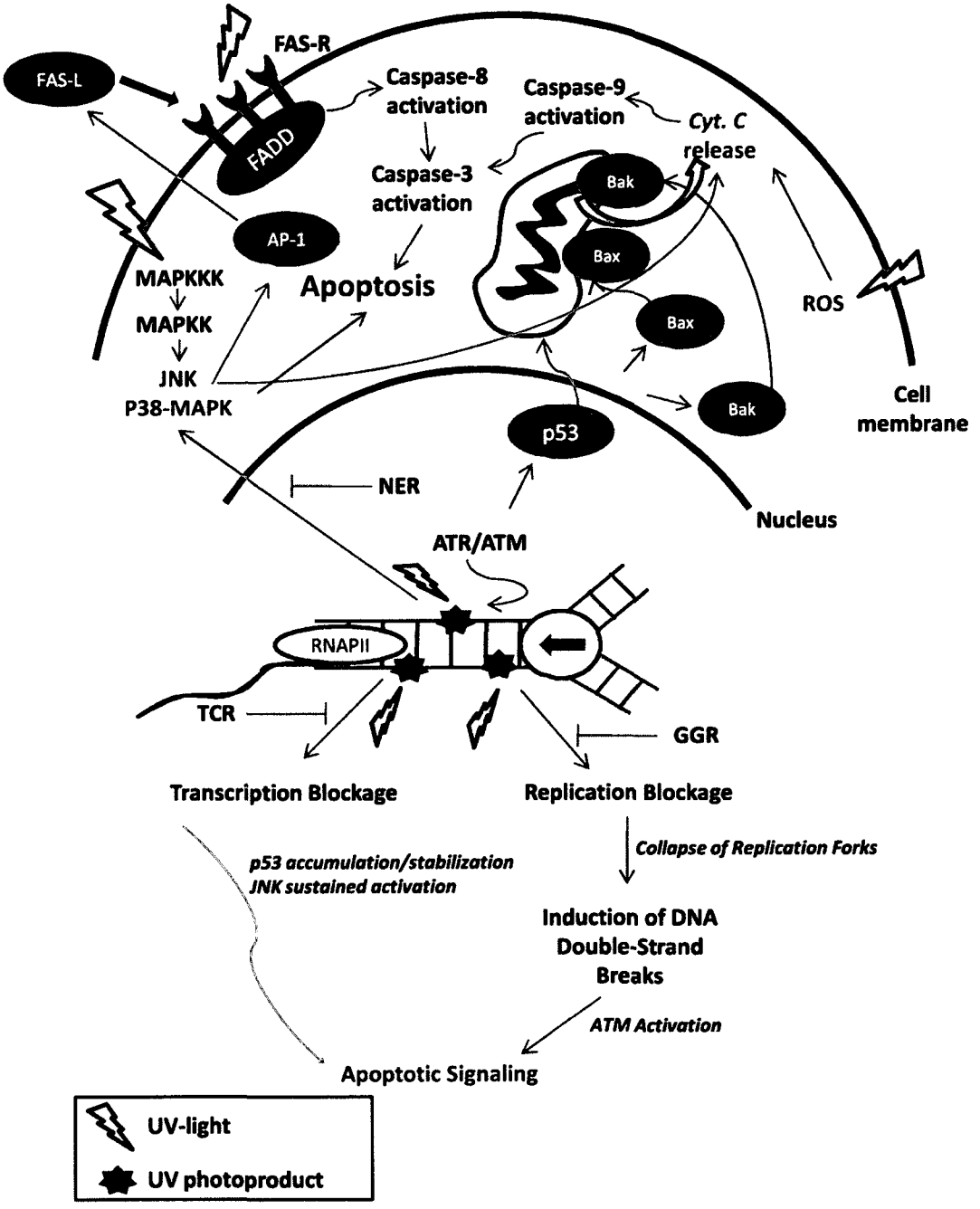
FAS-R
FAS-L
FADD
Caspase-8 activation
Caspase-9 activation
Cyt. C release
Caspase-3 activation
Bak
Bax
AP-1
Apoptosis
MAPKKK
MAPKK
JNK
P38-MAPK
ROS
Cell membrane
p53
Bak
NER
Nucleus
ATR/ATM
RNAPII
TCR
GGR
Transcription Blockage
Replication Blockage
p53 accumulation/stabilization
JNK sustained activation
Collapse of Replication Forks
Induction of DNA Double-Strand Breaks
ATM Activation
Apoptotic Signaling
UV-light
UV photoproduct

logical stage, location and type of the malignancy and general health of the patient.[272-278] Solid tumours are most successfully treated by surgery, where possible, often in combination with ionizing radiation and/or anti-neoplastic chemotherapy. Successful treatment of human cancer by chemotherapy and ionizing radiation depends predominantly on the concept that tumour cells succumb more readily than normal cells to the chosen treatment since they are dividing rapidly. The most effective therapies both inhibit the growth and increase cell death of tumours and often do so by imparting a cytotoxic level of DNA damage or cell cycle perturbations in the more rapidly dividing cancerous tissue and rely on the greater rate of replication inherent to tumour cells that have deregulated growth control. Thus, regularly dividing normal tissue, such as haematopoietic, cardiac, hair follicle and germ-line cells may also succumb. The accumulation of this therapeutic DNA damage is of real concern since it often leaves the patient reproductively sterile, temporarily immune suppressed, with cognitive deficits, at risk of future treatment-linked malignancies and often exhibiting a systemic acceleration of the ageing process.[279-283] An additional drawback to any DNA damage-inducing treatment regimen is the potential for eventual recurrence of resistant disease through selective processes.[276, 284, 285] Thus, a consideration of any chemotherapeutic regimen is the management of side effects while maximising efficacy, with the long-term goal of lowering rates of recurrence of disease. To combat recurrence patients receive the maximum tolerated dose of genotoxic drugs, often in the form of a combinatorial cocktail or in sequential monotherapy, possibly in concert with other interventions such as IR therapy and oncologic surgery, in a tissue-specific manner.[276, 278] DNA repair capacity appears to affect tumour responses in some

clinical situations. For example, the high cure rate of early stage testicular cancer after cisplatin monotherapy is thought to be due to the low expression of certain DNA repair proteins within this tissue.[285-287] Recently, cancer cell expression profiles have indicated that poor expression of certain DNA repair proteins may be both prognostic of positive outcome as well as indicate use of drugs whose mechanism is specifically linked to that repair pathway. For example, a deficit in homologous recombination due to breast cancer protein (BRCA) or Fanconi Anemia (FANC) family protein mutations increases the likelihood of certain cancers but also sensitizes the subsequent tumours to ionizing radiation and multiple chemotherapeutics.[288, 289] Additionally, reduced ERCC1 expression combined with cisplatin in several solid tumour types can be linked to a favourable outcome compared with normal expression.[290-297] It is also recognized that a significant proportion of solid tumours exhibit some form of DNA repair defect.[298] Taken together, these data suggest that certain tumours, by nature of their individual DNA repair defect(s), may be sensitive to specific forms of therapeutic DNA damage[287, 288, 290, 299-303]

1.9 Cisplatin Chemotherapy

The bulky adducts induced by UV light are similar in size and in DNA repair response they garner, to the inter- and intra-strand cross-links caused by cisplatin.[304-306] If left unrepaired the bulky DNA adducts caused by both UV and cisplatin can result in transcription blocks[187, 188, 243, 246] and replication stress[307-309] that may lead to the formation of DSB, through replication fork collapse.[42, 263, 310-312] DNA strand breaks can occur at the

replication fork, during mitosis and meiosis, as a normal step in immune cell development and as a result of DNA exposure to free-radicals.[302]

Amongst all chemotherapeutic interventions, platinum-based anti-neoplastic drugs are by far the most ubiquitous for germ cell, gynaecologic and gastrointestinal tumours.[277, 313, 314] Of these, cisplatin, discovered fortuitously as a potent inhibitor of bacterial cell division,[315] is the best studied and most frequently used clinically.[316] Two unfortunate drawbacks of clinical use of cisplatin are nephro- and neuro-toxicity and, as with all chemotherapeutic strategies, eventual resistance to the drug in previously sensitive tumours.[277, 313, 317-319] These factors have driven the search for platinum compounds with similar anti-tumour properties but fewer toxicity-related side-effects. Two more recent clinically relevant platinum compounds are carboplatin, used predominantly in palliative instead of curative regimens,[277, 320, 321] and oxaliplatin, which shows lower toxicity and better response in platinum resistant colorectal cancer treatment[277, 322, 323] (reviewed in Hartmann 2003[317]). Despite its long history of use, recent work suggests that the useful lifespan of cisplatin is being enhanced. Cisplatin treatment modalities, combination therapy and patient dosing are constantly being refined suggesting that the extensive experience from decades of use is being distilled into new potential in the clinical setting.[314]

1.9.1 DNA Repair and Cisplatin Response

From early use of 'caustics' to treat visible tumour tissue to the latest modern chemotherapeutics, the major clinical concerns for patients undergoing cancer therapy have been both toxicity and the recurrence of resistant and often fatal disease.[275, 276, 324,

[325] Despite a patient's initial positive response to therapeutic platinum drugs, or even prolonged cancer-free status, advanced disease often follows that does not respond to initial or similar subsequent therapy.[275, 284, 285, 319] Cells that escape therapeutic killing are often resistant to further rounds of the original therapy as well as being demonstrably more resistant to future therapeutic stress.[275, 285, 326, 327] The mechanisms by which small numbers of tumour cells evade cell death resultant of the original treatment are complex and thus far not fully understood. However, there is evidence that cisplatin treatment selects for: enhanced detoxification of the drug,[277, 284, 319, 326, 328] avoidance of apoptosis through loss or mutation of this multi-step mechanism[277, 285, 329-334] and abnormalities in DNA repair.[130, 188, 277, 284, 293, 294, 313, 318, 326, 328, 335-347] Conversely, there is significant evidence to suggest that certain nucleotide excision repair (NER) defects sensitize cells to cisplatin.[187, 188, 247, 277, 288, 299, 301, 302, 311, 348-350] It is therefore not surprising that amongst the many strategies to increase the efficacy of cisplatin, selectively manipulating DNA repair or devising tumour sensitivity profiling techniques could represent improved outcome for countless patients.[223, 288, 289, 300-303, 349-355]

1.9.2 Prognostic Implications of NER capacity: Cisplatin Response and NER protein expression

In addition to repairing bulky DNA adducts, UV lesions and cross-links, NER is implicated in generation of resistance to cisplatin treatment[284, 285, 296, 297, 319, 328, 337, 344, 356-359] while the absence, impairment or lowered expression of NER factors may play a role in cisplatin sensitivity.[285, 290, 294, 296, 297, 319, 344, 348, 354, 357, 358]

Early in the characterization of DDB2, a correlation between *in vitro* resistance of tumour cells to cisplatin and increased expression of DDB2, absent in XPE cell lines, was reported.[130] DDB2 recognizes and binds cisplatin lesions[360] and is necessary for their removal from the genome,[130, 132, 135] observations that accompanied the first suggestion that heightened NER could contribute to tumour cell resistance.[132] Further exhibiting the importance of GG-NER in recognizing cisplatin lesions, the completely NER deficient XPA cell line was found to remove one fifth of cisplatin lesions compared to normal fibroblasts.[336] This was followed shortly by recognition that the XPA protein binds and recognizes cisplatin lesions as part of the lesion verification step of NER.[157] Examining proteins involved in both sub-pathways (lesion verification step and onwards in NER), it is clear there are links between over-expression and cisplatin resistance. For example, increased expression of XPA and ERCC1 is linked to cisplatin resistance in ovarian tumour cells,[361] while increased expression of XPF-ERCC1 is also thought to be a determinant of cisplatin resistance *in vitro*.[344] This relationship is also seen for both XPA and XPD where increased levels of transcript measured from biopsies can predict cisplatin resistance in non-small cell lung cancer.[359]

Patients with XP are deficient in NER of UV-induced DNA lesions and are at a greatly increased risk of skin cancer and other malignancies. As such, XP-E patients have an increased risk of UV-induced tumour development.[59, 143, 362] XPE patients, the most numerous XP group, are considered GG-NER impaired but exhibit the mildest form of XP, due to retention of repair of 6-4-PP while remaining deficient in repair of CPD.[145, 363-365]

In the context of tumour cells, GG-NER likely repairs cisplatin lesions, so is a determinant of cisplatin resistance,[366] while efficient TC-NER would seem to predict resistance to or effective recovery from potentially apoptotic blockages in transcription.[187, 188, 367] The corollary, that NER deficient tumour cells are sensitive to cisplatin, has also been suggested where NER capacity is indicative of outcome, specifically where positive outcome is correlated with reduced NER capacity.[296, 349, 366, 368]

Conversely, low expression of NER factors XPA, ERCC1 and XPF in the typically cisplatin responsive testicular cancer is indicative of the prognostic potential of determining NER capacity in tumour cells.[286, 287] Under-expression of ERCC1 is thought to predict chemosensitivity and positive outcome in several human tumour types.[287, 291, 293, 294, 296, 311, 369] Similarly, certain XPG polymorphisms predict better outcome after cisplatin treatment.[358] However, the role of CSB in therapeutic outcome has not been investigated to date.

1.9.3 Targeting NER as a Therapeutic Strategy

TC-NER is known to protect primary human fibroblasts from cisplatin-induced apoptosis. There is clinical data supporting a role for TC-NER proteins, including XPA, ERCC1 and XPF, in therapeutic response.[286, 287, 291, 292, 294, 297, 361, 366, 370] Based on this, we suggest that impaired TC-NER may sensitize tumour cells to cisplatin. As CSB is similarly crucial to functional TC-NER, it represents a potential novel target in combined cisplatin therapy. As these proteins are all required for TC-NER, it is possible that TC-NER deficient tumours may respond well to cisplatin treatment. If so, impairing TC-NER by targeting re-

pair proteins would provide the basis for a clinical strategy. As a key protein in GG-NER, it has been suggested that DDB2 is required for appropriate regulation of p53-meditated apoptosis.[371] This is the only GG-NER protein that may represent a therapeutic target in tumour cells. If this relationship can be confirmed, it is possible that over-expression of DDB2 could sensitize tumour cells to apoptosis.

1.10 Hypothesis

TC-NER is required for tumour cells to recover from UV- and cisplatin-induced DNA damage.

1.11 Specific Aims

i) Determine the role of DDB2 in the sensitivity to UV-induced apoptosis

ii) Determine the importance of CSB, XAB2 and XPA to recovery from UV- and cisplatin-induced DNA damage in several human tumour cell lines

iii) Establish a xenograft tumour model of impaired TC-NER *in vivo*

2.0 The Anti-apoptotic Role for p53 Following Exposure to Ultraviolet Light does not Involve DDB2.

The following chapter has been published as a manuscript in the journal **Mutation Research/Fundamental and Molecular Mechanisms of Mutagenesis.**

All experiments were designed and performed by the first author, except where the co-authors assisted as follows: Jennifer Smith assisted with the caspase 3 assays, preparation of the adenoviruses, in experimental design and editing the manuscript. Jeffrey Hamill provided assistance in performing cell counting experiments, flow cytometry and western immunoblot analyses. Tanya Arcand provided assistance in performing the caspase 8 and caspase 9 experiments. Assistance with experimental design, data analysis and manuscript preparation was provided by the senior author, Bruce McKay.

The anti-apoptotic role for p53 following exposure to ultraviolet light does not involve DDB2

Stubbert, L.J., Cancer Therapeutics Program, Ottawa Health Research Institute, Department of Cellular and Molecular Medicine, University of Ottawa, 501 Smyth Rd, Ottawa, ON, Canada K1H 8L6

Smith, J.M., Cancer Therapeutics Program, Ottawa Health Research Institute, Department of Cellular and Molecular Medicine, University of Ottawa, 501 Smyth Rd, Ottawa, ON, Canada K1H 8L6

Hamill, J.D., Cancer Therapeutics Program, Ottawa Health Research Institute, 501 Smyth Rd, Ottawa, ON, Canada K1H 8L6

Arcand, T.L., Cancer Therapeutics Program, Ottawa Health Research Institute, 501 Smyth Rd, Ottawa, ON, Canada K1H 8L6

McKay, B.C., Cancer Therapeutics Program, Ottawa Health Research Institute, and the Departments of Radiology and Cellular and Molecular Medicine, University of Ottawa, 501 Smyth Rd, Ottawa, ON, Canada K1H 8L6

Corresponding author:
Bruce C. McKay
Cancer Therapeutics Program
Ottawa Health Research Institute
503 Smyth Rd, Box 926
Ottawa, ON K1H 8L6
Canada
Phone: 613-737-7700 x70338
Fax: 613-247-3524
bmckay@ohri.ca

Keywords: apoptosis, DDB2, nucleotide excision repair, p53, ultraviolet light, Xeroderma pigmentosum group E

Abstract

The p53 tumour suppressor is a transcription factor that can either activate or repress the expression of specific genes in response to cellular stresses such as exposure to ultraviolet light. The p53 protein can exert both pro- and anti-apoptotic effects depending on cellular context. In primary human fibroblasts, p53 protects cells from UV-induced apoptosis at moderate doses but this is greatly affected by the nucleotide excision repair (NER) capacity of the cells. The damage-specific DNA binding protein 2 (DDB2) is involved in NER and is associated with Xeroderma pigmentosum subgroup E (XP-E). Importantly, DDB2 is also positively regulated by the p53 protein. To study the potential interplay between DDB2 and p53 in determining the apoptotic response of primary fibroblasts exposed to UV light, the expression of these proteins was manipulated in primary normal and XP-E fibroblast strains using human papillomavirus E6 protein (HPV-E6), RNA interference and recombinant adenoviruses expressing either p53 or DDB2. Normal and XP-E fibroblast strains were equally sensitive to UV-induced apoptosis over a broad range of doses and disruption of p53 in these strains using HPV-E6 or RNA interference led to a similar increase in apoptosis following exposure to UV light. In contrast, forced expression of p53 or DDB2 did not affect UV-induced apoptosis greatly in these normal or XP-E fibroblast strains. Collectively, these results indicate that p53 is primarily protective against UV-induced apoptosis in primary human fibroblasts and this activity of p53 does not require DDB2.

Introduction

Ultraviolet light (UV light) induces DNA damage that poses a block to the progression of both DNA and RNA polymerases.[185, 372] These DNA lesions are repaired by two related but genetically separable subpathways of nucleotide excision repair (NER) termed transcription-coupled repair (TCNER) and global genomic repair (GGNER). TCNER is required for the selective removal of transcription-blocking UV lesions from the template strand of active genes.[373] In contrast, GGNER is responsible for the removal of UV lesions from the bulk of the genome and does not require ongoing transcription.[373] Through the concerted action of these repair processes, cells are able to survive genotoxic challenges and restore the integrity of genomic DNA.

The p53 transcription factor is activated by diverse cellular stresses.[374, 375] In response to UV light, p53 is activated and accumulates in the nuclei of cells where it either increases or decreases the expression of target genes, including DNA repair genes like DDB2.[374-376] Also prominent among p53 targets, are genes encoding proteins involved in inducing apoptosis through the intrinsic mitochondrial cell death pathway.[377-380] Apoptosis plays a critical role in suppressing carcinogenesis in sun exposed skin so the tumour suppressive activity of p53 is in part dependent on the regulation of apoptosis. [381, 382] TCNER-deficient fibroblasts accumulate p53 and undergo apoptosis in response to lower doses of UV light compared to repair proficient controls so there is a very tight correlation between the induction of p53 and UV-induced apoptosis in primary human fibroblasts.[242, 383-387] Initially this led to the assumption that UV-induced apoptosis was p53-mediated in primary human fibroblasts.[242, 383, 386, 387] However, this view has been challenged because

inhibition of p53 activity in primary human fibroblasts did not protect these cells from UV-induced apoptosis.[187, 388] In fact, loss of p53 in TCNER-proficient strains increased their sensitivity to moderate doses of UV light.[187, 367, 389] Therefore, p53 has both pro-apoptotic and anti-apoptotic activities depending in large part on the DNA repair capacity of the cells.[390, 391]

Xeroderma pigmentosum is a UV-sensitive syndrome associated with defects in the repair of UV-induced DNA lesions along with a concomitant increase in risk of sun-light-induced skin cancers.[129] There are eight known XP complementation groups: XP-A through XP-G and the variant form XP-V. Each is caused by mutations in a single protein.[129] Mutations in the damage-specific DNA binding protein 2 (DDB2) are associated with XP-E.[362, 392] DDB2 is not required *in vitro* for NER[183] but is required *in vivo* for GGNER of cyclobutane pyrimidine dimers (CPD).[376] DDB2 is associated with a large cullin 4A (Cul4A)-dependent ubiquitin ligase E3 complex (DDB1-Cul4A-DDB2).[213] DDB1-Cul4A-DDB2 activity appears to be required for the recruitment of other NER proteins to bind UV lesions.[147, 152, 393-395] There is also considerable evidence suggesting that DDB2 loss could impact various DNA damage responses, largely independent of its role in GG-NER. For example, DDB2 is a transcriptional coactivator of E2F1[396, 397] and DDB2 binds the histone acetyltransferase p300/CBP.[398] Furthermore, it has been reported that XP-E fibroblasts express very little p53 and that this results in decreased susceptibility to UV-induced apoptosis.[371]

Here, p53 and DDB2 levels were manipulated in normal and XP-E fibroblasts using HPV-E6 expression, siRNA targeting p53 and recombinant adenoviruses expressing either

p53 or DDB2. We found that DDB2 expression had no effect on the sensitivity of primary fibroblasts to UV-induced apoptosis. Similarly, forced expression of p53 had very little effect on the sensitivity of these cells to UV-induced apoptosis. Conversely, disruption of p53 in normal and XP-E fibroblasts led to similar increases in the sensitivity of these strains to UV-induced apoptosis, suggesting that p53 protects fibroblasts from cell death in a DDB2-independent manner. Taken together, we found no evidence to support a role for DDB2 in regulating p53 function in these cells.

Materials and Methods

Cell Culture and UV-irradiation

Normal neonatal foreskin fibroblasts (NF) were obtained from Dr. Mats Ljungman (University of Michigan). Normal (GM00038 and AG1522) and XP-E (GM01389 and GM02415) fibroblasts were obtained from Coriell Repositories (Camden, NJ). GM01389 carry a missense mutation (L350P) in one allele and a 3 bp in frame deletion (N349Del) in the second allele of DDB2.[392] GM02415 (XP2RO) is homozygous for a missense mutation (R273H).[392] Normal and XP-E fibroblasts expressing HPV-E6 were described previously.[187, 399] Cells were maintained in DMEM supplemented with either 10 or 15% fetal bovine serum (Wisent, St. Bruno, QC), as recommended by Coriell Repositories. Medium was supplemented with gentamicin (5 μg/ml, Sigma-Aldrich Canada Ltd, Oakville, ON).

To UV irradiate cells, medium was removed and cells were exposed to UV light at a dose rate of 1 $J/m^2/s$, at room temperature using a germicidal bulb (Philips) emitting UV predominantly at 254 nm. A hand held UV-radiometer was used to estimate fluence prior to each experiment (UVX Radiometer, UVP Inc, Uplands, CA). Following UV exposure, fresh pre-warmed medium was replaced and cells were returned to the incubator for the indicated period of time.

Adenovirus infections

Virus was propagated and titer was determined using standard methods.[400] Cells were seeded in 10 cm tissue culture dishes in order to obtain cultures approximately 70%

confluent at the time of infection. Cells from one plate were collected with trypsin and the number of cells was determined using a cell counter (Vi-Cell XR, Beckman Coulter). Unless otherwise stated, infections were performed at a multiplicity of infection of 25 plaque-forming units (pfu) per cell. To infect cells, DMEM was removed and replaced with 1 mL of serum free DMEM with the required amount of virus. Virus was allowed to adsorb for 1 hr at 37°C in the virus suspension, while dishes were rocked every 15 min to ensure even distribution of virus. Fresh pre-warmed medium was added and cells were returned to the incubator. To prevent cells from reaching confluence, infected cells were split 1:2 six hours following infection and again returned to the incubator for the indicated time.

The adenovirus expressing DDB2 was generated by standard methods using the AdMax vector system (Microbix, Toronto, ON). The coding region of the DDB2 cDNA was subcloned from pBJ5 (kind gift from Dr. Gilbert Chu) into the pDC316 adenoviral shuttle vector. The pDC316-DDB2 plasmid was co-transfected into 293 cells along with pBHGCre-loxdelta1,3 along with a Cre recombinase expressing plasmid. The resulting virus (AdDDB2) was plaque purified, expanded and the integrity of the DDB2 cDNA was confirmed by DNA sequencing. Infection of primary fibroblasts with AdDDB2 led to the overexpression of DDB2 protein (Supplementary Figure 1).

Apoptosis

Three conceptually different methods were used to assess apoptosis. First, changes in forward light scatter, side light scatter and membrane integrity of unfixed cells were used to discriminate early stages of apoptosis from late apoptosis and secondary necrosis using flow cytometry.[401-403] Briefly, control and UV-irradiated cells were collected at various times following UV treatment, rinsed in PBS and then were resuspended in PBS containing propidium iodide (PI, 18 μg/ml, Sigma-Aldrich Canada Ltd, Oakville, ON). The early apoptotic cells were identified as the population with low forward light scatter, high side light scatter and low red fluorescence,[401-403] using a BD LSRII Flow cytometer (Becton Dickenson, Mississauga, ON). Data was analyzed using FCS Express 3.0 (De Novo Software, Los Angeles, CA).

Second, internucleosomal DNA fragmentation that occurs during apoptosis was detected as an increase in the proportion of ethanol fixed cells with sub-diploid DNA content. Briefly, control and UV-irradiated cells were collected 72 hours following UV treatment, washed twice with PBS, fixed with 70% ethanol and stored at –20°C for a minimum of 30 minutes. The fixed cells were rinsed twice in PBS and then incubated in phosphate buffered saline (PBS, Hyclone) with RNase A (40 μg/ml, Sigma-Aldrich Canada Ltd, Oakville, ON) and PI for a minimum of 30 minutes. The proportion of sub-diploid cells was identified using a BD LSRII flow cytometer (Becton Dickenson, Mississauga, ON). Data was analyzed using FCS Express 3.0 (De Novo Software, Los Angeles, CA).

Third, fluorometric immunosorbent enzyme assays for caspase 3 (Roche Canada, Mississauga, ON), 8 and 9 (Clontech, BD Biosciences, Mississauga, ON) activity were performed according to the supplier's instructions using cell lysates collected at various times between 0 and 48 hours following UV treatment. Cells were counted at the time of collection using a ViCell XR automated cell counter (Beckman Coulter, Mississauga, ON) and caspase activity is expressed as units of activity per 10^6 cells.

Cell viability

Viable cell number was assessed by trypan blue dye exclusion. Adherent cells were collected at the indicated times, rinsed and resuspended in PBS. Viable cell number was determined using a ViCell XR automated cell counter (Beckman Coulter) and is expressed relative to the number of viable cells at the time of irradiation.

Western Blotting

Whole cell lysates were collected with either 1% SDS or RIPA buffer. Samples were sonicated for 10s using a microtip (Branson Sonifier, VWR International Ltd., Mississauga, ON) and protein concentrations determined using the BioRad Protein Assay (BioRad, Mississauga, ON). Proteins (20 μg per lane) in LDS NuPAGE sample buffer were separated using 10 or 12% Bis-Tris NuPAGE pre-cast gel (Invitrogen, Burlington, ON). Proteins were then transferred to Hybond-C Extra nitrocellulose membranes (Amersham, Baie d'Urfé, QC), stained with Ponceau S Red (5 mg/ml Ponceau S Red, 2% glacial acetic acid) and

blocked for a minimum of 1 hr at room temperature in PBSMT-A (PBS, 5% nonfat dry milk powder, 0.05% Tween 20). Membranes were incubated with primary antibody directed against p53 (Ab-6, 1:250, Calbiochem, Cambridge, MA), $p21^{WAF1}$ (Ab-1, 1:250, Calbiochem), DDB2 (AF3297, 1:1000, R&D Systems, Minneapolis, MN) or β-actin (clone AC-74, 1:15000, Sigma-Aldrich Canada Ltd, Oakville, ON) for 1.5 hr at room temperature in PBSMT-B (PBS, 0.5% nonfat dry milk powder, 0.05% Tween 20). SuperSignal West Pico Chemiluminescent Substrate (Pierce, Rockford, IL) in combination with either Kodak film (Rochester, NY) or a gel documentation system (Gene Gnome, Synoptics, Bristol, UK) was used to detect bands. Multiple proteins were detected using the same blots using Restore Western Blot Stripping Buffer (Pierce, Rockford, IL).

RNA interference

Transfection of siRNAs was performed as previously described [399]. Briefly, cells were maintained in antibiotic-free media at least 48 hours prior to transfection. Cells at 50-80% confluence in 10 cm culture dishes were transfected with SmartPool siRNA duplexes targeting p53 or control duplex (Dharmacon Inc., Lafayette, CO) at 50 nM final concentration using Oligofectamine Reagent and Opti-MEM I (Invitrogen, Burlington, ON) according to manufacturer's instructions. Cells were split 1:2, 24 hours following transfection and treated with the indicated doses of UV light 72 hours following transfection.

Results

UV induced apoptosis in normal and XP-E fibroblasts

Normal and XP-E fibroblasts were exposed to 10 J/m^2 of UV light and cell lysates were collected for immunoblot analysis. The p53 protein levels were low in untreated cells and p53 was induced in both fibroblast strains following exposure to UV light (Figure 1A). The proportion of cells undergoing apoptosis was assessed using three independent indicators of apoptosis. Apoptosis was not significantly increased in any normal fibroblast strain in response to 10 J/m^2 of UV light (Figure 1B-D). Despite heterogeneity in the proportion of normal fibroblasts undergoing apoptosis following exposure to high doses, 30 J/m^2 of UV light induced apoptosis in all three normal fibroblast strains (Figure 1B-D). Both XP-E fibroblast strains were similarly insensitive to the induction of apoptosis following exposure to 10 J/m^2 of UV light but apoptosis was again detectable in response to 30 J/m^2 (Figure 1B-D). Similar results were obtained when viability was assessed by trypan blue dye exclusion (Figure 1E). These results support a model in which GGNER capacity does not impact the sensitivity of primary fibroblasts to UV-induced apoptosis.[187, 242, 383, 386]

Disruption of p53 leads to increased sensitivity of XP-E fibroblasts to UV-induced apoptosis

HPV-E6 was used to target p53 for proteasome-mediated degradation in XP-E fibroblasts. The expression of p53 was induced following UV-irradiation in normal and XP-E fibroblasts and HPV-E6 expression prevented the UV-induced accumulation of p53 in normal and HPV-E6 (Figure 2A). Targeting p53 in this way led to a significant increase in

Figure 1. Ultraviolet Light-induced Apoptosis in Normal and XP- E Fibroblasts.

(A) Normal and XP-E fibroblasts were exposed to 10 J/m^2 of UV light and cell lysates were collected for immunoblot analysis. (B-E) Normal (NF, GM00038 and AG1522) and XP-E fibroblasts (GM01389 and GM02415) were exposed to the indicated dose of UV light and cell death was assessed 72 hours later by subdiploid DNA content (B) and PI-negative early apoptosis (C). Similarly, caspase 3 activity was assessed 48 hours following exposure to the indicated dose of UV light (D). Viable cell number was determined by trypan blue exclusion up to 3 days following exposure to 10 Jm^{-2} of UV light (E). Each value in B, C, D and E represents the mean ($\pm$ SEM) determined from a minimum of 3 independent experiments. Significant differences (* $P < 0.05$, ** $P < 0.001$ in E) were determined using student t-tests.

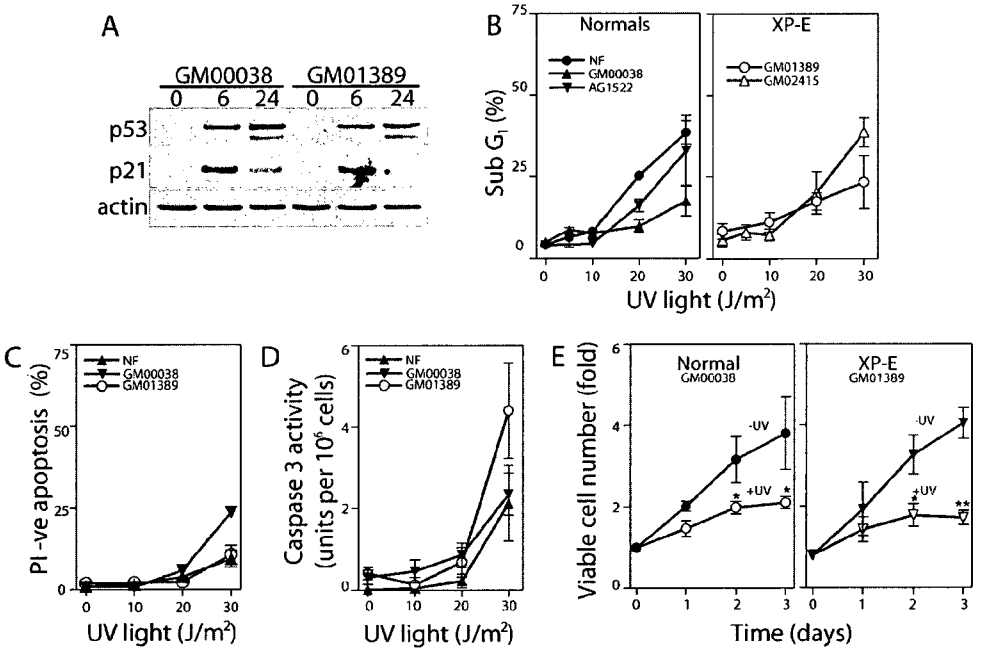
A
GM00038
GM01389
0 6 24 0 6 24
p53
p21
actin
B
Normals
XP-E
NF
GM00038
AG1522
GM01389
GM02415
Sub G1 (%)
UV light (J/m2)
C
PI -ve apoptosis (%)
UV light (J/m2)
D
Caspase 3 activity (units per 10^6 cells)
UV light (J/m2)
E
Normal
GM00038
XP-E
GM01389
-UV
+UV
Viable cell number (fold)
Time (days)

Figure 2. The Effect of HPV-E6 on UV-induced Apoptosis in Normal and XP-E Fibroblasts. (A) Cell lysates were collected from primary human fibroblasts and derivative HPV-E6 expressing sublines 24 hours following exposure of cells to either 10 or 30 Jm^{-2} of UV light, as indicated. (B) Normal (GM00038) and XP-E (GM01389) and their respective HPV-E6 expressing sublines were exposed to the indicated dose of UV light and 72 hours later cell death was measured by assessing subdiploid DNA content (B) and PI-negative early apoptosis (D). (C) Other normal (NF) and XP-E (GM2415) fibroblasts and their respective HPV-E6 expressing sublines were exposed to 0 or 10 Jm^{-2} of UV light and apoptosis was measured 72 hours later by assessing subdiploid DNA content. (E) Trypan blue exclusion was determined up to 3 days following exposure to 10 Jm^{-2} of UV light. Each value in B to E represents the mean (± SEM) determined from a minimum of 3 independent experiments. Significant differences (* $P < 0.05$, ** $P < 0.001$) between the indicated value and its respective control collected at the same time was determined using a student t-test.

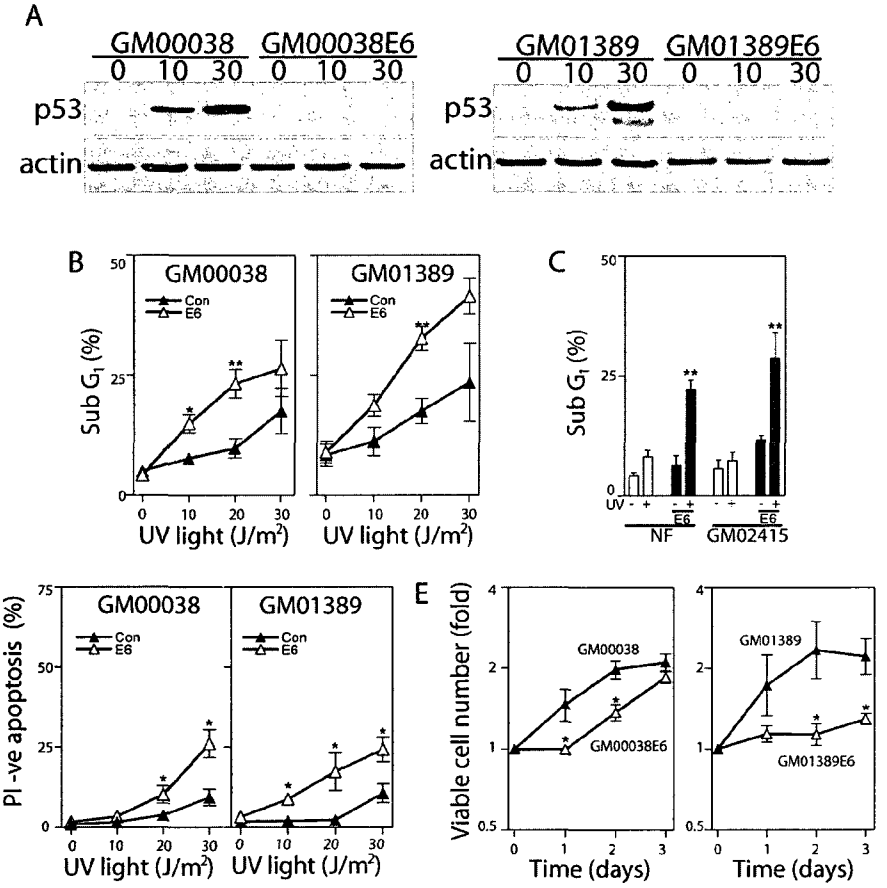
A
GM00038
GM00038E6
GM01389
GM01389E6
0 10 30 0 10 30
0 10 30 0 10 30
p53
actin
p53
actin
B
GM00038
GM01389
Con
E6
Sub G1 (%)
UV light (J/m2)
UV light (J/m2)
C
Sub G1 (%)
UV - +
E6
E6
NF
GM02415
D
GM00038
GM01389
Con
E6
PI -ve apoptosis (%)
UV light (J/m2)
UV light (J/m2)
E
Viable cell number (fold)
GM00038
GM00038E6
GM01389
GM01389E6
Time (days)
Time (days)

the sensitivity of normal and XP-E fibroblast strains to UV-induced apoptosis (Figure 2B-D). Furthermore, UV light led to a more substantial decrease in viable cell number in both HPV-E6 expressing strains compared to their respective controls (Figure 2E). Therefore, these results suggest that XP-E fibroblasts retain anti-apoptotic p53 activity.

Small inhibitory RNAs (siRNA) were used to target p53 as an alternative means of inactivating p53. Transient transfection of these siRNAs significantly decreased p53 protein levels before and after UV treatment (Figures 3A and B). Consistent with the results obtained in HPV-E6 expressing strains, transient knockdown of p53 increased the sensitivity of normal and XP-E fibroblast strains to UV-induced apoptosis (Figure 3C and D). Taken together, the expression of wildtype p53 protected primary human fibroblasts against UV-induced apoptosis, in a DDB2-independent manner.

Caspases 3 and 9 are activated in a p53- and DDB2-independent manner following UV exposure

Caspases are highly specific cysteine proteases involved in the execution of apoptosis.[3, 404] The activity of caspases 3, 8 and 9 was assessed at various times following exposure to several doses of UV light because the activity of these caspases is frequently used to discriminate between the intrinsic (caspase 3- and 9-dependent) and extrinsic (caspase 3- and 8-dependent) apoptotic pathways [3, 404]. The activity of caspase 3 and caspase 9 increased in a dose-dependent manner between 24 and 48 hours following UV exposure and this increase correlated with the induction of apoptosis in these primary human fibroblasts

Figure 3. The effect of targeting p53 by RNA interference on UV-induced apoptosis in normal and XP-E fibroblasts.

Normal (GM00038 in A) and XP-E (GM01389 in B) fibroblasts were transfected with control non-targeting (NT) or anti-p53 siRNAs. At 0, 6 or 24 hours following exposure to 10 J/m2 of UV light, cell lysates were subjected to immunoblot analysis. Similarly, normal and XP-E fibroblasts were transfected with siRNAs described in A and B and apoptosis was measured by assessing subdiploid DNA content (C) and PI negative early apoptosis (D). Each value in (C) and (D) represents the mean (± SEM) determined from a minimum of 3 independent experiments. Significant differences (* $P < 0.05$, ** $P < 0.001$) between the indicated value and its respective control exposed to the same dose of UV light was determined using a student t-test.

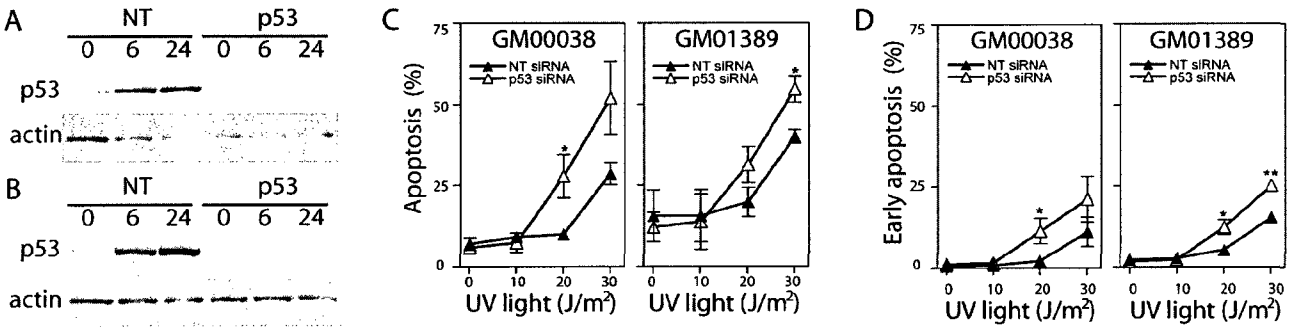
A
NT
p53
0 6 24 0 6 24
p53
actin
B
NT
p53
0 6 24 0 6 24
p53
actin
C
GM00038
GM01389
NT siRNA
p53 siRNA
Apoptosis (%)
75
50
25
0
0 10 20 30
UV light (J/m2)
D
GM00038
GM01389
NT siRNA
p53 siRNA
Early apoptosis (%)
75
50
25
0
0 10 20 30
UV light (J/m2)

Figure 4. Ultraviolet light-induced apoptosis is associated with increased activity of caspases 3 and 9 but not caspase 8.

(A) GM00038, GM01389 and their respective HPV-E6 expressing sublines were exposed to the indicated dose of UV light and the activity of caspases 8 and 9 was determined 48 hours later. (B) The indicated fibroblast strains and their respective HPV-E6 expressing sublines were exposed to 20 J/m2 of UV light and the activity of caspases 3, 8 and 9 was determined at the indicated time following UV exposure. Each value represents the mean (± SEM) determined from a minimum of 3 independent experiments. Significant differences (* $P < 0.05$, ** $P < 0.001$) between the indicated value and its respective control exposed to the same dose of UV light were determined with a student t-test.

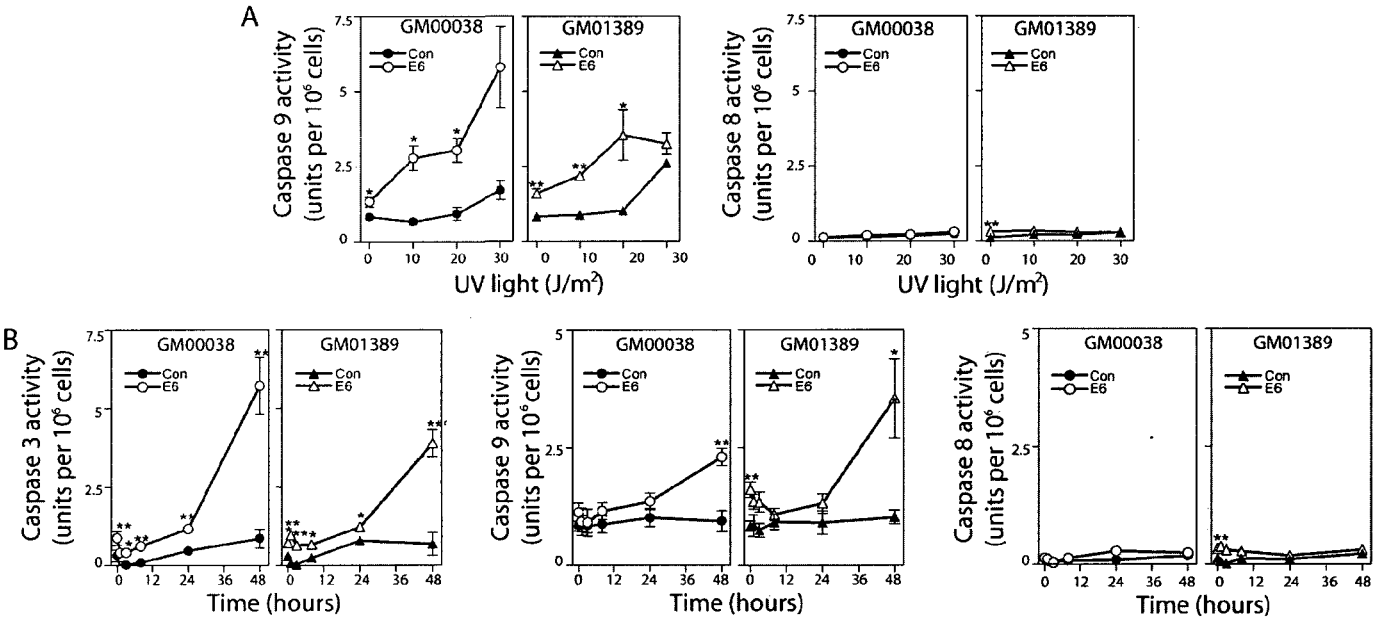
A
Caspase 9 activity (units per 10^6 cells)
GM00038
GM01389
Con
E6
UV light (J/m2)
Caspase 8 activity (units per 10^6 cells)
B
Caspase 3 activity (units per 10^6 cells)
Time (hours)

(Figures 1 and 4A and B). Importantly, the activity of caspase 9 was greater in both HPV-E6 expressing sub-lines compared to isogenic controls (Figure 4A and B). In contrast, caspase 8 activity was very low in all fibroblast strains and changes in caspase 8 activity following UV exposure did not correlate with apoptosis (Figure 4A and see Supplementary Figure 2). Therefore, UV-induced apoptosis was associated with increased activity of caspases 3 and 9 but not caspase 8, suggesting that cell death was mediated through the intrinsic mitochondrial cell death pathway.

The effect of DDB2 and p53 overexpression on UV-induced apoptosis

Primary human fibroblasts carrying mutations in DDB2 exhibited a normal dose-response for the induction of apoptosis following UV exposure (recall Figure 1). To determine whether overexpression of DDB2 altered the sensitivity of primary fibroblasts to UV-induced apoptosis, AdDDB2 was used to express DDB2 in normal and XP-E fibroblasts. Infection of normal and XP-E cells with AdDDB2 24 hours prior to UV-irradiation yielded readily detectable DDB2 protein that peaked 24 hours following infection (Figure 5A and B). Exogenously expressed DDB2 was detectable in both fibroblast strains for several days (Figure 5A and B Supplementary Figure 1). Consistent with the fact that XP-E fibroblasts exhibited a normal UV dose-response relationship, overexpression of DDB2 did not significantly alter the sensitivity of normal or XP-E fibroblasts to UV-induced apoptosis measured through two independent methods (Figure 5C and D). Our results indicate that neither DDB2 mutations nor over-expression of DDB2 altered the sensitivity of fibroblasts to apoptosis following UV exposure.

Supplementary figure 1. Expression of p53 and DDB2 from recombinant adenoviruses. (A) Normal (GM00038) and XP-E (GM01389) fibroblasts were infected with adenoviruses expressing lacZ, DDB2 or p53 at a MOI of 25, 24 hours prior to UV exposure, as indicated. Immunoblot analysis indicates that expression of p53 and DDB2 is maintained for at least 3 days following exposure to 10 J/m2 of UV light. (B) The normal and XP-E fibroblast strains were infected with AdDDB2, 24 hours prior to cell treatment. DDB2 levels were reduced approximately 4 fold within 3 hours following UV exposure when translation was blocked with simultaneous cycloheximide. UV-induced degradation of DDB2 is required for GG-NER so the UV-induced decrease in DDB2 protein is indicative of functional DDB2 protein.

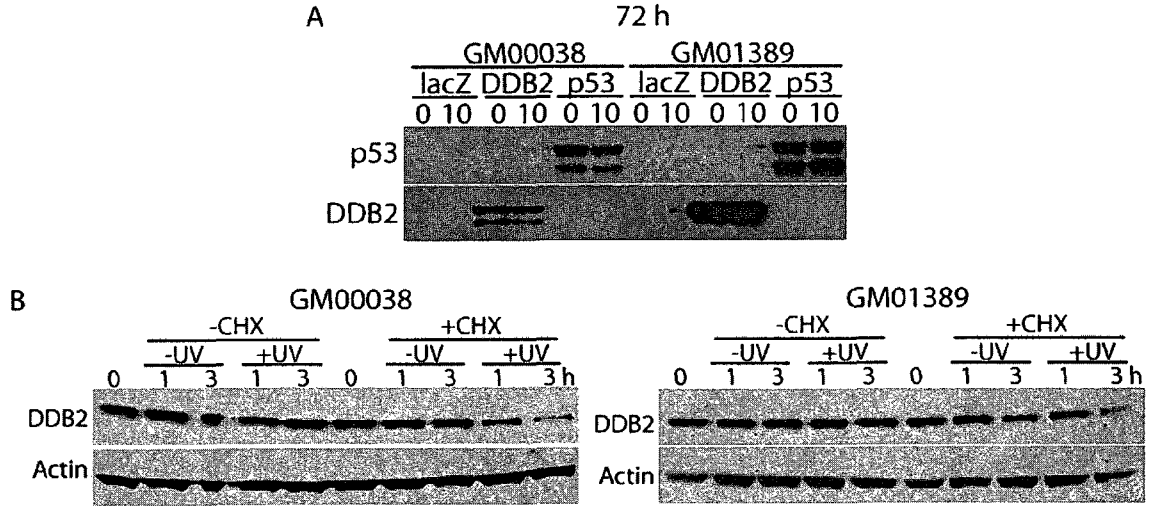
A
72 h
GM00038
GM01389
lacZ DDB2 p53 lacZ DDB2 p53
0 10 0 10 0 10 0 10 0 10 0 10
p53
DDB2
B
GM00038
GM01389
-CHX
+CHX
-UV
+UV
0 1 3 1 3 0 1 3 1 3 h
DDB2
Actin

Figure 5. Forced expression of DDB2 did not alter the sensitivity of normal or XP- E fibroblasts to UV-induced apoptosis.

Normal (GM00038) and XP-E (GM01389) fibroblasts were infected with the adenoviruses expressing either lacZ or DDB2, 24 hours prior to UV exposure. Cell lysates were collected for immunoblot analysis from normal (A) and XP-E (B) fibroblasts at 0, 24 and 48 hours following exposure to 0 or 10 Jm^{-2} of UV light. Similarly, subdiploid DNA content (C) and by PI-negative early apoptosis (D) were assessed 72 hours following exposure to the indicated dose of UV light. Each value in C and D represents the mean (± SEM) determined from a minimum of 3 independent experiments.

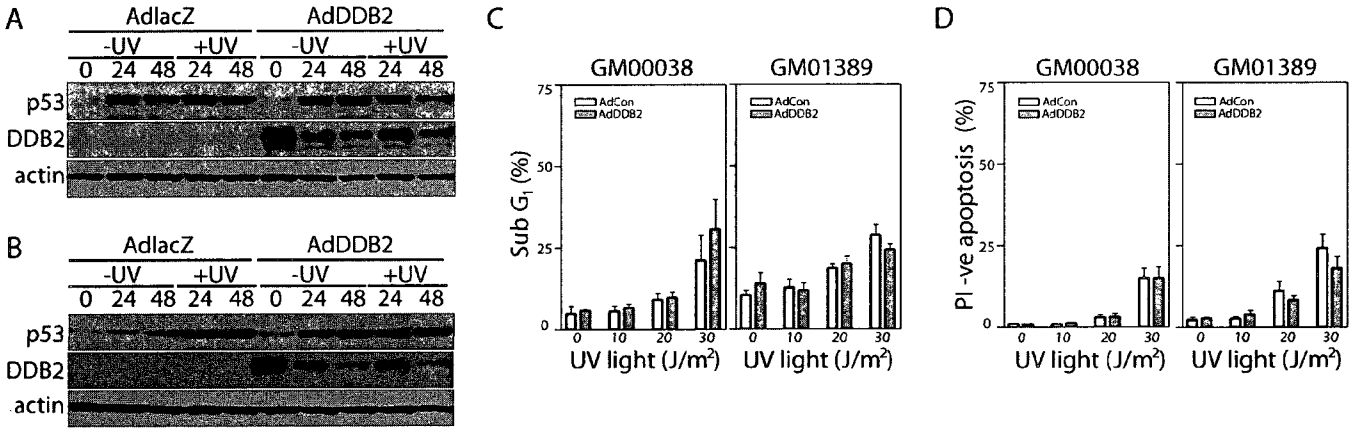
A
AdlacZ
AdDDB2
-UV
+UV
-UV
+UV
0 24 48 24 48 0 24 48 24 48
p53
DDB2
actin
B
AdlacZ
AdDDB2
-UV
+UV
-UV
+UV
0 24 48 24 48 0 24 48 24 48
p53
DDB2
actin
C
GM00038
GM01389
AdCon
AdDDB2
Sub G1 (%)
75
50
25
0
0 10 20 30
UV light (J/m2)
D
GM00038
GM01389
PI -ve apoptosis (%)
UV light (J/m2)

Supplementary figure 2. Ultraviolet light-induced apoptosis does not correlate with increased activity of caspase 8.

Caspase 8 activity data presented in Figure 4B is plotted over a narrower range to highlight small changes in activity following UV exposure. (A) GM00038, GM01389 and their respective HPV-E6 expressing sublines were exposed to the indicated dose of UV light and the activity of caspase 8 was determined 48 hours later. (B) The indicated fibroblasts strains and their respective HPV-E6 expressing sublines were exposed to 20 Jm^{-2} of UV light and the activity of caspase 8 was determined at the indicated time following UV exposure. Changes in caspase activity did not correlate with the dose-dependent differences in UV-induced apoptosis. Each value represents the mean (± SEM) determined from a minimum of 3 independent experiments. Significant differences (* $P < 0.05$) between the indicated value and its respective control exposed to the same dose of UV light were determined with a student t-test.

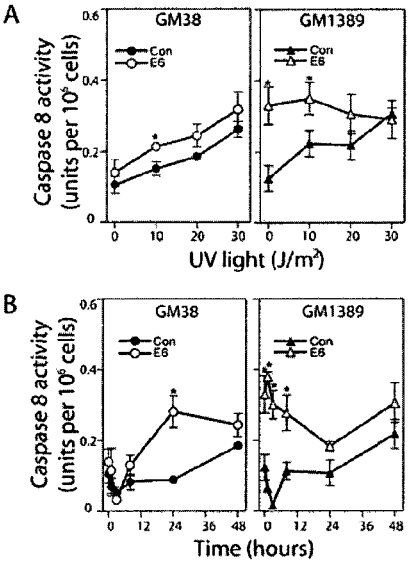
A
GM38
GM1389
Con
E6
Caspase 8 activity
(units per 10⁶ cells)
0.6
0.4
0.2
0
0
10
20
30
UV light (J/m²)
B
GM38
GM1389
Con
E6
Caspase 8 activity
(units per 10⁶ cells)
0.6
0.4
0.2
0
0
12
24
36
48
Time (hours)

In many model systems, p53 contributes strongly to DNA damage-induced apoptosis and the overexpression of p53 can be sufficient to induce apoptosis in many cell types.[378, 379, 391, 405] In primary human fibroblasts, p53 appears to be primarily protective against UV-induced apoptosis because disruption of p53 by mutation,[367, 389] HPV-E6[187] and present study, pharmacological inhibitors of p53[388] or siRNA (present study) increased the sensitivity of primary fibroblasts to UV-induced apoptosis. To complement these loss of function experiments, a recombinant adenovirus expressing wildtype p53 (Adp53) was used to determine if forced expression of p53 could drive p53-dependent apoptosis alone or in combination with UV light in these cells. Adp53 infection of normal and XP-E fibroblasts led to a large increase in p53 levels that were further increased following UV exposure (Figure 6A). Surprisingly, Adp53 did not induce significant apoptosis alone. Adp53 did not protect fibroblasts from UV-induced apoptosis but appeared to stimulate cell death marginally (Figure 6B and C). This only approached statistical significance in XP-E fibroblasts following exposure to 30 J/m^2 of UV light. Unlike the disruption of p53, the overexpression of p53 had very little effect on the sensitivity of primary human fibroblasts to UV-induced apoptosis. We interpret these results to indicate that primary human fibroblasts are relatively insensitive to p53-mediated apoptosis.

Figure 6. The effect of p53 overexpression on UV-induced apoptosis in primary human fibroblasts.

Normal (GM00038) and XP-E (GM01389) fibroblasts were infected with control or p53 expressing adenoviruses 24 hours prior to mock- or UV-irradiation. (A) Cell lysates were collected for p53 immunoblot analysis at the indicated times following exposure to either 0 or 10 Jm^{-2} of UV light. Subdiploid DNA content (B) and PI negative early apoptosis (C) were measured in normal and XP-E fibroblasts exposed to the indicated dose of UV light infected with the indicated adenovirus. Each value in (B) and (C) represents the mean ($\pm$ SEM) determined from a minimum of 4 independent experiments. Significant differences (* $P < 0.05$) between the indicated value and its respective control exposed to the same dose of UV light was determined using a student t-test.

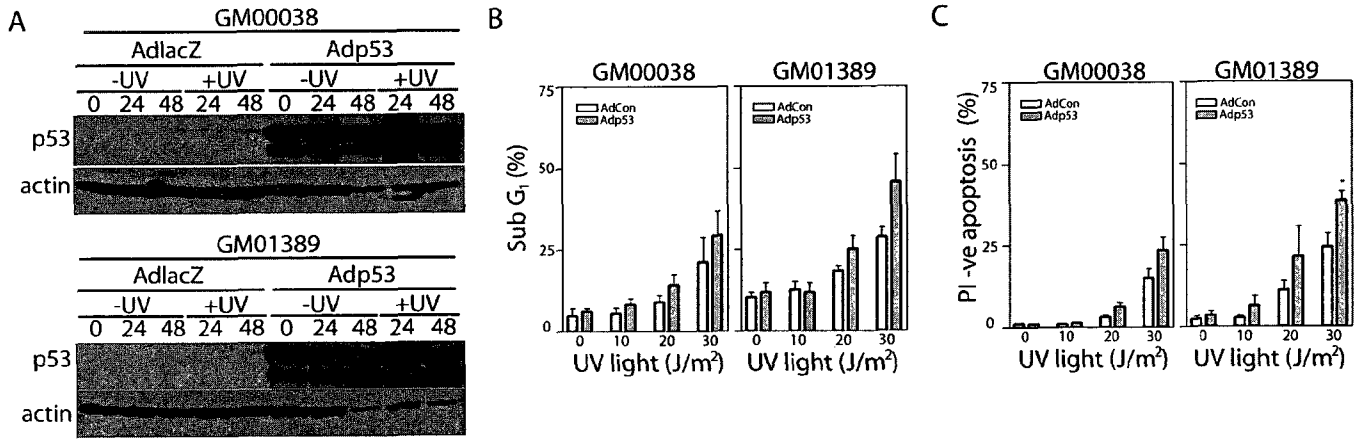
A
GM00038
AdlacZ
Adp53
-UV
+UV
-UV
+UV
0 24 48 24 48 0 24 48 24 48
p53
actin
GM01389
AdlacZ
Adp53
-UV
+UV
-UV
+UV
0 24 48 24 48 0 24 48 24 48
p53
actin
B
GM00038
GM01389
AdCon
Adp53
Sub G1 (%)
75
50
25
0
0 10 20 30
UV light (J/m2)
C
GM00038
GM01389
PI -ve apoptosis (%)
UV light (J/m2)

Discussion

The relationship between nucleotide excision repair and UV-induced apoptosis

The relationship between DNA repair capacity and apoptosis has important implications for DNA damage responses. We, and others, have reported that TCNER-deficient XP and CS fibroblasts are hypersensitive to the induction of apoptosis following exposure to low doses of UV light.[187, 242, 244, 383, 386, 406] By contrast, GGNER defects in XP-C strains do not increase the susceptibility of these cells to apoptosis.[187, 242, 244, 383, 386, 406] There is a very tight inverse correlation between the ability of primary fibroblasts to recover transcription and their sensitivity to UV-induced apoptosis.[187, 242, 243] Collectively these results indicate that the initial amount of DNA damage does not determine the apoptotic response because there is time to recover from damage before commitment to cell death. Furthermore, it is primarily unrepaired lesions in the template strand of active genes (i.e. transcription-blocking DNA lesions) that trigger the apoptotic response following UV exposure. In the present work, XP-E fibroblast strains exhibited normal responses for caspase activation and apoptosis following UV exposure. The response of these GGNER deficient XP-E fibroblasts is similar to that of other GGNER-deficient fibroblast strains (i.e. XP-C cells). The present work reaffirms previous observations indicating that TCNER-deficiency alters the apoptotic response to UV light whereas GGNER-deficiency has little effect.[187, 242, 383, 386] Furthermore, these results imply that the DNA repair phenotype of XP-E fibroblasts contributes more to their apoptotic response than the proposed role of DDB2 in regulating apoptosis through p53.[371, 407]

Anti-apoptotic activity of p53 in primary human fibroblasts

The p53 protein is a central player in the regulation of DNA damage-induced apoptosis in many cell types.[405] However, it is also well-established that p53 has anti-apoptotic activities in some contexts.[390, 391] Here we report that normal and XP-E fibroblasts activated caspases 3 and 9 and underwent apoptosis following UV exposure but that expression of HPV-E6 or targeting p53 by RNA interference increased the sensitivity of these fibroblast strains to UV-induced apoptosis. A similarly protective effect provided by p53 was reported in normal[187, 367, 386, 389, 408] and TCNER-proficient fibroblasts[187] but not in TCNER-deficient strains.[187] The increased sensitivity to UV-induced apoptosis in the absence of functional p53 was associated with a delay in the recovery of mRNA synthesis following UV exposure.[187, 243, 367] Taken together, p53 contributes to the recovery from UV-induced transcriptional arrest and this plays a significant role in determining the apoptotic response of primary human fibroblasts.

Although persistently blocked transcription is clearly one important determinant of the sensitivity of fibroblasts to UV-induced apoptosis,[187, 242, 243, 375] a sustained blockage of transcription is not sufficient to trigger cell death.[244] There is also a requirement for cells to enter S phase prior to apoptosis.[244, 409, 410] Briefly, nascent DNA can be detected in fibroblasts undergoing apoptosis following exposure to UV light[244] and blocking the entry of UV treated cells into S phase significantly inhibits apoptosis despite prolonged inhibition of transcription.[244, 409, 410] Entry of cells in S phase is regulated in large part by the E2F family of transcription under control of pRb. Interestingly, DDB2 binds the transactivation domain of E2F1 and stimulates E2F1-dependent transcription.[396] In addition, forced ex-

pression of E2F1 can increase the sensitivity of primary fibroblasts to UV-induced apoptosis.[383] Despite the link among DDB2, E2F1 and UV-induced apoptosis,[383, 396] XP-E fibroblasts exhibited a normal apoptotic response following UV exposure.

Persistently stalled replication forks can be converted to replication-associated DNA double strand breaks (DSB) and these DNA lesions form predominantly in the absence of functional p53.[308, 309, 399] The p53 tumour suppressor prevents DNA DSB formation in response to other replication stressors.[411] We recently reported that loss of p53 in normal and XP-E fibroblasts led to a dramatic UV-induced S phase arrest that was associated with the accumulation of γ-H2AX foci, consistent with DNA DSB formation in p53-deficient cells.[399] These S phase abnormalities may contribute to the increased sensitivity of p53-deficient fibroblasts to UV-induced apoptosis. Taken together, a model is emerging whereby p53-independent UV-induced apoptosis is triggered indirectly by DNA DSB formation, resulting from a combination of transcription and replication abnormalities.

p53 overexpression in primary human fibroblasts

Overexpression of p53 typically triggers either apoptosis[378, 412, 413] or G_1 arrest[412, 414] in a cell type specific manner. In some model systems, UV light can shift the outcome of p53 overexpression from G_1 cell cycle arrest to apoptosis.[391] Here, the massive overexpression of p53 failed to induce apoptosis in primary human fibroblasts regardless of UV dose. These results indicate that primary human fibroblasts are relatively unresponsive to apoptosis triggered by p53. This explains, in large part, why pro-survival activities of p53

are readily observed in primary human fibroblasts while they may not be detected in other cell lines or model systems.

DDB2 and UV-induced apoptosis

Certain aspects of the present work contrast a previous report. [371] Whereas we find that XP-E fibroblasts exhibit a normal sensitivity to UV-induced apoptosis, it was reported that XP-E fibroblasts were significantly more resistant to UV-induced apoptosis than normal fibroblasts due to decreased expression of p53.[371] Although the precise reason for the disparity is not entirely clear, the control fibroblast strains used in the prior publication underwent apoptosis faster and at lower doses of UV light than observed by other laboratories.[187, 242, 244, 367, 383, 386, 387, 389, 406, 410, 415-420] A precise reason for the disparity remains elusive. Nonetheless, our work indicates that XP-E fibroblasts exhibit normal sensitivity to UV-induced apoptosis.

Two independent laboratories have generated DDB2 targeted mice.[407, 421] Disruption of the DDB2 gene was associated with a small decrease in GG-NER while overexpression of DDB2 enhanced repair in UV-treated embryonic fibroblasts and keratinocytes.[50, 421] In both mouse models, the resulting DDB2-nullizygous mice were susceptible to UVB-induced skin cancers compared to wildtype litter mates while DDB2 heterozygous mice exhibited an intermediate susceptibility.[50, 407, 421] Transgenic mice overexpressing DDB2 under control of the keratin 14 promoter were markedly resistant to UVB-induced skin cancer.[421] Both strains clearly indicate that DDB2 is anti-neoplastic in mouse skin exposed to UV light. However one group reported that DDB2-/- mouse embryonic fibroblasts were

resistant to UV-induced apoptosis[407] while the other group reported a normal apoptotic response in both embryonic fibroblasts and keratinocytes from DDB2 nullizygous and DDB2 transgenic mice.[421] Our work with primary XP-E fibroblasts and fibroblasts overexpressing DDB2 are fully consistent with this latter report.[421] Therefore, we conclude that DDB2 does not affect the sensitivity of primary human or mouse cells to UV-induced apoptosis.

In summary, DDB2-deficient fibroblasts derived from patients affected with XP group E exhibit a normal sensitivity to UV-induced apoptosis and overexpression of DDB2 had no effect on the sensitivity of these cells to this form of cell death. Furthermore, UV-induced apoptosis was largely p53-independent and occurred through the intrinsic mitochondrial cell death pathway. In fact, p53 was primarily protective against UV-induced apoptosis, even in the absence of functional DDB2 protein. Our results suggest that the susceptibility of XP-E patients to solar carcinogenesis is more likely a consequence of their GG-NER defect and not the consequence of a combined defect in DNA repair and p53-dependent apoptosis. The present work has important implications for understanding the anti-neoplastic role of DDB2 in solar carcinogenesis.

Acknowledgements

We would like to thank Dr. G. Chu (Stanford University) for the DDB2 cDNA, Dr. R. Slack (University of Ottawa) for the p53 expressing recombinant adenovirus and Dr. F.L. Graham (McMaster University) for empty vector and lacZ expressing control adenoviruses. This work was supported by the National Cancer Institute of Canada with Funds from the Terry Fox Run. L.J.S. was supported by an Ontario Premier's Research Excellence Award to B.C.M. B.C.M. is a Research Scientist of the Canadian Cancer Society. L.J.S. and J.M.S. were supported with an Ontario Graduate Scholarship in Science and Technology.

3.0 Targeting Cockayne Syndrome Group B Protein Sensitizes Tumour Cells to Ultraviolet Light and Cisplatin Independent of p53 and MLH1

The following manuscript chapter is currently under editorial review at the journal **Neoplasia**. This work represents our efforts in establishing a role for TC-NER in human cancer therapy, specifically in combination with platinum chemotherapy.

The authors contributions to this manuscript are as follows: Jennifer Smith provided assistance in performing some of the caspase assays as well as assistance in manuscript organization and editing. All other experiments were designed and carried out by the first author, who also wrote the first draft and participated in the editing process. The senior author, Bruce McKay, supervised experimental design, assisted with data analysis and manuscript preparation.

Targeting Cockayne syndrome group B protein sensitizes tumour cells to ultraviolet light and cisplatin independent of p53 and MLH1

Stubbert LJ, Cancer Therapeutics Program, Ottawa Health Research Institute and the Department of Cellular and Molecular Medicine, University of Ottawa, Ottawa, K1H 8L6, Canada

Smith JM, Cancer Therapeutics Program, Ottawa Health Research Institute and the Department of Cellular and Molecular Medicine, University of Ottawa, Ottawa, K1H 8L6, Canada

McKay BC, Cancer Therapeutics Program, Ottawa Health Research Institute, and the Departments of Radiology and Cellular and Molecular Medicine, University of Ottawa, Ottawa, K1H 8L6, Canada

Corresponding author:

Bruce C. McKay
Cancer Therapeutics Program
Ottawa Hospital Research Institute
501 Smyth Rd, Box 926
Ottawa, ON K1H 8L6
Canada
Phone: 613-737-7700 x70338
Fax: 613-247-3524
bmckay@ohri.ca

Keywords: apoptosis, CSB, MLH1, XAB2 XPA and transcription-coupled nucleotide excision repair
Running title: MLH1, TC-NER and apoptosis

Abstract

Transcription-coupled nucleotide excision repair (TC-NER) removes a variety of DNA adducts from the template strand of active genes, including those induced by UV light and cisplatin. Fibroblasts with a specific defect in TC-NER are exquisitely sensitive to apoptosis induced by UV light and cisplatin. In contrast, TC-NER does not greatly affect the acute response of murine embryonic stem cells to UV light. Therefore, it was unclear whether TC-NER contributed to the decision of tumour cells to die in response to these agents. We used RNA interference (RNAi) to target the Cockayne syndrome group B (CSB) in several colon and prostate cancer cell lines. Decreased expression of CSB in these cell lines led to a decrease in TC-NER capacity and led to a significant increase in the sensitivity of cells to UV- and cisplatin-induced apoptosis, independent of p53 and DNA mismatch repair capacity. RNAi against XAB2 (XPA binding protein 2) and XPA (xeroderma pigmentosum group A protein) required for TC-NER and both TC-NER and GG-NER, respectively, similarly led to increased sensitivity to cisplatin treatment. Our results suggest that TC-NER proteins are potential targets for cancer therapy and may be important to overcoming cisplatin resistance in the clinic.

Introduction

Cisplatin [*cis*-diammine-dichloroplatinum (II)] has been used in the treatment of neoplastic diseases for over 30 years.[319] The effectiveness of cisplatin is dependent on its interaction with DNA. This drug forms a variety of DNA adducts but more than 99% of these are intrastrand DNA adducts, predominantly intrastrand DNA adducts involving adjacent purines with only a very small number of interstrand-crosslinks and monoadducts.[305] These lesions are repaired by the nucleotide excision repair (NER) pathway so the response of tumours to cisplatin and other platinum-based drugs may be affected by nucleotide excision repair capacity of tumour cells.[319]

The vast majority of what is known about nucleotide excision repair (NER) stems from studies using the model DNA damaging agent UV light but NER of cisplatin-induced DNA adducts is thought to occur through an identical mechanism.[188, 210, 335, 422-424] The rate-limiting step in NER is lesion recognition and this occurs through two distinct mechanisms yielding two interrelated yet genetically separable subpathways of NER.[425] Global-genomic nucleotide excision repair (GG-NER) is responsible for the removal of the vast majority of UV and cisplatin-lesions throughout the genome whereas transcription-coupled nucleotide excision repair (TC-NER) is responsible for the selective removal of only those lesions that are present in the template strand of expressed genes.[193, 197, 422, 423, 426]

Cockayne syndrome (CS) and xeroderma pigmentosum (XP) are heterogeneous disorders characterized by clinical photosensitivity.[416] Based on cell fusion and complementation studies, patients with CS were classified into two groups (CS groups A and B)

whereas XP patients were grouped into 8 groups (XP groups A through G and V). CS and XP cells (with the exception of the variant form, XP-V) have defects in NER. These defects can be specific to TC-NER, GG-NER or both sub-pathways of NER. Therefore, fibroblasts derived from patients with these UV-sensitive syndromes have been instrumental in identifying proteins involved specifically in TC-NER and GG-NER and provided a model system to study the relative contribution of GG-NER and TC-NER to cisplatin response.

All TC-NER-deficient and completely NER-deficient fibroblasts are exquisitely sensitive to apoptosis induced by UV light and cisplatin.[187, 210, 242, 246, 367, 383, 386] A similar relationship was subsequently confirmed in mouse embryonic fibroblasts, murine keratinocytes and mouse skin exposed to UV light[427-429] but intriguingly, TC-NER deficiency does not appear to affect the acute response to UV light in murine embryonic stem cells.[428] Therefore, the effect of targeting TC-NER on the acute response of tumour cells to UV light and cisplatin could not be accurately predicted.

Notably, CS-B fibroblasts have a specific defect in TC-NER but not GG-NER, supported by the observation that CS-B fibroblasts are exquisitely sensitive to cisplatin.[187, 243, 246] Here, we report that consistent with previous work in primary fibroblasts but in contrast to the situation in embryonic stem cells, decreasing CSB levels by RNA interference increased the sensitivity of a variety of tumour cells to UV light and cisplatin. Importantly, cell death under these conditions was largely independent of the p53 tumour suppressor and the DNA mismatch repair (MMR) capacity of the tumour cells. These results suggest that TC-NER plays a role in determining the sensitivity of tumour cells to cisplatin and further suggests that TC-NER represents a potential therapeutic target for cancer therapy.

Materials and Methods

Cell Culture and UV-irradiation

HCT116, DU145 and PC-3 cells were obtained from the American Tissue Type Collection (Camden, NJ). HCT116 was established from a colon adenocarcinoma,[430] DU145 was established from a brain lesion of a patient with metastatic prostate cancer [431] while PC-3 was established from a bony metastasis of a prostate cancer patient.[432] All three of these cell lines are considered MMR deficient due to varying degrees of inefficient repair of specific DNA mismatches in an *in vitro* repair assay.[433] Although mRNA transcripts of all relevant MMR gene products can be detected in each of these three cell lines,[433] neither HCT116 nor DU145 cells express hMLH1 protein,[433-435] DU145 cells also express very low levels of hMSH2 and hPMS2,[433] while PC-3 cells are considered mismatch repair deficient due to low expression of both hMLH1 and hPMS2.[433] The MLH1-corrected HCT116 strain (HCT116+chr3) was described previously.[434] HCT116 and HCT116+chr3 cells were cultured in McCoy's media (Wisent, St. Bruno, QC) while DU145 cells were grown in DMEM (Hyclone, Logan, UT). McCoy's and DMEM used for tumour cell culture was supplemented with 10% fetal bovine serum (Wisent, St. Bruno, QC). GM00739 (CS-B), GM00671 (XP-C), GM05509 (XP-A) human fibroblasts were obtained from National Institute of General Medical Sciences Mutant Cell Repository (Camden, NJ) and maintained in DMEM (Hyclone, Logan, UT) supplemented with 15% fetal bovine serum (Wisent). All cell lines were grown in humidified incubators at 37°C and 5% CO_2. Where indicated, cisplatin (Mayne

Pharma Canada Inc., Montreal, QC) was added to fresh, pre-warmed media at the indicated final concentration.

To UV-irradiate cells, media was removed and cells were irradiated with the indicated dose using a germicidal bulb emitting predominantly at 254 nm at $1J/m^2/s$ as measured with a hand-held UV dosimeter (UVX Radiometer, UVP Inc., Uplands, CA). Fresh, pre-warmed media was replaced and dishes were returned to an incubator for the indicated period of time.

RNA interference

Sub-confluent cells were transfected with the indicated siRNA (Dharmacon, Lafayette, CO) using OptiMEM II and Oligofectamine (Invitrogen, Burlington, ON). The target sequences for CSB, XPA and XAB2 were GTGTGCATGTGTCTTACGA, AGAATTGCGGCGAGCAGTA and TAGCGACTAAACACATCAA, respectively. These RNA duplexes were used at a final concentration of 100, 50 and 50 nM for CSB, XPA and XAB2, respectively. A non-targeting siRNA (TAGCGACTAAACACATCAA) was used as a negative control.

Real-time RT-PCR

Cells were transfected with siRNA and collected at indicated time points. Samples analyzed by RT-PCR had RNA purified using an RNeasy kit (Qiagen, Mississauga, ON) and then reversed transcribed using the First Strand cDNA Synthesis kit (Stratagene, La Jolla, CA). CSB transcript was quantified using a Lightcycler 2.0 PCR instrument (Roche, Mississauga, ON) with primers to CSB (CCAAGGAACAGAGCAATGAC and AAGAGTGAGGAG-

GAAGCGAG) with quantification compared to β-actin (GGGCATGGGTCAGAAGGAT and GTGGCCATCTCTTGCTCGA).

Preparation of nuclear lysates

Crude nuclear lysates were prepared by sucrose centrifugation as follows (modified from http://home.ncifcrf.gov/ccr/flowcore/nuclei.pdf). Cells were rinsed with PBS then trypsinized and collected by centrifugation. Cell pellets were resuspended in nuclear extraction buffer (320mM sucrose, 10mM HEPES, 5mM $MgCl_2$, 1% triton-X-100, pH 7.4), incubated on ice and then collected by centrifugation at 2500xg. The resulting pellets were rinsed twice with nuclear wash buffer (320mM sucrose, 10mM HEPES, 5mM $MgCl_2$, pH 7.4) and collected by centrifugation at 2500xg then resuspended in RIPA buffer (50mM Tris-HCl pH6.8, 150mM NaCl, 1mM EDTA, 1% Triton-X-100, 1% sodium deoxycholate, 0.1% SDS). Pellets were disrupted using a sonicator equipped with a chilled microtip (Thermo Fisher Scientific, Ottawa, ON) and protein quantified using the Bradford assay (Bio-Rad, Mississauga, ON).

Immunoblotting

Two hundred micrograms of nuclear protein per well was subjected to gel electrophoresis using NuPAGE 3-8% gradient polyacrylamide gels (Invitrogen), to visualize CSB protein (predicted at 168 kDa) and Ku86 (86 kDa) whereas MLH1, XAB2, XPA and ß-actin were resolved using NuPAGE 4-12% gradient polyacrylamide gels (Invitrogen). Proteins were transferred to Hybond-C nitrocellulose (GE Healthcare, Baie d'Urfé, QC) and blots

were stained with Ponceau S Red (5 mg/ml Ponceau S Red, 2% glacial acetic acid) to visualize total transferred proteins. Blots were then blocked in PBSMT-A (PBS, 5% nonfat milk powder, 0.05% Tween 20) proteins were detected using antibodies against XPA (FL-273), CSB (E-18) and Ku86 (M-20) (Santa Cruz Biotech, Santa Cruz, CA), against XAB2 (Pab-10266, Orbigen, San Diego, CA), against ß-actin (AC-74, Sigma-Aldrich, Oakville, ON) and against MLH-1 (clone G168-15, BD Biosciences, Mississauga, ON) diluted in PBSMT-B (PBS, 0.5% nonfat milk powder) and were visualized using SuperSignal West Pico Chemillumi-nescent Substrate (Thermo Fisher Scientific) in combination with X-ray film (Kodak, Roch-ester, NY). Multiple proteins were detected using the same blots using Restore Western Blot Stripping Buffer (Thermo Fisher Scientific).

The recovery of RNA synthesis

Sub-confluent cells were transfected with siRNA and subsequently grown in media supplemented with 5μCi/mL of [^{14}C] thymidine (GE Healthcare) to uniformly label DNA. Seventy-two hours later, cells were treated with 10 Jm^{-2} UV-C. One hour before indicated collection time, the media was replaced with fresh media containing 50μCi/mL [^{3}H] uridine (GE Healthcare) to label nascent RNA. Samples were rinsed in PBS containing 0.2% sodium azide (PBS-Z), collected by trypsin in PBS-Z, rinsed with PBS-Z and cell pellets were stored at -80°C. Samples were lysed in 1% SDS and nucleic acids were precipitated in 10% trichloroacetic acid (TCA)/0.1M sodium pyrophosphate and precipitated nucleic acids were collected on glass fiber filters (Thermo Fisher Scientific). Incorporation of [^{3}H] and [^{14}C] was determined using a scintillation counter and [^{3}H] counts were normalized to

[^{14}C] counts to control for cell number. RNA synthesis is expressed as the proportion of [^{3}H] uridine incorporated in UV-treated samples compared to unirradiated controls.

Host cell reactivation

Recombinant adenovirus expressing the *lacZ* gene under control of the murine cytomegalovirus promoter (AdCA35-1, hereafter referred to as AdlacZ, a kind gift from Dr. Frank Graham, McMaster University, Hamilton, ON), was suspended in a minimal volume of PBS and was subsequently irradiated with the indicated dose of UV light on ice, as previously described.[436] Cells were infected with UV- or mock-treated AdlacZ at a multiplicity of infection (MOI) of 20 for primary cells or an MOI of 5 for tumour cells. Forty-eight hours following infection, media was removed and monolayers were incubated with 1 mM chlorophenolred-β-D-galactopyranoside (Fluka Biochemika, Buchs, Switzerland) in 0.01% Triton X-100, 1 mM $MgCl_2$, and 100 mM phosphate buffer (pH 8.3).[437] Absorbance at 570 nm was determined using a Thermo Multiskan Ascent microplate photometer (Thermo Fischer Scientific). β-galatosidase activity from the indicated dose is expressed relative to the activity obtained by infection with un-irradiated virus.

Flow cytometry

Cells were treated with indicated dose of UV light or cisplatin, 72 hours following transfection of the indicated siRNA. Detached and adherent cells were collected 48 hours following treatment, fixed in 70% ethanol for a minimum of 2 hours at -20° C and stained in 30μM propidium iodide (Sigma-Aldrich) in PBS with 40 μg/mL of RNAse A (Sigma-

Aldrich).[391] Samples were analyzed by fluorescence activated cell sorting using a Becton Dickenson LSR II Facstation and CellQuest software (Becton Dickinson, Franklin Lakes, NJ) and data files were analysed using FCS Express (De Novo Software, Los Angeles, CA). Apoptosis was quantified as the proportion of cells with subdiploid DNA content (sample histograms, Appendix 1, Figure 1). Where indicated, Z-VAD-fmk (Bio-Rad) was added to the medium to a final concentration of 10 μM at the time of UV-C irradiation or treatment with cisplatin.

Caspase activity assays

Cells were transfected with the indicated siRNA and treated with either UV light or cisplatin. Twenty four hours following treatment, cells were collected with trypsin, rinsed thoroughly with PBS and cell number was determined using an automated cell counter (Vi-Cell XR, Beckman Coulter, Mississauga, ON). Caspase 3, 8 and 9 activities were determined from 10^6 cells using ApoAlert caspase-3/8 or ApoAlert capase-9/6 Fluorescent Assay Kits as per manufacturer's instructions (Clontech, Mountain View, CA). Fluorescence was measured using a Thermo Fluoroskan Ascent microplate fluorometer (Thermo Fisher Scientific).

Results

RNA interference against CSB in prostate cancer cells inhibits transcription-coupled nucleotide excision repair

Prostate cancer cells, PC-3 and DU145, were transfected with control or two different anti-CSB siRNAs. Cells were collected for RNA and nuclear protein extraction 72 hours later. Using quantitative real-time reverse transcriptase PCR, the relative expression of CSB mRNA was determined. One targeting siRNA (CSB1) reduced mRNA levels by approximately 50%, while the second siRNA (CSB2) was less effective (Figure 1A and C). Immunoblot analysis indicated that the more effective siRNA (CSB1) reduced CSB protein levels by over 75% while the second siRNA was relatively ineffective. Therefore, the CSB1 siRNA was used in subsequent experiments. As described later, siRNAs against other proteins involved in TC-NER were also used to control for potential off target effects of the single effective CSB siRNA.

A single UV-induced dimer in the template strand of an active gene is sufficient to block its expression.[372, 438, 439] This principal forms the conceptual basis of host cell reactivation assays that are commonly used to measure the repair of transcription-blocking DNA lesions.[436, 439, 440] In this assay, exposure of a recombinant adenovirus expressing the lacZ gene to UV light results in decreased β-galactosidase activity, in a dose-dependent manner.[441] The dose required to block β-galactosidase activity is greatly affected by the capacity of the host cell to repair transcription-blocking DNA lesions.[441] Here, DU145 and PC-3 cells exhibited a similar capacity to repair the UV damaged reporter gene (Figure 2A). Transfection of siRNAs directed at CSB led to a significant decrease in host cell reactivation of the UV-damaged reporter gene in both prostate cancer cell lines (Figure 2A). The dose of UV light required to reduce β-galactosidase activity to 50% (D50) was significantly lower in CSB1 siRNA-transfected cells compared to control transfected cells (Figure 2B).

Figure 1. Expression of CSB in PC-3 and DU145 cells.

The expression of CSB was assessed in PC-3 (A and B) and DU145 (C and D) cells in which CSB has been targeted with siRNA. Indicated cells were transfected with control (NT) or CSB siRNA (CSB1 and CSB2) and collected 72 hours later for purification of mRNA and nuclear extracts. RNA was purified, then reversed transcribed and cDNA was amplified using real-time quantitative PCR. CSB transcript abundance was compared to β-actin expression and data shown represents the mean (± SEM) of at least 3 independent experiments and * represents statistical significance compared to NT by student's t-test where $P < 0.05$. For nuclear extracts, two hundred micrograms of nuclear proteins were separated on 3-8% tris-acetate SDS-PAGE gels and immunoblotted with antibodies recognizing CSB (B and D). Immunoblots were stripped and re-probed with an antibody to Ku86 to serve as a loading control. CSB and Ku86 migrated with apparent molecular weights of approximately 170 and 85 kDa, respectively.

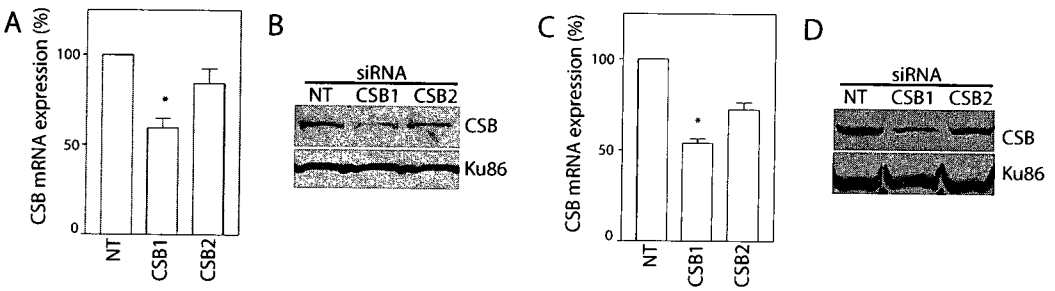
A
CSB mRNA expression (%)
100
50
0
*
NT
CSB1
CSB2
B
siRNA
NT
CSB1
CSB2
CSB
Ku86
C
CSB mRNA expression (%)
100
50
0
*
NT
CSB1
CSB2
D
siRNA
NT
CSB1
CSB2
CSB
Ku86

These results indicate that the ability of these cell lines to repair transcription-blocking DNA lesions was significantly reduced following transfection of CSB siRNAs. The specificity of the CSB knockdown on TC-NER was tested in primary human fibroblasts with known NER defects. Targeting CSB did not affect HCR of the UV-damaged reporter gene in CS-B or XP-A fibroblasts that are unable to perform TC-NER (Figure 2C). In contrast, targeting CSB in TC-NER-proficient XP-C fibroblasts decreased HCR to a level comparable to that observed in completely NER-deficient XP-A fibroblasts (Figure 2C). Therefore, siRNAs against CSB effectively reduced the TC-NER capacity of primary human fibroblasts. Furthermore, our results suggest that PC-3 and DU145 cells are TC-NER-proficient cell lines and that transfection of the siRNA against CSB reduced their ability to perform TC-NER.

Figure 2. Host cell reactivation of a UV-damaged reporter gene.

Host cell reactivation (HCR) of β-galactosidase (β-gal) activity was determined two days following infection with AdlacZ irradiated with the indicated dose of UV light. β-gal activity is expressed relative to unirradiated controls. β-gal activity over a range of UV doses was measured in PC-3 and DU145 cells (A, left and right panels, respectively) transfected with control (closed symbols) or CSB siRNA (open symbols). Data shown is mean (± SEM) from 5-7 individual experiments, each done in 8 replicate wells. In (B) the D50 was calculated from (A) and represents the dose at which 50 percent reduction of β-gal activity occurred, compared to controls. In (C), indicated primary fibroblast cell lines were transfected with non-targeting or CSB siRNA. Host cell reactivation D50 values were assessed as in (B) from at least 3 inde-pendent experiments. * indicates statistical significance of compared to NT control by student's t-test where $P < 0.05$.

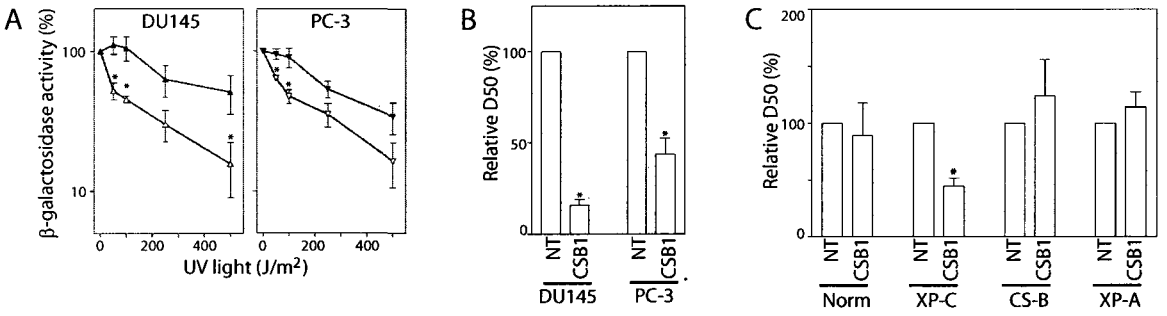
A
DU145
PC-3
β-galactosidase activity (%)
100
10
0
200
400
UV light (J/m2)
B
Relative D50 (%)
100
50
0
NT
CSB1
DU145
PC-3
C
Relative D50 (%)
200
100
0
Norm
XP-C
CS-B
XP-A

RNA interference against CSB sensitizes prostate cancer cells to cisplatin

As discussed already, TC-NER-deficient fibroblasts and keratinocytes are very sensitive to UV- and cisplatin-induced apoptosis whereas TC-NER-deficient murine embryonic stem cells are not.[187, 210, 242, 246, 367, 383, 386, 427-429] Therefore, it was unclear whether targeting CSB in cancer cell lines would increase their sensitivity to cisplatin-induced apoptosis. To address this issue, CSB was again targeted by RNAi in PC-3 and DU145 cells and the sensitivity of targeted cells to cisplatin-induced apoptosis was assessed as the proportion of cells with sub-diploid DNA content. Targeting CSB in this way led to a large increase in the sensitivity of DU145 cells and to a smaller increase in the sensitivity of PC-3 cells (Figure 3). Tumour cells frequently express mutant forms of DNA response proteins that may influence their sensitivity to therapeutic agents like cisplatin. For example, DU145 cells carry point mutations in both alleles of p53 and do not express MLH1.[433, 435] Similarly, PC-3 cells do not express detectable p53 and they exhibit a defect in MMR.[433, 435] Loss of p53 and MMR have been associated with resistance to cisplatin,[329-331, 442-444] therefore the sensitization of these cells lines suggests that targeting CSB may have therapeutic applications.

Figure 3. The effect of RNAi against CSB on the sensitivity of DU145 and PC-3 cells to cis-platin-induced apoptosis.

Indicated cell lines were transfected for 72h with control (NT- closed symbols) or CSB targeting (open symbols) siRNA. Apoptosis was assessed as the proportion of cells with sub-diploid DNA content 48 hours following exposure to the indicated dose of cisplatin. All data points are mean (± SEM) from at least 3 individual experiments and * indicates statistical significance compared to NT control by student's t-test where $P < 0.05$.

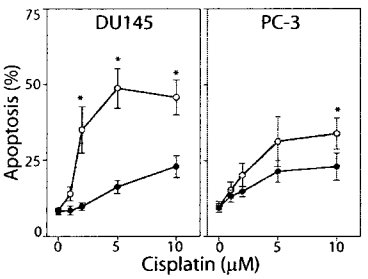
DU145
PC-3
Apoptosis (%)
75
50
25
0
0
5
10
0
5
10
Cisplatin (μM)
*
*
*
*

Targeting CSB in HCT116 colon cancer cells

Given the effect of targeting CSB in p53 and MMR-deficient prostate cancer cell lines, we decided to use an isogenic series of cell lines derived from HCT116 colorectal cancer cells to better test the impact of p53- and MMR-deficiency under conditions in which CSB is targeted by RNAi. HCT116 cells express wildtype p53 but do not express MLH1 and are considered MMR-defective.[434] Again, the anti-CSB siRNA was highly effective at reducing CSB levels in HCT116 cells (Figure 4A) and led to a decrease in HCR of the UV-damaged reporter gene (Figure 4B). As a second measure of TC-NER, we assessed the ability of cells to recover nascent RNA synthesis (RRS) following UV exposure. Exposure of HCT116 cells to 10 J/m^2 of UV light reduced the incorporation of [^{3}H] uridine by 40 to 50 % immediately following UV exposure (Figure 4C). Whereas mock and control siRNA transfected cells recovered nascent RNA synthesis within 8 hours, CSB siRNA-transfected did not recover RNA synthesis within 24 hours (Figure 4C). Consistent with the results in prostate cancer cell lines, targeting CSB in HCT116 cells increased their sensitivity to cisplatin-induced apoptosis (Figure 4D) and this was associated with increased activity of caspases 3, 8 and 9 (Figure 4E-G). So despite the absence of MLH1 in these cells, RNAi against CSB greatly increased the sensitivity of these cells to cisplatin and UV-induced apoptosis. Taken together, HCT116 cells are TC-NER proficient and RNAi against CSB reduced the capacity of these cells to perform this repair.

Similar experiments were performed in MLH1-corrected HCT116 cells (HCT116+chr3) (Figure 5A and B). No significant difference in TC-NER capacity as assessed by host cell reactivation or the recovery of nascent RNA synthesis was detected in these

Figure 4. Measuring the effects of RNAi against CSB in HCT116 cells.

RNAi of CSB was measured by protein expression (A) and HCR of β-gal activity (B) as described in Figure 1. Synthesis of nascent RNA synthesis was assessed between 0 and 24 hours following exposure to 10 Jm^{-2} of UV light. RNA synthesis is expressed relative to unirradiated control samples collected simultaneously where each point represents the mean (± SEM) determined from a minimum of 3 independent experiments (C). (D) Apoptosis was assessed by measuring sub-diploid proportion of cells as in Figure 3. Abundances of capases 3, 8 and 9 (E, F, G, respectively) were measured 24h after treatment with indicated doses of cisplatin in cells that had been transfected 96h previously with siRNA, as indicated. All data points are mean (± SEM) from at least 3 individual experiments and * indicates statistical significance compared to NT control by student's t-test where $P < 0.05$.

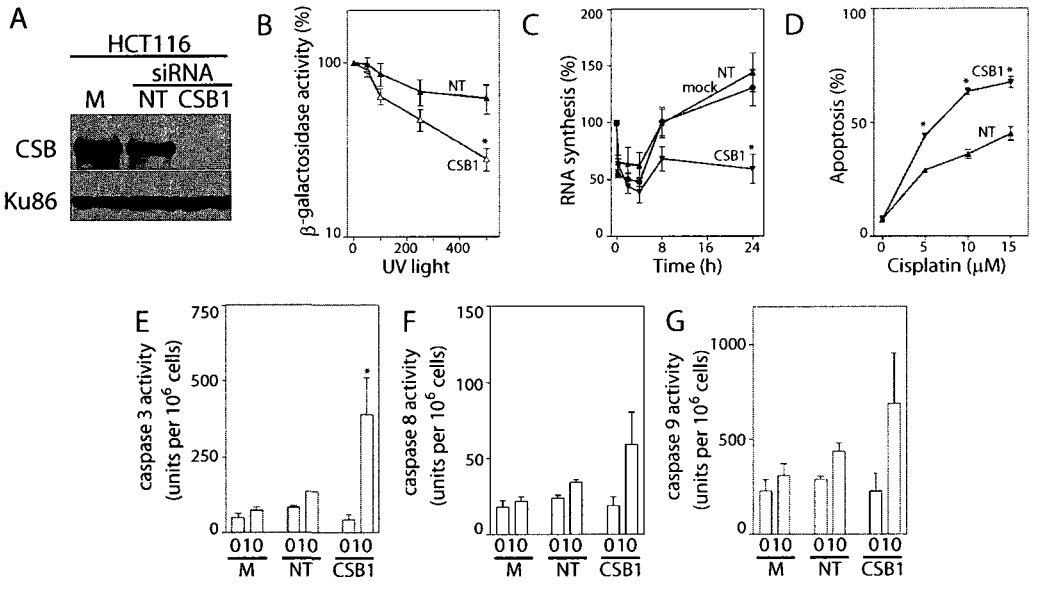
A
HCT116
siRNA
M
NT CSB1
CSB
Ku86
B
β-galactosidase activity (%)
100
10
NT
CSB1
*
0
200
400
UV light
C
RNA synthesis (%)
200
150
100
50
0
NT
mock
CSB1
*
0
8
16
24
Time (h)
D
Apoptosis (%)
100
50
0
CSB1
*
NT
0
5
10
15
Cisplatin (μM)
E
caspase 3 activity (units per 10^6 cells)
750
500
250
0
*
010
M
010
NT
010
CSB1
F
caspase 8 activity (units per 10^6 cells)
150
100
50
0
010
M
010
NT
010
CSB1
G
caspase 9 activity (units per 10^6 cells)
1000
500
0
010
M
010
NT
010
CSB1

Figure 5. Measuring the effects of RNAi against CSB in HCT116+chr3 cells.

HCT116+chr3 cells were either mock-transfected or transfected with the indicated siRNA, 72 hours before collection for immunoblotting (A and B) or measurements of HCR of β-gal activity (C), recovery of nascent RNA synthesis (D), sub-G1 apoptosis (E) and abundance of caspases 3, 8 and 9 (F, G, H), all as previously described (Figure 4). For immunoblots, levels of hMLH1 protein were measured in HCT116 and HCT116+chr3 using an antibody to human MLH1. † represents a non-specific band that appears in all samples, regardless of MLH1 status. All data points are mean (± SEM) from at least 3 individual experiments and * indicates statistical significance compared to NT control by student's t-test where $P < 0.05$.

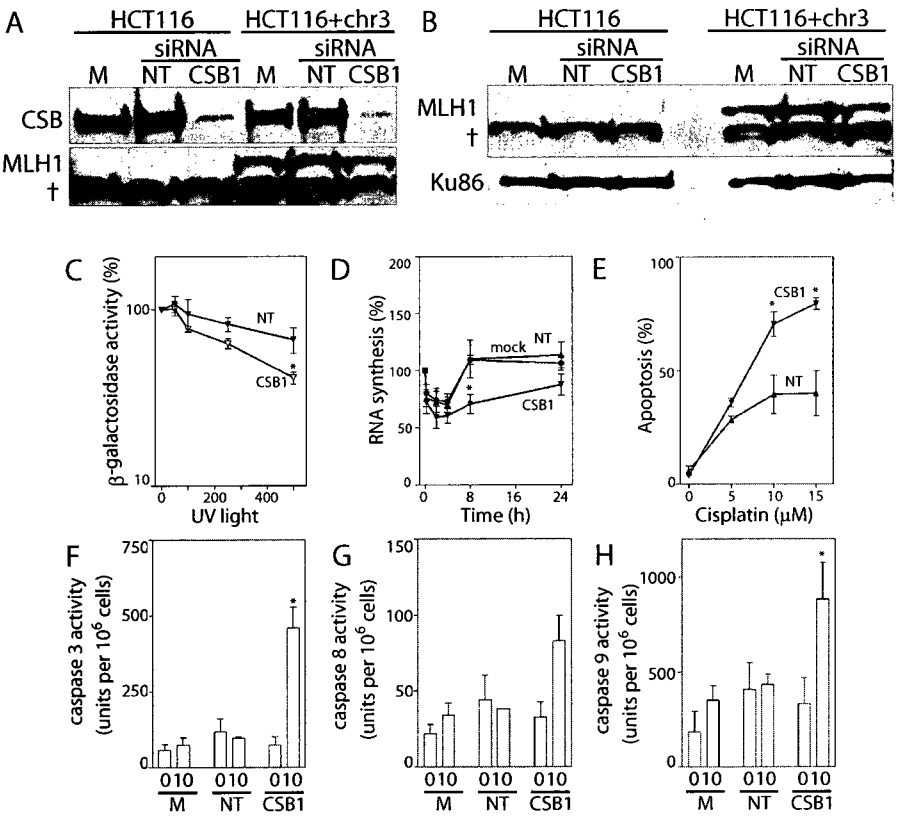
A
HCT116
HCT116+chr3
siRNA
M
NT
CSB1
CSB
MLH1
†
B
Ku86
C
β-galactosidase activity (%)
UV light
D
RNA synthesis (%)
mock
Time (h)
E
Apoptosis (%)
Cisplatin (μM)
F
caspase 3 activity (units per 10^6 cells)
G
caspase 8 activity (units per 10^6 cells)
H
caspase 9 activity (units per 10^6 cells)
010

cells compared to the parental strain (Figures 5C and D). Again, targeting CSB by RNAi in HCT116+chr3 cells inhibited TC-NER (Figures 5C and D) and increased their sensitivity to cisplatin- and UV-induced apoptosis (Figures 5C-H and Supplementary Figure 1B). Therefore, MLH1 expression had no effect on the response of HCT116 cells to UV light or cisplatin under the present conditions and targeting CSB by RNAi was similarly effective at increasing the sensitivity of this cell line to cisplatin-induced apoptosis. The apoptotic response was confirmed in parental cells by showing that the sub-diploid fraction of cells could be decreased by treating cells with a pan-specific caspase inhibitor (Supplementary Figure 2).

CSB was also targeted by RNAi in HCT116 cells in which p53 was disrupted by homologous recombination (HCT116p53-/-) (Figure 6A). These p53 null cells appeared to be reduced in their capacity to repair the UV damaged reporter gene compared to parental cells so host cell reactivation of the UV-damaged reporter gene could not be further reduced by siRNA against CSB (Figure 6B). Nonetheless, these cells recovered nascent RNA synthesis within 8 hours following UV exposure (Figure 6C). Decreased expression of CSB prevented the recovery of nascent RNA synthesis even 24 hours following UV exposure in these p53-/- cells (Figure 6C). Despite these differences in the repair of episomal and genomic DNA, the present results suggest that these HCT116p53-/- can perform TC-NER and that RNAi against CSB again abrogated this repair process. Importantly, decreased expression of CSB was associated with increased sensitivity of cells to cisplatin- and UV-induced apoptosis (Figure 6D and Supplementary figure 1C) that was again associated with activation of caspases 3, 8 and 9 (Figures 6E-G). Overall, there was little difference

Supplementary Figure 1. UV-C induced apoptosis in HCT116 parental and derivative cell lines.

HCT116 parental (A), HCT116+chr3 (B) and HCT116p53-/- (C) were either mock-transfected or transfected with the indicated siRNA, 72 hours before exposure to indicated doses of UV-C. Cells were returned to incubator for a 48h recovery period and then apoptosis as measured by sub-diploid DNA content was determined. All data points are mean (± SEM) from at least 3 individual experiments.

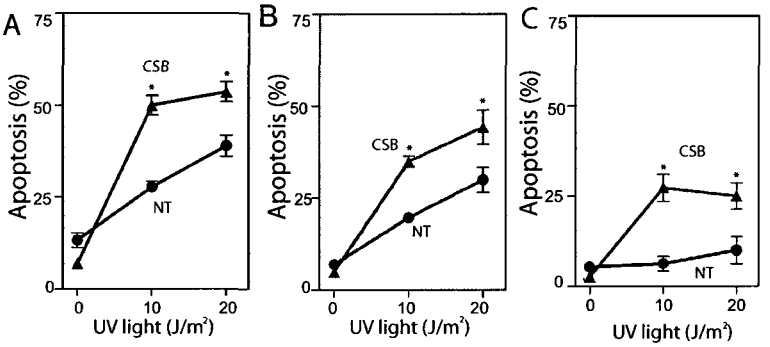
A
B
C
75
50
25
0
Apoptosis (%)
CSB
NT
*
0
10
20
UV light (J/m²)

Supplementary Figure 2. Assessment of apoptosis in the presence of a pan-specific caspase inhibitor in HCT116 cells.

Cells, as indicated, were either mock-transfected or transfected with the indicated siRNA, 72 hours before exposure to indicated doses of cisplatin or UV-C. Apoptosis was assessed as the proportion of cells with sub-diploid DNA content 48 hours following DNA damage treatment. Z-VAD-fmk was added upon exposure to 0 or 10 Jm^{-2} UV-C (A) or addition of 0 or 10 μM cisplatin (B). Each value in represents the mean (± SEM) from a minimum of 3 independent experiments. * represents statistical significance between Z-VAD-fmk treatments while † represents statistical significance between NT and CSB values.

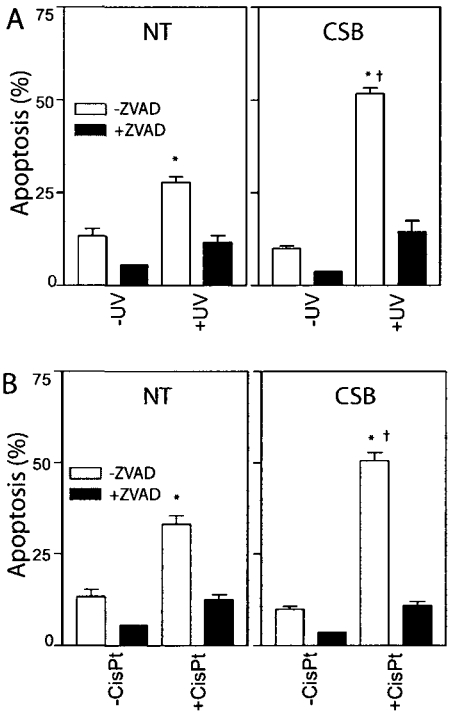
A
75
50
25
0
Apoptosis (%)
NT
CSB
-ZVAD
+ZVAD
*
* †
-UV
+UV
-UV
+UV
B
75
50
25
0
Apoptosis (%)
NT
CSB
-ZVAD
+ZVAD
*
* †
-CisPt
+CisPt
-CisPt
+CisPt

between the apoptotic response of any of the three HCT116 derived cell lines to DNA damage after targeting CSB by RNAi, except that the p53-deficient cells exhibited slightly lower rates of apoptosis after all treatments. This is likely due to the well described pro-apoptotic activity of p53. However, the present work suggests that p53 is not absolutely required to sensitize tumour cells to cisplatin by targeting TC-NER.

RNA interference against XPA and XAB2 sensitizes cancer cells to UV light and cisplatin

The CS proteins have been known to participate in TC-NER for many years,[445] however, the CSB protein may play an additional role in regulating transcription more directly.[234, 446, 447] Therefore, we decided to target two other proteins required for TC-NER. First, XPA is a DNA damage binding protein required for both TC-NER and GG-NER to which no additional functions have been ascribed.[373] XPA protein levels were reduced by RNA in HCT116 cells and the sensitivity of the targeted cells to UV- and cisplatin-induced apoptosis was assessed (Figures 7A and B). Decreased expression of XPA was associated with an increase in the sensitivity of HCT116 cells to UV- and cisplatin-induced apoptosis (Figure 7B). Similar results were obtained in HCT116p53-/- cells (Appendix 1, Figure 3).

Second, the XPA-binding protein 2 (XAB2) is involved in TC-NER and perhaps pre-mRNA splicing.[214, 217-219] RNAi against XAB2 efficiently reduced protein levels in HCT116 cells (Figure 8A). RNAi against XAB2 led to an increase in apoptosis in HCT116 cells in the absence of DNA damage (Figure 8B). The targeted cells exhibited an increase in their sensitivity to cisplatin- and UV-induced apoptosis but this was complicated by the cytotoxic effect of the siRNA alone. Strikingly, RNAi against XAB2 did not induce apoptosis in

HCT116p53-/- alone yet effectively increased the sensitivity of these p53 null cells to cis-platin- and UV-induced apoptosis (Figure 8C). These results suggest that targeting XAB2 induced p53-dependent apoptosis alone and sensitized cells to cisplatin. Taken together, our results indicate that the MMR-defective HCT116, PC-3 and DU145 cells and p53 null HCT116 cells appear to have a functional TC-NER pathway that can be abrogated using siRNAs targeting CSB, XPA and XAB2.

Figure 6. Measuring the effects of RNAi against CSB in HCT116p53-/- cells.

Experiments described in Figure 4 are repeated here using the p53 null HCT116p53-/- cells.

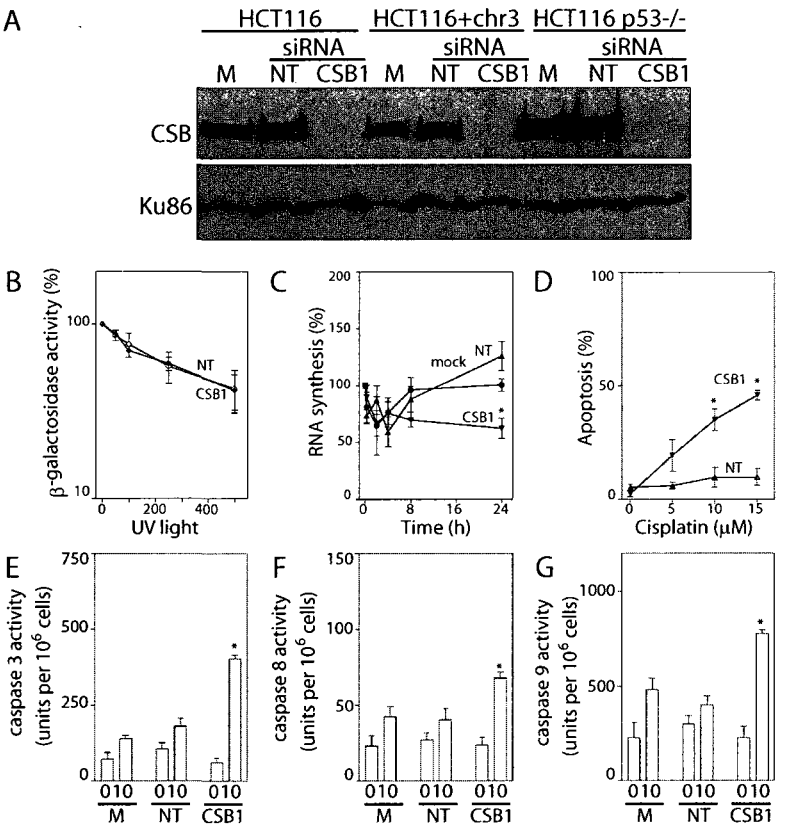
A
HCT116
HCT116+chr3
HCT116 p53-/-
siRNA
M NT CSB1 M NT CSB1 M NT CSB1
CSB
Ku86
B
β-galactosidase activity (%)
100
10
0 200 400
UV light
NT
CSB1
C
RNA synthesis (%)
200
150
100
50
0
0 8 16 24
Time (h)
mock
NT
CSB1
D
Apoptosis (%)
100
50
0
0 5 10 15
Cisplatin (μM)
CSB1
NT
E
caspase 3 activity (units per 10^6 cells)
750
500
250
0
010 010 010
M NT CSB1
F
caspase 8 activity (units per 10^6 cells)
150
100
50
0
010 010 010
M NT CSB1
G
caspase 9 activity (units per 10^6 cells)
1000
500
0
010 010 010
M NT CSB1

Figure 7. Targeting XPA sensitizes colon cancer cells to DNA damage.

HCT116 cells were either mock-transfected or transfected with the indicated siRNA at 50nM, 48 hours before collection for immunoblotting (A) or treatment with UV-C or cis-platin for measurement of sub-G1 apoptosis (B). XPA migrates with an apparent molecular weight of approximately 38 kDa. All data points are mean (± SEM) from at least 3 individual experiments. * represents statistical significance as measured by student's t-test where $P < 0.05$.

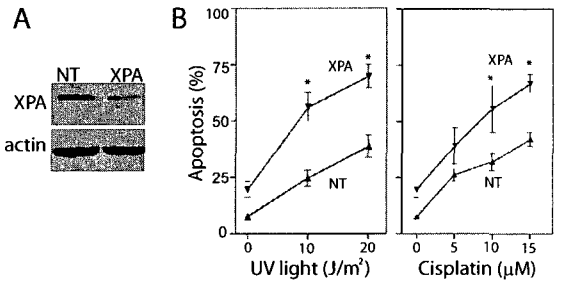
A
NT
XPA
XPA
actin
B
Apoptosis (%)
100
75
50
25
0
XPA
NT
0
10
20
UV light (J/m²)
0
5
10
15
Cisplatin (μM)

Figure 8. Targeting XAB2 sensitizes colon cancer cells to DNA damage.

HCT116 cells were either mock-transfected or transfected with the indicated siRNA at 50nM, 48 hours before collection for immunoblotting (A) or treatment with UV-C or cis-platin for measurement of sub-G1 apoptosis (B and C). HCT116 parental cells were used in (B) while HCT116p53-/- cells were used in (C). XAB2 migrates with an apparent molecular weight of approximately 98 kDa. All data points are mean (± SEM) from at least 3 individual experiments.

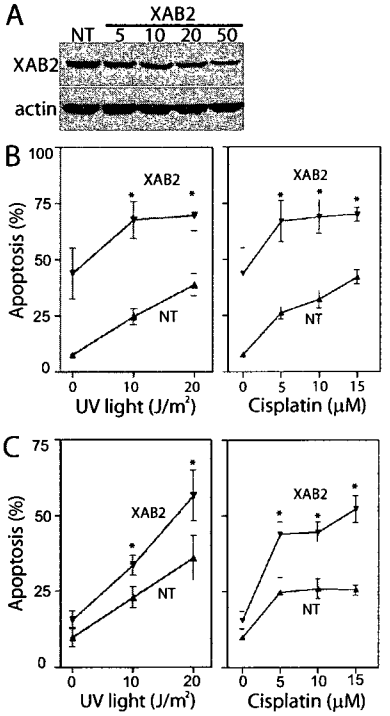
A
XAB2
NT 5 10 20 50
XAB2
actin
B
XAB2
NT
Apoptosis (%)
UV light (J/m²)
Cisplatin (μM)
C
XAB2
NT
Apoptosis (%)
UV light (J/m²)
Cisplatin (μM)

Discussion

Link between nucleotide excision repair and sensitivity to cisplatin

Cells with defects in NER are sensitive to cisplatin. For example, Cockayne syndrome fibroblasts have a specific defect in TC-NER and are more sensitive to cisplation-induced apoptosis than GG-NER deficient XP-C fibroblasts.[187, 188, 243, 246] A similar relationship exists for UV light in primary human fibroblasts, mouse embryonic fibroblasts, murine keratinocytes but not murine embryonic stem cells.[187, 210, 242, 246, 367, 383, 386, 427-429] Therefore, it was unclear whether TC-NER deficiency would affect the response of tumour cells to these agents.

The CSB protein is required for a rate limiting step of TC-NER.[83, 214, 448] Therefore, we targeted this protein in a variety of tumour cell lines and found that disruption of TC-NER increased the sensitivity of tumour cells to this important chemotherapeutic agent. Similarly, targeting downstream proteins in the same repair pathway (XPA and XAB2) increased the responsiveness of these tumours to cisplatin-induced apoptosis. There are several important interpretations of these results. First, the tumour cells tested must have been TC-NER proficient. Second, targeting TC-NER was an effective means of increasing the responsiveness of tumour cells to this drug.

Role of MMR protein in TC-NER

As indicated above, our data clearly indicate that the tumour cell lines tested were TC-NER proficient because disruption of this DNA repair pathway similarly resulted in decreased repair and enhanced the sensitivity of all cell lines to UV- and cisplatin-induced

apoptosis. As described already, HCT116, HCT116p53-/-, DU145 and PC-3 cells are all MMR-deficient. The MMR system is critical for the recognition and repair of post-replicative errors including DNA base mismatches[442] however, these proteins have been reported to play a role in TC-NER.[449]

In this previous paper,[449] TC-NER was measured using a Southern blot method that detects the removal of T4 endonuclease V sensitive sites (cyclobutane pyrimidine dimers (CPD)) from the transcribed strand of the DHFR gene.[449] Mellon and co-workers found that MMR-deficient tumour cells, including HCT116 cells, were TC-NER-deficient and that the hMLH1-corrected sub-line (HCT116+chr3) were repair proficient.[449] These cells were therefore considered to be more resistant to UV light compared to parental lines.[449] The initial findings of Mellon and co-workers[449] have not been reproduced in studies using the same DNA repair assay[450, 451] or a ligation-mediated PCR based repair assay that similarly measures DNA repair at T4-endonuclease sensitive sites.[452] Similarly, mouse embryonic fibroblasts derived from MSH2-knockout mice displayed no difference in their ability to remove CPD from the transcribed region of active genes compared to wild type cells.[451] The reason for the disparity among studies remains unclear, however, MMR-deficient cells exhibit microsatellite instability[434, 453, 454] and secondary mutations in both DNA repair genes and other DNA damage response genes have been reported[298, 455] so alterations in DNA repair phenotype may reflect additional mutations in the cell lines used. In the present work, transient transfection of siRNAs against CSB, XPA and XAB2 eliminates the risk of secondary mutation contributing to differences in TC-NER capacity. Our data clearly indicate that all tested tumour cell lines were capable of repairing UV- and cis-

platin-induced DNA lesions by TC-NER and this is unaffected by hMLH1 and hMSH2 deficiency.

Role of p53 in TC-NER

The tumour cells examined here included PC-3 cells that are considered effectively p53 null, DU145 that carry inactivating mutations in both alleles of p53 and HCT116p53-/- that are nullizygous for p53. By contrast, the HCT116 and the chromosome 3 complemented derivative cell lines express functional p53. RNAi against CSB reduced HCR of the UV-damaged reporter gene in DU145 and PC-3 and the recovery of nascent RNA synthesis DU145 in DU145 (Supplementary Figure 3) indicating that these p53-deficient cells were able to perform TC-NER. In partial contrast, HCT116p53-/- cells exhibited a reduced capacity to support the repair of the UV-damaged reporter and RNAi against CSB did not result in a further decrease in HCR. Nonetheless, RNAi against CSB decreased the ability of these p53 nullizygous cells to recover RNA synthesis and increased their sensitivity to UV- and cisplatin-induced apoptosis. The present data suggest that TC-NER is intact in these p53-deficient cell lines even though there may be some subtle differences in the repair of transcription-blocking DNA lesions that were only apparent in HCR experiments.

Supplementary Figure 3. Recovery of RNA synthesis after UV-C in DU145 cells.

DU145 cells were either mock-transfected or transfected with the indicated siRNA, 72 hours before exposure to 10 Jm^{-2} UV-C. RRS was measured as previously described. Each value in represents the mean (± SEM) from a minimum of 3 independent experiments. * represents statistical significance by student's t-test where $P < 0.05$.

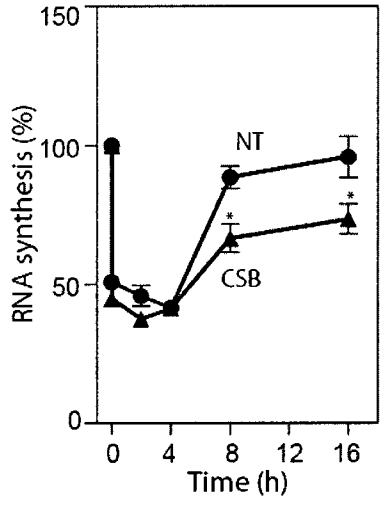
150
100
50
0
RNA synthesis (%)
NT
CSB
*
*
0
4
8
12
16
Time (h)

MMR proteins and p53 in cisplatin resistance

A major drawback of the platinum family of chemotherapeutics is the recurrence of resistant disease.[275, 276, 285, 313, 316, 317, 319, 326, 456] This can in some cases be attributed to increased DNA repair response[285, 313, 327, 337, 342, 344, 456, 457] but may also result from decreased death signalling in response to this form of DNA damage. Two key genetic changes that have been associated with resistance to cisplatin are: p53- and MMR-deficiency.[329, 330, 442-444, 456, 458-460] Despite the association of p53 and MMR defects with cisplatin resistance, RNAi against CSB, XPA and XAB2 in our panel of tumour cell lines deficient in p53 (PC-3, DU145 and HCT116p53-/-) and MMR (PC-3, DU145, HCT116 and HCT116p53-/-) resulted in defects in TC-NER and hypersensitivity to cisplatin. The present results indicate that targeting TC-NER sensitizes tumour cells to cisplatin independent of p53 and MMR.

In summary, we found that both p53 and MMR-deficient colorectal and prostate cancer cells retain the ability to perform TC-NER and targeting TC-NER in these cells increases their sensitivity to UV light and cisplatin. These results have important implications for platinum-based therapies, where the therapeutic DNA lesion is recognized by NER. CSB may represent a rational target to augment cisplatin responsiveness of tumours, independent of MMR or p53 capacity. Our work, coupled with recent clinical evidence that ERCC1 levels predict response to platinum based therapies in non-small cells lung cancer,[294, 319, 368, 461] small cell lung cancer,[462] esophageal cancer,[463] head and neck cancer,[464] bladder cancer[465] and testicular cancer,[287] supports the concept that TC-NER capacity may be a predictor of therapeutic response in diverse tumours. Further, these

data support the concept that targeting TC-NER as a therapeutic option is a promising approach for cancer therapy.

Acknowledgements

This work was initially supported with an IDEA grant from the Prostate Cancer Research Initiative and later from the National Cancer Institute of Canada with funds from the Terry Fox Run. L.J.S. was supported by an Ontario Premier's Research Excellence Award to B.C.M. with support from the Ottawa Regional Cancer Foundation and an Ontario Graduate Scholarship in Science and Technology. J.M.S. was supported with an Ontario Graduate Scholarship and subsequently an Ontario Graduate Scholarship in Science and Technology. B.C.M. is a Research Scientist of the National Cancer Institute of Canada supported with funds provided by the Canadian Cancer Society.

4.0 Targeting TC-NER Sensitizes Human Tumour Cells in an *In Vivo* Xenograft Model

In the previous chapter we targeted three key proteins in the TC-NER pathway and sensitized tumour cells to cisplatin and UV-induced DNA damage, in cell culture. The following chapter describes our preliminary efforts to test the therapeutic potential of targeting TC-NER *in vivo*. The chapter has been written as a short report.

I am grateful for the assistance of Jeffrey Hamill, Jennifer Smith, Brian Melanson and Christine MacKinnon-Roy in the measurement of xenograft tumours in the experiments described herein. Reetesh Bose contributed data for Figures 2D-E.

RNAi of CSB *in vivo* and delivery by an adenovirus vector in culture sensitizes human colon cancer cells to cisplatin.

Stubbert LJ, Cancer Therapeutics Program, Ottawa Health Research Institute and the Department of Cellular and Molecular Medicine, University of Ottawa, Ottawa, K1H 8L6, Canada

Reetesh Bose, Cancer Therapeutics Program, Ottawa Health Research Institute

McKay BC, Cancer Therapeutics Program, Ottawa Health Research Institute, and the Departments of Radiology and Cellular and Molecular Medicine, University of Ottawa, Ottawa, K1H 8L6, Canada

Corresponding author:

Bruce C. McKay
Cancer Therapeutics Program
Ottawa Hospital Research Institute
501 Smyth Rd, Box 926
Ottawa, ON K1H 8L6
Canada
Phone: 613-737-7700 x70338
Fax: 613-247-3524
bmckay@ohri.ca

Keywords: apoptosis, CSB, cisplatin, xenograft, adenovirus and transcription-coupled nucleotide excision repair
Running title: CSB, TC-NER and apoptosis

Abstract

We have previously shown that targeting the Cockayne syndrome B (CSB) protein using siRNA is effective at impairing the transcription-coupled nucleotide excision repair (TC-NER) pathway in a variety of tumour cell lines. RNAi against CSB greatly increased the sensitivity to UV light and cisplatin-induced apoptosis. In order to test the effect of inhibiting TC-NER on tumour response in vivo, we generated shRNA expressing retrovirus constructs that permitted stable knockdown of CSB. Using this viral construct, we were able to generate stable TC-NER deficient tumour cells. These CSB targeted cells remained tumourigenic in nude mice. Exposure of CSB-targeted tumours to cisplatin significantly delayed tumour growth. These results suggest that CSB and potentially other TC-NER proteins may represent targets for combined cancer therapy.

Abstract Word Count: 121
Manuscript Word Count: 3743

Introduction

Platinum-based chemotherapeutics are important in the treatment of human cancer and have seen some success in the treatment of gastrointestinal and reproductive tumours.[275, 313] Curiously, in some germ-cell testicular cancer, cisplatin is almost always successful in treatment with little recurrence of disease. [466-468] It has since been suggested that this may be due to inherent low levels of nucleotide excision repair (NER) proteins[287] a pathway also known to correct cisplatin lesions.[304, 360] Conversely, recurrent cisplatin resistant tumours can also have increased NER.[284, 326, 327, 337, 456] Together, NER capacity appears to be an important determinant of cisplatin response.

NER can be subdivided into both global-genomic (GG-) NER and transcription-coupled (TC-) NER, that differ only in their DNA lesion recognition step.[75, 85] We have shown previously that human fibroblast cells, deficient in TC-NER are exquisitely sensitive to cisplatin and that this was independent of p53.[187] Similarly, transient transfection of siRNAs targeting a series of proteins required for TC-NER (CSB, XAB2 and XPA) sensitized a variety of colon and prostate cancer cell lines. Importantly, this was largely independent of DNA mismatch repair and p53, that when genetically altered have been associated with cisplatin resistance.[223, 329, 331, 338, 341, 443, 469, 470] Here we constructed a retroviral CSB shRNA expression construct that was effective at reducing CSB protein, inhibiting TC-NER and sensitizing tumour cells to cisplatin. Cells stably expressing shRNA targeting CSBs formed subcutaneous tumours in CD-1 nude mice. Inhibition of CSB expression resulted in a significant delay in tumour growth in mice treated with cisplatin.

Materials and Methods

Cell Culture and UV-irradiation

HCT116 cells were obtained from the American Tissue Type Collection (Camden, NJ) and the RetroPack™ PT67 cell line was purchased from Clontech (Mountainview, CA). HCT116 were established from a colon adenocarcinoma[430] while PT67 are an NIH 3T3-derived cell line containing the Moloney murine leukemia virus *gag, pol* and *env* genes (Clontech). Parental HCT116 and cells derived from this cell line were cultured in McCoy's media (Wisent, St. Bruno, QC). McCoy's media was supplemented with 10% fetal bovine serum (Wisent, St. Bruno, QC). All cell lines were grown in humidified incubators at 37°C and 5% CO_2. Where indicated, cisplatin (Mayne Pharma Canada Inc., Montreal, QC) was added to fresh, pre-warmed media at the indicated final concentration.

To UV-irradiate cells, media was removed and cells were irradiated with the indicated dose using a germicidal bulb emitting predominantly at 254 nm at $1J/m^2/s$ as measured with a hand-held UV dosimeter (UVX Radiometer, UVP Inc., Uplands, CA). Fresh, pre-warmed media was replaced and dishes were returned to an incubator for the indicated period of time.

Construction of retrovirus vectors and shRNA expressing cell lines

The pLXSN retroviral vector (Clontech, Mountain View, CA) was modified for use as a retroviral delivery for shRNA according to Hao *et al.* (2005).[471] Briefly pLXSN was double digested with XbaI and NheI (New England Biolabs, Pickering, ON) and resulting large fragments re-ligated to form pXSN.[471] Based on our CSB targeting sequence used previ-

ously[223] and the validated green fluorescence protein (GFP) targeting sequence (Dharmacon), we inserted synthetic DNA oligonucleotides with appropriate linkers, into the pSUPER plasmid, a kind gift from Dr. Thomas Tuschl (Rockefeller University). The following oligos were annealed and ligated into pSUPER under control of the H1 RNA polymerase III promoter between the restriction sites BglII and HindIII:

CSB1+

GATCCCCGTGTGCATGTGTCTTACGATTCAAGAGATCGTAAGACACATGCACACTTTTTGGAAA,

CSB1-

AGCTTTTCCAAAAAGTGTGCATGTGTCTTACGATCTCTTGAATCGTAAGACACATGCACACGGG;

GFP+

GATCCCCGGCTACGTCCAGGAGCGCACCTTCAAGAGAGGTGCGCTCCTGGACGTAGCCTTTTTGG

AAA,

GFP-

AGCTTTTCCAAAAAGGCTACGTCCAGGAGCGCACCTCTCTTGAAGGTGCGCTCCTGGACGTAGCC

GGG. Subsequently, the H1-shRNA expression cassette from pSUPER-CSB1 was removed at BamHI and XhoI and ligated into pXSN, creating the new vector pXSN-H1-shRNA. The shRNA sequences were validated by DNA sequencing.

PT67 cells were then transfected with pXSN-H1-shRNA constructs and placed under G418 (Sigma-Aldrich, Oakville, ON) selection as per manufacturer's instructions[472]. Individual cell colonies were amplified and characterized by protein immunoblotting to assess the effectiveness of the integrated shRNA (Figure 1). The clones selected for future use were designated HCT116-shCSB1 and HCT116-shGFP.

Construction of adenovirus vectors and infections with AdshRNA viruses

The adenoviruses expressing shRNA were generated by standard methods using the AdMax vector system (Microbix, Toronto, ON). The BglII-HindIII fragment of pSUPER-shRNA was cloned into the promoter-less pDC311 adenoviral shuttle vector. The pDC311-H1-shRNA plasmid was co-transfected into 293 cells along with pBHGCreloxdelta1,3. The resulting virus (AdshRNA) was plaque purified, expanded and the integrity of the H1-shRNA cDNA was confirmed by DNA sequencing. To infect cells, media was removed and virus was adsorbed for thirty minutes in one millilitre of serum-free media, with regular gentle rocking in a humidified incubator at 37°C and 5% CO_2. Infection of HCT116 cells with AdshCSB1 led to the knockdown of the CSB protein (Figure 3).

Preparation of nuclear lysates

Crude nuclear lysates were prepared by sucrose centrifugation as follows (modified from http://home.ncifcrf.gov/ccr/flowcore/nuclei.pdf). Cells were rinsed with PBS then trypsinized and collected by centrifugation. Cell pellets were resuspended in nuclear extraction buffer (320mM sucrose, 10mM HEPES, 5mM $MgCl_2$, 1% triton-X-100, pH 7.4), incubated on ice and then collected by centrifugation at 2500xg. The resulting pellets were rinsed twice with nuclear wash buffer (320mM sucrose, 10mM HEPES, 5mM $MgCl_2$, pH 7.4) and collected by centrifugation at 2500xg then resuspended in RIPA buffer (50mM Tris-HCl pH6.8, 150mM NaCl, 1mM EDTA, 1% Triton-X-100, 1% sodium deoxycholate, 0.1% SDS). Pellets were disrupted using a sonicator equipped with a chilled microtip (Thermo

Fisher Scientific, Ottawa, ON) and protein quantified using the Bradford assay (Bio-Rad, Mississauga, ON).

Immunoblotting

Nuclear extracts were resuspended in RIPA buffer after being purified as indicated. Samples were sonicated for 10 s using a microtip (Branson Sonifier, VWR International Ltd., Mississauga, ON) and protein concentrations determined using the BioRad Protein Assay (BioRad, Mississauga, ON). Two hundred micrograms of nuclear protein per well was subjected to gel electrophoresis using NuPAGE 3-8% gradient polyacrlyamide gels (Invitrogen) to visualize CSB protein (predicted at 168 kDa) or Ku86 (86 kDa). Proteins were transferred to Hybond-C nitrocellulose (GE Healthcare, Baie d'Urfé, QC) and blots were stained with Ponceau S Red (5 mg/ml Ponceau S Red, 2% glacial acetic acid) to visualize total transferred proteins. Blots were then blocked in PBSMT-A (PBS, 5% nonfat milk powder, 0.05% Tween 20) proteins were detected using antibodies against CSB (E-18) and Ku86 (M-20) (Santa Cruz Biotech, Santa Cruz, CA) diluted in PBSMT-B (PBS, 0.5% non-fat milk powder) and were visualized using SuperSignal West Pico Chemilluminescent Substrate (Thermo Fisher Scientific) in combination with X-ray film (Kodak, Rochester, NY). Multiple proteins were detected using the same blots using Restore Western Blot Stripping Buffer (Thermo Fisher Scientific).

The recovery of RNA synthesis

Sub-confluent cells were grown in media supplemented with 5μCi/mL of [^{14}C] thymidine (GE Healthcare) to uniformly label DNA. As indicated some HCT116 cells were infected at an MOI of 5 just prior to the labelling period. Seventy-two hours later, cells were treated with 10 Jm^{-2} UV. One hour before indicated collection time, the media was replaced with fresh media containing 50μCi/mL [^{3}H] uridine (GE Healthcare) to label nascent RNA. Samples were rinsed in PBS containing 0.2% sodium azide (PBS-Z), collected by trypsin in PBS-Z, rinsed with PBS-Z and cell pellets were stored at -80ºC. Samples were lysed in 1% SDS and nucleic acids were precipitated in 10% trichloroacetic acid (TCA)/0.1M sodium pyrophosphate (NaPPi) and preciptiated nucleic acids were collected on glass fiber filters (Thermo Fisher Scientific). Incorporation of [^{3}H] and [^{14}C] was determined using a scintillation counter and [^{3}H] counts were normalized to [^{14}C] counts to control for cell number. RNA synthesis is expressed as the proportion of [^{3}H] uridine incorporated in UV-treated samples compared to unirradiated controls.

Host cell reactivation

Recombinant adenovirus expressing the *lacZ* gene under control of the murine cytomegalovirus promoter (AdCA35-1, hereafter referred to as AdlacZ, a kind gift from Dr. Frank Graham, McMaster University, Hamilton, ON), was suspended in a minimal volume of PBS and was subsequently irradiated with the indicated dose of UV light on ice, as previously described.[436] Cells were infected with UV- or mock-treated AdlacZ at a multiplicity of infection (MOI) of 20 for primary cells or an MOI of 5 for tumour cells. Forty-eight

hours following infection, media was removed and monolayers were incubated with 1 mM chlorophenolred-β-D-galactopyranoside (Fluka Biochemika, Buchs, Switzerland) in 0.01% Triton X-100, 1 mM $MgCl_2$, and 100 mM phosphate buffer (pH 8.3).[437] Absorbance at 570 nm was determined using a Thermo Multiskan Ascent microplate photometer (Thermo Fischer Scientific). β-galatosidase activity from the indicated dose is expressed relative to the activity obtained by infection with un-irradiated virus.

Flow cytometry

Cells, as indicated were treated with indicated dose of UV light or cisplatin. In the case of AdshRNA infections, HCT116 were treated with indicated dose of UV light or cis-platin 72 hours following infection with the indicated AdshRNA virus at an MOI of 5. Detached and adherent cells were collected 48 hours following treatment, fixed in 70% ethanol for a minimum of 2 hours at -20° C and stained in 30μM propidium iodide (Sigma-Aldrich, Oakville, ON) in PBS with 40 μg/mL of RNAse A (Sigma-Aldrich).[391] Samples were analyzed by fluorescence activated cell sorting using a Becton Dickenson LSR II Facstation and CellQuest software (Becton Dickinson, Franklin Lakes, NJ) and data files were analysed using FCS Express (De Novo Software, Los Angeles, CA). Apoptosis was quantified as the proportion of cells with sub-diploid DNA content. Where indicated, Z-VAD-fmk (Bio-Rad) was added to the medium to a final concentration of 10 μM at the time of irradiation or treatment with cisplatin.

Animal Experimentation

All animal experimentation was approved by the University of Ottawa Animal Research Ethics Committee, conducted at the University of Ottawa Animal Care Facilities and supervised by the veterinary research technicians. Animals were given food and water ad libidim and wellness was monitored daily. Our experimental protocol has been previously described.[473] Briefly, ten million parental HCT116 or HCT116-shCSB1 were injected subcutaneously into the flanks of 8 week-old athymic male nude mice (Jackson Laboratories, Bar Harbour, ME). Once palpable tumours formed (approximately $50mm^3$ in one to two weeks), mice were treated 3 times over a 5 day period (day 0, day 2 and day 4) at 0, 1 or 4mg/kg cisplatin (Mayne Pharmaceuticals, Montreal, QC) in phosphate buffered saline, by intraperitoneal injection. Tumours were then measured using callipers every 2-3 days over a four week period and this experiment was completed 3 times. Mice were sacrificed at either humane endpoints as per University of Ottawa Animal Research Ethics guidelines, or termination of the studies. During the ensuing necropsy, cells from the subcutaneous tumours were removed and established in cell culture using no selective media. In several cases, cell lines were amplified and protein immunoblotting done to determine the state of CSB expression. All tumours tested in this way yielded CSB expression that was identical to the original HCT116-shCSB1 cell line prior xenograft (see Figure 2C).

Results

Targeting CSB with stably expressed shRNA sensitizes tumour cells to DNA damage

We recently reported that targeting CSB by RNAi was effective at increasing sensitivity to cisplatin-induced apoptosis in a variety of tumour cell lines *in vitro*.[223] Here we used RNAi to target CSB by stably inserting an shRNA into HCT116 colon carcinoma cells by retrovirus integration. After selecting for stable integration, individual clones were grown and the expression of CSB was assessed by western blotting (Figure 1A). Several clones were identified with decreased CSB expression and their response to UV-C and cisplatin was assessed (Figure 1A and 1B). Decreased expression of CSB was associated with increased sensitivity to UV- and cisplatin-induced apoptosis in 3 of 4 clones selected. Clone 15-16 (clone 6 in Figure 1A) exhibited a pronounced TC-NER defect as evidenced by decreased HCR of a UV-damaged reporter gene (Figure 1C) and in their ability to recover nascent RNA synthesis (Figure 1D). Together, this clone (henceforth referred to as HCT116-shCSB) exhibited the expected decrease in TC-NER and increased sensitivity to UV- and cisplatin-induced apoptosis.

RNAi against CSB increases responsiveness of a tumour xenograft to cisplatin

HCT116 colon carcinoma, HCT116-shGFP and TC-NER deficient HCT116-shCSB cells, were injected subcutaneously in the flank of CD-1 nude mice. All three cell lines formed tumours at similar rates (Figure 2A, 0mg/kg plots). Tumours were allowed to reach a minimum volume of 50mm^3 prior to treatment. The time required for tumours to reach treatment volume and mean tumour volume prior to treatment were not significantlydif-

Figure 1. Generation and Characterization of Stably Expressed shRNA Targeting CSB.

Cell lines stably expressing shRNA to CSB were assessed for CSB expression by immunoblotting (A) using Ku86 as a loading control. From these cell lines (clone numbers from 1A), sensitivity to DNA damage-induced apoptosis was determined by assessing the sub-diploid fraction of the cell cycle after treatment with cisplatin (B, left panel) or UV-C (B, right panel). TC-NER capacity was then measured by host cell reactivation (HCR) of β-galactosidase (β-gal) activity, determined two days following infection with AdlacZ irradiated with the indicated dose of UV light. β-gal activity is expressed relative to unirradiated controls. β-gal activity over a range of UV doses was measured in indicated cells (either parental HCT116 or clone 6, HCT116-shCSB). Data shown is mean (± SEM) from 3 individual experiments, each done in 8 replicate wells (C). Recovery of RNA synthesis (RRS) was determined in HCT116 and HCT116-shCSB cells. Synthesis of nascent RNA synthesis was assessed between 0 and 24 hours following exposure to 10 Jm^{-2} of UV light. RNA synthesis is expressed relative to unirradiated control samples collected simultaneously where each point represents the mean (± SEM) determined from a minimum of 3 independent experiments (D). * indicates statistical significance compared to controls determined by student t-test where $P < 0.05$.

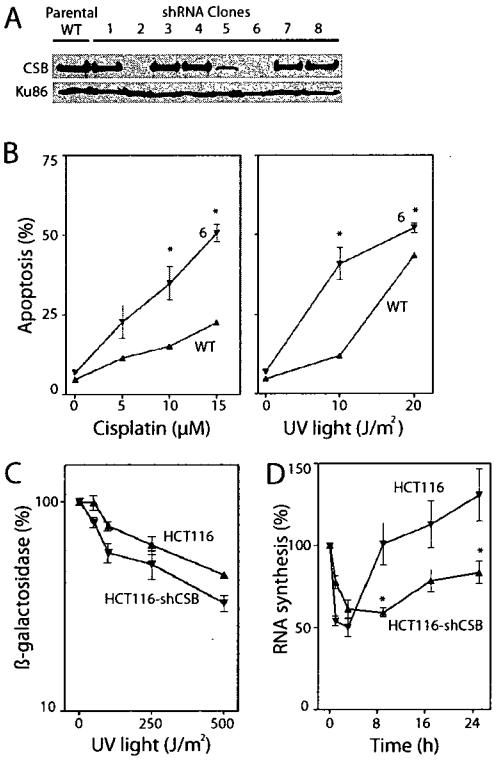
A
Parental
WT
shRNA Clones
1 2 3 4 5 6 7 8
CSB
Ku86
B
Apoptosis (%)
75
50
25
0
6
WT
0 5 10 15
Cisplatin (μM)
0 10 20
UV light (J/m²)
C
β-galactosidase (%)
100
10
HCT116
HCT116-shCSB
0 250 500
UV light (J/m²)
D
RNA synthesis (%)
150
100
50
0
HCT116
HCT116-shCSB
0 8 16 24
Time (h)

ferent. Cisplatin (1 or 4 mg/kg/day) was administered three times over a five day period for a total of 3 or 12mg/kg cisplatin per mouse. Tumour volume was measured three times per week.

As expected, cisplatin delayed the growth of all tumour xenografts to some extent. In response to both doses, HCT116-shCSB tumours were significantly smaller than control tumours (Figure 2A). This was noticeable within 2 days of the first treatment (Figure 2B). These results are consistent with the rapid onset of apoptosis in HCT116-shCSB tumours. The shCSB1-expressing cells that were tested maintained their original low level expression of CSB (Figure 2C). During necropsy, cells were recovered from tumours and established in culture. To determine the long-term expression status of CSB, immunoblotting was done. All tumours re-established in culture that were tested maintained their original low level expression of CSB (Figure 2D). Targeting CSB by stably expressing shRNA appears to yield long-term knockdowns and in xenograft studies exhibit sensitivity to cisplatin.

Figure 2. Tumour Xenografts From Cells Deficient in CSB are Sensitive to Cisplatin.

HCT116 parental, HCT116-shGFP and HCT116-shCSB1 cells were established as subcutaneous tumours in nude mice. Mice were treated on day 0, 2 and 4 with indicated doses of cisplatin then tumour volumes were measured with callipers. Data in 2A-B represents pooled results from three independent experiments with a total of 6-17 animals per group. Each point represents the mean (± SEM). Figure 2B shows just the first 7 days after treatment. After necropsy, individual tumours were excised and re-established in cell culture. Nuclear extracts were analysed by immunoblotting, as indicated, from three tumours treated with and compared to transient RNAi from cell culture to verify that knockdown was stable (C). * represents statistical significance compared to control by one-way ANOVA and Bonferonni post-testing, where $P < 0.05$. In 2D, parental cells (square symbols) and post-xenograft cells established in culture after necropsy (triangles) were treated with cisplatin and sub-diploid fraction of cells was determined. In 2E, post-xenograft cells (triangles from 2D) expressing shGFP and or shCSB maintained their sensitivity to DNA damage-induced apoptosis after re-establishment in cell culture. † represents statistical significance between pooled shNT values compared to pooled shCSB values by student's t-test where $P < 0.05$. There was no evidence that cisplatin treatment *in vivo* selected for cells with low shCSB expression.

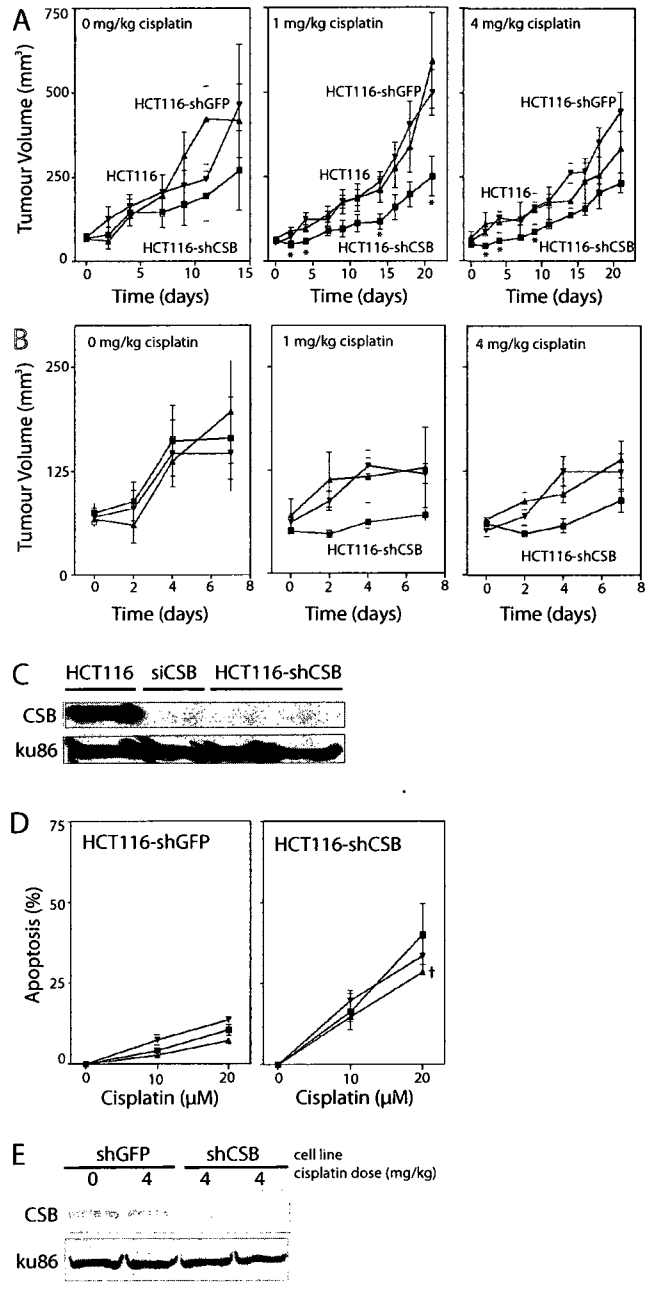
A
0 mg/kg cisplatin
1 mg/kg cisplatin
4 mg/kg cisplatin
HCT116-shGFP
HCT116
HCT116-shCSB
Tumour Volume (mm³)
Time (days)
B
C
HCT116
siCSB
HCT116-shCSB
CSB
ku86
D
HCT116-shGFP
HCT116-shCSB
Apoptosis (%)
Cisplatin (μM)
E
shGFP
shCSB
cell line
cisplatin dose (mg/kg)
0
4
4
4
CSB
ku86

Discussion

Platinum-based chemotherapeutic agents, while being a common component of many therapies, are curative in only a few tumour types [275, 276, 313, 350, 467]. The more likely outcome is a period of progression-free survival with modest increases in lifespan.[313] Recently, clinical trials suggest combining platinum therapies with other agents to further increase efficacy, however without dramatic differences in survival.[275, 313] The mechanisms for recurrence of resistant disease are complex but include various aspects of cell survival culminating in a selective advantage for the remaining tumour cells that escape initial therapy.[276, 284, 285, 313, 316] Hence the call for novel and targeted approaches to improve the clinical outcome and increase the useful life of platinum-based therapy.[275]

Low expression levels of NER proteins are known to be positively predictive of outcome of cisplatin chemotherapy.[286, 292, 293, 296, 355] Alternatively, where NER proteins are found to be expressed at higher than normal levels, there is evidence for poorer outcome[292, 355, 356, 366, 369] and in some of these cases cisplatin therapy may be discouraged.[355] Taken together, NER may represent a therapeutic target in combined cisplatin therapy.

We recently reported that RNAi against a variety of proteins required for TC-NER resulted in increased cisplatin responsiveness in cell culture.[223] As a preliminary experiment to determine the contribution of TC-NER to tumour response *in vivo*, we have stably introduced shRNA targeting CSB in colon cancer cells. The targeted cells generated here exhibited the same TC-NER deficiency as cells treated with siRNAs against CSB.[223] These cells remained tumourigenic in nude mice and the resulting tumours grew at a similar rate to tumours from parental HCT116 cells and cells expressing shRNA against GFP.

Using these TC-NER-impaired tumour cells, we generated CSB deficient tumours in nude mice that we then treated with cisplatin. We were not able to cure any of the mice, a difficult task in this model due to short tumour doubling time (see Figure 2A, first panel), yet we suggest that TC-NER is indeed important for tumour cell growth after cisplatin therapy *in vivo*. There is a clear difference between the tumour volumes of parental, HCT116-shGFP and HCT116-shCSB treated with 1 mg/kg and 4 mg/kg cisplatin (Figure 2A-B). This suggests that CSB-targeted tumours respond more rapidly and at apparently lower doses.

Eventually all tumours grew. To better understand the re-growth of the tumours, cells lines were established at endpoint. Re-established cell lines, examined for CSB expression, showed very low levels of CSB protein and retained their sensitivity to cisplatin-induced apoptosis (Figure 2C-D). Collectively our results support the concept that CSB may be an attractive therapeutic target. Future strategies to disrupt CSB could include the use of biologicals or small molecule inhibitors. We constructed an adenovirus expressing shRNA against CSB under control of the same RNA polymerase III H1 promoter. Infection at low low MOI was sufficient to inhibit expression of CSB (Supplementary Figure 1A). Decreased CSB expression was associated with impaired TC-NER and hypersensitivity to UV light and cisplatin (Supplementary Figure 1B-C). These results suggest that virally expressed shRNAs can functionally inhibit TC-NER. These strategies will need to be combined with tumour-specific methods of delivery to be therapeutically useful.

Supplementary Figure 1. Adenovirus-delivered shRNA Targets CSB and Impairs TC-NER in Colon Cancer Cells.

Adenovirus constructs were used to infect HCT116 cells for 72 h after which nuclear extracts were used for immunoblotting (A). RRS (B) and HCR (C) were assessed as previously described, after HCT116 cells were infected with indicated virus for 72 h. Results plotted in (B) and (C) are the mean (± SEM) of three individual experiments. HCT116 cells were infected with indicated virus for 72 h then treated as indicated with cisplatin or UV-C. Apoptosis, as the sub-diploid content of the cell cycle, was assessed and representative experiments are shown (D).

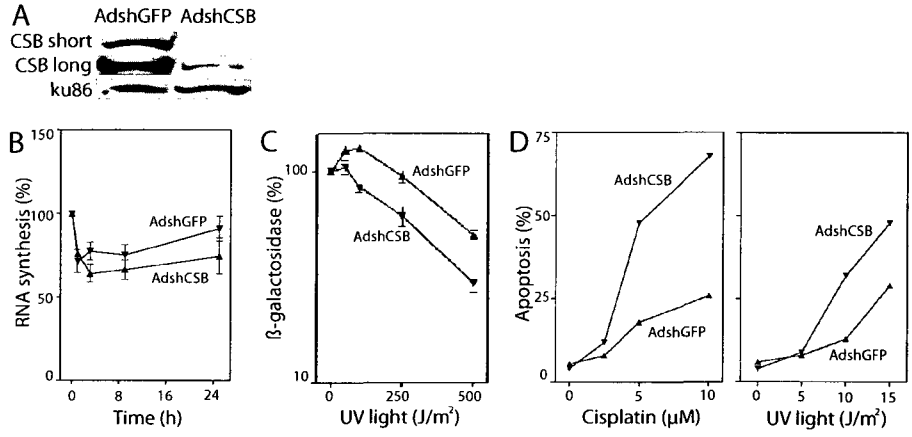
A
AdshGFP AdshCSB
CSB short
CSB long
ku86
B
RNA synthesis (%)
150
100
50
0
AdshGFP
AdshCSB
0 8 16 24
Time (h)
C
β-galactosidase (%)
100
10
AdshGFP
AdshCSB
0 250 500
UV light (J/m²)
D
Apoptosis (%)
75
50
25
0
AdshCSB
AdshGFP
0 5 10
Cisplatin (μM)
AdshCSB
AdshGFP
0 5 10 15
UV light (J/m²)

Acknowledgements

This work was initially supported by the National Cancer Institute of Canada with funds from the Terry Fox Run. L.J.S. was supported by an Ontario Premier's Research Excellence Award to B.C.M. with support from the Ottawa Regional Cancer Foundation and an Ontario Graduate Scholarship in Science and Technology. B.C.M. was a Research Scientist of the National Cancer Institute of Canada supported with funds provided by the Canadian Cancer Society throughout this work.

5.0 General Discussion

5.1 MMR and cisplatin resistance

Mismatch repair (MMR) is a post-replicative DNA repair mechanism that recognizes small loops generated by DNA base substitution mismatches and insertion-deletion mismatches (IDL) due to replication errors that escape the proofreading function of DNA polymerases.[474, 475] MMR is highly conserved between species with *E.coli*, *S.cerevisiae* and humans utilizing essentially homologous mechanisms.[476] Loss of any one component, such as MLH1, results in a crippling of MMR capacity.[444, 477] MMR deficiency is most commonly associated with colorectal cancer,[434, 478, 479] but ovarian, uterine, prostate and gastric cancers are frequently associated with defects in MMR.[75, 435, 454] MMR mutant cells exhibit genomic and microsatellite instability and are assigned to a mutator phenotype.[453] Loss of MMR in cancer is positively correlated with acquired cisplatin resistance[338, 340, 343, 469, 480] (reviewed in Stewart *et al.* 2007[285] and Pani *et al.* 2007[481]). In fact an enrichment for MMR deficient cells has been seen *in vitro*, with xenograft tumour models and when examining patient-derived tissue after clinical treatment with cisplatin.[442, 480]

The reported MMR-associated resistance to DNA damaging chemotherapeutic agents stems from the observation that MMR-deficient cells are unable to properly signal for programmed cell death, or apoptosis[263, 443, 444, 474, 482] and this has been attributed to MMR-dependent roles in apoptosis signalling through the p53 tumour suppressor.[263, 443, 483-485] and perhaps S-phase arrest.[486]

In the work presented here, we do not detect significant cisplatin resistance in MMR-deficient cell lines compared to controls. Specifically, HCT116 (MMR deficient) and

HCT116+chr3 (MMR proficient) cells responded identically to cisplatin in a battery of assays (Chapter 2, Figures 4 and 5, Supplementary Figures 1 and 2). We also tested the clonogenic survival of these cells after treatment with cisplatin and UV-C and also saw no difference (Appendix 1, Figure 2), though the same paired cell lines have been reported to exhibit up to a 2-fold difference in sensitivity to cisplatin.[338] While MMR-deficient tumours may exhibit resistance to chemotherapeutics, this may not always be observed in cell culture. Importantly, our data from both cell culture and *in vivo* experiments indicate that we can indeed measure significant cisplatin responsiveness in CSB-targeted cell lines despite inherent MMR defects.

5.2 MMR and Reported Links to TC-NER

It has been suggested that components of MMR participate in TC-NER of UV-induced DNA damage.[437, 449, 487, 488] More specifically, Mellon and Champe (1996) [487] confirmed that there was indeed a link between MMR and TC-NER in *E. coli* that had been previously suggested by Feng *et al.* (1991)[489] and Skandalis *et al.* (1994).[490] However, a concurrent study, acknowledging this link in bacterial repair mechanisms, dismissed this same possibility in yeast where no MMR requirement for TC-NER was detected.[491] This assertion was partially challenged by Yang *et al.* (1996) who showed that a protein required for yeast TC-NER increased the efficiency of MMR.[488] Mellon *et al.* (1996) then suggested a dependency of TC-NER on functional MMR since they reported an increase in TC-NER after correcting MMR in paired cell lines of parental HCT116 and the MMR-

corrected HCT116-chr3.[449] Unfortunately, this high profile work, published in the journal Science, remains to be supported by others.

No deficiency in TC-NER has been seen in the same paired human tumour cell lines[452] or MMR deficient cells derived from mice.[451] Additionally, others have reported that HCT116 cells are indeed proficient in performing TC-NER.[450] Kobayashi *et al.* (2004) introduced an MMR deficiency into XPC cells (GG-NER deficient yet TC-NER proficient) but this had no effect on their capacity to remove CPD from transcribed strands.[492]

Despite overwhelming evidence dissociating the processes of TC-NER and MMR, the controversial link between the two is still referenced in discussion of mechanisms of human skin cancer.[36] Here we found that RNAi against CSB decreased the repair of transcription-blocking DNA lesions. This clearly indicates that MMR-deficient cells were TC-NER proficient and this was CSB, XPA and XAB2 dependent, as expected.

5.3 p53 and Apoptosis

A significant hurdle to effective tumour therapy is the often abnormal expression of the p53 tumour suppressor, an important transcriptional regulator of many genes involved in cellular stress responses. p53 expression and function is limited by the human double minute 2 protein (hDM2) that ubiquitinates and targets it for proteasome degradation (reviewed in Lahav *et al.* 2004[493]). After DNA damage, p53 is stabilized post-translationally by DNA damage sensors (i.e. ATM and ATR) through phosphorylation of serine residues, thus causing dissociation of hDM2 (reviewed in Perry *et al.* 2004[494]). p53 can then transcriptionally activate pro-apoptotic BH3 family members such as p53

upregulated modulator of apoptosis (PUMA),[495] DNA repair genes,(reviewed in Ford 2005[496]) and cell cycle regulators such as p21.[497] The complex balance between these pro- and anti-apoptotic factors determines the ultimate cellular outcome (reviewed in Helton and Chen 2007[498]).

Mutated in over half of all human tumours, aberrant function or loss of p53 function is associated with transformation of normal cells (reviewed in Harris and Hollstein 1993[499]). p53 status can be predictive in some clinical settings. For example, mutations in p53 positively predict clinical resistance to cisplatin[329-331] such that p53-deficient tumour cells are more resistant to apoptosis, a relationship we see here. Although, cisplatin resistance can also be associated with enhanced drug efflux, increased expression of multi-drug resistance genes, alteration of cellular pH and mutations in DNA repair genes.[285]

The cellular mechanisms by which p53 regulates survival versus apoptosis is not completely understood. As reviewed in Helton and Chen (2007) there are accounts that confound current models of p53 function.[498] Inhibition of the E3-ubiquitin ligase hDM2 activates p53 function without inducing phosphorylation at key serines,[500] while mutation of perceived stability promoting C-terminal lysines, failed to alter p53 protein stability.[501] This is in addition to a recent report that necessitates the review of the mechanistic roles of certain internal regions involved in transactivation of p53 target genes.[379] Due to its apparent ubiquity in cellular processes, p53 function is likely specific to its cellular context. However, in the context of UV-induced DNA damage, the greater the dose, the greater the likelihood that the p53 response will follow an apoptotic program.[498] In fact, we reported a similar dose-response relationship and this was associated with a shift in

the spectrum of p53-induced genes, enriched for pro-apoptotic BH3 family members. We attributed this shift to a passive mechanism whereby smaller, pro-apoptotic p53 target genes with fewer and shorter introns evaded DNA damage and were expressed at the expense of larger anti-apoptotic p53 targets and genes encoding proteins involved in p53 negative feedback. This passive mechanism of gene regulation acts as a molecular dosimeter, thereby eliminating cells sustaining irreparable transcription-blocking DNA damage.[380] We have shown that p53 is required to protect cells from the generation of γ-H2AX loci, that indicate generation of DSBs, after exposure to low doses of UV irradiation. We also see an S-phase arrest in cells lacking p53 which is consistent with the notion that cells, after generation of UV-induced DSBs in S-phase, are unable to complete the cell cycle due to replication blocking, catastrophic accumulation of DNA damage.[399] This data is consistent with previous reports that show that in the absence of p53, UV irradiated cells undergo an S-phase arrest.[391]

Persistently stalled RNPII at a UV- or cisplatin-induced DNA lesion results in a potent apoptotic response (reviewed in van den Boom *et al.* 2002[207]). It has previously been well-established that stalled RNPII evokes a strong p53-dependent apoptotic response.[243, 367, 502] Consistent with previous work in human fibroblasts[187] however, p53 is not absolutely required for an apoptotic response when transcription is blocked by UV or cisplatin lesions because HPV-E6 expression or RNAi against p53 does not inhibit UV or cisplatin-induced apoptosis.[187, 367, 503] As expected, p53-deficient prostate cancer cells (DU145 and PC-3) and HCT116p53-/- cells (p53 deleted) were relatively resistant to UV- and cisplatin-induced apoptosis. However, RNAi targeting essential components of TC-NER, increased

the sensitivity of these p53 deficient cells to DNA damage-induced apoptosis (Chapter 2, Figures 1, 2, 6, 8 and Appendix 1, Figure 3). Therefore we suggest that TC-NER shares a significant yet separable role with p53 in determining apoptotic response in tumour cells, consistent with a p53-independent role for persistently stalled RNA polymerase II in the apoptotic response. These results indicate that abrogation of TC-NER could render cis-platin-resistant, p53-deficient tumours sensitive to platinum therapy.

5.4 Involvement of p53 in NER

The p53 tumour suppressor is an important part of the cellular response to DNA damage (reviewed in Ford 2005[496] and Roos and Kaina 2006[263]). The p53 response to DNA damage activates a G1 checkpoint and the ensuing G1-S phase arrest allows time for DNA repair (reviewed in Lane 1992[504]).

Proper function of GG-NER requires the p53 protein, as first discovered in cells from a patient with the p53-deficiency (Li Fraumeni syndrome).[505] The p53 tumour suppressor regulates the expression of DNA repair proteins such as DDB2[506] and XPC,[507] in response to DNA damage, thereby regulating NER directly. After inactivating p53 with the human papilloma virus E6 protein, CPD were found to be repaired more slowly in untranscribed regions of the genome.[399, 508, 509]

There is some evidence for a role of p53 in the regulation of TC-NER as well.[510-512] The p53 protein may directly regulate NER-mediated DNA repair by interacting with the TFIIH complex[513] and by regulating XPB and XPD helicase activities.[514] Consistent with a role for p53 in regulation of TC-NER, HCT116p53-/- cells exhibited a defect in repair of UV-

damaged reporter gene (Chapter 2, Figure 6). Conversely, these cells did not exhibit a decrease in the ability to recover nascent mRNA synthesis after UV-induced DNA damage (Chapter 2, Figures 1 and 6). Importantly, RNAi against CSB, XPA and XAB2 resulted in decreased TC-NER and increased sensitivity to UV- and cisplatin-induced cell death. Therefore, our results suggest that these HCT116p53-/- cells retain some ability to perform TC-NER and this is CSB, XPA and XAB2-dependent.

5.5 Anti-apoptotic Role for p53

In primary human fibroblasts, p53 is primarily protective against UV- and cisplatin-induced apoptosis.[187, 367, 515] Cell death in this context requires S-phase progression[244] and seems to be associated with a variety of S-phase defects including prolonged S-phase arrest,[399] increased formation of replication-associated DSB[399] and unscheduled expression of cyclin E.[516]

Surprisingly, it was reported that XP-E cells were resistant to cell death due to abnormal regulation of p53.[371] Given the fact that p53 is primarily protective against UV- and cisplatin-induced apoptosis, this report seemed to be inconsistent with previous literature. Given the conflicting reports, we explored the relationship between DDB2 and p53 in the context of UV damage in primary human fibroblasts. Contrary to the reports by the Linn group however, we found that disruption of p53 by RNAi or HPV-E6 expression increased resistance of fibroblasts to UV light. We concluded that p53 is primarily anti-apoptotic in this model system and this may be due to the accumulation of DSB due to defects in S-phase progression following UV exposure.

5.6 Future Directions

Future work pursued in the lab will address the therapeutic potential in targeting TC-NER in combined cisplatin cancer therapy. We propose to screen a library of small molecules to discover inhibitors of TC-NER. A method using an enhanced HCR technique to screen such a chemical library would allow high throughput analysis of existing chemical compounds to detect perturbed TC-NER, possibly reflective of inhibition of repair.

6.0 References

1. Canadian Cancer Statistics 2008. Toronto, Canada: Canadian Cancer Society/National Cancer Institute of Canada, 2008:108.
2. Hanahan D, Weinberg RA. The hallmarks of cancer. Cell 2000; 100:57-70.
3. Green DR, Evan GI. A matter of life and death. Cancer Cell 2002; 1:19-30.
4. Hager JH, Hanahan D. Tumor cells utilize multiple pathways to down-modulate apoptosis. Lessons from a mouse model of islet cell carcinogenesis. Ann N Y Acad Sci 1999; 887:150-63.
5. Venkatesan RN, Bielas JH, Loeb LA. Generation of mutator mutants during carcinogenesis. DNA repair 2006; 5:294-302.
6. Beckman RA, Loeb LA. Efficiency of carcinogenesis with and without a mutator mutation. Proceedings of the National Academy of Sciences of the United States of America 2006; 103:14140-5.
7. Bielas JH, Loeb KR, Rubin BP, True LD, Loeb LA. Human cancers express a mutator phenotype. Proceedings of the National Academy of Sciences of the United States of America 2006; 103:18238-42.
8. Renan MJ. How many mutations are required for tumorigenesis? Implications from human cancer data. Molecular carcinogenesis 1993; 7:139-46.
9. Jackson AL, Loeb LA. The contribution of endogenous sources of DNA damage to the multiple mutations in cancer. Mutation research 2001; 477:7-21.
10. Morton. Case of Encephaloid Tumor springing from the Fundus of the Eye-ball simulating Glaucoma. Trans Am Ophthalmol Soc 1868; 1:39.
11. Turner. An Account of an Enormous Tumour, presenting the Type of Structure of the Chorda Dorsalis. J Anat Physiol 1868; 2:247-52.
12. Maguire R. Case of Primary Cancer of the Femur. J Anat Physiol 1881; 15:496-501.
13. Maguire R. The Histology of some of the Rarer Forms of Malignant Bone Tumours. J Anat Physiol 1881; 15:405-21.
14. Dixon K, Kopras E. Genetic alterations and DNA repair in human carcinogenesis. Semin Cancer Biol 2004; 14:441-8.
15. Martinez ME, Marshall JR, Giovannucci E. Diet and cancer prevention: the roles of observation and experimentation. Nature reviews 2008; 8:694-703.
16. McTiernan A. Mechanisms linking physical activity with cancer. Nature reviews 2008; 8:205-11.
17. Akgul B, Cooke JC, Storey A. HPV-associated skin disease. J Pathol 2006; 208:165-75.
18. Benjamin CL, Ananthaswamy HN. p53 and the pathogenesis of skin cancer. Toxicol Appl Pharmacol 2007; 224:241-8.
19. Marrot L, Meunier JR. Skin DNA photodamage and its biological consequences. J Am Acad Dermatol 2008; 58:S139-48.
20. Matsumura Y, Ananthaswamy HN. Toxic effects of ultraviolet radiation on the skin. Toxicol Appl Pharmacol 2004; 195:298-308.
21. Vink AA, Roza L. Biological consequences of cyclobutane pyrimidine dimers. J Photochem Photobiol B 2001; 65:101-4.
22. Levine AJ. The common mechanisms of transformation by the small DNA tumor viruses: The inactivation of tumor suppressor gene products: p53. Virology 2009; 384:285-93.

23. Burnett-Hartman AN, Newcomb PA, Potter JD. Infectious agents and colorectal cancer: a review of Helicobacter pylori, Streptococcus bovis, JC virus, and human papillomavirus. Cancer Epidemiol Biomarkers Prev 2008; 17:2970-9.
24. Beliveau R, Gingras D. Role of nutrition in preventing cancer. Can Fam Physician 2007; 53:1905-11.
25. Shrivastav M, De Haro LP, Nickoloff JA. Regulation of DNA double-strand break repair pathway choice. Cell research 2008; 18:134-47.
26. Roschke AV, Glebov OK, Lababidi S, Gehlhaus KS, Weinstein JN, Kirsch IR. Chromosomal instability is associated with higher expression of genes implicated in epithelial-mesenchymal transition, cancer invasiveness, and metastasis and with lower expression of genes involved in cell cycle checkpoints, DNA repair, and chromatin maintenance. Neoplasia (New York, NY 2008; 10:1222-30.
27. Hoeijmakers JH. Genome maintenance mechanisms are critical for preventing cancer as well as other aging-associated diseases. Mech Ageing Dev 2007; 128:460-2.
28. Zhu W, Abbas T, Dutta A. DNA replication and genomic instability. Advances in experimental medicine and biology 2005; 570:249-79.
29. Zhivotovsky B, Kroemer G. Apoptosis and genomic instability. Nat Rev Mol Cell Biol 2004; 5:752-62.
30. Hegde ML, Hazra TK, Mitra S. Early steps in the DNA base excision/single-strand interruption repair pathway in mammalian cells. Cell research 2008; 18:27-47.
31. Hazra TK, Das A, Das S, Choudhury S, Kow YW, Roy R. Oxidative DNA damage repair in mammalian cells: a new perspective. DNA repair 2007; 6:470-80.
32. Sedgwick B, Bates PA, Paik J, Jacobs SC, Lindahl T. Repair of alkylated DNA: recent advances. DNA repair 2007; 6:429-42.
33. Friedberg EC, McDaniel LD, Schultz RA. The role of endogenous and exogenous DNA damage and mutagenesis. Current opinion in genetics & development 2004; 14:5-10.
34. Lewtas J. Air pollution combustion emissions: characterization of causative agents and mechanisms associated with cancer, reproductive, and cardiovascular effects. Mutation research 2007; 636:95-133.
35. Rigel DS. Cutaneous ultraviolet exposure and its relationship to the development of skin cancer. J Am Acad Dermatol 2008; 58:S129-32.
36. Rass K, Reichrath J. UV damage and DNA repair in malignant melanoma and nonmelanoma skin cancer. Advances in experimental medicine and biology 2008; 624:162-78.
37. D'Errico M, Lemma T, Calcagnile A, Proietti De Santis L, Dogliotti E. Cell type and DNA damage specific response of human skin cells to environmental agents. Mutation research 2007; 614:37-47.
38. Sinha RP, Hader DP. UV-induced DNA damage and repair: a review. Photochem Photobiol Sci 2002; 1:225-36.
39. Courdavault S, Baudouin C, Charveron M, Canguilhem B, Favier A, Cadet J, Douki T. Repair of the three main types of bipyrimidine DNA photoproducts in human keratinocytes exposed to UVB and UVA radiations. DNA repair 2005; 4:836-44.
40. Pfeifer GP, You YH, Besaratinia A. Mutations induced by ultraviolet light. Mutation research 2005; 571:19-31.
41. de Lima-Bessa KM, Armelini MG, Chigancas V, Jacysyn JF, Amarante-Mendes GP, Sarasin A, Menck CF. CPDs and 6-4PPs play different roles in UV-induced cell death in normal and NER-deficient human cells. DNA repair 2008; 7:303-12.
42. Batista LF, Kaina B, Meneghini R, Menck CF. How DNA lesions are turned into powerful killing structures: insights from UV-induced apoptosis. Mutation research 2009; 681:197-208.

43. Cadet J, Sage E, Douki T. Ultraviolet radiation-mediated damage to cellular DNA. Mutation research 2005; 571:3-17.
44. Douki T, Leccia MT, Beani JC, Mouret S, Cadet J, Favier A. [Harmful effects of solar UVA radiation: new indices in DNA]. Med Sci (Paris) 2007; 23:124-6.
45. Ichihashi M, Ueda M, Budiyanto A, Bito T, Oka M, Fukunaga M, Tsuru K, Horikawa T. UV-induced skin damage. Toxicology 2003; 189:21-39.
46. Jiang Y, Rabbi M, Kim M, Ke C, Lee W, Clark RL, Mieczkowski PA, Marszalek PE. UVA generates pyrimidine dimers in DNA directly. Biophys J 2009; 96:1151-8.
47. Ravanat JL, Douki T, Cadet J. Direct and indirect effects of UV radiation on DNA and its components. J Photochem Photobiol B 2001; 63:88-102.
48. de Winter S, Vink AA, Roza L, Pavel S. Solar-simulated skin adaptation and its effect on subsequent UV-induced epidermal DNA damage. J Invest Dermatol 2001; 117:678-82.
49. Szymkowski DE, Lawrence CW, Wood RD. Repair by human cell extracts of single (6-4) and cyclobutane thymine-thymine photoproducts in DNA. Proceedings of the National Academy of Sciences of the United States of America 1993; 90:9823-7.
50. Pines A, Backendorf C, Alekseev S, Jansen JG, de Gruijl FR, Vrieling H, Mullenders LH. Differential activity of UV-DDB in mouse keratinocytes and fibroblasts: Impact on DNA repair and UV-induced skin cancer. DNA repair 2008.
51. Mouret S, Charveron M, Favier A, Cadet J, Douki T. Differential repair of UVB-induced cyclobutane pyrimidine dimers in cultured human skin cells and whole human skin. DNA repair 2008; 7:704-12.
52. D'Errico M, Teson M, Calcagnile A, Proietti De Santis L, Nikaido O, Botta E, Zambruno G, Stefanini M, Dogliotti E. Apoptosis and efficient repair of DNA damage protect human keratinocytes against UVB. Cell Death Differ 2003; 10:754-6.
53. D'Errico M, Teson M, Calcagnile A, Nardo T, De Luca N, Lazzari C, Soddu S, Zambruno G, Stefanini M, Dogliotti E. Differential role of transcription-coupled repair in UVB-induced response of human fibroblasts and keratinocytes. Cancer research 2005; 65:432-8.
54. Otto AI, Riou L, Marionnet C, Mori T, Sarasin A, Magnaldo T. Differential behaviors toward ultraviolet A and B radiation of fibroblasts and keratinocytes from normal and DNA-repair-deficient patients. Cancer research 1999; 59:1212-8.
55. Hayflick L. The Limited in Vitro Lifetime of Human Diploid Cell Strains. Experimental cell research 1965; 37:614-36.
56. Hahn WC. Immortalization and transformation of human cells. Molecules and cells 2002; 13:351-61.
57. Fridman AL, Tainsky MA. Critical pathways in cellular senescence and immortalization revealed by gene expression profiling. Oncogene 2008; 27:5975-87.
58. Clarkson SG. The XPG story. Biochimie 2003; 85:1113-21.
59. Cleaver JE, Thompson LH, Richardson AS, States JC. A summary of mutations in the UV-sensitive disorders: xeroderma pigmentosum, Cockayne syndrome, and trichothiodystrophy. Hum Mutat 1999; 14:9-22.
60. Giannelli F, Croll PM, Lewin SA. DNA repair synthesis in human heterokaryons formed by normal and UV-sensitive fibroblasts. Experimental cell research 1973; 78:175-85.
61. Kraemer KH, Cleaver JE. Xeroderma pigmentosum and Cockayne Syndrome. . In: Scriver CR, Beaudet AL, Sly WS, Valle D, eds. The Metabolic and Molecular Bases of Inherited Disease. New York: McGraw-Hill, 1995:4393-419.
62. Kleijer WJ, Laugel V, Berneburg M, Nardo T, Fawcett H, Gratchev A, Jaspers NG, Sarasin A, Stefanini M, Lehmann AR. Incidence of DNA repair deficiency disorders in western Europe:

Xeroderma pigmentosum, Cockayne syndrome and trichothiodystrophy. DNA repair 2008; 7:744-50.
63. Saebo J. Xeroderma Pigmentosum with Affection of the Eye. Br J Ophthalmol 1948; 32:398-411.
64. Weisman PA. Xeroderma pigmentosum; report of occurrence in two Japanese siblings, with secondary epidermoid carcinoma in one case. Ohio Med 1949; 45:138-40.
65. Setlow RB, Regan JD, German J, Carrier WL. Evidence that xeroderma pigmentosum cells do not perform the first step in the repair of ultraviolet damage to their DNA. Proceedings of the National Academy of Sciences of the United States of America 1969; 64:1035-41.
66. Cleaver JE, Bootsma D, Friedberg E. Human diseases with genetically altered DNA repair processes. Genetics 1975; 79 Suppl:215-25.
67. Chu G, Mayne L. Xeroderma pigmentosum, Cockayne syndrome and trichothiodystrophy: do the genes explain the diseases? Trends Genet 1996; 12:187-92.
68. Anttinen A, Koulu L, Nikoskelainen E, Portin R, Kurki T, Erkinjuntti M, Jaspers NG, Raams A, Green MH, Lehmann AR, Wing JF, Arlett CF, Marttila RJ. Neurological symptoms and natural course of xeroderma pigmentosum. Brain 2008; 131:1979-89.
69. San RH, Stich W, Stich HF. Differential sensitivity of Xeroderma pigmentosum cells of different repair capacities towards the chromosome breaking action of carcinogens and mutagens. International journal of cancer 1977; 20:181-7.
70. Parshad R, Sanford KK, Jones GM. Chromatid damage after G2 phase x-irradiation of cells from cancer-prone individuals implicates deficiency in DNA repair. Proceedings of the National Academy of Sciences of the United States of America 1983; 80:5612-6.
71. Kondo S, Satoh Y, Kuroki T. Reduced levels of UV-induced unscheduled DNA synthesis in epidermal keratinocytes of patients with xeroderma pigmentosum and correlation with development of skin neoplasms. Cancer research 1989; 49:1927-30.
72. Araujo SJ, Wood RD. Protein complexes in nucleotide excision repair. Mutation research 1999; 435:23-33.
73. Sarasin A. The molecular pathways of ultraviolet-induced carcinogenesis. Mutation research 1999; 428:5-10.
74. Benhamou S, Sarasin A. Variability in nucleotide excision repair and cancer risk: a review. Mutation research 2000; 462:149-58.
75. Friedberg EC. How nucleotide excision repair protects against cancer. Nature reviews 2001; 1:22-33.
76. Cleaver JE. Mending human genes: a job for a lifetime. DNA repair 2005; 4:635-8.
77. Cockayne EA. Dwarfism with retinal atrophy and deafness. Arch Dis Child 1936; 11:1-8.
78. Nance MA, Berry SA. Cockayne syndrome: review of 140 cases. Am J Med Genet 1992; 42:68-84.
79. Meira LB, Graham JM, Jr., Greenberg CR, Busch DB, Doughty AT, Ziffer DW, Coleman DM, Savre-Train I, Friedberg EC. Manitoba aboriginal kindred with original cerebro-oculo- facio-skeletal syndrome has a mutation in the Cockayne syndrome group B (CSB) gene. Am J Hum Genet 2000; 66:1221-8.
80. Hanawalt PC. DNA repair. The bases for Cockayne syndrome. Nature 2000; 405:415-6.
81. Hanawalt PC. Controlling the efficiency of excision repair. Mutation research 2001; 485:3-13.
82. Cleaver JE, Revet I. Clinical implications of the basic defects in Cockayne syndrome and xeroderma pigmentosum and the DNA lesions responsible for cancer, neurodegeneration and aging. Mech Ageing Dev 2008; 129:492-7.

83. Fousteri M, Mullenders LH. Transcription-coupled nucleotide excision repair in mammalian cells: molecular mechanisms and biological effects. Cell research 2008; 18:73-84.
84. Lehmann AR. DNA repair-deficient diseases, xeroderma pigmentosum, Cockayne syndrome and trichothiodystrophy. Biochimie 2003; 85:1101-11.
85. Hanawalt PC, Spivak G. Transcription-coupled DNA repair: two decades of progress and surprises. Nat Rev Mol Cell Biol 2008; 9:958-70.
86. Fujiwara Y, Ichihashi M, Kano Y, Goto K, Shimizu K. A new human photosensitive subject with a defect in the recovery of DNA synthesis after ultraviolet-light irradiation. J Invest Dermatol 1981; 77:256-63.
87. Horibata K, Iwamoto Y, Kuraoka I, Jaspers NG, Kurimasa A, Oshimura M, Ichihashi M, Tanaka K. Complete absence of Cockayne syndrome group B gene product gives rise to UV-sensitive syndrome but not Cockayne syndrome. Proceedings of the National Academy of Sciences of the United States of America 2004; 101:15410-5.
88. Spivak G, Hanawalt PC. Host cell reactivation of plasmids containing oxidative DNA lesions is defective in Cockayne syndrome but normal in UV-sensitive syndrome fibroblasts. DNA repair 2006; 5:13-22.
89. Bergmann E, Egly JM. Trichothiodystrophy, a transcription syndrome. Trends Genet 2001; 17:279-86.
90. Stefanini M, Dalpra L, Zei G, Giorgi R, Falaschi A, Nuzzo F. Incorporation of (3H)thymidine stimulated by ultraviolet radiation into human fibroblast cultures. Mutation research 1976; 34:313-26.
91. Pena SD, Shokeir MH. Autosomal recessive cerebro-oculo-facio-skeletal (COFS) syndrome. Clin Genet 1974; 5:285-93.
92. Harrison PV, Shuster S. De Sanctis-Cacchione syndrome. Arch Dermatol 1979; 115:676.
93. Ford JM, Hanawalt PC. Role of DNA excision repair gene defects in the etiology of cancer. Curr Top Microbiol Immunol 1997; 221:47-70.
94. Cleaver JE. Common pathways for ultraviolet skin carcinogenesis in the repair and replication defective groups of xeroderma pigmentosum. J Dermatol Sci 2000; 23:1-11.
95. Friedberg EC. DNA damage and repair. Nature 2003; 421:436-40.
96. Cleaver JE. Cancer in xeroderma pigmentosum and related disorders of DNA repair. Nature reviews 2005; 5:564-73.
97. Sancar A. Structure and function of photolyase and in vivo enzymology: 50th anniversary. The Journal of biological chemistry 2008; 283:32153-7.
98. Kelner A. Effect of Visible Light on the Recovery of Streptomyces Griseus Conidia from Ultra-violet Irradiation Injury. Proceedings of the National Academy of Sciences of the United States of America 1949; 35:73-9.
99. Rupert CS, Goodgal SH, Herriott RM. Photoreactivation in vitro of ultraviolet-inactivated Hemophilus influenzae transforming factor. J Gen Physiol 1958; 41:451-71.
100. Rupert CS. Photoreactivation of transforming DNA by an enzyme from bakers' yeast. J Gen Physiol 1960; 43:573-95.
101. Hanawalt P, Buehler J. Photoreactivation of macromolecular synthesis in Escherichia coli. Biochim Biophys Acta 1960; 37:141-3.
102. Rupert CS. Photoenzymatic repair of ultraviolet damage in DNA. II. Formation of an enzyme-substrate complex. J Gen Physiol 1962; 45:725-41.
103. Rupert CS. Photoenzymatic repair of ultraviolet damage in DNA. I. Kinetics of the reaction. J Gen Physiol 1962; 45:703-24.
104. Carell T, Burgdorf LT, Kundu LM, Cichon M. The mechanism of action of DNA photolyases. Curr Opin Chem Biol 2001; 5:491-8.

105. Pettijohn D, Hanawalt P. Evidence for Repair-Replication of Ultraviolet Damaged DNA in Bacteria. Journal of molecular biology 1964; 9:395-410.
106. Pettijohn DE, Hanawalt PC. Deoxyribonucleic acid replication in bacteria following ultraviolet irradiation. Biochim Biophys Acta 1963; 72:127-9.
107. Kozinski AW, Kozinski PB. Fragmentary transfer of P32-labeled parental DNA to progeny phage. II. The average size of the transferred parental fragment. Two-cycletransfer. Repair of the polynucleotide chain after fragmentation. Virology 1963; 20:213-29.
108. Kozinski AW, Kozinski PB, Shannon P. Replicative Fragmentation in T4 Phage: Inhibition by Chloramphenicol. Proceedings of the National Academy of Sciences of the United States of America 1963; 50:746-53.
109. Riklis E. Studies on mechanism of repair of ultraviolet-irradiated viral and bacterial DNAin vivo and in vitro. Can J Biochem 1965; 43:1207-19.
110. Friedberg EC. DNA repair of ultraviolet-irradiated bacteriophage T4. Photochem Photobiol 1975; 21:277-89.
111. Painter RB, Rasmussen RE. Organization of the Deoxyribonucleic Acid Replicating System in Mammalian Cells as Revealed by the Use of X-Radiation and Bromuracil Deoxyriboside. Nature 1964; 201:162-5.
112. Kanner L, Hanawalt P. Efficiency of utilization of thymine and 5-bromouracil for normal and repair DNA synthesis in bacteria. Biochim Biophys Acta 1968; 157:532-45.
113. Cleaver JE. Defective repair replication of DNA in xeroderma pigmentosum. Nature 1968; 218:652-6.
114. Cleaver JE. Repair replication and degradation of bromouracil-substituted DNA in mammalian cells after irradiation with ultraviolet light. Biophys J 1968; 8:775-91.
115. Friedberg EC. The discovery that xeroderma pigmentosum (XP) results from defective nucleotide excision repair. DNA repair 2004; 3:183, 95.
116. Barbis DP, Schultz RA, Friedberg EC. Isolation and partial characterization of virus-transformed cell lines representing the A, G and variant complementation groups of xeroderma pigmentosum. Mutation research 1986; 165:175-84.
117. Cook K, Friedberg EC, Cleaver JE. Excision of thymine dimers from specifically incised DNA by extracts of xeroderma pigmentosum cells. Nature 1975; 256:235-6.
118. Mortelmans K, Friedberg EC, Slor H, Thomas G, Cleaver JE. Defective thymine dimer excision by cell-free extracts of xeroderma pigmentosum cells. Proceedings of the National Academy of Sciences of the United States of America 1976; 73:2757-61.
119. Moustacchi E, Ehmann UK, Friedberg EC. Defective recovery of semi-conservative DNA synthesis in xeroderma pigmentosum cells following split-dose ultraviolet irradiation. Mutation research 1979; 62:159-71.
120. Lehmann AR, Stevens S. A rapid procedure for measurement of DNA repair in human fibroblasts and for complementation analysis of xeroderma pigmentosum cells. Mutation research 1980; 69:177-90.
121. Abrahams PJ, Van der Eb AJ. Host-cell reactivation of ultraviolet-irradiated SV40 DNA in five complementation groups of xeroderma pigmentosum. Mutation research 1976; 35:13-22.
122. Stary A, Sarasin A. The genetics of the hereditary xeroderma pigmentosum syndrome. Biochimie 2002; 84:49-60.
123. Lehmann AR. Replication of damaged DNA. Cell cycle (Georgetown, Tex 2003; 2:300-2.
124. Friedberg EC. A brief history of the DNA repair field. Cell research 2008; 18:3-7.
125. Lehmann AR, Niimi A, Ogi T, Brown S, Sabbioneda S, Wing JF, Kannouche PL, Green CM. Translesion synthesis: Y-family polymerases and the polymerase switch. DNA repair 2007; 6:891-9.

126. Fornace AJ, Jr., Kohn KW, Kann HE, Jr. DNA single-strand breaks during repair of UV damage in human fibroblasts and abnormalities of repair in xeroderma pigmentosum. Proceedings of the National Academy of Sciences of the United States of America 1976; 73:39-43.
127. Kannouche P, Broughton BC, Volker M, Hanaoka F, Mullenders LH, Lehmann AR. Domain structure, localization, and function of DNA polymerase eta, defective in xeroderma pigmentosum variant cells. Genes & development 2001; 15:158-72.
128. Gratchev A, Strein P, Utikal J, Sergij G. Molecular genetics of Xeroderma pigmentosum variant. Exp Dermatol 2003; 12:529-36.
129. Kraemer KH, Patronas NJ, Schiffmann R, Brooks BP, Tamura D, DiGiovanna JJ. Xeroderma pigmentosum, trichothiodystrophy and Cockayne syndrome: a complex genotype-phenotype relationship. Neuroscience 2007; 145:1388-96.
130. Chu G, Chang E. Cisplatin-resistant cells express increased levels of a factor that recognizes damaged DNA. Proceedings of the National Academy of Sciences of the United States of America 1990; 87:3324-7.
131. Kataoka H, Fujiwara Y. UV damage-specific DNA-binding protein in xeroderma pigmentosum complementation group E. Biochem Biophys Res Commun 1991; 175:1139-43.
132. Hwang BJ, Chu G. Purification and characterization of a human protein that binds to damaged DNA. Biochemistry 1993; 32:1657-66.
133. Takao M, Abramic M, Moos M, Jr., Otrin VR, Wootton JC, McLenigan M, Levine AS, Protic M. A 127 kDa component of a UV-damaged DNA-binding complex, which is defective in some xeroderma pigmentosum group E patients, is homologous to a slime mold protein. Nucleic acids research 1993; 21:4111-8.
134. Keeney S, Eker AP, Brody T, Vermeulen W, Bootsma D, Hoeijmakers JH, Linn S. Correction of the DNA repair defect in xeroderma pigmentosum group E by injection of a DNA damage-binding protein. Proceedings of the National Academy of Sciences of the United States of America 1994; 91:4053-6.
135. Payne A, Chu G. Xeroderma pigmentosum group E binding factor recognizes a broad spectrum of DNA damage. Mutation research 1994; 310:89-102.
136. Dualan R, Brody T, Keeney S, Nichols AF, Admon A, Linn S. Chromosomal localization and cDNA cloning of the genes (DDB1 and DDB2) for the p127 and p48 subunits of a human damage-specific DNA binding protein. Genomics 1995; 29:62-9.
137. Hwang BJ, Liao JC, Chu G. Isolation of a cDNA encoding a UV-damaged DNA binding factor defective in xeroderma pigmentosum group E cells. Mutation research 1996; 362:105-17.
138. Chu G, Yang W. Here comes the sun: recognition of UV-damaged DNA. Cell 2008; 135:1172-4.
139. Otrin VR, McLenigan M, Takao M, Levine AS, Protic M. Translocation of a UV-damaged DNA binding protein into a tight association with chromatin after treatment of mammalian cells with UV light. Journal of cell science 1997; 110 (Pt 10):1159-68.
140. Wakasugi M, Kawashima A, Morioka H, Linn S, Sancar A, Mori T, Nikaido O, Matsunaga T. DDB accumulates at DNA damage sites immediately after UV irradiation and directly stimulates nucleotide excision repair. The Journal of biological chemistry 2002; 277:1637-40.
141. Sugasawa K, Okuda Y, Saijo M, Nishi R, Matsuda N, Chu G, Mori T, Iwai S, Tanaka K, Hanaoka F. UV-induced ubiquitylation of XPC protein mediated by UV-DDB-ubiquitin ligase complex. Cell 2005; 121:387-400.
142. Zelle B, Berends F, Lohman PH. Repair of damage by ultraviolet radiation in xeroderma pigmentosum cell strains of complementation groups E and F. Mutation research 1980; 73:157-69.
143. Fischer E, Schnyder UW, Jung EG. Report of three sisters with XP-E, a rare xeroderma pigmentosum complementation group. Photodermatol 1984; 1:232-6.

144. Patterson M, Chu G. Evidence that xeroderma pigmentosum cells from complementation group E are deficient in a homolog of yeast photolyase. Molecular and cellular biology 1989; 9:5105-12.
145. Reardon JT, Nichols AF, Keeney S, Smith CA, Taylor JS, Linn S, Sancar A. Comparative analysis of binding of human damaged DNA-binding protein (XPE) and Escherichia coli damage recognition protein (UvrA) to the major ultraviolet photoproducts: T[c,s]T, T[t,s]T, T[6-4]T, and T[Dewar]T. The Journal of biological chemistry 1993; 268:21301-8.
146. Scrima A, Konickova R, Czyzewski BK, Kawasaki Y, Jeffrey PD, Groisman R, Nakatani Y, Iwai S, Pavletich NP, Thoma NH. Structural basis of UV DNA-damage recognition by the DDB1-DDB2 complex. Cell 2008; 135:1213-23.
147. Kapetanaki MG, Guerrero-Santoro J, Bisi DC, Hsieh CL, Rapic-Otrin V, Levine AS. The DDB1-CUL4ADDB2 ubiquitin ligase is deficient in xeroderma pigmentosum group E and targets histone H2A at UV-damaged DNA sites. Proceedings of the National Academy of Sciences of the United States of America 2006; 103:2588-93.
148. Sugasawa K. UV-induced ubiquitylation of XPC complex, the UV-DDB-ubiquitin ligase complex, and DNA repair. J Mol Histol 2006.
149. Sugasawa K. The xeroderma pigmentosum group C protein complex and ultraviolet-damaged DNA-binding protein: functional assays for damage recognition factors involved in global genome Repair. Methods in enzymology 2006; 408:171-88.
150. Sugasawa K, Ng JM, Masutani C, Iwai S, van der Spek PJ, Eker AP, Hanaoka F, Bootsma D, Hoeijmakers JH. Xeroderma pigmentosum group C protein complex is the initiator of global genome nucleotide excision repair. Molecular cell 1998; 2:223-32.
151. Sugasawa K, Shimizu Y, Iwai S, Hanaoka F. A molecular mechanism for DNA damage recognition by the xeroderma pigmentosum group C protein complex. DNA repair 2002; 1:95-107.
152. El-Mahdy MA, Zhu Q, Wang QE, Wani G, Praetorius-Ibba M, Wani AA. Cullin 4A-mediated proteolysis of DDB2 protein at DNA damage sites regulates in vivo lesion recognition by XPC. The Journal of biological chemistry 2006; 281:13404-11.
153. van der Spek PJ, Smit EM, Beverloo HB, Sugasawa K, Masutani C, Hanaoka F, Hoeijmakers JH, Hagemeijer A. Chromosomal localization of three repair genes: the xeroderma pigmentosum group C gene and two human homologs of yeast RAD23. Genomics 1994; 23:651-8.
154. Li L, Lu X, Peterson C, Legerski R. XPC interacts with both HHR23B and HHR23A in vivo. Mutation research 1997; 383:197-203.
155. Luijsterburg MS, Goedhart J, Moser J, Kool H, Geverts B, Houtsmuller AB, Mullenders LH, Vermeulen W, van Driel R. Dynamic in vivo interaction of DDB2 E3 ubiquitin ligase with UV-damaged DNA is independent of damage-recognition protein XPC. Journal of cell science 2007; 120:2706-16.
156. Uchida A, Sugasawa K, Masutani C, Dohmae N, Araki M, Yokoi M, Ohkuma Y, Hanaoka F. The carboxy-terminal domain of the XPC protein plays a crucial role in nucleotide excision repair through interactions with transcription factor IIH. DNA repair 2002; 1:449-61.
157. Kuraoka I, Morita EH, Saijo M, Matsuda T, Morikawa K, Shirakawa M, Tanaka K. Identification of a damaged-DNA binding domain of the XPA protein. Mutation research 1996; 362:87-95.
158. Xu N, Pasa-Tolic L, Smith RD, Ni S, Thrall BD. Electrospray ionization-mass spectrometry study of the interaction of cisplatin-adducted oligonucleotides with human XPA minimal binding domain protein. Anal Biochem 1999; 272:26-33.
159. Turchi JJ, Henkels KM, Hermanson IL, Patrick SM. Interactions of mammalian proteins with cisplatin-damaged DNA. J Inorg Biochem 1999; 77:83-7.

160. Araki M, Masutani C, Maekawa T, Watanabe Y, Yamada A, Kusumoto R, Sakai D, Sugasawa K, Ohkuma Y, Hanaoka F. Reconstitution of damage DNA excision reaction from SV40 minichromosomes with purified nucleotide excision repair proteins. Mutation research 2000; 459:147-60.
161. Maltseva EA, Rechkunova NI, Gillet LC, Petruseva IO, Scharer OD, Lavrik OI. Crosslinking of the NER damage recognition proteins XPC-HR23B, XPA and RPA to photoreactive probes that mimic DNA damages. Biochim Biophys Acta 2007; 1770:781-9.
162. Mustra DJ, Warren AJ, Wilcox DE, Hamilton JW. Preferential binding of human XPA to the mitomycin C-DNA interstrand crosslink and modulation by arsenic and cadmium. Chem Biol Interact 2007; 168:159-68.
163. Koberle B, Roginskaya V, Wood RD. XPA protein as a limiting factor for nucleotide excision repair and UV sensitivity in human cells. DNA repair 2006; 5:641-8.
164. Lambert MW, Yang L. Xeroderma pigmentosum complementation group A protein acts as a processivity factor. Biochem Biophys Res Commun 2000; 271:782-7.
165. Mer G, Bochkarev A, Gupta R, Bochkareva E, Frappier L, Ingles CJ, Edwards AM, Chazin WJ. Structural basis for the recognition of DNA repair proteins UNG2, XPA, and RAD52 by replication factor RPA. Cell 2000; 103:449-56.
166. Nikiforov AA, Svetlova MP, Solov'eva LV, Pleskach NM, Hanawalt PC, Tomilin NV. [UV-induced immobilization of DNA repair protein XPA in different human cell line]. Tsitologiia 2000; 42:181-9.
167. Buchko GW, Isern NG, Spicer LD, Kennedy MA. Human nucleotide excision repair protein XPA: NMR spectroscopic studies of an XPA fragment containing the ERCC1-binding region and the minimal DNA-binding domain (M59-F219). Mutation research 2001; 486:1-10.
168. Saijo M, Matsuda T, Kuraoka I, Tanaka K. Inhibition of nucleotide excision repair by anti-XPA monoclonal antibodies which interfere with binding to RPA, ERCC1, and TFIIH. Biochem Biophys Res Commun 2004; 321:815-22.
169. Croteau DL, Peng Y, Van Houten B. DNA repair gets physical: mapping an XPA-binding site on ERCC1. DNA repair 2008; 7:819-26.
170. Park CH, Mu D, Reardon JT, Sancar A. The general transcription-repair factor TFIIH is recruited to the excision repair complex by the XPA protein independent of the TFIIE transcription factor. The Journal of biological chemistry 1995; 270:4896-902.
171. Kuhnlein U, Penhoet EE, Linn S. An altered apurinic DNA endonuclease activity in group A and group D xeroderma pigmentosum fibroblasts. Proceedings of the National Academy of Sciences of the United States of America 1976; 73:1169-73.
172. Tomkinson AE, Bonk RT, Kim J, Bartfeld N, Linn S. Mammalian mitochondrial endonuclease activities specific for ultraviolet-irradiated DNA. Nucleic acids research 1990; 18:929-35.
173. Flejter WL, McDaniel LD, Askari M, Friedberg EC, Schultz RA. Characterization of a complex chromosomal rearrangement maps the locus for in vitro complementation of xeroderma pigmentosum group D to human chromosome band 19q13. Genes Chromosomes Cancer 1992; 5:335-42.
174. Flejter WL, McDaniel LD, Johns D, Friedberg EC, Schultz RA. Correction of xeroderma pigmentosum complementation group D mutant cell phenotypes by chromosome and gene transfer: involvement of the human ERCC2 DNA repair gene. Proceedings of the National Academy of Sciences of the United States of America 1992; 89:261-5.
175. Frederick GD, Amirkhan RH, Schultz RA, Friedberg EC. Structural and mutational analysis of the xeroderma pigmentosum group D (XPD) gene. Human molecular genetics 1994; 3:1783-8.
176. Boulikas T. Xeroderma pigmentosum and molecular cloning of DNA repair genes. Anticancer Res 1996; 16:693-708.
177. Iyer N, Reagan MS, Wu KJ, Canagarajah B, Friedberg EC. Interactions involving the human RNA polymerase II transcription/nucleotide excision repair complex TFIIH, the nucleotide excision

repair protein XPG, and Cockayne syndrome group B (CSB) protein. Biochemistry 1996; 35:2157-67.
178. Evans E, Moggs JG, Hwang JR, Egly JM, Wood RD. Mechanism of open complex and dual incision formation by human nucleotide excision repair factors. The EMBO journal 1997; 16:6559-73.
179. Sijbers AM, de Laat WL, Ariza RR, Biggerstaff M, Wei YF, Moggs JG, Carter KC, Shell BK, Evans E, de Jong MC, Rademakers S, de Rooij J, Jaspers NG, Hoeijmakers JH, Wood RD. Xeroderma pigmentosum group F caused by a defect in a structure-specific DNA repair endonuclease. Cell 1996; 86:811-22.
180. Miura M, Nakamura S, Sasaki T, Takasaki Y, Shiomi T, Yamaizumi M. Roles of XPG and XPF/ERCC1 endonucleases in UV-induced immunostaining of PCNA in fibroblasts. Experimental cell research 1996; 226:126-32.
181. Constantinou A, Gunz D, Evans E, Lalle P, Bates PA, Wood RD, Clarkson SG. Conserved residues of human XPG protein important for nuclease activity and function in nucleotide excision repair. The Journal of biological chemistry 1999; 274:5637-48.
182. Bowman KK, Smith CA, Hanawalt PC. Excision-repair patch lengths are similar for transcription-coupled repair and global genome repair in UV-irradiated human cells. Mutation research 1997; 385:95-105.
183. Aboussekhra A, Biggerstaff M, Shivji MK, Vilpo JA, Moncollin V, Podust VN, Protic M, Hubscher U, Egly JM, Wood RD. Mammalian DNA nucleotide excision repair reconstituted with purified protein components. Cell 1995; 80:859-68.
184. Shivji MK, Podust VN, Hubscher U, Wood RD. Nucleotide excision repair DNA synthesis by DNA polymerase epsilon in the presence of PCNA, RFC, and RPA. Biochemistry 1995; 34:5011-7.
185. Mayne LV, Lehmann AR. Failure of RNA synthesis to recover after UV irradiation: an early defect in cells from individuals with Cockayne's syndrome and xeroderma pigmentosum. Cancer research 1982; 42:1473-8.
186. Mayne LV, Lehmann AR, Waters R. Excision repair in Cockayne syndrome. Mutation research 1982; 106:179-89.
187. McKay BC, Becerril C, Ljungman M. P53 plays a protective role against UV- and cisplatin-induced apoptosis in transcription-coupled repair proficient fibroblasts. Oncogene 2001; 20:6805-8.
188. Furuta T, Ueda T, Aune G, Sarasin A, Kraemer KH, Pommier Y. Transcription-coupled nucleotide excision repair as a determinant of cisplatin sensitivity of human cells. Cancer research 2002; 62:4899-902.
189. Yamada A, Masutani C, Hanaoka F. Detection of reduced RNA synthesis in UV-irradiated Cockayne syndrome group B cells using an isolated nuclear system. Biochim Biophys Acta 2002; 1592:129-34.
190. Bohr VA, Smith CA, Okumoto DS, Hanawalt PC. DNA repair in an active gene: removal of pyrimidine dimers from the DHFR gene of CHO cells is much more efficient than in the genome overall. Cell 1985; 40:359-69.
191. Madhani HD, Bohr VA, Hanawalt PC. Differential DNA repair in transcriptionally active and inactive proto-oncogenes: c-abl and c-mos. Cell 1986; 45:417-23.
192. Mellon I, Bohr VA, Smith CA, Hanawalt PC. Preferential DNA repair of an active gene in human cells. Proceedings of the National Academy of Sciences of the United States of America 1986; 83:8878-82.
193. Mellon I, Spivak G, Hanawalt PC. Selective removal of transcription-blocking DNA damage from the transcribed strand of the mammalian DHFR gene. Cell 1987; 51:241-9.

194. Hanawalt PC. Preferential DNA repair in expressed genes. Environ Health Perspect 1987; 76:9-14.
195. Mullenders LH, van Kesteren van Leeuwen AC, van Zeeland AA, Natarajan AT. Nuclear matrix associated DNA is preferentially repaired in normal human fibroblasts, exposed to a low dose of ultraviolet light but not in Cockayne's syndrome fibroblasts. Nucleic acids research 1988; 16:10607-22.
196. Carreau M, Hunting D. Transcription-dependent and independent DNA excision repair pathways in human cells. Mutation research 1992; 274:57-64.
197. Tu Y, Bates S, Pfeifer GP. Sequence-specific and domain-specific DNA repair in xeroderma pigmentosum and Cockayne syndrome cells. The Journal of biological chemistry 1997; 272:20747-55.
198. Kantor GJ, Bastin SA. Repair of some active genes in Cockayne syndrome cells is at the genome overall rate. Mutation research 1995; 336:223-33.
199. Kantor GJ, Barsalou LS, Hanawalt PC. Selective repair of specific chromatin domains in UV-irradiated cells from xeroderma pigmentosum complementation group C. Mutation research 1990; 235:171-80.
200. Venema J, van Hoffen A, Natarajan AT, van Zeeland AA, Mullenders LH. The residual repair capacity of xeroderma pigmentosum complementation group C fibroblasts is highly specific for transcriptionally active DNA. Nucleic acids research 1990; 18:443-8.
201. Hanawalt PC. Heterogeneity of DNA repair at the gene level. Mutation research 1991; 247:203-11.
202. Corda Y, Job C, Anin MF, Leng M, Job D. Transcription by eucaryotic and procaryotic RNA polymerases of DNA modified at a d(GG) or a d(AG) site by the antitumor drug cis-diamminedichloroplatinum(II). Biochemistry 1991; 30:222-30.
203. Tornaletti S, Donahue BA, Reines D, Hanawalt PC. Nucleotide sequence context effect of a cyclobutane pyrimidine dimer upon RNA polymerase II transcription. The Journal of biological chemistry 1997; 272:31719-24.
204. Balajee AS, May A, Dianov GL, Friedberg EC, Bohr VA. Reduced RNA polymerase II transcription in intact and permeabilized Cockayne syndrome group B cells. Proceedings of the National Academy of Sciences of the United States of America 1997; 94:4306-11.
205. Selby CP, Sancar A. Cockayne syndrome group B protein enhances elongation by RNA polymerase II. Proceedings of the National Academy of Sciences of the United States of America 1997; 94:11205-9.
206. Tantin D, Kansal A, Carey M. Recruitment of the putative transcription-repair coupling factor CSB/ERCC6 to RNA polymerase II elongation complexes. Molecular and cellular biology 1997; 17:6803-14.
207. van den Boom V, Jaspers NG, Vermeulen W. When machines get stuck--obstructed RNA polymerase II: displacement, degradation or suicide. Bioessays 2002; 24:780-4.
208. van den Boom V, Citterio E, Hoogstraten D, Zotter A, Egly JM, van Cappellen WA, Hoeijmakers JH, Houtsmuller AB, Vermeulen W. DNA damage stabilizes interaction of CSB with the transcription elongation machinery. The Journal of cell biology 2004; 166:27-36.
209. Bregman DB, Halaban R, van Gool AJ, Henning KA, Friedberg EC, Warren SL. UV-induced ubiquitination of RNA polymerase II: a novel modification deficient in Cockayne syndrome cells. Proceedings of the National Academy of Sciences of the United States of America 1996; 93:11586-90.
210. McKay BC, Chen F, Clarke ST, Wiggin HE, Harley LM, Ljungman M. UV light-induced degradation of RNA polymerase II is dependent on the Cockayne's syndrome A and B proteins but not p53 or MLH1. Mutation research 2001; 485:93-105.

211. van Gool AJ, Citterio E, Rademakers S, van Os R, Vermeulen W, Constantinou A, Egly JM, Bootsma D, Hoeijmakers JH. The Cockayne syndrome B protein, involved in transcription-coupled DNA repair, resides in an RNA polymerase II-containing complex. The EMBO journal 1997; 16:5955-65.
212. Kamiuchi S, Saijo M, Citterio E, de Jager M, Hoeijmakers JH, Tanaka K. Translocation of Cockayne syndrome group A protein to the nuclear matrix: possible relevance to transcription-coupled DNA repair. Proceedings of the National Academy of Sciences of the United States of America 2002; 99:201-6.
213. Groisman R, Polanowska J, Kuraoka I, Sawada J, Saijo M, Drapkin R, Kisselev AF, Tanaka K, Nakatani Y. The ubiquitin ligase activity in the DDB2 and CSA complexes is differentially regulated by the COP9 signalosome in response to DNA damage. Cell 2003; 113:357-67.
214. Fousteri M, Vermeulen W, van Zeeland AA, Mullenders LH. Cockayne syndrome A and B proteins differentially regulate recruitment of chromatin remodeling and repair factors to stalled RNA polymerase II in vivo. Molecular cell 2006; 23:471-82.
215. Citterio E, Van Den Boom V, Schnitzler G, Kanaar R, Bonte E, Kingston RE, Hoeijmakers JH, Vermeulen W. ATP-dependent chromatin remodeling by the Cockayne syndrome B DNA repair-transcription-coupling factor. Molecular and cellular biology 2000; 20:7643-53.
216. Sarker AH, Tsutakawa SE, Kostek S, Ng C, Shin DS, Peris M, Campeau E, Tainer JA, Nogales E, Cooper PK. Recognition of RNA polymerase II and transcription bubbles by XPG, CSB, and TFIIH: insights for transcription-coupled repair and Cockayne Syndrome. Molecular cell 2005; 20:187-98.
217. Nakatsu Y, Asahina H, Citterio E, Rademakers S, Vermeulen W, Kamiuchi S, Yeo JP, Khaw MC, Saijo M, Kodo N, Matsuda T, Hoeijmakers JH, Tanaka K. XAB2, a novel tetratricopeptide repeat protein involved in transcription-coupled DNA repair and transcription. The Journal of biological chemistry 2000; 275:34931-7.
218. Yonemasu R, Minami M, Nakatsu Y, Takeuchi M, Kuraoka I, Matsuda Y, Higashi Y, Kondoh H, Tanaka K. Disruption of mouse XAB2 gene involved in pre-mRNA splicing, transcription and transcription-coupled DNA repair results in preimplantation lethality. DNA repair 2005; 4:479-91.
219. Kuraoka I, Ito S, Wada T, Hayashida M, Lee L, Saijo M, Nakatsu Y, Matsumoto M, Matsunaga T, Handa H, Qin J, Nakatani Y, Tanaka K. Isolation of XAB2 complex involved in pre-mRNA splicing, transcription, and transcription-coupled repair. The Journal of biological chemistry 2008; 283:940-50.
220. Troelstra C, van Gool A, de Wit J, Vermeulen W, Bootsma D, Hoeijmakers JH. ERCC6, a member of a subfamily of putative helicases, is involved in Cockayne's syndrome and preferential repair of active genes. Cell 1992; 71:939-53.
221. Troelstra C, Hesen W, Bootsma D, Hoeijmakers JH. Structure and expression of the excision repair gene ERCC6, involved in the human disorder Cockayne's syndrome group B. Nucleic acids research 1993; 21:419-26.
222. Troelstra C, Landsvater RM, Wiegant J, van der Ploeg M, Viel G, Buys CH, Hoeijmakers JH. Localization of the nucleotide excision repair gene ERCC6 to human chromosome 10q11-q21. Genomics 1992; 12:745-9.
223. Stubbert LJ, Smith, J.M., Hamill, J.D., McKay, B.C. Sensitizing tumour cells to DNA damage by targeting transcription-coupled nucleotide excision repair. in preparation 2009.
224. Eisen JA, Sweder KS, Hanawalt PC. Evolution of the SNF2 family of proteins: subfamilies with distinct sequences and functions. Nucleic acids research 1995; 23:2715-23.
225. Selby CP, Sancar A. Human transcription-repair coupling factor CSB/ERCC6 is a DNA-stimulated ATPase but is not a helicase and does not disrupt the ternary transcription complex of stalled RNA polymerase II. The Journal of biological chemistry 1997; 272:1885-90.

226. Brosh RM, Jr., Balajee AS, Selzer RR, Sunesen M, Proietti De Santis L, Bohr VA. The ATPase domain but not the acidic region of Cockayne syndrome group B gene product is essential for DNA repair. Molecular biology of the cell 1999; 10:3583-94.
227. Balajee AS, Proietti De Santis L, Brosh RM, Jr., Selzer R, Bohr VA. Role of the ATPase domain of the Cockayne syndrome group B protein in UV induced apoptosis. Oncogene 2000; 19:477-89.
228. Beerens N, Hoeijmakers JH, Kanaar R, Vermeulen W, Wyman C. The CSB protein actively wraps DNA. The Journal of biological chemistry 2005; 280:4722-9.
229. Laine JP, Egly JM. Initiation of DNA repair mediated by a stalled RNA polymerase IIO. The EMBO journal 2006; 25:387-97.
230. Selby CP, Drapkin R, Reinberg D, Sancar A. RNA polymerase II stalled at a thymine dimer: footprint and effect on excision repair. Nucleic acids research 1997; 25:787-93.
231. Henning KA, Li L, Iyer N, McDaniel LD, Reagan MS, Legerski R, Schultz RA, Stefanini M, Lehmann AR, Mayne LV, Friedberg EC. The Cockayne syndrome group A gene encodes a WD repeat protein that interacts with CSB protein and a subunit of RNA polymerase II TFIIH. Cell 1995; 82:555-64.
232. Itoh T, Shiomi T, Shiomi N, Harada Y, Wakasugi M, Matsunaga T, Nikaido O, Friedberg EC, Yamaizumi M. Rodent complementation group 8 (ERCC8) corresponds to Cockayne syndrome complementation group A. Mutation research 1996; 362:167-74.
233. Seroz T, Hwang JR, Moncollin V, Egly JM. TFIIH: a link between transcription, DNA repair and cell cycle regulation. Current opinion in genetics & development 1995; 5:217-21.
234. Dianov GL, Houle JF, Iyer N, Bohr VA, Friedberg EC. Reduced RNA polymerase II transcription in extracts of cockayne syndrome and xeroderma pigmentosum/Cockayne syndrome cells. Nucleic acids research 1997; 25:3636-42.
235. Svejstrup JQ. Contending with transcriptional arrest during RNAPII transcript elongation. Trends Biochem Sci 2007; 32:165-71.
236. Choi JH, Lindsey-Boltz LA, Sancar A. Reconstitution of a human ATR-mediated checkpoint response to damaged DNA. Proceedings of the National Academy of Sciences of the United States of America 2007; 104:13301-6.
237. Lindsey-Boltz LA, Sancar A. RNA polymerase: the most specific damage recognition protein in cellular responses to DNA damage? Proceedings of the National Academy of Sciences of the United States of America 2007; 104:13213-4.
238. Brueckner F, Armache KJ, Cheung A, Damsma GE, Kettenberger H, Lehmann E, Sydow J, Cramer P. Structure-function studies of the RNA polymerase II elongation complex. Acta Crystallogr D Biol Crystallogr 2009; 65:112-20.
239. Brueckner F, Hennecke U, Carell T, Cramer P. CPD damage recognition by transcribing RNA polymerase II. Science (New York, NY 2007; 315:859-62.
240. Tornaletti S, Reines D, Hanawalt PC. Structural characterization of RNA polymerase II complexes arrested by a cyclobutane pyrimidine dimer in the transcribed strand of template DNA. The Journal of biological chemistry 1999; 274:24124-30.
241. Atanassov B, Velkova A, Mladenov E, Anachkova B, Russev G. Comparison of the global genomic and transcription-coupled repair rates of different lesions in human cells. Z Naturforsch C 2004; 59:445-53.
242. Ljungman M, Zhang F. Blockage of RNA polymerase as a possible trigger for u.v. light-induced apoptosis. Oncogene 1996; 13:823-31.
243. Ljungman M, Zhang F, Chen F, Rainbow AJ, McKay BC. Inhibition of RNA polymerase II as a trigger for the p53 response. Oncogene 1999; 18:583-92.

244. McKay BC, Becerril C, Spronck JC, Ljungman M. Ultraviolet light-induced apoptosis is associated with S-phase in primary human fibroblasts. DNA repair 2002; 1:811-20.
245. Cullinane C, Mazur SJ, Essigmann JM, Phillips DR, Bohr VA. Inhibition of RNA polymerase II transcription in human cell extracts by cisplatin DNA damage. Biochemistry 1999; 38:6204-12.
246. Andera L, Wasylyk B. Transcription abnormalities potentiate apoptosis of normal human fibroblasts. Mol Med 1997; 3:852-63.
247. Bulmer JT, Zacal NJ, Rainbow AJ. Human cells deficient in transcription-coupled repair show prolonged activation of the Jun N-terminal kinase and increased sensitivity following cisplatin treatment. Cancer Chemother Pharmacol 2005; 56:189-98.
248. Wyllie AH, Golstein P. More than one way to go. Proceedings of the National Academy of Sciences of the United States of America 2001; 98:11-3.
249. Taylor RC, Cullen SP, Martin SJ. Apoptosis: controlled demolition at the cellular level. Nat Rev Mol Cell Biol 2008; 9:231-41.
250. Wyllie AH. Apoptosis: an overview. Br Med Bull 1997; 53:451-65.
251. Janicke RU, Sprengart ML, Wati MR, Porter AG. Caspase-3 is required for DNA fragmentation and morphological changes associated with apoptosis. The Journal of biological chemistry 1998; 273:9357-60.
252. Earnshaw WC, Martins LM, Kaufmann SH. Mammalian caspases: structure, activation, substrates, and functions during apoptosis. Annu Rev Biochem 1999; 68:383-424.
253. Aragane Y, Kulms D, Metze D, Wilkes G, Poppelmann B, Luger TA, Schwarz T. Ultraviolet light induces apoptosis via direct activation of CD95 (Fas/APO-1) independently of its ligand CD95L. The Journal of cell biology 1998; 140:171-82.
254. Chatterjee M, Wu S. Involvement of Fas receptor and not tumor necrosis factor-alpha receptor in ultraviolet-induced activation of acid sphingomyelinase. Molecular carcinogenesis 2001; 30:47-55.
255. Hama-Inaba H, Choi KH, Wang B, Haginoya K, Yamada T, Hayata I, Ohyama H. Fas-independent apoptosis induced by UVC in p53-mutated human epithelial tumor A431 cells through activation of caspase-8 and JNK/SAPK. J Radiat Res (Tokyo) 2001; 42:201-15.
256. Zhan Q, Jin S, Ng B, Plisket J, Shangary S, Rathi A, Brown KD, Baskaran R. Caspase-3 mediated cleavage of BRCA1 during UV-induced apoptosis. Oncogene 2002; 21:5335-45.
257. Denning MF, Wang Y, Tibudan S, Alkan S, Nickoloff BJ, Qin JZ. Caspase activation and disruption of mitochondrial membrane potential during UV radiation-induced apoptosis of human keratinocytes requires activation of protein kinase C. Cell Death Differ 2002; 9:40-52.
258. Wyllie AH. Apoptosis. Death gets a brake. Nature 1994; 369:272-3.
259. Mazumder S, Plesca D, Almasan A. Caspase-3 activation is a critical determinant of genotoxic stress-induced apoptosis. Methods Mol Biol 2008; 414:13-21.
260. Youle RJ, Strasser A. The BCL-2 protein family: opposing activities that mediate cell death. Nat Rev Mol Cell Biol 2008; 9:47-59.
261. Riedl SJ, Shi Y. Molecular mechanisms of caspase regulation during apoptosis. Nat Rev Mol Cell Biol 2004; 5:897-907.
262. Letai AG. Diagnosing and exploiting cancer's addiction to blocks in apoptosis. Nature reviews 2008; 8:121-32.
263. Roos WP, Kaina B. DNA damage-induced cell death by apoptosis. Trends Mol Med 2006; 12:440-50.
264. Durocher D, Jackson SP. DNA-PK, ATM and ATR as sensors of DNA damage: variations on a theme? Current opinion in cell biology 2001; 13:225-31.
265. Falck J, Coates J, Jackson SP. Conserved modes of recruitment of ATM, ATR and DNA-PKcs to sites of DNA damage. Nature 2005; 434:605-11.

266. Stiff T, Walker SA, Cerosaletti K, Goodarzi AA, Petermann E, Concannon P, O'Driscoll M, Jeggo PA. ATR-dependent phosphorylation and activation of ATM in response to UV treatment or replication fork stalling. The EMBO journal 2006; 25:5775-82.
267. Myers JS, Cortez D. Rapid activation of ATR by ionizing radiation requires ATM and Mre11. The Journal of biological chemistry 2006; 281:9346-50.
268. Jazayeri A, Falck J, Lukas C, Bartek J, Smith GC, Lukas J, Jackson SP. ATM- and cell cycle-dependent regulation of ATR in response to DNA double-strand breaks. Nature cell biology 2006; 8:37-45.
269. Tomimatsu N, Tahimic CG, Otsuki A, Burma S, Fukuhara A, Sato K, Shiota G, Oshimura M, Chen DJ, Kurimasa A. Ku70/80 modulates ATM and ATR signaling pathways in response to DNA double strand breaks. The Journal of biological chemistry 2007; 282:10138-45.
270. Colton SL, Xu XS, Wang YA, Wang G. The involvement of ataxia-telangiectasia mutated protein activation in nucleotide excision repair-facilitated cell survival with cisplatin treatment. The Journal of biological chemistry 2006; 281:27117-25.
271. Lewis KA, Lilly KK, Reynolds EA, Sullivan WP, Kaufmann SH, Cliby WA. Ataxia telangiectasia and rad3-related kinase contributes to cell cycle arrest and survival after cisplatin but not oxaliplatin. Mol Cancer Ther 2009; 8:855-63.
272. Rass K, Tilgen W. Treatment of melanoma and nonmelanoma skin cancer. Advances in experimental medicine and biology 2008; 624:296-318.
273. Park DJ, Stoehlmacher J, Lenz HJ. Tailoring chemotherapy in advanced colorectal cancer. Curr Opin Pharmacol 2003; 3:378-85.
274. Barroca H. Fine needle biopsy and genetics, two allied weapons in the diagnosis, prognosis, and target therapeutics of solid pediatric tumors. Diagnostic cytopathology 2008; 36:678-84.
275. Tao X, Hu W, Ramirez PT, Kavanagh JJ. Chemotherapy for recurrent and metastatic cervical cancer. Gynecologic oncology 2008; 110:S67-71.
276. Gonzalez-Martin A. Treatment of recurrent disease: randomized trials of monotherapy versus combination chemotherapy. Int J Gynecol Cancer 2005; 15 Suppl 3:241-6.
277. Guminski AD, Harnett PR, deFazio A. Scientists and clinicians test their metal-back to the future with platinum compounds. Lancet Oncol 2002; 3:312-8.
278. Muller H, Hilger R. Curative and palliative aspects of regional chemotherapy in combination with surgery. Support Care Cancer 2003; 11:1-10.
279. Arnon J, Meirow D, Lewis-Roness H, Ornoy A. Genetic and teratogenic effects of cancer treatments on gametes and embryos. Human reproduction update 2001; 7:394-403.
280. Grillari J, Katinger H, Voglauer R. Contributions of DNA interstrand cross-links to aging of cells and organisms. Nucleic acids research 2007; 35:7566-76.
281. Havelka AM, Berndtsson M, Olofsson MH, Shoshan MC, Linder S. Mechanisms of action of DNA-damaging anticancer drugs in treatment of carcinomas: is acute apoptosis an "off-target" effect? Mini reviews in medicinal chemistry 2007; 7:1035-9.
282. L'Ecuyer T, Sanjeev S, Thomas R, Novak R, Das L, Campbell W, Heide RV. DNA damage is an early event in doxorubicin-induced cardiac myocyte death. American journal of physiology 2006; 291:H1273-80.
283. Rogers LR. Cerebrovascular complications in cancer patients. Neurologic clinics 2003; 21:167-92.
284. Borst P, Rottenberg S, Jonkers J. How do real tumors become resistant to cisplatin? Cell cycle (Georgetown, Tex 2008; 7:1353-9.
285. Stewart DJ. Mechanisms of resistance to cisplatin and carboplatin. Critical reviews in oncology/hematology 2007; 63:12-31.

286. Koberle B, Masters JR, Hartley JA, Wood RD. Defective repair of cisplatin-induced DNA damage caused by reduced XPA protein in testicular germ cell tumours. Curr Biol 1999; 9:273-6.
287. Welsh C, Day R, McGurk C, Masters JR, Wood RD, Koberle B. Reduced levels of XPA, ERCC1 and XPF DNA repair proteins in testis tumor cell lines. International journal of cancer 2004; 110:352-61.
288. Powell SN, Kachnic LA. Therapeutic exploitation of tumor cell defects in homologous recombination. Anti-cancer agents in medicinal chemistry 2008; 8:448-60.
289. Willers H, Kachnic LA, Luo CM, Li L, Purschke M, Borgmann K, Held KD, Powell SN. Biomarkers and mechanisms of FANCD2 function. Journal of biomedicine & biotechnology 2008; 2008:821529.
290. Gurubhagavatula S, Liu G, Park S, Zhou W, Su L, Wain JC, Lynch TJ, Neuberg DS, Christiani DC. XPD and XRCC1 genetic polymorphisms are prognostic factors in advanced non-small-cell lung cancer patients treated with platinum chemotherapy. J Clin Oncol 2004; 22:2594-601.
291. Huang ZH, Hua D, Du X, Li LH, Mao Y, Liu ZH, Song MX, Zhou XK. ERCC1 polymorphism, expression and clinical outcome of oxaliplatin-based adjuvant chemotherapy in gastric cancer. World J Gastroenterol 2008; 14:6401-7.
292. Moreno V, Gemignani F, Landi S, Gioia-Patricola L, Chabrier A, Blanco I, Gonzalez S, Guino E, Capella G, Canzian F. Polymorphisms in genes of nucleotide and base excision repair: risk and prognosis of colorectal cancer. Clin Cancer Res 2006; 12:2101-8.
293. Olaussen KA, Dunant A, Fouret P, Brambilla E, Andre F, Haddad V, Taranchon E, Filipits M, Pirker R, Popper HH, Stahel R, Sabatier L, Pignon JP, Tursz T, Le Chevalier T, Soria JC. DNA repair by ERCC1 in non-small-cell lung cancer and cisplatin-based adjuvant chemotherapy. The New England journal of medicine 2006; 355:983-91.
294. Olaussen KA, Mountzios G, Soria JC. ERCC1 as a risk stratifier in platinum-based chemotherapy for nonsmall-cell lung cancer. Current opinion in pulmonary medicine 2007; 13:284-9.
295. Pantaleo MA, Astolfi A, Nannini M, Paterini P, Piazzi G, Ercolani G, Brandi G, Martinelli G, Pession A, Pinna AD, Biasco G. Gene expression profiling of liver metastases from colorectal cancer as potential basis for treatment choice. British journal of cancer 2008; 99:1729-34.
296. Wei J, Zou Z, Qian X, Ding Y, Xie L, Sanchez JJ, Zhao Y, Feng J, Ling Y, Liu Y, Yu L, Rosell R, Liu B. ERCC1 mRNA levels and survival of advanced gastric cancer patients treated with a modified FOLFOX regimen. British journal of cancer 2008; 98:1398-402.
297. Zhou W, Gurubhagavatula S, Liu G, Park S, Neuberg DS, Wain JC, Lynch TJ, Su L, Christiani DC. Excision repair cross-complementation group 1 polymorphism predicts overall survival in advanced non-small cell lung cancer patients treated with platinum-based chemotherapy. Clin Cancer Res 2004; 10:4939-43.
298. Takebayashi Y, Nakayama K, Kanzaki A, Miyashita H, Ogura O, Mori S, Mutoh M, Miyazaki K, Fukumoto M, Pommier Y. Loss of heterozygosity of nucleotide excision repair factors in sporadic ovarian, colon and lung carcinomas: implication for their roles of carcinogenesis in human solid tumors. Cancer letters 2001; 174:115-25.
299. D'Andrea AD. The Fanconi Anemia/BRCA signaling pathway: disruption in cisplatin-sensitive ovarian cancers. Cell cycle (Georgetown, Tex 2003; 2:290-2.
300. Burkitt K, Ljungman M. Phenylbutyrate interferes with the Fanconi anemia and BRCA pathway and sensitizes head and neck cancer cells to cisplatin. Molecular cancer 2008; 7:24.
301. Helleday T. Amplifying tumour-specific replication lesions by DNA repair inhibitors - a new era in targeted cancer therapy. Eur J Cancer 2008; 44:921-7.
302. Helleday T, Petermann E, Lundin C, Hodgson B, Sharma RA. DNA repair pathways as targets for cancer therapy. Nature reviews 2008; 8:193-204.

303. Martin SA, Lord CJ, Ashworth A. DNA repair deficiency as a therapeutic target in cancer. Current opinion in genetics & development 2008; 18:80-6.
304. Reed E. Platinum-DNA adduct, nucleotide excision repair and platinum based anti-cancer chemotherapy. Cancer Treat Rev 1998; 24:331-44.
305. Kartalou M, Essigmann JM. Recognition of cisplatin adducts by cellular proteins. Mutation research 2001; 478:1-21.
306. Wu Y, Bhattacharyya D, King CL, Baskerville-Abraham I, Huh SH, Boysen G, Swenberg JA, Temple B, Campbell SL, Chaney SG. Solution structures of a DNA dodecamer duplex with and without a cisplatin 1,2-d(GG) intrastrand cross-link: comparison with the same DNA duplex containing an oxaliplatin 1,2-d(GG) intrastrand cross-link. Biochemistry 2007; 46:6477-87.
307. Hendel A, Ziv O, Gueranger Q, Geacintov N, Livneh Z. Reduced efficiency and increased mutagenicity of translesion DNA synthesis across a TT cyclobutane pyrimidine dimer, but not a TT 6-4 photoproduct, in human cells lacking DNA polymerase eta. DNA repair 2008; 7:1636-46.
308. Limoli CL, Giedzinski E, Morgan WF, Cleaver JE. Inaugural article: polymerase eta deficiency in the xeroderma pigmentosum variant uncovers an overlap between the S phase checkpoint and double-strand break repair. Proceedings of the National Academy of Sciences of the United States of America 2000; 97:7939-46.
309. Squires S, Coates JA, Goldberg M, Toji LH, Jackson SP, Clarke DJ, Johnson RT. p53 prevents the accumulation of double-strand DNA breaks at stalled-replication forks induced by UV in human cells. Cell cycle (Georgetown, Tex 2004; 3:1543-57.
310. Ahmad A, Robinson AR, Duensing A, van Drunen E, Beverloo HB, Weisberg DB, Hasty P, Hoeijmakers JH, Niedernhofer LJ. ERCC1-XPF endonuclease facilitates DNA double-strand break repair. Molecular and cellular biology 2008; 28:5082-92.
311. Clingen PH, Arlett CF, Hartley JA, Parris CN. Chemosensitivity of primary human fibroblasts with defective unhooking of DNA interstrand cross-links. Experimental cell research 2007; 313:753-60.
312. Zhang Y, Rohde LH, Emami K, Hammond D, Casey R, Mehta SK, Jeevarajan AS, Pierson DL, Wu H. Suppressed expression of non-DSB repair genes inhibits gamma-radiation-induced cytogenetic repair and cell cycle arrest. DNA repair 2008; 7:1835-45.
313. Muggia F. Platinum compounds 30 years after the introduction of cisplatin: implications for the treatment of ovarian cancer. Gynecologic oncology 2009; 112:275-81.
314. Jones B. Toxicity after cervical cancer treatment using radiotherapy and chemotherapy. Clin Oncol (R Coll Radiol) 2009; 21:56-63.
315. Rosenberg B, Vancamp L, Krigas T. Inhibition of Cell Division in Escherichia Coli by Electrolysis Products from a Platinum Electrode. Nature 1965; 205:698-9.
316. Wang D, Lippard SJ. Cellular processing of platinum anticancer drugs. Nat Rev Drug Discov 2005; 4:307-20.
317. Hartmann JT, Lipp HP. Toxicity of platinum compounds. Expert Opin Pharmacother 2003; 4:889-901.
318. Farrell NP. Preclinical perspectives on the use of platinum compounds in cancer chemotherapy. Semin Oncol 2004; 31:1-9.
319. Rabik CA, Dolan ME. Molecular mechanisms of resistance and toxicity associated with platinating agents. Cancer Treat Rev 2007; 33:9-23.
320. Calvert AH, Harland SJ, Newell DR, Siddik ZH, Jones AC, McElwain TJ, Raju S, Wiltshaw E, Smith IE, Baker JM, Peckham MJ, Harrap KR. Early clinical studies with cis-diammine-1,1-cyclobutane dicarboxylate platinum II. Cancer Chemother Pharmacol 1982; 9:140-7.
321. Waterhouse DM, Reynolds RK, Natale RB. Combined carboplatin and cisplatin. Limited prospects for dose intensification. Cancer 1993; 71:4060-6.

322. Mathe G, Kidani Y, Triana K, Brienza S, Ribaud P, Goldschmidt E, Ecstein E, Despax R, Musset M, Misset JL. A phase I trial of trans-1-diaminocyclohexane oxalato-platinum (l-OHP). Biomed Pharmacother 1986; 40:372-6.
323. Levi F, Perpoint B, Garufi C, Focan C, Chollet P, Depres-Brummer P, Zidani R, Brienza S, Itzhaki M, Iacobelli S, et al. Oxaliplatin activity against metastatic colorectal cancer. A phase II study of 5-day continuous venous infusion at circadian rhythm modulated rate. Eur J Cancer 1993; 29A:1280-4.
324. Lewis D. II. The Use and Place of Caustics in the Treatment of Cancer. Ann Surg 1893; 17:392-7.
325. Ragnhammar P, Hafstrom L, Nygren P, Glimelius B. A systematic overview of chemotherapy effects in colorectal cancer. Acta oncologica (Stockholm, Sweden) 2001; 40:282-308.
326. Kartalou M, Essigmann JM. Mechanisms of resistance to cisplatin. Mutation research 2001; 478:23-43.
327. Zamble DB, Lippard SJ. Cisplatin and DNA repair in cancer chemotherapy. Trends Biochem Sci 1995; 20:435-9.
328. Brabec V, Kasparkova J. Molecular aspects of resistance to antitumor platinum drugs. Drug Resist Updat 2002; 5:147-61.
329. Fajac A, Da Silva J, Ahomadegbe JC, Rateau JG, Bernaudin JF, Riou G, Benard J. Cisplatin-induced apoptosis and p53 gene status in a cisplatin-resistant human ovarian carcinoma cell line. International journal of cancer 1996; 68:67-74.
330. Perego P, Giarola M, Righetti SC, Supino R, Caserini C, Delia D, Pierotti MA, Miyashita T, Reed JC, Zunino F. Association between cisplatin resistance and mutation of p53 gene and reduced bax expression in ovarian carcinoma cell systems. Cancer research 1996; 56:556-62.
331. Righetti SC, Perego P, Corna E, Pierotti MA, Zunino F. Emergence of p53 mutant cisplatin-resistant ovarian carcinoma cells following drug exposure: spontaneously mutant selection. Cell Growth Differ 1999; 10:473-8.
332. O'Connor DJ, Lu X. Stress signals induce transcriptionally inactive E2F-1 independently of p53 and Rb. Oncogene 2000; 19:2369-76.
333. Seluanov A, Gorbunova V, Falcovitz A, Sigal A, Milyavsky M, Zurer I, Shohat G, Goldfinger N, Rotter V. Change of the death pathway in senescent human fibroblasts in response to DNA damage is caused by an inability to stabilize p53. Molecular and cellular biology 2001; 21:1552-64.
334. Armstrong JL, Veal GJ, Redfern CP, Lovat PE. Role of Noxa in p53-independent fenretinide-induced apoptosis of neuroectodermal tumours. Apoptosis 2007; 12:613-22.
335. Zhen W, Link CJ, Jr., O'Connor PM, Reed E, Parker R, Howell SB, Bohr VA. Increased gene-specific repair of cisplatin interstrand cross-links in cisplatin-resistant human ovarian cancer cell lines. Molecular and cellular biology 1992; 12:3689-98.
336. Zhen W, Evans MK, Haggerty CM, Bohr VA. Deficient gene specific repair of cisplatin-induced lesions in Xeroderma pigmentosum and Fanconi's anemia cell lines. Carcinogenesis 1993; 14:919-24.
337. Chao CC. Enhanced excision repair of DNA damage due to cis-diamminedichloroplatinum(II) in resistant cervix carcinoma HeLa cells. Eur J Pharmacol 1994; 268:347-55.
338. Aebi S, Kurdi-Haidar B, Gordon R, Cenni B, Zheng H, Fink D, Christen RD, Boland CR, Koi M, Fishel R, Howell SB. Loss of DNA mismatch repair in acquired resistance to cisplatin. Cancer research 1996; 56:3087-90.
339. States JC, Reed E. Enhanced XPA mRNA levels in cisplatin-resistant human ovarian cancer are not associated with XPA mutations or gene amplification. Cancer letters 1996; 108:233-7.

340. Aebi S, Fink D, Gordon R, Kim HK, Zheng H, Fink JL, Howell SB. Resistance to cytotoxic drugs in DNA mismatch repair-deficient cells. Clin Cancer Res 1997; 3:1763-7.
341. Fink D, Zheng H, Nebel S, Norris PS, Aebi S, Lin TP, Nehme A, Christen RD, Haas M, MacLeod CL, Howell SB. In vitro and in vivo resistance to cisplatin in cells that have lost DNA mismatch repair. Cancer research 1997; 57:1841-5.
342. Damia G, Guidi G, D'Incalci M. Expression of genes involved in nucleotide excision repair and sensitivity to cisplatin and melphalan in human cancer cell lines. Eur J Cancer 1998; 34:1783-8.
343. Vaisman A, Varchenko M, Umar A, Kunkel TA, Risinger JI, Barrett JC, Hamilton TC, Chaney SG. The role of hMLH1, hMSH3, and hMSH6 defects in cisplatin and oxaliplatin resistance: correlation with replicative bypass of platinum-DNA adducts. Cancer research 1998; 58:3579-85.
344. Ferry KV, Hamilton TC, Johnson SW. Increased nucleotide excision repair in cisplatin-resistant ovarian cancer cells: role of ERCC1-XPF. Biochemical pharmacology 2000; 60:1305-13.
345. Zdraveski ZZ, Mello JA, Marinus MG, Essigmann JM. Multiple pathways of recombination define cellular responses to cisplatin. Chem Biol 2000; 7:39-50.
346. Bassett E, Vaisman A, Tropea KA, McCall CM, Masutani C, Hanaoka F, Chaney SG. Frameshifts and deletions during in vitro translesion synthesis past Pt-DNA adducts by DNA polymerases beta and eta. DNA repair 2002; 1:1003-16.
347. Albertella MR, Green CM, Lehmann AR, O'Connor MJ. A role for polymerase eta in the cellular tolerance to cisplatin-induced damage. Cancer research 2005; 65:9799-806.
348. Arnould S, Hennebelle I, Canal P, Bugat R, Guichard S. Cellular determinants of oxaliplatin sensitivity in colon cancer cell lines. Eur J Cancer 2003; 39:112-9.
349. Rosell R, Taron M, Alberola V, Massuti B, Felip E. Genetic testing for chemotherapy in non-small cell lung cancer. Lung cancer (Amsterdam, Netherlands) 2003; 41 Suppl 1:S97-102.
350. Stevens EV, Nishizuka S, Antony S, Reimers M, Varma S, Young L, Munson PJ, Weinstein JN, Kohn EC, Pommier Y. Predicting cisplatin and trabectedin drug sensitivity in ovarian and colon cancers. Mol Cancer Ther 2008; 7:10-8.
351. Lord CJ, McDonald S, Swift S, Turner NC, Ashworth A. A high-throughput RNA interference screen for DNA repair determinants of PARP inhibitor sensitivity. DNA repair 2008; 7:2010-9.
352. Mohrenweiser HW, Jones IM. Variation in DNA repair is a factor in cancer susceptibility: a paradigm for the promises and perils of individual and population risk estimation? Mutation research 1998; 400:15-24.
353. Proietti De Santis L, Garcia CL, Balajee AS, Brea Calvo GT, Bassi L, Palitti F. Transcription coupled repair deficiency results in increased chromosomal aberrations and apoptotic death in the UV61 cell line, the Chinese hamster homologue of Cockayne's syndrome B. Mutation research 2001; 485:121-32.
354. Saldivar JS, Lu KH, Liang D, Gu J, Huang M, Vlastos AT, Follen M, Wu X. Moving toward individualized therapy based on NER polymorphisms that predict platinum sensitivity in ovarian cancer patients. Gynecologic oncology 2007; 107:S223-9.
355. Simon GR, Ismail-Khan R, Bepler G. Nuclear excision repair-based personalized therapy for non-small cell lung cancer: from hypothesis to reality. Int J Biochem Cell Biol 2007; 39:1318-28.
356. Dabholkar M, Thornton K, Vionnet J, Bostick-Bruton F, Yu JJ, Reed E. Increased mRNA levels of xeroderma pigmentosum complementation group B (XPB) and Cockayne's syndrome complementation group B (CSB) without increased mRNA levels of multidrug-resistance gene (MDR1) or metallothionein-II (MT-II) in platinum-resistant human ovarian cancer tissues. Biochemical pharmacology 2000; 60:1611-9.
357. Yu JJ, Mu C, Lee KB, Okamoto A, Reed EL, Bostick-Bruton F, Mitchell KC, Reed E. A nucleotide polymorphism in ERCC1 in human ovarian cancer cell lines and tumor tissues. Mutation research 1997; 382:13-20.

358. Sun X, Li F, Sun N, Shukui Q, Baoan C, Jifeng F, Lu C, Zuhong L, Hongyan C, Yuandong C, Jiazhong J, Yingfeng Z. Polymorphisms in XRCC1 and XPG and response to platinum-based chemotherapy in advanced non-small cell lung cancer patients. Lung cancer (Amsterdam, Netherlands) 2009.
359. Weaver DA, Crawford EL, Warner KA, Elkhairi F, Khuder SA, Willey JC. ABCC5, ERCC2, XPA and XRCC1 transcript abundance levels correlate with cisplatin chemoresistance in non-small cell lung cancer cell lines. Molecular cancer 2005; 4:18.
360. Chu G, Chang E. Xeroderma pigmentosum group E cells lack a nuclear factor that binds to damaged DNA. Science (New York, NY 1988; 242:564-7.
361. Dabholkar M, Vionnet J, Bostick-Bruton F, Yu JJ, Reed E. Messenger RNA levels of XPAC and ERCC1 in ovarian cancer tissue correlate with response to platinum-based chemotherapy. The Journal of clinical investigation 1994; 94:703-8.
362. Nichols AF, Ong P, Linn S. Mutations specific to the xeroderma pigmentosum group E Ddb- phenotype. The Journal of biological chemistry 1996; 271:24317-20.
363. Tang JY, Hwang BJ, Ford JM, Hanawalt PC, Chu G. Xeroderma pigmentosum p48 gene enhances global genomic repair and suppresses UV-induced mutagenesis. Molecular cell 2000; 5:737-44.
364. van der Wees CG, Vreeswijk MP, Persoon M, van der Laarse A, van Zeeland AA, Mullenders LH. Deficient global genome repair of UV-induced cyclobutane pyrimidine dimers in terminally differentiated myocytes and proliferating fibroblasts from the rat heart. DNA repair 2003; 2:1297-308.
365. Wittschieben BO, Iwai S, Wood RD. DDB1-DDB2 (xeroderma pigmentosum group E) protein complex recognizes a cyclobutane pyrimidine dimer, mismatches, apurinic/apyrimidinic sites, and compound lesions in DNA. The Journal of biological chemistry 2005; 280:39982-9.
366. Rosell R, Taron M, Ariza A, Barnadas A, Mate JL, Reguart N, Margel M, Felip E, Mendez P, Garcia-Campelo R. Molecular predictors of response to chemotherapy in lung cancer. Semin Oncol 2004; 31:20-7.
367. McKay BC, Ljungman M. Role for p53 in the recovery of transcription and protection against apoptosis induced by ultraviolet light. Neoplasia (New York, NY 1999; 1:276-84.
368. Felip E, Rosell R. Testing for excision repair cross-complementing 1 in patients with non-small-cell lung cancer for chemotherapy response. Expert review of molecular diagnostics 2007; 7:261-8.
369. Fautrel A, Andrieux L, Musso O, Boudjema K, Guillouzo A, Langouet S. Overexpression of the two nucleotide excision repair genes ERCC1 and XPC in human hepatocellular carcinoma. J Hepatol 2005; 43:288-93.
370. Booton R, Ward T, Ashcroft L, Morris J, Heighway J, Thatcher N. ERCC1 mRNA expression is not associated with response and survival after platinum-based chemotherapy regimens in advanced non-small cell lung cancer. J Thorac Oncol 2007; 2:902-6.
371. Itoh T, O'Shea C, Linn S. Impaired regulation of tumor suppressor p53 caused by mutations in the xeroderma pigmentosum DDB2 gene: mutual regulatory interactions between p48(DDB2) and p53. Molecular and cellular biology 2003; 23:7540-53.
372. Sauerbier W, Hercules K. Gene and transcription unit mapping by radiation effects. Annual review of genetics 1978; 12:329-63.
373. Friedberg EC, Aguilera A, Gellert M, Hanawalt PC, Hays JB, Lehmann AR, Lindahl T, Lowndes N, Sarasin A, Wood RD. DNA repair: from molecular mechanism to human disease. DNA repair 2006; 5:986-96.
374. Latonen L, Laiho M. Cellular UV damage responses--functions of tumor suppressor p53. Biochim Biophys Acta 2005; 1755:71-89.

375. Ljungman M, Lane DP. Transcription - guarding the genome by sensing DNA damage. Nature reviews 2004; 4:727-37.
376. Hwang BJ, Ford JM, Hanawalt PC, Chu G. Expression of the p48 xeroderma pigmentosum gene is p53-dependent and is involved in global genomic repair. Proceedings of the National Academy of Sciences of the United States of America 1999; 96:424-8.
377. Zhao R, Gish K, Murphy M, Yin Y, Notterman D, Hoffman WH, Tom E, Mack DH, Levine AJ. Analysis of p53-regulated gene expression patterns using oligonucleotide arrays. Genes & development 2000; 14:981-93.
378. Polyak K, Xia Y, Zweier JL, Kinzler KW, Vogelstein B. A model for p53-induced apoptosis. Nature 1997; 389:300-5.
379. Smith JM, Stubbert LJ, Hamill JD, McKay BC. The contribution of transactivation subdomains 1 and 2 to p53-induced gene expression is heterogeneous but not subdomain-specific. Neoplasia (New York, NY 2007; 9:1057-65.
380. McKay BC, Stubbert LJ, Fowler CC, Smith JM, Cardamore RA, Spronck JC. Regulation of ultraviolet light-induced gene expression by gene size. Proceedings of the National Academy of Sciences of the United States of America 2004; 101:6582-6.
381. Guzman E, Langowski JL, Owen-Schaub L. Mad dogs, Englishmen and apoptosis: the role of cell death in UV-induced skin cancer. Apoptosis 2003; 8:315-25.
382. Brash DE. Roles of the transcription factor p53 in keratinocyte carcinomas. Br J Dermatol 2006; 154 Suppl 1:8-10.
383. McKay BC, Ljungman M, Rainbow AJ. Persistent DNA damage induced by ultraviolet light inhibits p21waf1 and bax expression: implications for DNA repair, UV sensitivity and the induction of apoptosis. Oncogene 1998; 17:545-55.
384. Yamaizumi M, Sugano T. U.v.-induced nuclear accumulation of p53 is evoked through DNA damage of actively transcribed genes independent of the cell cycle. Oncogene 1994; 9:2775-84.
385. Dumaz N, Duthu A, Ehrhart JC, Drougard C, Appella E, Anderson CW, May P, Sarasin A, Daya-Grosjean L. Prolonged p53 protein accumulation in trichothiodystrophy fibroblasts dependent on unrepaired pyrimidine dimers on the transcribed strands of cellular genes. Molecular carcinogenesis 1997; 20:340-7.
386. Queille S, Drougard C, Sarasin A, Daya-Grosjean L. Effects of XPD mutations on ultraviolet-induced apoptosis in relation to skin cancer-proneness in repair-deficient syndromes. J Invest Dermatol 2001; 117:1162-70.
387. Conforti G, Nardo T, D'Incalci M, Stefanini M. Proneness to UV-induced apoptosis in human fibroblasts defective in transcription coupled repair is associated with the lack of Mdm2 transactivation. Oncogene 2000; 19:2714-20.
388. Proietti De Santis L, Balajee AS, Lorenti Garcia C, Pepe G, Worboys AM, Palitti F. Inhibition of p53, p21 and Bax by pifithrin-alpha does not affect UV induced apoptotic response in CS-B cells. DNA repair 2003; 2:891-900.
389. Wani MA, Zhu QZ, El-Mahdy M, Wani AA. Influence of p53 tumor suppressor protein on bias of DNA repair and apoptotic response in human cells. Carcinogenesis 1999; 20:765-72.
390. Smith ML, Fornace AJ, Jr. The two faces of tumor suppressor p53. Am J Pathol 1996; 148:1019-22.
391. McKay BC, Chen F, Perumalswami CR, Zhang F, Ljungman M. The tumor suppressor p53 can both stimulate and inhibit ultraviolet light-induced apoptosis. Molecular biology of the cell 2000; 11:2543-51.
392. Nichols AF, Itoh T, Graham JA, Liu W, Yamaizumi M, Linn S. Human damage-specific DNA-binding protein p48. Characterization of XPE mutations and regulation following UV irradiation. The Journal of biological chemistry 2000; 275:21422-8.

393. Li J, Wang QE, Zhu Q, El-Mahdy MA, Wani G, Praetorius-Ibba M, Wani AA. DNA damage binding protein component DDB1 participates in nucleotide excision repair through DDB2 DNA-binding and cullin 4A ubiquitin ligase activity. Cancer research 2006; 66:8590-7.
394. Matsuda N, Azuma K, Saijo M, Iemura S, Hioki Y, Natsume T, Chiba T, Tanaka K. DDB2, the xeroderma pigmentosum group E gene product, is directly ubiquitylated by Cullin 4A-based ubiquitin ligase complex. DNA repair 2005; 4:537-45.
395. Moser J, Volker M, Kool H, Alekseev S, Vrieling H, Yasui A, van Zeeland AA, Mullenders LH. The UV-damaged DNA binding protein mediates efficient targeting of the nucleotide excision repair complex to UV-induced photo lesions. DNA repair 2005; 4:571-82.
396. Hayes S, Shiyanov P, Chen X, Raychaudhuri P. DDB, a putative DNA repair protein, can function as a transcriptional partner of E2F1. Molecular and cellular biology 1998; 18:240-9.
397. Shiyanov P, Hayes SA, Donepudi M, Nichols AF, Linn S, Slagle BL, Raychaudhuri P. The naturally occurring mutants of DDB are impaired in stimulating nuclear import of the p125 subunit and E2F1-activated transcription. Molecular and cellular biology 1999; 19:4935-43.
398. Datta A, Bagchi S, Nag A, Shiyanov P, Adami GR, Yoon T, Raychaudhuri P. The p48 subunit of the damaged-DNA binding protein DDB associates with the CBP/p300 family of histone acetyltransferase. Mutation research 2001; 486:89-97.
399. Stubbert LJ, Hamill JD, Spronck JC, Smith JM, Becerril C, McKay BC. DDB2-independent role for p53 in the recovery from ultraviolet light-induced replication arrest. Cell cycle (Georgetown, Tex 2007; 6:1730-40.
400. Hitt MM, Addison CL, Graham FL. Human adenovirus vectors for gene transfer into mammalian cells. Advances in pharmacology (San Diego, Calif 1997; 40:137-206.
401. Bertho AL, Santiago MA, Coutinho SG. Flow cytometry in the study of cell death. Mem Inst Oswaldo Cruz 2000; 95:429-33.
402. Ormerod MG, Paul F, Cheetham M, Sun XM. Discrimination of apoptotic thymocytes by forward light scatter. Cytometry 1995; 21:300-4.
403. Darzynkiewicz Z, Bruno S, Del Bino G, Gorczyca W, Hotz MA, Lassota P, Traganos F. Features of apoptotic cells measured by flow cytometry. Cytometry 1992; 13:795-808.
404. Jin Z, El-Deiry WS. Overview of cell death signaling pathways. Cancer Biol Ther 2005; 4:139-63.
405. Vogelstein B, Lane D, Levine AJ. Surfing the p53 network. Nature 2000; 408:307-10.
406. Clement V, Dunand-Sauthier I, Clarkson SG. Suppression of UV-induced apoptosis by the human DNA repair protein XPG. Cell Death Differ 2006; 13:478-88.
407. Itoh T, Cado D, Kamide R, Linn S. DDB2 gene disruption leads to skin tumors and resistance to apoptosis after exposure to ultraviolet light but not a chemical carcinogen. Proceedings of the National Academy of Sciences of the United States of America 2004; 101:2052-7.
408. Lackinger D, Kaina B. Primary mouse fibroblasts deficient for c-Fos, p53 or for both proteins are hypersensitive to UV light and alkylating agent-induced chromosomal breakage and apoptosis. Mutation research 2000; 457:113-23.
409. Dunkern TR, Kaina B. Cell proliferation and DNA breaks are involved in ultraviolet light-induced apoptosis in nucleotide excision repair-deficient Chinese hamster cells. Molecular biology of the cell 2002; 13:348-61.
410. da Costa RM, Quayle C, de Fatima Jacysyn J, Amarante-Mendes GP, Sarasin A, Menck CF. Resistance to ultraviolet-induced apoptosis in DNA repair deficient growth arrested human fibroblasts is not related to recovery from RNA transcription blockage. Mutation research 2008; 640:1-7.
411. Kumari A, Schultz N, Helleday T. p53 protects from replication-associated DNA double-strand breaks in mammalian cells. Oncogene 2004; 23:2324-9.

412. Polyak K, Waldman T, He TC, Kinzler KW, Vogelstein B. Genetic determinants of p53-induced apoptosis and growth arrest. Genes & development 1996; 10:1945-52.
413. Yonish-Rouach E, Resnitzky D, Lotem J, Sachs L, Kimchi A, Oren M. Wild-type p53 induces apoptosis of myeloid leukaemic cells that is inhibited by interleukin-6. Nature 1991; 352:345-7.
414. el-Deiry WS, Harper JW, O'Connor PM, Velculescu VE, Canman CE, Jackman J, Pietenpol JA, Burrell M, Hill DE, Wang Y, et al. WAF1/CIP1 is induced in p53-mediated G1 arrest and apoptosis. Cancer research 1994; 54:1169-74.
415. Carvalho H, da Costa RM, Chigancas V, Weinlich R, Brumatti G, Amarante-Mendes GP, Sarasin A, Menck CF. Effect of cell confluence on ultraviolet light apoptotic responses in DNA repair deficient cells. Mutation research 2003; 544:159-66.
416. Cleaver JE. Ultraviolet photobiology: its early roots and insights into DNA repair. DNA repair 2002; 1:977-9.
417. Barley RD, Enns L, Paterson MC, Mirzayans R. Aberrant p21WAF1-dependent growth arrest as the possible mechanism of abnormal resistance to ultraviolet light cytotoxicity in Li-Fraumeni syndrome fibroblast strains heterozygous for TP53 mutations. Oncogene 1998; 17:533-43.
418. Latonen L, Taya Y, Laiho M. UV-radiation induces dose-dependent regulation of p53 response and modulates p53-HDM2 interaction in human fibroblasts. Oncogene 2001; 20:6784-93.
419. Gentile M, Latonen L, Laiho M. Cell cycle arrest and apoptosis provoked by UV radiation-induced DNA damage are transcriptionally highly divergent responses. Nucleic acids research 2003; 31:4779-90.
420. Hamdi M, Kool J, Cornelissen-Steijger P, Carlotti F, Popeijus HE, van der Burgt C, Janssen JM, Yasui A, Hoeben RC, Terleth C, Mullenders LH, van Dam H. DNA damage in transcribed genes induces apoptosis via the JNK pathway and the JNK-phosphatase MKP-1. Oncogene 2005; 24:7135-44.
421. Alekseev S, Kool H, Rebel H, Fousteri M, Moser J, Backendorf C, de Gruijl FR, Vrieling H, Mullenders LH. Enhanced DDB2 expression protects mice from carcinogenic effects of chronic UV-B irradiation. Cancer research 2005; 65:10298-306.
422. May A, Nairn RS, Okumoto DS, Wassermann K, Stevnsner T, Jones JC, Bohr VA. Repair of individual DNA strands in the hamster dihydrofolate reductase gene after treatment with ultraviolet light, alkylating agents, and cisplatin. The Journal of biological chemistry 1993; 268:1650-7.
423. Jones JC, Zhen WP, Reed E, Parker RJ, Sancar A, Bohr VA. Gene-specific formation and repair of cisplatin intrastrand adducts and interstrand cross-links in Chinese hamster ovary cells. The Journal of biological chemistry 1991; 266:7101-7.
424. Sancar A. DNA excision repair. Annu Rev Biochem 1996; 65:43-81.
425. Balajee AS, Bohr VA. Genomic heterogeneity of nucleotide excision repair. Gene 2000; 250:15-30.
426. Tu Y, Bates S, Pfeifer GP. The transcription-repair coupling factor CSA is required for efficient repair only during the elongation stages of RNA polymerase II transcription. Mutation research 1998; 400:143-51.
427. Brash DE, Wikonkal NM, Remenyik E, van der Horst GT, Friedberg EC, Cheo DL, van Steeg H, Westerman A, van Kranen HJ. The DNA damage signal for Mdm2 regulation, Trp53 induction, and sunburn cell formation in vivo originates from actively transcribed genes. J Invest Dermatol 2001; 117:1234-40.
428. de Waard H, Sonneveld E, de Wit J, Esveldt-van Lange R, Hoeijmakers JH, Vrieling H, van der Horst GT. Cell-type-specific consequences of nucleotide excision repair deficiencies: Embryonic stem cells versus fibroblasts. DNA repair 2008; 7:1659-69.

429. Garssen J, van Steeg H, de Gruijl F, de Boer J, van der Horst GT, van Kranen H, van Loveren H, van Dijk M, Fluitman A, Weeda G, Hoeijmakers JH. Transcription-coupled and global genome repair differentially influence UV-B-induced acute skin effects and systemic immunosuppression. J Immunol 2000; 164:6199-205.
430. Brattain MG, Fine WD, Khaled FM, Thompson J, Brattain DE. Heterogeneity of malignant cells from a human colonic carcinoma. Cancer research 1981; 41:1751-6.
431. Stone KR, Mickey DD, Wunderli H, Mickey GH, Paulson DF. Isolation of a human prostate carcinoma cell line (DU 145). International journal of cancer 1978; 21:274-81.
432. Kaighn ME, Narayan KS, Ohnuki Y, Lechner JF, Jones LW. Establishment and characterization of a human prostatic carcinoma cell line (PC-3). Invest Urol 1979; 17:16-23.
433. Yeh CC, Lee C, Dahiya R. DNA mismatch repair enzyme activity and gene expression in prostate cancer. Biochem Biophys Res Commun 2001; 285:409-13.
434. Koi M, Umar A, Chauhan DP, Cherian SP, Carethers JM, Kunkel TA, Boland CR. Human chromosome 3 corrects mismatch repair deficiency and microsatellite instability and reduces N-methyl-N'-nitro-N-nitrosoguanidine tolerance in colon tumor cells with homozygous hMLH1 mutation. Cancer research 1994; 54:4308-12.
435. Chen Y, Wang J, Fraig MM, Metcalf J, Turner WR, Bissada NK, Watson DK, Schweinfest CW. Defects of DNA mismatch repair in human prostate cancer. Cancer research 2001; 61:4112-21.
436. McKay BC, Rainbow AJ. Heat-shock enhanced reactivation of a UV-damaged reporter gene in human cells involves the transcription coupled DNA repair pathway. Mutation research 1996; 363:125-35.
437. Lee DF, Drouin R, Pitsikas P, Rainbow AJ. Detection of an involvement of the human mismatch repair genes hMLH1 and hMSH2 in nucleotide excision repair is dependent on UVC fluence to cells. Cancer research 2004; 64:3865-70.
438. Protic-Sabljic M, Kraemer KH. One pyrimidine dimer inactivates expression of a transfected gene in xeroderma pigmentosum cells. Proceedings of the National Academy of Sciences of the United States of America 1985; 82:6622-6.
439. Francis MA, Rainbow AJ. UV-enhanced reactivation of a UV-damaged reporter gene suggests transcription-coupled repair is UV-inducible in human cells. Carcinogenesis 1999; 20:19-26.
440. Boszko IP, Rainbow AJ. Removal of UV photoproducts from an adenovirus-encoded reporter gene following infection of unirradiated and UV-irradiated human fibroblasts. Somat Cell Mol Genet 1999; 25:301-15.
441. Rainbow AJ, McKay BC, Francis MA. Recombinant adenoviruses as expression vectors and as probes for DNA repair in human cells. Gene Therapy and Molecular Biology 2000; 5:87-100.
442. Fink D, Aebi S, Howell SB. The role of DNA mismatch repair in drug resistance. Clin Cancer Res 1998; 4:1-6.
443. Bernstein C, Bernstein H, Payne CM, Garewal H. DNA repair/pro-apoptotic dual-role proteins in five major DNA repair pathways: fail-safe protection against carcinogenesis. Mutation research 2002; 511:145-78.
444. Stojic L, Brun R, Jiricny J. Mismatch repair and DNA damage signalling. DNA repair 2004; 3:1091-101.
445. van Hoffen A, Natarajan AT, Mayne LV, van Zeeland AA, Mullenders LH, Venema J. Deficient repair of the transcribed strand of active genes in Cockayne's syndrome cells. Nucleic acids research 1993; 21:5890-5.
446. van Oosterwijk MF, Versteeg A, Filon R, van Zeeland AA, Mullenders LH. The sensitivity of Cockayne's syndrome cells to DNA-damaging agents is not due to defective transcription-coupled repair of active genes. Molecular and cellular biology 1996; 16:4436-44.

447. Proietti-De-Santis L, Drane P, Egly JM. Cockayne syndrome B protein regulates the transcriptional program after UV irradiation. The EMBO journal 2006; 25:1915-23.
448. Fousteri M, van Hoffen A, Vargova H, Mullenders LH. Repair of DNA lesions in chromosomal DNA impact of chromatin structure and Cockayne syndrome proteins. DNA repair 2005; 4:919-25.
449. Mellon I, Rajpal DK, Koi M, Boland CR, Champe GN. Transcription-coupled repair deficiency and mutations in human mismatch repair genes. Science (New York, NY 1996; 272:557-60.
450. Adimoolam S, Lin CX, Ford JM. The p53-regulated cyclin-dependent kinase inhibitor, p21 (cip1, waf1, sdi1), is not required for global genomic and transcription-coupled nucleotide excision repair of UV-induced DNA photoproducts. The Journal of biological chemistry 2001; 276:25813-22.
451. Sonneveld E, Vrieling H, Mullenders LH, van Hoffen A. Mouse mismatch repair gene Msh2 is not essential for transcription-coupled repair of UV-induced cyclobutane pyrimidine dimers. Oncogene 2001; 20:538-41.
452. Rochette PJ, Bastien N, McKay BC, Therrien JP, Drobetsky EA, Drouin R. Human cells bearing homozygous mutations in the DNA mismatch repair genes hMLH1 or hMSH2 are fully proficient in transcription-coupled nucleotide excision repair. Oncogene 2002; 21:5743-52.
453. Bhattacharyya NP, Ganesh A, Phear G, Richards B, Skandalis A, Meuth M. Molecular analysis of mutations in mutator colorectal carcinoma cell lines. Human molecular genetics 1995; 4:2057-64.
454. Boyer JC, Umar A, Risinger JI, Lipford JR, Kane M, Yin S, Barrett JC, Kolodner RD, Kunkel TA. Microsatellite instability, mismatch repair deficiency, and genetic defects in human cancer cell lines. Cancer research 1995; 55:6063-70.
455. Vassileva V, Millar A, Briollais L, Chapman W, Bapat B. Genes involved in DNA repair are mutational targets in endometrial cancers with microsatellite instability. Cancer research 2002; 62:4095-9.
456. Siddik ZH. Cisplatin: mode of cytotoxic action and molecular basis of resistance. Oncogene 2003; 22:7265-79.
457. Petersen LN, Mamenta EL, Stevnsner T, Chaney SG, Bohr VA. Increased gene specific repair of cisplatin induced interstrand crosslinks in cisplatin resistant cell lines, and studies on carrier ligand specificity. Carcinogenesis 1996; 17:2597-602.
458. Lupi M, Matera G, Natoli C, Colombo V, Ubezio P. The contribution of p53 in the dynamics of cell cycle response to DNA damage interpreted by a mathematical model. Cell cycle (Georgetown, Tex 2007; 6:943-50.
459. Bhana S, Lloyd DR. The role of p53 in DNA damage-mediated cytotoxicity overrides its ability to regulate nucleotide excision repair in human fibroblasts. Mutagenesis 2008; 23:43-50.
460. Vazquez A, Bond EE, Levine AJ, Bond GL. The genetics of the p53 pathway, apoptosis and cancer therapy. Nat Rev Drug Discov 2008; 7:979-87.
461. Simon GR, Sharma S, Cantor A, Smith P, Bepler G. ERCC1 expression is a predictor of survival in resected patients with non-small cell lung cancer. Chest 2005; 127:978-83.
462. Ceppi P, Longo M, Volante M, Novello S, Cappia S, Bacillo E, Selvaggi G, Saviozzi S, Calogero R, Papotti M, Scagliotti GV. Excision repair cross complementing-1 and topoisomerase IIalpha gene expression in small-cell lung cancer patients treated with platinum and etoposide: a retrospective study. J Thorac Oncol 2008; 3:583-9.
463. Kim MK, Cho KJ, Kwon GY, Park SI, Kim YH, Kim JH, Song HY, Shin JH, Jung HY, Lee GH, Choi KD, Kim SB. Patients with ERCC1-negative locally advanced esophageal cancers may benefit from preoperative chemoradiotherapy. Clin Cancer Res 2008; 14:4225-31.
464. Handra-Luca A, Hernandez J, Mountzios G, Taranchon E, Lacau-St-Guily J, Soria JC, Fouret P. Excision repair cross complementation group 1 immunohistochemical expression predicts ob-

jective response and cancer-specific survival in patients treated by Cisplatin-based induction chemotherapy for locally advanced head and neck squamous cell carcinoma. Clin Cancer Res 2007; 13:3855-9.
465. Bellmunt J, Paz-Ares L, Cuello M, Cecere FL, Albiol S, Guillem V, Gallardo E, Carles J, Mendez P, de la Cruz JJ, Taron M, Rosell R, Baselga J. Gene expression of ERCC1 as a novel prognostic marker in advanced bladder cancer patients receiving cisplatin-based chemotherapy. Ann Oncol 2007; 18:522-8.
466. Rick O, Siegert W, Beyer J. Chemotherapy in patients with metastatic or relapsed germ-cell tumours. Cancer Treat Rev 2001; 27:283-8.
467. Einhorn LH. Chemotherapeutic and surgical strategies for germ cell tumors. Chest Surg Clin N Am 2002; 12:695-706.
468. Einhorn LH. Curing metastatic testicular cancer. Proceedings of the National Academy of Sciences of the United States of America 2002; 99:4592-5.
469. de las Alas MM, Aebi S, Fink D, Howell SB, Los G. Loss of DNA mismatch repair: effects on the rate of mutation to drug resistance. J Natl Cancer Inst 1997; 89:1537-41.
470. Bunz F, Hwang PM, Torrance C, Waldman T, Zhang Y, Dillehay L, Williams J, Lengauer C, Kinzler KW, Vogelstein B. Disruption of p53 in human cancer cells alters the responses to therapeutic agents. The Journal of clinical investigation 1999; 104:263-9.
471. Hao DL, Liu CM, Dong WJ, Gong H, Wu XS, Liu DP, Liang CC. Knockdown of human p53 gene expression in 293-T cells by retroviral vector-mediated short hairpin RNA. Acta Biochim Biophys Sin (Shanghai) 2005; 37:779-83.
472. Clontech Laboratories I. Retroviral Gene Transfer and Expression User Manual. Protocol No PT3132-1, 2009:41.
473. Rose WC, Basler GA. In vivo model development of cisplatin-resistant and -sensitive A2780 human ovarian carcinomas. In Vivo 1990; 4:391-6.
474. Jiricny J. The multifaceted mismatch-repair system. Nat Rev Mol Cell Biol 2006; 7:335-46.
475. Hsieh P, Yamane K. DNA mismatch repair: molecular mechanism, cancer, and ageing. Mech Ageing Dev 2008; 129:391-407.
476. Strand M, Prolla TA, Liskay RM, Petes TD. Destabilization of tracts of simple repetitive DNA in yeast by mutations affecting DNA mismatch repair. Nature 1993; 365:274-6.
477. Harfe BD, Jinks-Robertson S. DNA mismatch repair and genetic instability. Annual review of genetics 2000; 34:359-99.
478. Papadopoulos N, Nicolaides NC, Wei YF, Ruben SM, Carter KC, Rosen CA, Haseltine WA, Fleischmann RD, Fraser CM, Adams MD, et al. Mutation of a mutL homolog in hereditary colon cancer. Science (New York, NY 1994; 263:1625-9.
479. Bronner CE, Baker SM, Morrison PT, Warren G, Smith LG, Lescoe MK, Kane M, Earabino C, Lipford J, Lindblom A, et al. Mutation in the DNA mismatch repair gene homologue hMLH1 is associated with hereditary non-polyposis colon cancer. Nature 1994; 368:258-61.
480. Fink D, Nebel S, Norris PS, Baergen RN, Wilczynski SP, Costa MJ, Haas M, Cannistra SA, Howell SB. Enrichment for DNA mismatch repair-deficient cells during treatment with cisplatin. International journal of cancer 1998; 77:741-6.
481. Pani E, Stojic L, El-Shemerly M, Jiricny J, Ferrari S. Mismatch repair status and the response of human cells to cisplatin. Cell cycle (Georgetown, Tex 2007; 6:1796-802.
482. Kaina B. DNA damage-triggered apoptosis: critical role of DNA repair, double-strand breaks, cell proliferation and signaling. Biochemical pharmacology 2003; 66:1547-54.
483. Peters AC, Young LC, Maeda T, Tron VA, Andrew SE. Mammalian DNA mismatch repair protects cells from UVB-induced DNA damage by facilitating apoptosis and p53 activation. DNA repair 2003; 2:427-35.

484. Yanamadala S, Ljungman M. Potential role of MLH1 in the induction of p53 and apoptosis by blocking transcription on damaged DNA templates. Mol Cancer Res 2003; 1:747-54.
485. Li HR, Shagisultanova EI, Yamashita K, Piao Z, Perucho M, Malkhosyan SR. Hypersensitivity of tumor cell lines with microsatellite instability to DNA double strand break producing chemotherapeutic agent bleomycin. Cancer research 2004; 64:4760-7.
486. van Oosten M, Stout GJ, Backendorf C, Rebel H, de Wind N, Darroudi F, van Kranen HJ, de Gruijl FR, Mullenders LH. Mismatch repair protein Msh2 contributes to UVB-induced cell cycle arrest in epidermal and cultured mouse keratinocytes. DNA repair 2005; 4:81-9.
487. Mellon I, Champe GN. Products of DNA mismatch repair genes mutS and mutL are required for transcription-coupled nucleotide-excision repair of the lactose operon in Escherichia coli. Proceedings of the National Academy of Sciences of the United States of America 1996; 93:1292-7.
488. Yang Y, Johnson AL, Johnston LH, Siede W, Friedberg EC, Ramachandran K, Kunz BA. A mutation in a Saccharomyces cerevisiae gene (RAD3) required for nucleotide excision repair and transcription increases the efficiency of mismatch correction. Genetics 1996; 144:459-66.
489. Feng WY, Lee EH, Hays JB. Recombinagenic processing of UV-light photoproducts in nonreplicating phage DNA by the Escherichia coli methyl-directed mismatch repair system. Genetics 1991; 129:1007-20.
490. Skandalis A, Ford BN, Glickman BW. Strand bias in mutation involving 5-methylcytosine deamination in the human hprt gene. Mutation research 1994; 314:21-6.
491. Sweder KS, Verhage RA, Crowley DJ, Crouse GF, Brouwer J, Hanawalt PC. Mismatch repair mutants in yeast are not defective in transcription-coupled DNA repair of UV-induced DNA damage. Genetics 1996; 143:1127-35.
492. Kobayashi K, O'Driscoll M, Macpherson P, Mullenders L, Vreeswijk M, Karran P. XPC lymphoblastoid cells defective in the hMutSalpha DNA mismatch repair complex exhibit normal sensitivity to UVC radiation and normal transcription-coupled excision repair of DNA cyclobutane pyrimidine dimers. DNA repair 2004; 3:649-57.
493. Lahav G, Rosenfeld N, Sigal A, Geva-Zatorsky N, Levine AJ, Elowitz MB, Alon U. Dynamics of the p53-Mdm2 feedback loop in individual cells. Nature genetics 2004; 36:147-50.
494. Perry ME. Mdm2 in the response to radiation. Mol Cancer Res 2004; 2:9-19.
495. Jeffers JR, Parganas E, Lee Y, Yang C, Wang J, Brennan J, MacLean KH, Han J, Chittenden T, Ihle JN, McKinnon PJ, Cleveland JL, Zambetti GP. Puma is an essential mediator of p53-dependent and -independent apoptotic pathways. Cancer Cell 2003; 4:321-8.
496. Ford JM. Regulation of DNA damage recognition and nucleotide excision repair: another role for p53. Mutation research 2005; 577:195-202.
497. el-Deiry WS, Tokino T, Velculescu VE, Levy DB, Parsons R, Trent JM, Lin D, Mercer WE, Kinzler KW, Vogelstein B. WAF1, a potential mediator of p53 tumor suppression. Cell 1993; 75:817-25.
498. Helton ES, Chen X. p53 modulation of the DNA damage response. J Cell Biochem 2007; 100:883-96.
499. Harris CC, Hollstein M. Clinical implications of the p53 tumor-suppressor gene. The New England journal of medicine 1993; 329:1318-27.
500. Thompson T, Tovar C, Yang H, Carvajal D, Vu BT, Xu Q, Wahl GM, Heimbrook DC, Vassilev LT. Phosphorylation of p53 on key serines is dispensable for transcriptional activation and apoptosis. The Journal of biological chemistry 2004; 279:53015-22.
501. Feng L, Lin T, Uranishi H, Gu W, Xu Y. Functional analysis of the roles of posttranslational modifications at the p53 C terminus in regulating p53 stability and activity. Molecular and cellular biology 2005; 25:5389-95.

502. Ljungman M, O'Hagan HM, Paulsen MT. Induction of ser15 and lys382 modifications of p53 by blockage of transcription elongation. Oncogene 2001; 20:5964-71.
503. Stubbert LJ, Smith JM, Hamill JD, Arcand TL, McKay BC. The anti-apoptotic role for p53 following exposure to ultraviolet light does not involve DDB2. Mutation research 2009; 663:69-76.
504. Lane DP. Cancer. p53, guardian of the genome. Nature 1992; 358:15-6.
505. Ford JM, Hanawalt PC. Li-Fraumeni syndrome fibroblasts homozygous for p53 mutations are deficient in global DNA repair but exhibit normal transcription-coupled repair and enhanced UV resistance. Proceedings of the National Academy of Sciences of the United States of America 1995; 92:8876-80.
506. Tan T, Chu G. p53 Binds and activates the xeroderma pigmentosum DDB2 gene in humans but not mice. Molecular and cellular biology 2002; 22:3247-54.
507. Adimoolam S, Ford JM. p53 and DNA damage-inducible expression of the xeroderma pigmentosum group C gene. Proceedings of the National Academy of Sciences of the United States of America 2002; 99:12985-90.
508. Ford JM, Baron EL, Hanawalt PC. Human fibroblasts expressing the human papillomavirus E6 gene are deficient in global genomic nucleotide excision repair and sensitive to ultraviolet irradiation. Cancer research 1998; 58:599-603.
509. El-Mahdy MA, Hamada FM, Wani MA, Zhu Q, Wani AA. p53-degradation by HPV-16 E6 preferentially affects the removal of cyclobutane pyrimidine dimers from non-transcribed strand and sensitizes mammary epithelial cells to UV-irradiation. Mutation research 2000; 459:135-45.
510. Wang XW, Yeh H, Schaeffer L, Roy R, Moncollin V, Egly JM, Wang Z, Freidberg EC, Evans MK, Taffe BG, et al. p53 modulation of TFIIH-associated nucleotide excision repair activity. Nature genetics 1995; 10:188-95.
511. McKay BC, Francis MA, Rainbow AJ. Wildtype p53 is required for heat shock and ultraviolet light enhanced repair of a UV-damaged reporter gene. Carcinogenesis 1997; 18:245-9.
512. Mathonnet G, Leger C, Desnoyers J, Drouin R, Therrien JP, Drobetsky EA. UV wavelength-dependent regulation of transcription-coupled nucleotide excision repair in p53-deficient human cells. Proceedings of the National Academy of Sciences of the United States of America 2003; 100:7219-24.
513. Wang QE, Zhu Q, Wani MA, Wani G, Chen J, Wani AA. Tumor suppressor p53 dependent recruitment of nucleotide excision repair factors XPC and TFIIH to DNA damage. DNA repair 2003; 2:483-99.
514. Leveillard T, Andera L, Bissonnette N, Schaeffer L, Bracco L, Egly JM, Wasylyk B. Functional interactions between p53 and the TFIIH complex are affected by tumour-associated mutations. The EMBO journal 1996; 15:1615-24.
515. McKay BC, Ljungman M, Rainbow AJ. Potential roles for p53 in nucleotide excision repair. Carcinogenesis 1999; 20:1389-96.
516. Stubbert LJ, Spronck JC, Hamill JD, McKay BC. Ultraviolet light induces the sustained unscheduled expression of cyclin E in the absence of functional p53. Cell cycle (Georgetown, Tex 2009; 8:2995-3002.

7.0 Tables

Table 1: Nucleotide Excision Repair Defects and Associated Clinical Manifestations

Clinical disease	Implicated gene	Hugo nomen-clature	Overlap with other diseases*	NER Sub-pathway		Cancer prone
				TC-NER	GG-NER	
XP	XPA	XPA	DSC	–	–	+
	XPB	ERCC3	CS and TTD	–	–	+
	XPC	XPC	Unknown	+	–	+
	XPD	ERCC2	CS, TTD and COFS	–	–	+
	XPE	DDB2	Unknown	+	–	+
	XPF	ERCC4	Unknown	–	–	+
	XPG	ERCC5	CS and COFS	–	–	+
CS	CSA	ERCC8	Unknown	–	+	–
	CSB	ERCC6	UV^SS, COFS and DSC	–	+	–
	XPB	ERCC3	XP and TTD	–	–	+
	XPD	ERCC2	XP and TTD	–	–	+
	XPG	ERCC5	XP	–	–	+
	ERCC1	ERCC1	COFS	–	–	Unknown
UV^SS	CSB	ERCC6	CS, COFS and DSC	–	+	–
	Unknown	Unknown	Unknown	–	+	–
TTD	XPB	ERCC3	XP and CS	–	–	–
	XPD	ERCC2	XP and CS	–	–	–
	TTDA	GTF2H5	Unknown	–	–	–
	TTDN1	C7orf11	Unknown	+	+	Unknown

Table modified from Hanawalt and Spivak (2008)[85] with additional data incorporated from Lehmann 2000.[84]

Table 2: NER Genes, their Roles and Homologous Versions

Human Gene	Role	Additional Comments	Rodent	*Saccharomyces cerevisiae*	*Escherichia coli*
GG-NER Genes					
XPE (DDB2)	Lesion recognition	Recruits XPC and is p53 inducible	Ddb2(Xpe)	Unknown	Unknown
DDB1	Lesion recognition	Forms a complex with DDB2	Ddb1	Unknown	Unknown
XPC	Lesion recognition	Opens DNA and is p53 inducible	Xpc	RAD4	UvrA
RAD23B	Lesion recognition	Forms a complex with XPC	Rad23b	RAD23	Unknown
Centrin-2	Lesion recognition	Forms a complex with XPC	Unknown	Unknown	Unknown
GG-NER and TC-NER genes					
XPB	Helicase and ATPase	TFIIH subunit	Ercc3 (Xpb)	RAD25	UvrB
XPD	Helicase and ATPase	TFIIH subunit	Ercc2 (Xpd)	RAD3	UvrB
XPA	Lesion verification	Stabilizes pre-incision complex	Xpa	RAD14	Unknown
RPA	ssDNA binding	Binds to XPA	Rpa	RFA-1–3	Ssb?
XPF	Structure-specific endonuclease	3' incision	Ercc4 (Xpf)	RAD1	UvrC
ERCC1	Forms a complex with XPF	3' incision	Ercc1	RAD10	Unknown
XPG	Structure-specific endonuclease	5' incision and stabilization of TFIIH	Ercc5 (Xpg)	RAD2	UvrC
PCNA	DNA replication sliding clamp	3 subunits; docking sites for DNA pol	Pcna	PCNA	β-clamp
RFC1	Loads PCNA on DNA	RFC large subunit	Rfc1	CDC44	Unknown
Unknown	Removal of incised oligo	None	Unknown	Unknown	UvrD||
DNA pol δ / ε	DNA replication and repair	None	DNA pol δ or ε	DNA pol δ or ε	DNA pol I
DNA pol κ	Bypass polymerase	None	DNA pol κ	DNA pol κ	Dinb1
DNA ligase-I	Ligase	None	Unknown	CDC9	Ligase
DNA ligase-III	Ligase complex		Unknown	Unknown	Ligase
XRCC1	Ligase complex		Xrcc1	Unknown	Unknown

TC-NER genes					
CSA	Ubiquitin-ligase complex	WD repeat	Ercc8 (Csa)	RAD28	Unknown
CSB	TCR coupling factor and chromatin re-modelling	Transcription elon-gation factor	Ercc6 (Csb)	RAD26	Mfd
XAB2	Transcription factor	Link between XPA and RNAPII	Unknown	Unknown	Unknown
TFIIS	RNAPII elongation factor?	Stimulates tran-script cleavage by RNAPII?	Unknown	Unknown	GreA and GreB
HMGN1	Chromatin relaxa-tion	Nucleosome re-moval?	Unknown	Unknown	Unknown
p300	Chromatin remod-elling	Nucleosome re-moval?	Unknown	Unknown	Unknown

Table modified from Hanawalt and Spivak (2008)[85] with additional data from Cleaver 2008[82], Lehmann 2003[84], Fousteri and Mullenders 2008[83]

8.0 Appendix 1 Supplementary Figures

Figure 1 Flow Cytometric Histograms of Cisplatin-treated siRNA Targeted HCT116 Tumour Cells

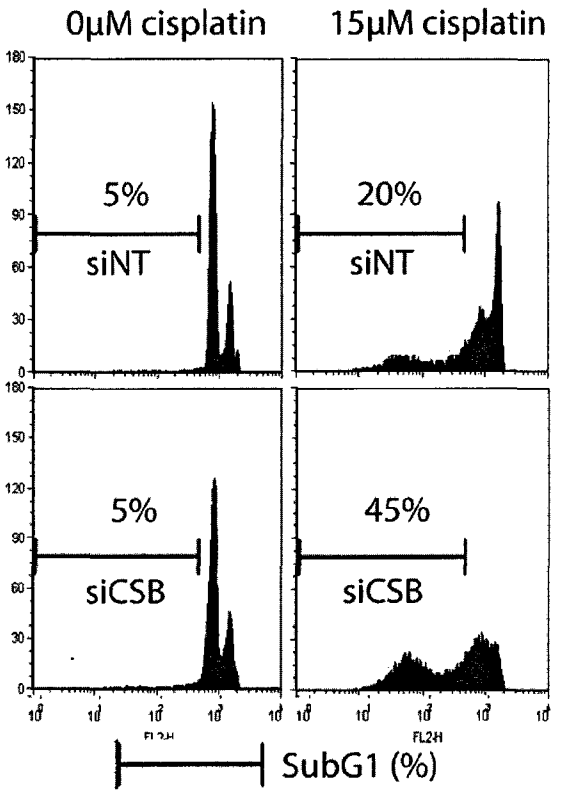

HCT116 cells, transfected as indicated then collected after 48h continuous treatment with cisplatin. Cells are fixed in ethanol then stained with the DNA stain propidium iodide then analysed by flow cytometry. Cell cycle distribution histograms are shown where marker indicates sub-diploid fraction of cells (percent apoptosis).

Appendix 1 Supplementary Figures

Figure 2 Colon Cancer Cells Exhibit Similar Clonogenic Survival after Cisplatin Treatment, Independent of MMR Status

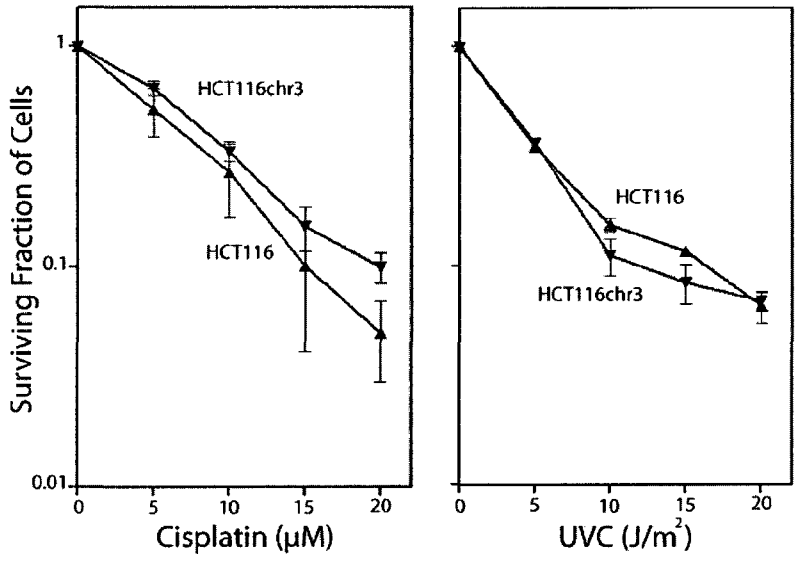

Cells as indicated were transfected with siRNA and 72h later re-plated at various densities after treatment for 12h with indicated dose of cisplatin or with indicated dose of UVC. After colonies formed, cells were fixed and stained in methylene blue in methanol and colonies were counted. Plots were normalized to 0 dose and error bars represent mean of normalized (± SEM) from 2-3 experiments.

Appendix 1 Supplementary Figures

Figure 3 Targeting XPA by siRNA Sensitizes HCT116p53-/- Colon Cancer Cells to DNA Damage

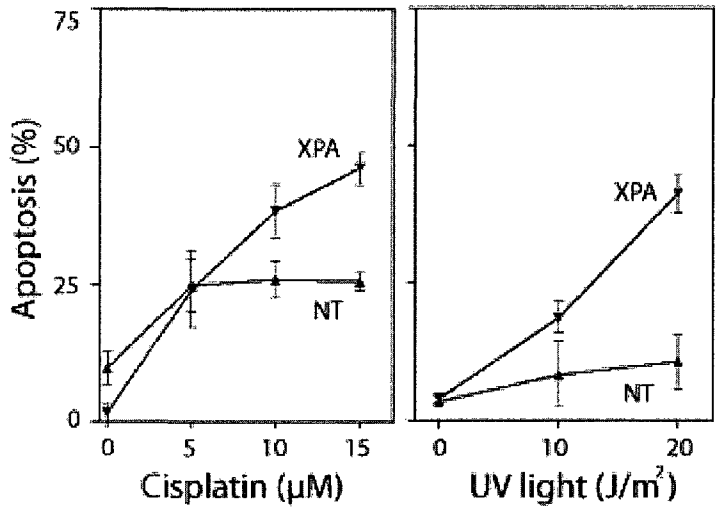

HCT116p53-/- cells were treated with UV and cisplatin after transient transfection with indicated siRNA (NT or XPA). Sub-diploid fraction of the cell cycle was measured as an indicator of apoptosis (as described previously). Data points represent means from at least 3 experiments (± SEM).

9.0 Appendix 2 Published Manuscripts

I was fortunate to be involved in a variety of peripheral projects that have resulted in journal publications that do not form an integral part of this thesis but which are presented here.

Regulation of ultraviolet light-induced gene expression by gene size

Bruce C. McKay*†‡§, Lawton J. Stubbert*‡, Casey C. Fowler*, Jennifer M. Smith*‡, Robin A. Cardamore*, and Jennifer C. Spronck*

*Centre for Cancer Therapeutics, Ottawa Regional Cancer Centre, Departments of †Radiology and ‡Cellular and Molecular Medicine, University of Ottawa, 503 Smyth Road, Ottawa, ON, Canada K1C 5T5

Edited by Philip C. Hanawalt, Stanford University, Stanford, CA, and approved March 11, 2004 (received for review December 9, 2003)

UV light induces the expression of a wide variety of genes. At present, it is unclear how cells sense the extent of DNA damage and alter the expression of UV-induced genes appropriately. UV light induces DNA damage that blocks transcription, and the probability that a gene sustains transcription-blocking DNA damage is proportional to locus size and dose of UV light. Using colon carcinoma cells that express a temperature-sensitive variant of p53 and undergo p53-dependent apoptosis after UV irradiation, we found that the number of p53-induced genes identified by oligonucleotide microarray analysis decreased in a UV dose-dependent manner. This was associated with a statistically significant shift in the spectrum of p53-induced genes toward compact genes with fewer and smaller introns. Genes encoding proapoptotic proteins involved in the initiation of the mitochondrial apoptotic cascade were prominent among the compact p53 target genes, whereas genes encoding negative regulators of p53 and the mitochondrial apoptotic pathway were significantly larger. We propose that the shift in spectrum of UV-responsive gene expression caused by passive effects of UV lesions on transcription acts as a molecular dosimeter, ensuring the elimination of cells sustaining irreparable transcription-blocking DNA damage.

DNA damage | microarray | p53 | transcription | stress responses

The human genome contains between 26,000 and 39,000 genes distributed throughout ≈3 billion base pairs of DNA (1). The coordinated regulation of this many genes presents a daunting task. Superimposed upon the complexity of transcriptional regulation is the fact that many DNA damaging agents can induce damage that inhibits elongation by RNA polymerase II (2). These transcription-blocking DNA lesions pose an obvious difficulty to the coordinated regulation of gene expression in those cells that have sustained sufficient damage. It is not fortuitous that highly conserved DNA repair pathways coupling transcription to DNA repair have evolved and that mechanisms exist to eliminate cells with excessive transcription-blocking lesions.

Transcription-coupled nucleotide excision repair (TC-NER) preferentially removes transcription-blocking lesions from the transcribed strand of active genes, facilitating the recovery from DNA damage-induced transcriptional arrest (3–5). Much of what is known about TC-NER and DNA damage-induced transcriptional stress stems from studies using the model DNA damaging agent, UV light. Cyclobutane pyrimidine dimers (CPDs) and 6-4 photoproducts (6-4PPs), the most common lesions induced by short-wavelength UV light, block transcription and are substrates for TC-NER (6, 7). After exposure to cytotoxic doses of UV light, cells fail to recover transcription and undergo apoptosis (4, 8), and this is thought to occur primarily through the mitochondrial pathway involving cytochrome *c*, Apaf1, and caspase 9 (9–11). There is a very tight correlation between the sustained inhibition of transcription and UV-induced apoptosis, indicating that cells sense sustained transcriptional stress as an indicator of irreparable DNA damage (4, 8, 12, 13).

UV light activates signaling cascades that ultimately result in the activation of transcription-factors such as AP-1 and the p53 tumor suppressor (14, 15). However, UV-induced DNA damage also inhibits transcription by posing a physical impediment to elongation by RNA polymerases (2). The likelihood that a gene sustains DNA damage after UV irradiation is proportional to gene size because the induction of UV photoproducts is a stochastic event (16). A moderate dose of 10 J/m^2 of UV light that induces apoptosis in <20% of UV-irradiated primary human fibroblasts or most other DNA repair-proficient human cell lines (4, 13, 17–20) yields ≈2.4 lesions per strand of an average gene (Fig. 4, which is published as supporting information on the PNAS web site) (1, 7, 21–25). This high lesion frequency led us to hypothesize that transcription-blocking UV lesions could dramatically effect the expression of UV-induced genes. Here we report that the spectrum of genes induced by UV light or by p53 in the presence of UV-induced DNA damage is significantly altered in a dose-dependent manner. The genes induced at cytotoxic doses of UV light were compact, with fewer and smaller introns, and were enriched for initiators of apoptosis acting through the mitochondrial pathway. We propose that cells use this passive mechanism of gene regulation to ensure that cells sustaining irreparable DNA damage are eliminated by apoptosis.

Materials and Methods

Cell Culture and UV Treatment. The HT29-tsp53 colorectal carcinoma cells expressing a temperature-sensitive variant of p53 and HT29-neo vector control cells (26) were obtained from Mats Ljungman and Jon Maybaum (University of Michigan, Ann Arbor). Cells were grown at the restrictive temperature (38°C) in 10-cm tissue culture dishes in DMEM supplemented with 10% FCS (GIBCO/BRL) and 5 μg/ml gentamicin (Sigma). Growth medium was removed before UV iradiation, and fresh medium was immediately replaced after treatment. Fluence was determined with a UV radiometer (Ultraviolet Products) to deliver ≈1 J/m^2/s from a germicidal bulb (Philips) emitting predominately at 254 nm.

RNA Isolation. Cells were seeded 48 h before treatment. At the time of treatment, cells were irradiated with the indicated doses of UV light and were either returned immediately to the restrictive temperature (38°C) or switched to the permissive temperature (32°C). Cells were harvested 6 h after treatment. Total RNA was isolated by using the RNeasy RNA isolation kit (Qiagen, Valencia, CA) according to manufacturer's specifications. The yield of total cellular RNA was not dramatically affected by UV dose by this time.

Quantitative RT-PCR. Five micrograms of total RNA was reverse-transcribed by using first-strand cDNA synthesis kit (MBI Fer-

This paper was submitted directly (Track II) to the PNAS office.

§To whom correspondence should be addressed. E-mail: bmckay@ohri.ca.

www.pnas.org/cgi/doi/10.1073/pnas.0308181101

mentas). Quantitative RT-PCR was performed by using the Sybr green fluorescent DNA stain (Molecular Probes), a LightCycler 2 quantitative PCR machine (Roche Diagnostics) and LIGHTCYCLER software version 3 (Roche Diagnostics). The primers used were CRYAB (AGCCGCCTCTTTGACCAGTTCTT and GCGGTGACAGCAGGCTTCTCTTC), p21WAF-1/CDKN1A (CCTCAAATCGTCCAGCGACCTT and CATTGTGGGAGGAGCTGTGAAA), FAS (CTCATCTTAATGGCCTAATGCA and GCTTCAGTTTATAACTATCTTCAC), DDB2 (CCACCTTCATCAAAGGGATTGG and CTCGGATCTCGCTCTTCTGGTC), serpinB5/maspin (CTTTTCTGTGGATGCCGATT and CCTGCCAGGGCTTAACATAA), XP-C (AAGTTCACTCGCCTCGGTTGC and TTCTTTCCTGATTTTAGCCTTTTT), SMAD-3 (AGGCGTGCGGCTCTACTACATC and GGGCGTTTCTGGTTGGACTG), EFNB1 (GGAGGCAGACAACACTGTCA and GAACAATGCCACCTTGGAGT), LOC254531 (CCGAATGTGAGTTTGTAGG and TTTGGTGTCTGGGAGGTG), MAX (CTCTCGTGGTATGTATGGG and AGTAGGAAAGGAAGTGGGATG), MYB (AACTCCTACACCATTCAAAC and CTGCTCCTCCATCTTTCC), PMAIP1/NOXA (TAAAGCAAGAATGGAAGAC and GACCGAAGAAATCAACAC), and ACTIN (GGGCATGGGTCAGAAGGAT and GTGGCCATCTCTTGCTCGA).

Microarray. Twenty micrograms of each RNA sample was labeled by using the Super Script II (Invitrogen) and the Enzo BioArray HighYield RNA transcript labeling kit (Affymetrix). Labeled complementary RNA was hybridized to the Affymetrix U95A microarrays containing 12558 probe sets according to the specifications of the manufacturer (Affymetrix) at the Affymetrix gene expression facility at the Ottawa Hospital Research Institute (Ottawa). Affymetrix MICROARRAY SUITE 5.0 software was used to compare each sample to mock-irradiated controls maintained at the restrictive temperature. A nonparametric Wilcoxon signed rank test was used to determine whether statistically meaningful differences in probe cell intensities were detected between samples (change calls were determined by using γ_1H and γ_1L values of 0.0025). We considered genes to be differentially expressed under a given condition if and only if they were statistically ($P \leq 0.0025$) increased or decreased 2-fold in all experiments compared to samples collected from cells maintained at the restrictive temperature. The NetAffx database was used to determine the identity of differentially expressed genes (27).

The National Centre for Biotechnology Information Locuslink database (www.ncbi.nlm.nih.gov/LocusLink) was used to obtain detailed information regarding the physical makeup of all differentially expressed genes. The size of genes, mRNAs, and introns did not fit a Gaussian distribution, so statistical analysis was performed on log-transformed data by using the PRISM software package (GraphPad, San Diego). However, similar results were obtained with nontransformed data by using a nonparametric Mann–Whitney U test.

Chromatin Immunoprecipitation. The chromatin immunoprecipitation assay was performed as described by Kallesen and Rosen (http://public.bcm.tmc.edu/rosenlab/protocols/ChIP.pdf), which represents a minor modification of the method of Boyd and Farnham (28). Briefly, proteins and DNA were crosslinked with 1% formaldehyde in growth medium. Chromatin was isolated and sonicated to an average length of 700 bp with a microtip sonifier (Branson Sonifier) in 20-sec bursts. Debris was cleared by centrifugation, and the resulting supernatants were frozen in liquid nitrogen and stored at −80°C.

Upon analysis, the chromatin was diluted 5-fold and precleared with protein A-agarose (Roche Diagnostics) for 50 min at 4°C. Twenty percent of the precleared chromatin was retained

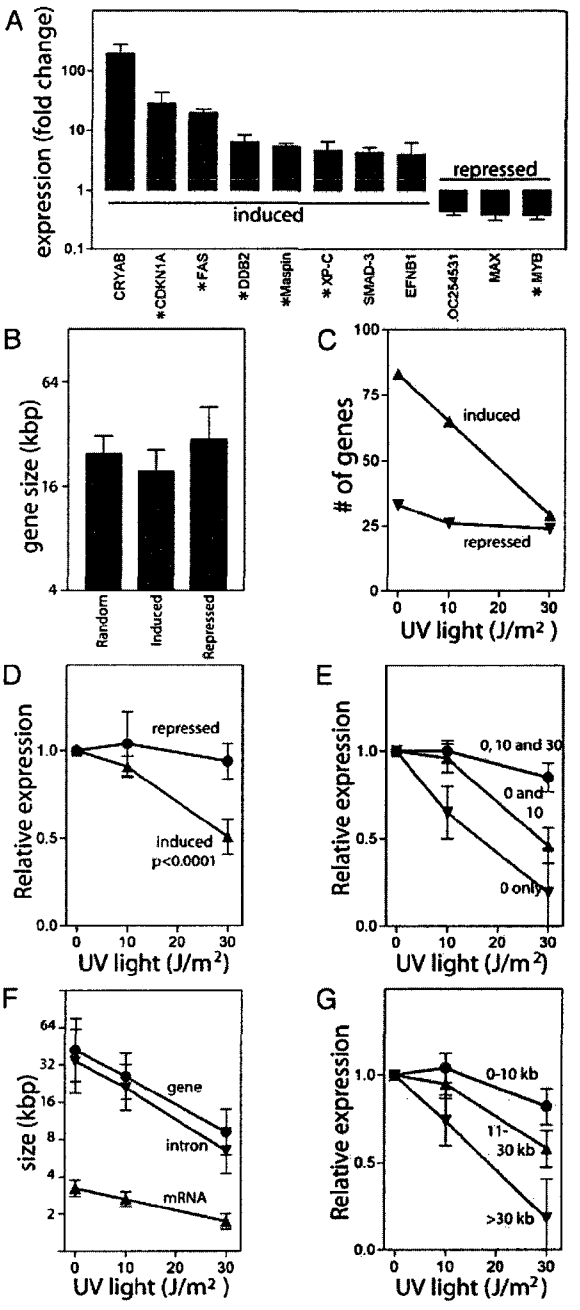

Fig. 1. The effect of UV light on expression of genes induced at the permissive temperature. (*A*) Fold increase in gene expression at the permissive temperature was determined by real-time RT-PCR. Known p53-regulated genes are denoted with asterisks. (*B*) The mean size of genes induced or repressed at the permissive temperature compared to the size of randomly selected genes. The effect of the UV light on the number (*C*) and expression (*D*) of genes induced or repressed at the permissive temperature. Expression in *D* for each gene was determined and normalized to the induced level of expression of that gene at the permissive temperature alone and is expressed as the mean level of expression determined from all genes in the group. (*E*) Genes were grouped by behavior to UV light: induced at 0 (inverted triangle), 0 and 10 (triangle), or 0, 10, and 30 (circle) J/m^2. Relative expression was determined as indicated in *D*. (*F*) The mean size of loci (circles), mean size of mRNA (triangles), and the total intron size (inverted triangles) are indicated for each group in *E*. (*G*) Genes were sorted into three groups by gene size (≤10 kb, 11–30 kb, and >30 kb, n = 28, 26, and 27, respectively) and the mean effect of UV light on gene expression in each group was determined. Error bars in *A* and *D–G* indicate the 95% confidence interval of the indicated mean. The *P* value in *D* was determined by one-way ANOVA.

Table 1. Effect of UV light on the expression of known p53-responsive genes

Expression	UV, J/m²	*n*	Median gene size, bp	mRNA size, $\log_2$ bp	Gene size, $\log_2$ bp	Gene size, bp†	Total intron size, $\log_2$ bp
Random‡	NA	132	29,104	11.1 ± 0.1	14.6 ± 0.2	24,800	14.4 ± 0.2
p53 induced	All	43	13,751	11.1 ± 0.1	14.0 ± 0.2	16,500	13.7 ± 0.3
	0	33	23,036	11.1 ± 0.1	14.1 ± 0.3	17,600	13.8 ± 0.3
	10	32	11,934	11.1 ± 0.1	13.7 ± 0.3*	13,300	13.5 ± 0.3*
	30	18	8,176	10.8 ± 0.2	13.2 ± 0.3**	9,400	12.8 ± 0.3**

Asterisks indicate that the indicated value is significantly different from randomly selected genes using a Student's *t* test at *, $P \leq 0.05$ or **, $P \leq 0.005$. NA, not applicable.

†For clarity, mean gene size is presented in a linear form but was determined from the mean of transformed values by using the following formula: (mean gene size = $2^{\text{meanlog2 gene size}}$).

‡A random number generator was used to generate a random series of Locuslink accession numbers.

as a positive control for PCR amplification. The remainder of the solution was divided into equal aliquots and incubated overnight at 4°C, either without antibody or with 5 μg of p53 antibody (Ab-1 antibody, Oncogene Science, or phospho-Ser-15 antibody, Cell Signaling Technologies). Immune complexes were collected overnight at 4°C with the addition of 60 μl of protein A-agarose (Roche Diagnostics).

Crosslinks were reversed by addition of NaCl to a final concentration of 0.3 M with RNase A and incubated at 65°C for 4–5 h. DNA was precipitated in 70% ethanol, collected by centrifugation, and proteinase K treated for 2 h at 45°C. DNA was purified by using QiaQuick spin columns (Qiagen) and was eluted in 10 mM Tris, pH 8.0. Semiquantitative PCRs were performed by using a GenAmp PCR System 9700 (Applied Biosystems). The binding of p53 to the serbinB5 (maspin), CDKN1A ($p21^{WAF1}$), and FAS p53 response elements was determined by using the following primer pairs: CTTTTCTGTGGATGCCGATT and CCTGCCAGGGCTTAACATAA, GTGGCTCTGATTGGCTTTCTG and CTGAAAACAGGCAGCCCAAG (29), and GGGACCCCGGTTGGAGAG and CTGCTTCGGTGCTGACTTATTTC, respectively. Amplification of upstream sequences of the GAPDH (GTATTCCCCCAGGTTTACAT and TTCTGTCTTCCACTCACTCC; ref. 29), XAB2 (AACGAGCTGGGACCCTCAGT and TATCAGTTTTTGGGGGCCGAGT) and KiSS-1 (CCTGGGGCCCGCACTTAGC and CCCCCGCACCTTCTCCATTTG) promoters and enhancers served as negative controls.

Results and Discussion

To evaluate the inhibitory affect of UV photoproducts on DNA damage-induced gene expression in a well controlled model system, we examined gene expression profiles in a human colorectal carcinoma cell line harboring a temperature sensitive allele of p53 (26). At the restrictive temperature (38°C), this variant of p53 is in a mutant conformation and cytoplasmic, but becomes nuclear and functional at the permissive temperature (32°C) (30). This variant is ideal for these studies because conditional expression of active p53 does not require *de novo* transcription of the transgene nor does it require a DNA damage signal. Statistically significant changes in gene expression were determined for each individual experiment by using the MICROARRAY SUITE 5.0 software (Affymetrix). We found 83 genes were induced at least 2-fold at the permissive temperature in each of four independent experiments. Thirty-three of these genes have previously been reported to be p53-induced (31–38). By similar criteria, 33 genes were repressed at the permissive temperature. The differential expression of several gene products was confirmed by using real-time RT-PCR (Fig. 1*A*). In all instances, RT-PCR data confirmed the differential expression detected by microarray analysis.

We obtained information regarding the physical makeup of all differentially expressed genes (Tables 3–5, which are published as supporting information on the PNAS web site). For statistical purposes, detailed information regarding the physical makeup of 132 randomly selected genes was also obtained (Table 6, which is published as supporting information on the PNAS web site). As expected, the average size of the randomly selected genes closely approximated that reported by the human genome project (1). Overall, the mean size of the genes induced at the permissive temperature was not significantly different from the size of randomly selected genes (Fig. 1*B*).

We determined the effect of UV light on the spectrum and expression of these p53 target genes. Of the 83 genes induced at the permissive temperature, only 29 were still induced after exposure to 30 J/m² (Fig. 1*C*). In contrast, the number of repressed genes was not dramatically altered by UV light (Fig. 1*C*). Whereas the expression of p53-induced genes was also strongly inhibited by UV light ($P < 0.0001$), the expression of the p53-repressed genes remained largely unaffected (Fig. 1*D*). Thus, UV irradiation dramatically altered the spectrum and expression of p53-induced but not p53-repressed genes.

Genes induced at the permissive temperature were grouped by behavior after exposure to UV light (i.e., induced at "0 J/m² only," "0 and 10 J/m²," or "0, 10, and 30 J/m²") (Fig. 1*E*). There was a significant UV dose-dependent decrease in the size of genes induced but not repressed at the permissive temperature (Fig. 1*F*, $P < 0.0001$, ANOVA). This was associated with a decrease in the number and average size of introns, but mRNA size was not significantly different from that of randomly selected genes ($P = 0.005$, 0.004, and 0.17, respectively). The p53-induced genes were sorted into groups based on gene size, and the effect of UV light on the expression of each group of genes was determined. The expression of large genes was strongly inhibited, whereas the

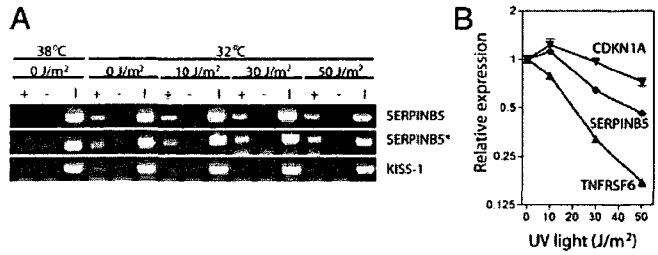

Fig. 2. The effect of UV dose on p53 binding and p53 target gene expression. (*A*) Representative chromatin immunoprecipitation experiments demonstrate an interaction of p53 and ser15 phosphorylated p53 (asterisk) with the SERPINB5 p53-response element at all doses of UV light. KiSS-1 served as a negative control. +, antibody; −, the no-antibody control; I, input DNA. (*B*) The effect of UV light on representative p53 target genes was determined by real-time RT-PCR. Values are expressed relative to the corresponding mean determined for p53 target genes induced at the permissive temperature alone. Values represent the mean ± standard error.

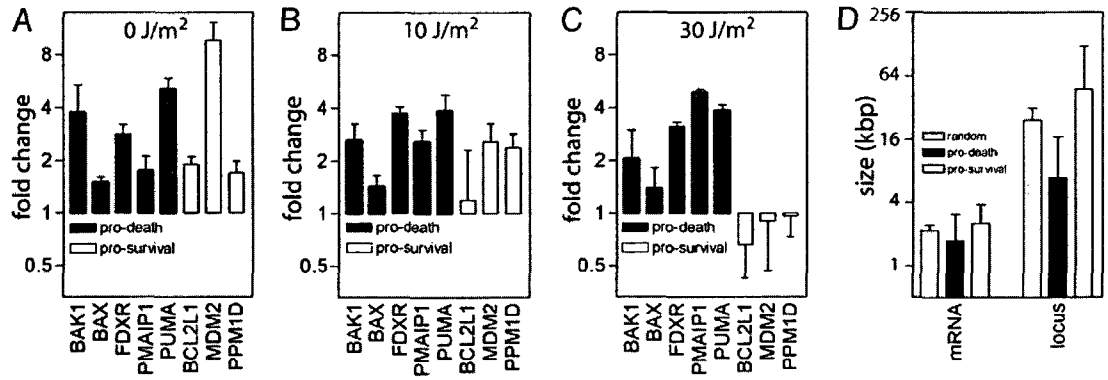

Fig. 3. p53 target genes involved in mitochondrial apoptotic pathways are resistant to inhibition of gene expression by UV light. (*A–C*) The fold change in the expression of genes encoding antiapoptotic (open symbols) and proapoptotic (filled symbols) proteins after exposure to 0 (*A*), 10 (*B*), or 30 (*C*) J/m². (*D*) The mean size of the mRNA and locus of genes encoding p53-regulated proapoptotic proteins or survival promoting proteins (in *A–C*).

expression of small genes was not (Fig. 1*G*). Because many of these putative p53-regulated genes identified through our microarray analysis have not been independently confirmed to be p53-regulated, we performed a similar analysis on the 43 previously reported target genes (31–40) (Table 5). Again, genes induced at higher doses of UV light were significantly smaller (Table 1), and this was associated with a significant decrease in the average number and size of introns ($P < 0.005$, *t* test). Thus, UV light inhibits the p53 response in a dose-dependent manner, resulting in the preferential induction of compact p53 target genes with fewer and smaller introns.

To ensure that p53 was associated with consensus response elements *in vivo* at high doses of UV light, we performed chromatin immunoprecipitation experiments. An interaction between p53 and the SERPINB5 (maspin, Fig. 2*A*), CDKN1A ($p21^{WAF1}$, data not shown), and TNFRSF6 (Fas, data not shown) p53-response elements *in vivo* by chromatin immunoprecipitation was detected even though UV light inhibited the expression of SERPINB5 and TNFRSF6 (Fig. 2*B*). The interactions were apparent for all three promoters using two different p53 antibodies. We interpret these results to indicate that dose-dependent variation in the spectrum of p53-induced genes cannot be explained by a decrease in the binding of p53 to its response elements.

We have previously reported that the HT29-tsp53 cells used here undergo extensive apoptosis at the permissive temperature after exposure to 30 but not after exposure to 0 or 10 J/m² of UV light (20). Of the 43 known p53 target genes differentially expressed in our microarray experiments, 17 have been reported to regulate the induction of apoptosis. Of these, five are inducers of apoptosis through the mitochondrial apoptotic pathway (Fig. 3) important for both p53- and UV-induced apoptosis (9–11, 32, 33, 41–45). All five genes implicated in the p53-mediated mitochondrial pathway were highly resistant to inhibition by UV light (Fig. 3 *A–C*), whereas the expression of genes known to inhibit p53-mediated apoptosis was strongly blocked by UV light (Fig. 3 *A–C*). The proapoptotic genes were significantly smaller than the prosurvival genes (Fig. 3*D*). The large size of MDM2 and PPM1D genes ensures that feedback inhibition is blocked at higher doses, permitting cells to be eliminated by apoptosis. Taken together, UV irradiation resulted in the expression of a restricted set of small p53-responsive genes at the expense of larger p53 targets, and this coincides with the induction of apoptosis in a dose-dependent manner.

To determine whether gene size had an effect on the p53-independent induction of UV-responsive genes, we assessed the effect of UV light on gene expression at the restrictive temperature, as well. We found that the size of genes induced after exposure to high doses of UV light at the restrictive temperature were again smaller ($P = 0.005$ and $P < 0.0001$, respectively, Table 2). Furthermore, we determined the average size of genes reported to be induced by UVC, UVB, and γ radiation in a variety of cell types by several other groups (38, 46–49). In striking support of our results, we found that these previously reported UVB- and UVC-induced genes were also significantly smaller than randomly selected genes (Table 7, which is published as supporting information on the PNAS web site). The compact UV-induced genes included p53-responsive genes, AP-1 responsive immediate early genes, cytokines, chemokines, and histones (38, 46–49). In contrast, exposure of tumor cells to γ radiation did not result in the striking induction of compact genes (Table 7). In fact, UV-induced genes were significantly smaller than genes induced by ionizing radiation ($0.05 < P < 0.0001$, depending on the studies compared). This is consistent with the fact that γ radiation does not strongly inhibit transcription (8). Therefore, gene size is an important determinant of UV-induced but not γ-radiation-induced gene expression.

In summary, we found that the induction of UV-induced gene expression is subject to a strong gene size constraint. The gamut of UV-induced genes was enriched for compact genes with fewer and smaller introns. We propose that this gene size constraint has played a significant role in the evolution of UV-response pathways and that the dose-dependent change in the spectrum of p53-induced and UV-induced genes acts as an elegant molecular dosimeter. Selective gene expression based on gene size represents a gene regulatory mechanism that acts at the level of transcript elongation because of blocked RNA polymerases. We propose that differences in gene expression caused by gene size are used to interpret the extent of irreparable transcription-blocking DNA damage sustained by the cell. This dose-

Table 2. Size of genes induced by UV light at the restrictive temperature

UV	*n*	Median	Gene size*	Mean†	*P*‡
Random§	132	29,104	14.6 ± 0.2	24,800	
10 J/m²	14	10,340	13.1 ± 0.4	8,800	0.005
30 J/m²	17	5,822	12.6 ± 0.3	6,200	<0.0001

*The size of individual genes in bp were $\log_2$ transformed, and the mean (±SEM) of these $\log_2$ transformed values is presented.

†For clarity, mean gene size is presented in a linear form, but was determined from the mean of transformed values by using the formula: mean gene size = $2^{\text{mean gene size (log2)}}$.

‡Each mean was compared to the mean determined from randomly selected genes by using a *t* test.

§Randomly selected genes.

GENETICS

dependent pattern of expression explains in large part the tight association between the UV-induced inhibition of transcription and the induction of apoptosis (4, 8, 12, 13, 20).

We thank Drs. Mats Ljungman and Jon Maybaum (University of Michigan) for providing the HT29-tsp53 cell line used in these studies and Dr. Douglas Gray for critical reading of the manuscript. We appreciate the technical assistance of the Ottawa Health Research Institute Gene Expression Facility. This work was supported by the National Cancer Institute of Canada with funds from the Terry Fox Run and the Ontario Premier's Research Excellence Award. B.C.M. is a Research Scientist of the Canadian Cancer Society.

1. Venter, J. C., Adams, M. D., Myers, E. W., Li, P. W., Mural, R. J., Sutton, G. G., Smith, H. O., Yandell, M., Evans, C. A., Holt, R. A., *et al.* (2001) *Science* **291,** 1304–1351.
2. Tornaletti, S. & Hanawalt, P. (1999) *Biochimie* **81,** 139–146.
3. Mayne, L. & Lehmann, A. (1982) *Cancer Res.* **42,** 1473–1478.
4. Ljungman, M. & Zhang, F. (1996) *Oncogene* **13,** 823–831.
5. McKay, B. C., Chen, F., Clarke, S. T., Wiggin, H. E., Harvey, L. M. & Ljungman, M. (2001) *Mutat. Res.* **485,** 93–105.
6. Mellon, I., Spivak, G. & Hanawalt, P. C. (1987) *Cell* **51,** 241–249.
7. van Hoffen, A., Venema, J., Meschini, R., Vanzeeland, A. A. & Mullenders, L. H. F. (1995) *EMBO J.* **14,** 360–367.
8. Ljungman, M., Zhang, F., Chen, F., Rainbow, A. J. & McKay, B. C. (1999) *Oncogene* **18,** 583–592.
9. Yoshida, H., Kong, Y. Y., Yoshida, R., Elia, A. J., Hakem, A., Hakem, R., Penninger, J. M. & Mak, T. W. (1998) *Cell* **94,** 739–750.
10. Hakem, R., Hakem, A., Duncan, G. S., Henderson, J. T., Woo, M., Soengas, M. S., Elia, A., de la Pompa, J. L., Kagi, D., Khoo, W., *et al.* (1998) *Cell* **94,** 339–352.
11. Sitailo, L. A., Tibudan, S. S. & Denning, M. F. (2002) *J. Biol. Chem.* **277,** 19346–19352.
12. McKay, B. C., Becerril, C. & Ljungman, M. (2001) *Oncogene* **20,** 6805–6808.
13. McKay, B. C. & Ljungman, M. (1999) *Neoplasia* **1,** 276–284.
14. Herrlich, P., Blattner, C., Knebel, A., Bender, K. & Rahmsdorf, H. J. (1997) *Biol. Chem.* **378,** 1217–1229.
15. Ljungman, M. (2000) *Neoplasia* **2,** 208–225.
16. Sauerbier, W. & Hercules, K. (1978) *Annu. Rev. Genet.* **12,** 329–363.
17. McKay, B. C., Ljungman, M. & Rainbow, A. J. (1998) *Oncogene* **17,** 545–555.
18. Queille, S., Drougard, C., Sarasin, A. & Daya-Grosjean, L. (2001) *J. Invest. Dermatol.* **117,** 1162–1170.
19. McKay, B. C., Becerril, C., Spronck, J. C. & Ljungman, M. (2002) *DNA Rep.* **1,** 811–820.
20. McKay, B. C., Chen, F., Perumalswami, C. R., Zhang, F. & Ljungman, M. (2000) *Mol. Biol. Cell* **11,** 2543–2551.
21. Venema, J., Mullenders, L. H. F., Natarajan, A. T., van Zeeland, A. A. & Mayne, L. V. (1990) *Proc. Natl. Acad. Sci. USA* **87,** 4707–4711.
22. Venema, J., van Hoffen, A., Natarajan, A. T., van Zeeland, A. A. & Mullenders, L. H. F. (1990) *Nucleic Acids. Res.* **18,** 443–448.
23. Evans, M. K., Robbins, J. H., Ganges, M. B., Tarone, R. E., Nairn, R. S. & Bohr, V. A. (1993) *J. Biol. Chem.* **268,** 4839–4847.
24. Tolbert, D. M. & Kantor, G. J. (1996) *Cancer Res.* **56,** 3324–3330.
25. Ford, J. M. & Hanawalt, P. C. (1997) *J. Biol. Chem.* **272,** 28073–28080.
26. Merchant, A. K., Loney, T. L. & Maybaum, J. (1996) *Oncogene* **13,** 2631–2637.
27. Liu, G., Loraine, A. E., Shigeta, R., Cline, M., Cheng, J., Valmeekam, V., Sun, S., Kulp, D. & Siani-Rose, M. A. (2003) *Nucleic Acids Res.* **31,** 82–86.
28. Boyd, K. E. & Farnham, P. J. (1999) *Mol. Biol. Cell* **19,** 8393–8399.
29. Kaeser, M. D. & Iggo, R. D. (2002) *Proc. Natl. Acad. Sci. USA* **99,** 95–100.
30. Gannon, J. & Lane, D. (1991) *Nature* **349,** 802–806.
31. Vousden, K. H. & Lu, X. (2002) *Nat. Rev. Cancer* **2,** 594–604.
32. Nakano, K. & Vousden, K. H. (2001) *Mol. Cell* **7,** 683–694.
33. Oda, E., Ohki, R., Murasawa, H., Nemoto, J., Shibue, T., Yamashita, T., Tokino, T., Taniguchi, T. & Tanaka, N. (2000) *Science* **288,** 1053–1058.
34. Zou, Z., Gao, C., Nagaich, A. K., Connell, T., Saito, S., Moul, J. W., Seth, P., Appella, E. & Srivastava, S. (2000) *J. Biol. Chem.* **275,** 6051–6054.
35. Kannan, K., Amariglio, N., Rechavi, G., Jakob-Hirsch, J., Kela, I., Kaminski, N., Getz, G., Domany, E. & Givol, D. (2001) *Oncogene* **20,** 2225–2234.
36. Kannan, K., Amariglio, N., Rechavi, G. & Givol, D. (2000) *FEBS Lett.* **470,** 77–82.
37. Yu, J., Hwang, P. M., Rago, C., Kinzler, K. W. & Vogelstein, B. (1999) *Proc. Natl. Acad. Sci. USA* **96,** 14517–14522.
38. Zhao, R., Gish, K., Murphy, M., Yin, Y., Notterman, D., Hoffman, W. H., Tom, E., Mack, D. H. & Levine, A. J. (2000) *Genes Dev.* **14,** 981–993.
39. Vogelstein, B., Lane, D. & Levine, A. J. (2000) *Nature* **408,** 307–310.
40. Polyak, K., Xia, Y., Zweier, J. L., Kinzler, K. W. & Vogelstein, B. (1997) *Nature* **389,** 300–305.
41. Soengas, M. S., Alarcon, R. M., Yoshida, H., Giaccia, A. J., Hakem, R., Mak, T. W. & Lowe, S. W. (1999) *Science* **284,** 156–159.
42. Bates, S. & Vousden, K. H. (1999) *Cell Mol. Life Sci.* **55,** 28–37.
43. Yu, J., Wang, Z., Kinzler, K. W., Vogelstein, B. & Zhang, L. (2003) *Proc. Natl. Acad. Sci. USA* **100,** 1931–1936.
44. Miyashita, T., Krajewsky, S., Krajewska, M., Wang, H., Lin, H., Hoffman, B., Lieberman, D. & Reed, J. (1994) *Oncogene* **9,** 1799–1805.
45. Pohl, U., Wagenknecht, B., Naumann, U. & Weller, M. (1999) *Cell Physiol. Biochem.* **9,** 29–37.
46. Dazard, J.-E., Gal, H., Amariglio, N., Rechavi, G., Domany, E. & Givol, D. (2003) *Oncogene* **22,** 2993–3006.
47. Gentile, M., Latonen, L. & Laiho, M. (2003) *Nucleic Acids Res.* **31,** 4779–4790.
48. Amundson, S. A., Bittner, M., Chen, Y., Trent, J., Meltzer, P. & Fornace, A. J. J. (1999) *Oncogene* **18,** 3666–3672.
49. Guo, Y., Chang, H., Tsai, J., Huang, J., Li, C., Young, K., Wu, L., Lai, M., Liu, H. & Huang, W. (2002) *Environ. Mol. Mutagen* **40,** 122–128.

The Contribution of Transactivation Subdomains 1 and 2 to p53-Induced Gene Expression Is Heterogeneous But Not Subdomain-Specific[1,2]

Jennifer M. Smith[*,†], *Lawton J. Stubbert*[*,†], *Jeffrey D. Hamill*[*] *and Bruce C. McKay*[*,†]

*Cancer Therapeutics Program, Ottawa Health Research Institute, 501 Smyth Rd, Ottawa, ON, Canada K1H 8L6; †Department of Cellular and Molecular Medicine, University of Ottawa, 451 Smyth Rd, Ottawa, ON, Canada K1H 8M5

Abstract

Two adjacent regions within the transactivation domain of p53 are sufficient to support sequence-specific transactivation when fused to a heterologous DNA binding domain. It has been hypothesized that these two subdomains of p53 may contribute to the expression of distinct p53-responsive genes. Here we have used oligonucleotide microarrays to identify transcripts induced by variants of p53 with point mutations within subdomains 1, 2, or 1 and 2 (QS1, QS2, and QS1/QS2, respectively). The expression of 254 transcripts was increased in response to wild-type p53 expression but most of these transcripts were poorly induced by these variants of p53. Strikingly, a number of known p53-regulated transcripts including *TNFRSF10B*, *BAX*, *BTG2*, and *POLH* were increased to wild-type levels by $p53^{QS1}$ and $p53^{QS2}$ but not $p53^{QS1/QS2}$, indicating that either subdomain 1 or 2 is sufficient for p53-dependent expression of a small subset of p53-responsive genes. Unexpectedly, there was no evidence for $p53^{QS1}$- or $p53^{QS2}$-specific gene expression. Taken together, we found heterogeneity in the requirement for transactivation subdomains 1 and 2 of p53 without any subdomain-specific contribution to p53-induced gene expression.

Neoplasia (2007) **9**, 1057–1065

Keywords: p53, gene expression, microarray, transcription factor, apoptosis.

Introduction

The p53 tumor suppressor plays a pivotal role in preventing oncogenic transformation [1]. More than half of all human cancers is associated with alterations in p53 [1]. Decreased p53 activity is associated with hereditary cancers [2] and p53 nullizygous mice are cancer-prone [3]. The p53 protein is a sequence-specific transcription factor that can regulate the expression of a plethora of genes [1]. This protein is activated and accumulates in cells in response to a variety of cellular stresses and thus is an important regulator of stress gene regulation [1].

The p53 protein is a modular protein with several well-characterized functional domains. The C-terminus of p53 is required for oligomerization and contains sequence-independent DNA, DNA damage, and RNA binding activities [4]. This region is dispensable for p53 to function as a transcriptional activator [5,6]. The central third of p53 contains the sequence-specific DNA binding domain required for p53 to function as a transcriptional activator [7]. The majority of tumor-associated p53 mutations fall within the DNA binding domain [8]. The N-terminus of p53 contains an activation domain (AD) that is also required for sequence-specific transcriptional activation [9,10].

The N-terminal 73 amino acids of p53 expressed as a fusion protein with the DNA binding domain of the yeast GAL4 protein functions as an activator of GAL4-dependent gene expression [10]. The minimal transactivation domain was subsequently localized to the N-terminal 42 amino acids of p53 [9] and critical hydrophobic amino acids (Leu-22 and Trp-23) within this acidic region were found to be important for transactivation [5,11,12]. The mutation of these residues (L22Q/W23S) decreased the ability of the N-terminal 42 amino acids of p53 to function as an AD [5,11,12]. The $p53^{L22Q/W23S}$ variant and the murine equivalent ($p53^{L25Q/W26S}$) are commonly used as transactivation-deficient versions of p53 [13–17]. Intriguingly, the L22Q/W23S variant (hereafter referred to as the QS1 variant) reportedly retains some p53 activity despite a profound transactivation defect [13,18–20]. Specifically, the QS1 variant retains the ability to induce apoptosis in some cellular contexts but is unable to induce G_1 arrest [13,14,19,20]. Intriguingly, the homozygous QS1 knock-in mice undergo embryonic lethality although p53 is not required for embryonic development [14,21]. The QS1 variant is not equivalent to the complete loss of p53.

Abbreviations: MALDI-TOF, matrix-assisted laser desorption/ionization time of flight; AD, activation domain; MEF, mouse embryonic fibroblast

Address all correspondence to: Bruce C. McKay, Cancer Therapeutics Program, Ottawa Health Research Institute, 501 Smyth Rd, Ottawa, ON, Canada K1H 8L6. E-mail: bmckay@ohri.ca

[1]This work was initially supported by the Cancer Research Society and, more recently, by the National Cancer Institute of Canada with Funds from the Terry Fox Run. J.M.S. was supported by an Ontario Graduate Scholarship in Science and Technology. L.J.S. was supported by an Ontario Premier's Research Excellence Award to B.C.M. B.C.M. is a Research Scientist of the National Cancer Institute of Canada funded through the Canadian Cancer Society.

[2]This article refers to supplementary materials, which are designated by Tables W1, W2, W3, and W4 and Figure W1 and are available online at www.neoplasia.com.

Received 3 August 2007; Revised 22 September 2007; Accepted 25 September 2007.

DOI 10.1593/neo.07688

A second functional transactivation subdomain in the N-terminus of p53 has also been identified through a similar strategy. Amino acids 43 to 73 of p53 fused to the DNA binding domain of GAL4 were able to drive Gal4-dependent reporter gene expression and two critical hydrophobic amino acids (Trp-53 and Phe-54) were again critical for this activity [5,11,20]. Like the QS1 variant of p53, the W53Q/F54S variant (hereafter referred to as the QS2 variant) is defective in sequence-specific transactivation, when the expression of a small number of well-characterized p53 target genes was assessed [16,18–20]. Intriguingly, the QS2 variant of p53 was reported to retain the ability to induce p53-dependent G_1 arrest but not p53-dependent apoptosis [20]. Therefore, despite the fact that the QS1 and QS2 variants of p53 have defects in sequence-specific transactivation, they exhibit some distinct biologic activities. This has led several laboratories to hypothesize that these domains function independently in regulating distinct subsets of p53 target genes [14,16,19–21].

Before this study, the relative contribution of these two AD subdomains to p53-mediated gene expression had not been assessed. Here we used recombinant adenoviruses expressing wild-type p53, $p53^{QS1}$, $p53^{QS2}$, and $p53^{QS1/QS2}$ to drive p53-dependent gene expression in colorectal carcinoma cell lines in which endogenous p53 expression had been abolished by gene targeting. Gene expression was assessed using Affymetrix Oligonucleotide microarrays containing over 50,000 features. The expression of 254 transcripts was increased in response to $Adp53^{wt}$ infection and approximately 10% of these transcripts was also induced by the QS1 and QS2 variants but not the compound mutant. A small number of these genes were induced to wild-type levels by the QS variants; however, the fold increase in expression of the transcripts induced by the QS1 and QS2 variants was strongly correlated. These results indicate that the two subdomains cooperate to activate transcription of most p53 target genes. Our work also identified another subgroup of p53 target genes that appear to use either subdomain interchangeably.

Materials and Methods

Cell Culture and UV Treatment

The HCT116 $p53^{-/-}$ cell line was kindly provided by Dr. Bert Vogelstein (John's Hopkins University). Cells were maintained in McCoy's 5A media supplemented with 10% fetal bovine serum (Wisent, St. Bruno, Quebec, Canada). Adenovirus constructs expressing $p53^{wt}$, $p53^{QS1}$, $p53^{QS2}$, and $p53^{QS1/QS2}$ were kindly provided by Dr. Ruth Slack (University of Ottawa, Ontario, Canada). The adenovirus Ad-$BHG^{\Delta E1\Delta E3}$ (Ad-empty) control was generously provided by Dr. Frank Graham (McMaster University, Canada). Viruses were propagated using human embryonic kidney (HEK293) cells and cesium chloride gradient purification [22]. Virus titers were determined in HEK293 cells by standard methods [22] and titers are expressed as plaque-forming units per milliliter (pfu/ml). Cell lines were routinely tested for mycoplasma contamination.

RNA Isolation and Quantitative Reverse Transcription–Polymerase Chain Reaction (RT-PCR)

HCT116 $p53^{-/-}$ cells at 70% to 80% confluence were infected at a multiplicity of infection of 25 with indicated adenovirus in serum-free media for 1 hour. Growth medium containing 10% fetal bovine serum was replaced and cells were returned to the incubator for the indicated time. Infected cells were collected and total RNA was isolated using the RNeasy RNA isolation kit (Qiagen, Valencia, CA) according to manufacturer's specifications. Five micrograms of total RNA was reverse-transcribed using a first-strand cDNA synthesis kit (MBI Fermentas, Burlington, ON, Canada). Quantitative RT-PCR was performed using the SYBR Green Fluorescent DNA stain (Invitrogen, Burlington, ON, Canada), a LightCycler 2 quantitative PCR machine (Roche Diagnostics, Mannheim, Germany), and LightCycler software version 3 (Roche Diagnostics). The primers used were ACTB (GGGCATGGGTCAGAAGGAT and GTGGCCATCTCTTGCTCGA), APAF1 (CAACGGGAGATGACAATG and CTGGAGAAAAGCAAAGGTC), BAK1 (GCCATCAGCAGGAACAGGAG and ACACCCAGAACCACCAGCAC), BTG2 (CACAGAGCACTACAAACACC and ACAAGACGCAGATGGAGC), CASP6 (GCTTTGTGTGTCTTCC and CTCAGTTATGTTGGTGTCC), CDKN1A (CCTCAAATCGTCCAGCGACCTT and CATTGTGGGAGGAGCTGTGAAA), TNFRSF6 (CTCATCTTAATGGCCTAATGCA and GCTTCAGTTTATAACTATCTTCAC), TNFRSF10B (GGCATCATCATAGGAGTCAC and GTCAAAGGGCACCAAGTC), TP53I3 (TCTCTATGGTCTGATGGG and TTGCCTATGTTCTTGTTG), and MafB (TGCTGAGAGAGAGAACCGAGAG and CACCACCAAGAACTCTTCCTAC).

Microarrays

Total RNA was collected from HCT116$p53^{-/-}$ cells infected for 16 hours with 25 pfu/cell of Ad-$BHG^{\Delta E1\Delta E3}$, $Adp53^{wt}$, $Adp53^{QS1}$, $Adp53^{QS2}$, or $Adp53^{QS1/QS2}$ using the RNeasy Mini kit (Qiagen). Human Genome U133plus2.0 oligonucleotide arrays (Affymetrix, Santa Clara, CA) were used for expression analysis. Experimental procedures were performed according to the manufacturer specifications at the Ottawa Genomics Innovation Centre Affymetrix GeneChip Facility (Ottawa, Ontario, Canada). Affymetrix Microarray Suite 6.0 (MAS6.0) software was used to analyze the microarray data. MAS6.0 software uses a nonparametric Wilcoxon signed rank test to determine whether statistically meaningful differences in probe cell intensities were detected between samples (change calls were determined using γ_{1H} and γ_{1L} values of 0.0025). Genes were considered to be induced if and only if they were statistically ($P \leq .0025$) increased in all experiments compared to Ad-$BHG^{\Delta E1\Delta E3}$ infected controls by an average of two-fold.

Western Blot Analysis

Total protein was extracted from cells using 1% sodium dodecyl sulfate and brief sonication. Protein samples were run on 4% to 12% Bis–Tris acrylamide gels, transferred to nitrocellulose membrane (Hybond-C; Amersham, Piscataway, NJ) and blocked with 5% skim milk–phosphate-buffered saline

with 1% Tween 20 (TBS–T). Monoclonal antibodies raised against p53 were DO-1 (Ab6; Calbiochem, San Diego, CA), Pab1801 (Ab2; Calbiochem), and Pab421 (Ab1; Calbiochem). Additional antibodies were raised against $p21^{WAF1}$ (Ab1; Calbiochem), PUMA (Ab1; Calbiochem), MDM2 (SMP14; Santa Cruz Biotechnology, Santa Cruz, CA) and MafB (P-20; Santa Cruz Biotechnology). Anti–mouse immunoglobulin (IgG) conjugated with horseradish peroxidase was used as a secondary antibody (Calbiochem), and protein bands were detected using the SuperSignal WestPico Chemiluminescent Substrate kit (Pierce, Rockford, IL) after being exposed to a film (X-OMAT; Kodak, Rochester, NY).

Immunoprecipitation and Mass Spectrometry

HCT116 $p53^{-/-}$ cells were infected with a multiplicity of infectionof 25 of $Adp53^{wt}$. Twenty-four hours postinfection cells were washed twice with PBS and scraped into PBS on ice. Cells were then treated as per manufacturer's instructions for the use of Protein A–agarose beads (Roche Diagnostics). Protein lysates were immunoprecipitated with p53 antibody Pab421. Precipitated protein extracts were run on a 4% to 12% Bis–Tris polyacrylamide gel and subsequently treated with GelCode Blue Stain Reagent according to manufacturer's specifications (Pierce). Bands of interest were excised and subjected to trypsin digestion. Matrix-assisted laser desorption/ionization time of flight tandem mass spectrometry (MALDI-TOF MS/MS) was performed at the Ontario Genomics Innovation Centre Proteomics Facility at the Ottawa Health Research Institute (Ottawa, Ontario, Canada). Peptides were identified using Mascot [23].

Results

The QS1 and QS2 Variants of p53 Are Impaired in p53-Dependent Gene Expression

HCT116 cells in which p53 had been inactivated by gene targeting (HCT116$p53^{-/-}$) [24] were infected with recombinant adenoviruses expressing wild-type, QS1, QS2, or QS1/QS2 variants of p53. Cell lysates were collected for immunoblot analysis at various times following infection using a panel of anti–p53 antibodies. The use of this panel of antibodies allowed us to distinguish between the variant forms of p53 in all experiments (Figure 1*A*). Immunoblot analysis revealed the presence of two immunoreactive bands that migrated at approximately 47 and 53 kDa (Figure 1*B*). Wild-type p53 was immunoprecipitated with Pab421 and separated by sodium dodecyl sulfate–polyacrylamide gel electrophoresis. The bands were gel excised and analyzed by MALDI-TOF mass spectrometry. The seven peptides identified were located within the DNA binding domain of p53 (Figure 1*A* and Table W1). These peptides coupled with our panel of anti–p53 antibodies indicated that both bands represent full-length p53 (Figure 1*A*). The two forms likely correspond to

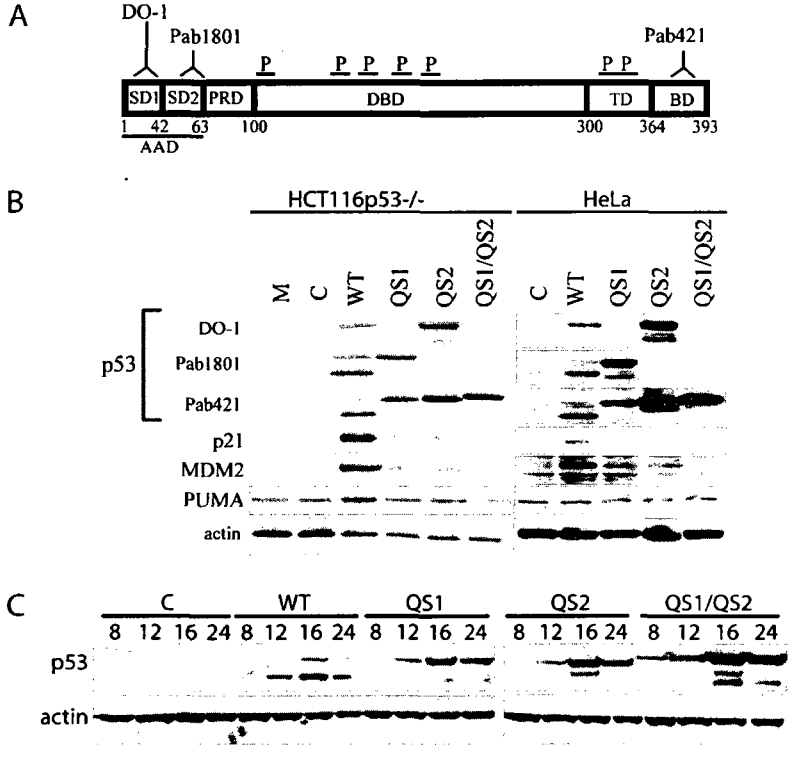

Figure 1. *Expression of transactivation subdomain variants of p53. (A) Schematic representation of epitopes recognized by the indicated monoclonal antibodies (DO-1, Pab1801, and Pab421), peptides (P) identified by mass spectroscopy (see Table W1), and p53 functional domains. SD1 and SD2 denote subdomains 1 and 2 within the acidic AD.* PRD, *proline-rich domain;* DBD, *DNA binding domain;* TD, *tetramerization domain;* BD, *basic domain. Numbers below indicate the amino acid position. (B) Immunoblot analysis of p53 expression 16 hours following infection of either HCT116*$p53^{-/-}$ *or HeLa cells with the indicated recombinant adenovirus, using three different anti–p53 monoclonal antibodies. M and C represent mock- and control virus–infected samples whereas WT, QS1, QS2, and QS1/QS2 denote the wild-type and variant forms of p53. Similar blots were obtained with cell lysates derived from HCT116 and MDAH041 cells (data not shown). (C) Samples were collected at 8, 16, or 24 hours and subsequently analyzed by immunoblot analysis with the Pab421 monoclonal antibody.*

differentially modified forms. However, the N- and C-termini of p53, containing the known modification sites, were not represented among the identified peptides and thus the specific modifications were not ascertained. The increased expression of these variants relative to wild-type p53 was expected because the QS variants do not induce mdm2 expression (Figure 1*B*), the ubiquitin ligase responsible for the rapid turnover of wild-type p53 [25].

To identify transcripts induced in response to Adp53^{wt}, Adp53^{QS1}, Adp53^{QS2} and Adp53$^{QS1/QS2}$ infection, microarray analysis was performed using total RNA collected from HCT116p53$^{-/-}$ cells 16 hours post infection because maximal p53 levels were achieved within this time frame (Figure 1*C*). The expression of 254 transcripts increased significantly following infection with the Adp53^{wt} virus compared to control virus infection (Table W2). Of these, only 28, 23, and 1 were induced by Adp53^{QS1}, Adp53^{QS2}, and Adp53$^{QS1/QS2}$, respectively (Figure 2*A* and Table W3). The mean induction of the Adp53^{wt}-induced transcripts was significantly higher than the fold increase in expression due to the expression of any of the QS variants (Figure 2*B*). In fact, very few of the Adp53^{wt}-induced genes appeared to be induced to wild-type levels by either the QS1 or QS2 variants (Figure 2*C*). Infection with the Adp53^{wt} virus resulted in a greater increase in gene expression even when examining genes determined to be induced in response to either Adp53^{QS1} or Adp53^{QS2} infection (Figure 2, *D* and *E*). Therefore, the majority of WT-, QS1-, and QS2-regulated genes were poorly induced by the QS variants.

Correlation between Genes Induced By the QS1 and QS2 Variants

Having determined that most Adp53^{wt}-induced genes were poorly induced by the variants, we sought to determine whether distinct subgroups of p53 target genes were preferentially responsive to the QS variants of p53. The fold change in p53 target gene expression in response to Adp53^{QS1} infection was plotted with respect to Adp53^{QS2} infection (Figure 3*B*). We observed a very striking linear correlation between the fold change in expression induced by the QS1 and QS2 variants of p53 regardless of whether the expression of Adp53^{wt}-, Adp53^{QS1}-, or Adp53^{QS2}-induced genes were considered (Figure 3*B*; R^2 values were 0.73, 0.64, and 0.61, respectively). Therefore, the Adp53^{QS1}- and Adp53^{QS2}-induced genes were induced to a similar extent by both variants (Figure 3*B* and Table W3). These results indicate that the disruption of either subdomain of p53 similarly affected the overall pattern of p53 transcriptional activation. We interpret these results to indicate that the contribution of transactivation subdomains 1 and 2 to p53-mediated gene expression was heterogeneous but not subdomain-specific.

Based on our definition of induced genes (see Materials and Methods section), the expression of 18 genes increased in response to both QS variants but 10 and 5 wild-type p53-induced transcripts appeared to be increased in response to either QS1 or QS2, respectively (Figure 3*A*). To determine whether these apparently p53^{QS1}- and p53^{QS2}-specific genes were in fact specifically and preferentially upregulated by one of the variants, the pattern of allele-specific gene expression was confirmed by quantitative RT-PCR for 11 different transcripts at several different times following viral infection. The majority of p53 target genes were poorly induced by the QS1 and QS2 variants (Figure 4*A*). Several p53 target genes were significantly induced by the QS variants but were induced more strongly by wild-type p53 (Figure 4*B*). Lastly, a few target genes were induced to near wild-type levels by p53^{QS1} and p53^{QS2} (Figure 4*C*). The quantitative RT-PCR data correlated well with the microarray analysis and none of the p53-upregulated transcripts examined displayed a subdomain-specific pattern of gene expression (Figure 4 and Tables W3 and W4). The expression of several p53-regulated proteins was assessed by immunoblot in independent cell lines and no subdomain-specific differences in protein expression were detected (Figure 1*B*). Collectively, we interpret our results to indicate that the apparently p53^{QS1}- and p53^{QS2}-specific targets were not specifically induced by a single variant. Therefore, the response of p53-induced transcripts to the QS variants was heterogeneous but not subdomain-specific.

The 254 Adp53^{wt}-induced genes were subjected to gene ontology (GO) analysis (http://www.geneontology.org/). Several genes were associated with the GO terms apoptosis (GO:0006915), cell cycle (GO:0007049), and DNA repair (GO:0006281) (Table 1), consistent with known p53 biology [26]. Of these terms, only apoptosis was statistically overrepresented ($P < .01$) based on analysis using the web-based GOstat software (http://gostat.wehi.edu.au/). Consistent with the preponderance of proapoptotic genes, Adp53^{wt} infection resulted in a significant increase in the proportion of apoptotic cells (Figure 5, *A* and *B*). Both QS variants were reduced in their capacity to induce cell death and there was no significant difference in their ability to induce apoptosis in these cells (Figure 5, *A* and *B*). Most of the apoptosis annotated genes were poorly induced by the QS1 and QS2 variants of p53 compared to wild-type p53 (Table 1). Therefore, decreased p53-dependent gene expression correlated with decreased p53-dependent apoptosis in these cells. Similarly, the cell cycle–annotated genes were poorly induced by all variants (Table 1). Interestingly, two of the three genes associated with DNA repair (*BTG2* and *POLH*) were induced to near wild-type levels by the QS1 and QS2 variants but not the QS1/QS2 variant (Table 1 and Figure 4*C*). Due to the limited number of repair-related genes, the significance of this specific observation remains unclear. Overall, our results suggest that there is substantial heterogeneity in the contribution of subdomains 1 and 2 to p53-mediated gene expression but there are no subdomain-specific effects.

Discussion

The p53 protein can act as both a positive and negative regulator of gene expression but p53 is best understood as a transcriptional activator. The p53 protein is a positive regulator of several hundred genes and this is mediated by the sequence-specific binding of p53 to consensus elements found in promoters, enhancer regions, introns, or the 5′

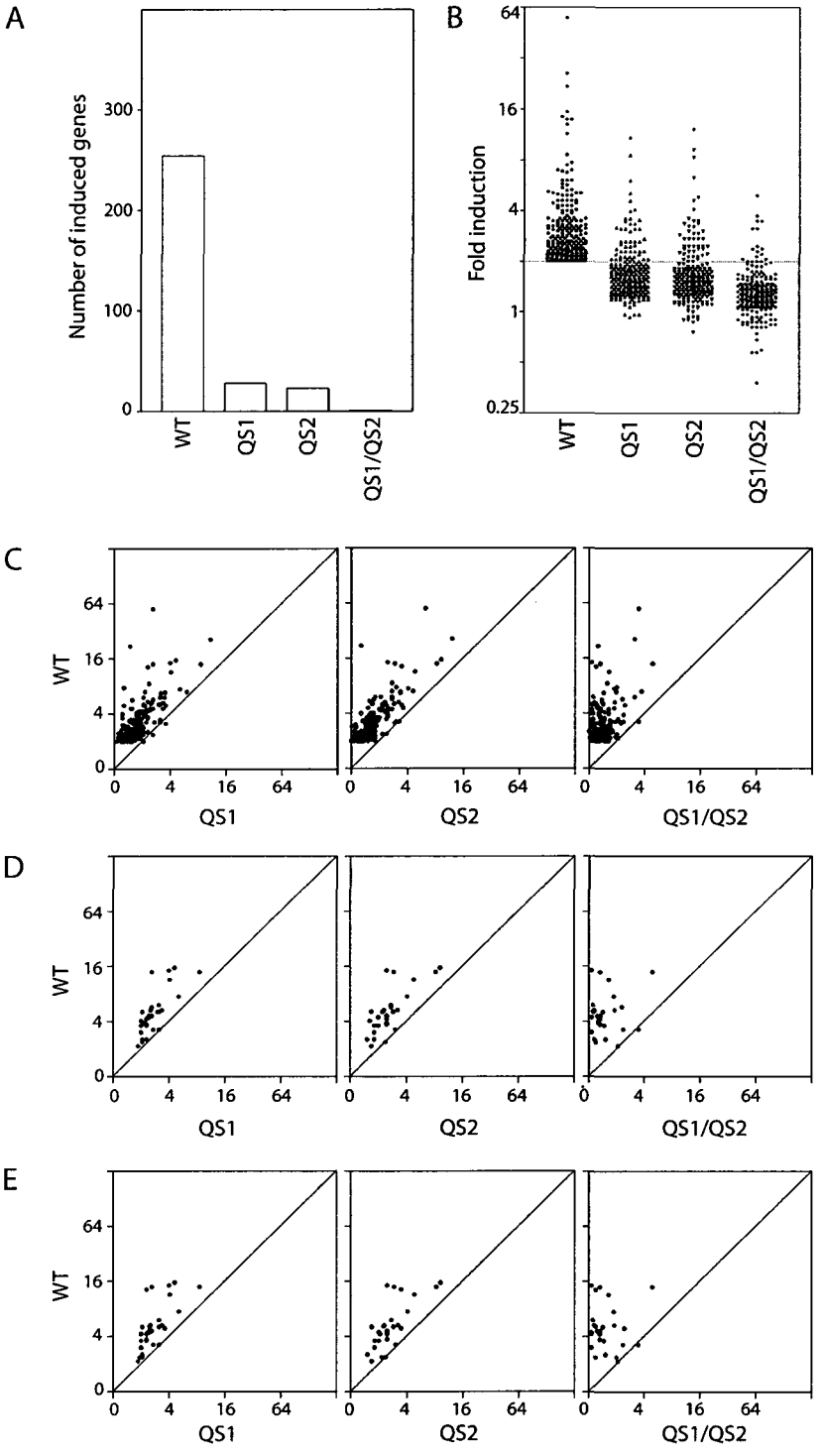

Figure 2. *Most p53 target genes are poorly induced by the QS variants. (A) Two hundred and fifty-four genes were induced by Adp53^{wt}. Of these, only 28, 23, and 1 were induced by QS1, QS2, and QS1/QS2, respectively. (B) The fold increase in expression of these 254 genes was determined following infection of cells with adenoviruses expressing wild-type, QS1, QS2, or QS1/QS2 variant of p53. The fold increase in the expression following infection with Adp53^{QS1}, Adp53^{QS2}, or Adp53$^{QS1/QS2}$ was less than the fold increase in response to Adp53^{wt} infection (one-way analysis of variance followed by a Tukey's Multiple Comparisons test, $P \leq .001$). (C–E) The fold increase in expression due to Adp53^{wt} expression was compared to the fold increase in expression due to indicated transactivation subdomain variant of p53 for Adp53^{wt}-, Adp53^{QS1}-, and Adp53^{QS2}-induced genes (C, D, and E, respectively). The 254, 28, and 23 genes induced by Adp53^{wt}, Adp53^{QS1}, and Adp53^{QS2} are listed in Tables W2 and W3.*

untranslated regions of these genes [1]. Transcriptional activation further requires the p53-dependent recruitment of the histone acetyl transferases CBP/p300, general transcription factors, and RNA polymerase II to the promoter of target genes [27–30]. The N-terminal AD is required for the recruitment of these proteins and subsequent p53-dependent gene activation [11,30]. Amino acids 1 to 42 were found to function as a minimal transcriptional AD [9,10]. However, it was subsequently shown that this minimal region was part of a larger AD with each of the two subdomains capable of supporting

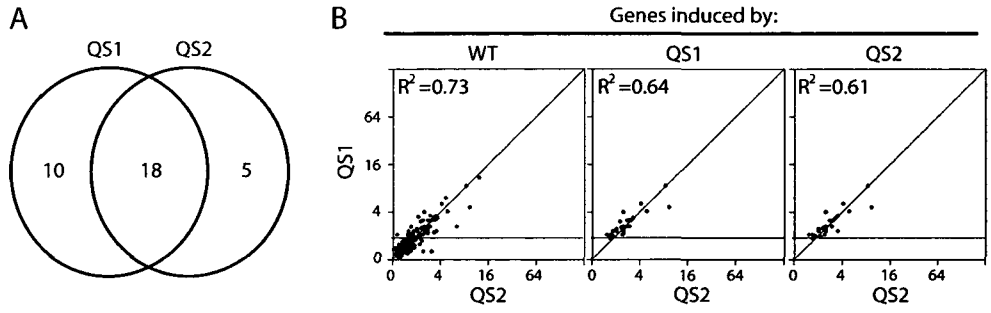

Figure 3. *Correlation between Adp53^{QS1}- and Adp53^{QS2}-induced genes. (A) A Venn diagram is used to represent the overlap between Adp53^{QS1}- and Adp53^{QS2}-induced genes, as defined in the Materials and Methods section. (B) The effect of Adp53^{QS1} and Adp53^{QS2} infection on the expression of the 254 Adp53^{wt}-, 28 Adp53^{QS1}-, and 23 Adp53^{QS2}-induced genes was determined. The genes induced by Adp53^{wt}, Adp53^{QS1}, and Adp53^{QS2} are listed in Tables W2 and W3. A very tight correlation (R^2 values are inset) between Adp53^{QS1}- and Adp53^{QS2}-induced gene expression was observed within the subset of target genes.*

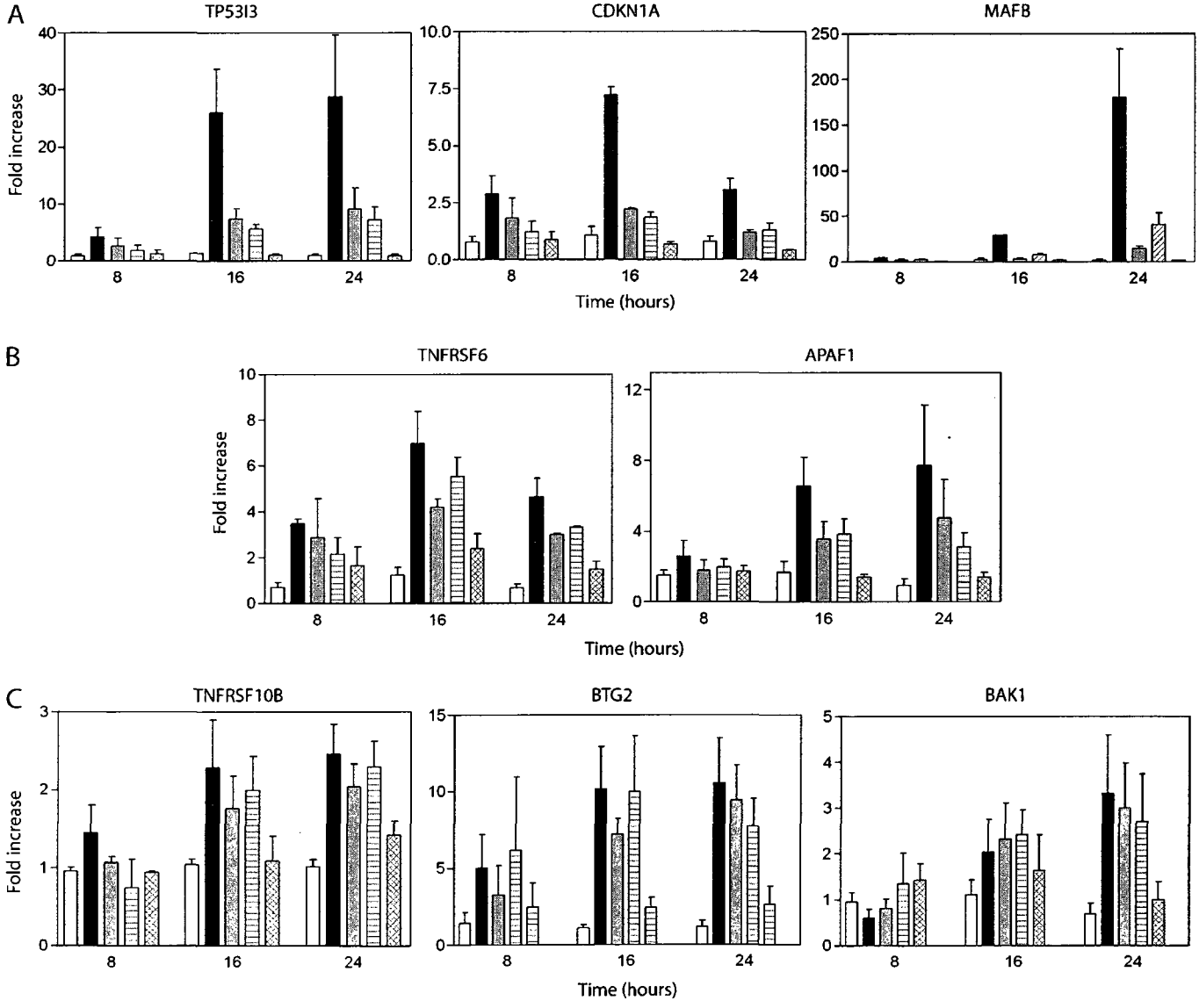

Figure 4. *Representative transcripts induced by wild-type p53. (A–C) Expression of the indicated transcript was determined by real-time RT-PCR using samples collected at the indicated time following virus infection (8, 16, or 24 hours). Expression of β-actin was used to normalize all RT-PCR results. Open, black, grey, hatched, and crosshatched bars represent control, Adp53^{wt}-, Adp53^{QS1}-, Adp53^{QS2}-, and Adp53$^{QS1/QS2}$-infected samples. Each value represents the mean fold increase in expression (± SEM) determined from a minimum of three independent experiments.*

Table 1. Adp53^{wt}-Induced Genes Involved in Apoptosis, Cell Cycle, and/or DNA Repair.

GO Term*	Locus	p53 Variant			
		WT	QS1	QS2	QS1/QS2
Apoptosis (GO:0006915)	*TP53I3*	3.9†	2.0	1.3	0.1
	TP53INP1	3.8	1.4	1.5	0.4
	APAF1	2.8	1.8	1.8	1.0
	TNFRSF6	2.4	1.8	1.7	0.9
	CASP6	1.7	0.8	0.7	0.4
	TNFRSF10B	1.5	0.9	0.8	0.5
	MDM2	1.4	0.3	0.1	0.0
	BAX	1.4	1.2	0.9	0.2
	AKTIP	1.2	0.3	0.4	0.4
	AMID	1.2	0.4	0.2	0.2
	BID	1.1	0.4	0.3	0.3
	CARD10	1.1	0.5	0.4	0.4
	BAK1	1.0	0.5	0.4	0.3
	TRAF4	1.0	0.4	−0.1	−0.2
Cell Cycle (GO:0007049)	*CDKN1A*	2.4	1.1	0.8	−0.8
	SESN1	2.0	0.9	0.8	0.1
	GAS2L1	1.4	0.8	0.6	0.4
	MDM2	1.4	0.3	0.1	0.0
	RB1	1.3	0.8	0.6	0.8
	RHOB	1.2	0.4	0.3	0.5
	PARD6G	1.2	0.7	0.6	0.4
	SFN	1.2	0.4	0.3	−0.3
	SESN2	1.1	0.3	0.2	0.0
	LATS2	1.1	0.5	0.4	0.4
	HRAS	1.0	0.5	0.4	0.2
DNA Repair (GO:0006281)	*BTG2*	2.9	2.4	2.0	0.9
	POLH	2.2	1.8	1.9	0.9
	DDB2	1.1	0.4	0.3	−0.3

*Genes involved in apoptosis, cell cycle and DNA repair were identified using the Gene Ontology database (http://geneontology.org/). Of these GO terms, only apoptosis (GO:0006915) and related GO terms were significantly over represented among the Adp53^{wt}-induced genes based on GOstat analysis (http://gostat.wehi.edu.au/).

†The mean fold increase in expression (log_2) determined from microarray experiments, as described in the Materials and Methods section.

sequence-specific transactivation when expressed as a fusion protein with a heterologous DNA binding domain [5,11].

The relative contribution of subdomains 1 and 2 to p53 activity has been examined at the cell biologic level by two laboratories. Zhu et al. [20] reported that p53^{QS1} is unable to induce G_1 arrest but retains the ability to induce apoptosis in tumor cell lines [18]. In contrast, p53^{QS2} was reportedly able to induce cell cycle arrest but was impaired in its ability to induce apoptosis in these same cell lines [20]. Cregan et al. [16] reported that overexpression of either p53^{QS1} or p53^{QS2} in neuronal cells led to similar levels of apoptosis but that forced expression of the p53^{QS2} variant in p53 nullizygous neuronal cells led to significantly more apoptosis than the p53^{QS1} variant when these cells were subsequently treated with camptothecin. Based on these studies, it was hypothesized that the p53 transactivation subdomains contribute to the regulation of distinct subsets of p53 target genes that affect the biologic activity of these variants. However, the relative contribution of the two distinct subdomains in the AD to p53-dependent transcriptional activity had remained untested.

Here we found that infection of these cells with recombinant adenoviruses expressing p53^{QS1}, p53^{QS2}, and p53$^{QS1/QS2}$ resulted in the induction of far fewer p53 target genes than Adp53^{wt} infection. Approximately 10% of the Adp53-induced genes were also increased on Adp53^{QS1} and Adp53^{QS2} infection. The identity and fold increase in expression of the p53^{QS1}- and p53^{QS2}-upregulated genes were strongly correlated, indicating that these subdomains do not contribute to the expression of distinct subsets of genes. The majority of p53-regulated genes were induced poorly by p53^{QS1}, p53^{QS2}, and p53$^{QS1/QS2}$, indicating that both subactivation domains are required to increase the expression of most p53 target genes. Conversely, a relatively small number of p53-target genes including *TNFRSF10B*, *BAX*, *BTG2*, and *POLH* were induced to near wild-type levels by p53^{QS1} and p53^{QS2}, but were poorly induced by p53$^{QS1/QS2}$. Therefore, the p53-dependent induction of this subgroup of p53 target genes requires a functional transactivation domain but subdomain 1 or 2 appears to be sufficient and used interchangeably for p53 target gene expression within this group of genes. We did not detect any subdomain-specific p53 target genes.

Like many other transactivation domains, the N-terminus of p53 is not highly conserved overall at the level of amino acid sequence; however, there is a high level of sequence conservation among rodents and primates within subdomain 1 (34% identity; see Figure W1). The region of highest homology includes amino acids 13 through 26 (93% identity), a region of p53 termed box 1 [31]. The N-terminus of p53 is rich in acidic residues characteristic of acidic ADs and is mostly unstructured under physiological conditions [32]. Box 1 contains a number of hydrophobic residues and nuclear magnetic resonance studies indicate that amino acids 18 to 26 within box 1 form a helix within the context of the larger disordered transactivation domain [32]. Mutation of Leu-22 and Trp-23 within the helical region in the QS1 variant is predicted to disrupt this region of limited secondary structure [32]. The high

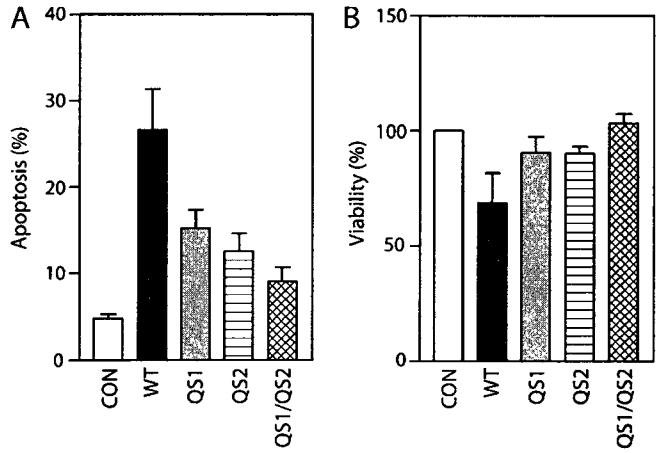

Figure 5. *Effect of QS variants of p53 on cell viability and apoptosis. Apoptosis and cell viability were assessed 48 hours following infection with either control adenovirus or adenoviruses expressing the indicated variants of p53. Apoptosis was assessed by subdiploid DNA content (A) and viability was assessed by Trypan blue exclusion (B). Each point represents the mean (±SEM) determined from three independent experiments. Adp53wt induced more apoptosis than the variants (one-way analysis of variance followed by Tukey's Multiple Comparisons test, $P \leq .01$ for apoptosis and $P \leq .05$ for viability). No significant difference in viability or apoptosis was observed when comparing QS1 and QS2 variants.*

level of conservation between mouse and human p53 has made it possible to generate knock-in mice expressing the QS1 variant from the endogenous p53 locus [14], as discussed later. It is likely that this secondary structure is important for the activity of subdomain 1.

Subdomain 2, within the transactivation domain of p53, is well conserved among primate species but is poorly conserved when the sequence comparison is extended to rodent versions of p53 (Figure W1). The limited homology between mouse and human p53 makes the QS2 variant more difficult to model in mice. Much like subdomain 1, hydrophobic residues within subdomain 2 of human p53 give rise to localized secondary structure within the mostly unstructured acidic AD (nascent turns between Met-40 and Met-44 and between Asp-48 and Trp-53) [32–34]. Regions of limited secondary structure within mostly unstructured ADs are common among transcriptional activators [12,30,34,35]. The second subdomain of p53 reportedly binds to many proteins known to interact with subdomain 1, such as mdm2, RPA, TFIID, TFIIH, and p300 [11,27,30,34,36–44]. The QS2 point mutations are thought to disrupt the localized secondary structure and would be expected to disrupt protein–protein interactions important for transcriptional activation [12,30,32–34].

As indicated above, knock-in mice expressing the QS1 variant from the endogenous p53 locus have been generated [14]. Homozygous $p53^{QS1}$ expression results in embryonic lethality; however, homozygous $p53^{QS1}$-targeted mouse embryonic fibroblasts (MEFs) were obtained [14]. Using these MEFs, the induction of five of the six p53 target genes tested was reduced in the QS1-expressing MEFs compared to control cell lines following doxorubicin treatment [14]. The single gene induced by the QS1 variant of murine p53 was *BAX* [14] and we similarly found that the human QS1 variant was able to upregulate *BAX* expression. Unexpectedly, we found that the QS1 and QS2 variants similarly increased the expression of *BAX* along with three other known p53 target genes (*TNFRSF10B*, *BTG2*, and *POLH*). Therefore, only one of the two subdomains appears to be necessary and sufficient for p53-dependent gene expression of this subset of p53 target genes. We interpret the heterogenous requirement for subdomains 1 and 2 to indicate that the requirement for specific protein–p53 AD interactions must vary in a p53 target gene–specific manner.

In summary, our results suggest that compound mutations of critical hydrophobic amino acids in either subdomain 1 or 2 decrease the affinity of the AD for cofactors or other components of basal transcription apparatus that are rate-limiting for p53-dependent gene expression, at most p53-induced promoters. Surprisingly, the induction of a small subset of p53-responsive genes, including *BAX*, *TNFRSF10B*, *BTG2*, and *POLH*, is not limited by mutations in either of the subdomains alone. Therefore, this latter group of genes appears to have a less stringent requirement for as yet unidentified protein–protein interactions. Importantly, we did not find any genes that were preferentially induced by any single AD variant. Our results support a model in which the transcription activation subdomains of p53 contribute equally to p53-dependent target gene expression.

Acknowledgements

We thank Ruth Slack (University of Ottawa) and Frank Graham (McMaster University) for the recombinant adenoviruses. We acknowledge the assistance of Microarray Core Facility of StemCore Laboratories in the Sprott Center for Stem Cell Research at the Ottawa Health Research Institute.

References

[1] Harris SL and Levine AJ (2005). The p53 pathway: positive and negative feedback loops. *Oncogene* **24**, 2899–2908.

[2] Iwakuma T, Lozano G, and Flores ER (2005). Li-Fraumeni syndrome: a p53 family affair. *Cell Cycle* **4**, 865–867.

[3] Donehower LA, Harvey M, Slagle BL, McArthur MJ, Montgomery CA Jr, Butel JS, and Bradley A (1992). Mice deficient for p53 are developmentally normal but susceptible to spontaneous tumours. *Nature* **356**, 215–221.

[4] Ahn J and Prives C (2001). The C-terminus of p53: the more you learn the less you know. *Nat Struct Biol* **8**, 730–732.

[5] Candau R, Scolnick DM, Darpino P, Ying CY, Halazonetis TD, and Berger SL (1997). Two tandem and independent sub-activation domains in the amino terminus of p53 require the adaptor complex for activity. *Oncogene* **15**, 807–816.

[6] Unger T, Mietz JA, Scheffner M, Yee CL, and Howley PM (1993). Functional domains of wild-type and mutant p53 proteins involved in transcriptional regulation, transdominant inhibition, and transformation suppression. *Mol Cell Biol* **13**, 5186–5194.

[7] El Deiry WS, Kern SE, Pietenpol JA, Kinzler KW, and Vogelstein B (1992). Definition of a consensus binding site for p53. *Nat Genet* **1**, 45–49.

[8] Hollstein M, Sidransky D, Vogelstein B, and Harris CC (1991). p53 mutations in human cancers. *Science* **253**, 49–53.

[9] Unger T, Nau MM, Segal S, and Minna JD (1992). p53: a transdominant regulator of transcription whose function is ablated by mutations occurring in human cancer. *EMBO J* **11**, 1383–1390.

[10] Fields S and Jang SK (1990). Presence of a potent transcription activating sequence in the p53 protein. *Science* **249**, 1046–1049.

[11] Chang J, Kim DH, Lee SW, Choi KY, and Sung YC (1995). Transactivation ability of p53 transcriptional activation domain is directly related to the binding affinity to TATA-binding protein. *J Biol Chem* **270**, 25014–25019.

[12] Lin J, Chen J, Elenbaas B, and Levine AJ (1994). Several hydrophobic amino acids in the p53 amino-terminal domain are required for transcriptional activation, binding to mdm-2 and the adenovirus 5 E1B 55-kD protein. *Genes Dev* **8**, 1235–1246.

[13] Haupt Y, Rowan S, Shaulian E, Vousden KH, and Oren M (1995). Induction of apoptosis in HeLa cells by trans-activation–deficient p53. *Genes Dev* **9**, 2170–2183.

[14] Johnson TM, Hammond EM, Giaccia A, and Attardi LD (2005). The $p53^{QS}$ transactivation-deficient mutant shows stress-specific apoptotic activity and induces embryonic lethality. *Nat Genet* **37**, 145–152.

[15] Attardi LD, Lowe SW, Brugarolas J, and Jacks T (1996). Transcriptional activation by p53, but not induction of the p21 gene, is essential for oncogene-mediated apoptosis. *EMBO J* **15**, 3693–3701.

[16] Cregan SP, Arbour NA, Maclaurin JG, Callaghan SM, Fortin A, Cheung EC, Guberman DS, Park DS, and Slack RS (2004). p53 activation domain 1 is essential for PUMA upregulation and p53-mediated neuronal cell death. *J Neurosci* **24**, 10003–10012.

[17] Jimenez GS, Nister M, Stommel JM, Beeche M, Barcarse EA, Zhang XQ, O'Gorman S, and Wahl GM (2000). A transactivation-deficient mouse model provides insights into Trp53 regulation and function. *Nat Genet* **26**, 37–43.

[18] Chen X, Ko LJ, Jayaraman L, and Prives C (1996). p53 levels, functional domains, and DNA damage determine the extent of the apoptotic response of tumor cells. *Genes Dev* **10**, 2438–2451.

[19] Zhu J, Zhou W, Jiang J, and Chen X (1998). Identification of a novel p53 functional domain that is necessary for mediating apoptosis. *J Biol Chem* **273**, 13030–13036.

[20] Zhu J, Zhang S, Jiang J, and Chen X (2000). Definition of the p53 functional domains necessary for inducing apoptosis. *J Biol Chem* **275**, 39927–39934.

[21] Johnson TM and Attardi LD (2005). $p53^{QS}$: an old mutant teaches us new tricks. *Cell Cycle* **4**, 731–734.

[22] Ng P and Graham FL (2002). Construction of first-generation adenoviral vectors. *Methods Mol Med* **69**, 389–414.

[23] Perkins DN, Pappin DJ, Creasy DM, and Cottrell JS (1999). Probability-based protein identification by searching sequence databases using mass spectrometry data. *Electrophoresis* **20**, 3551–3567.
[24] Bunz F, Dutriaux A, Lengauer C, Waldman T, Zhou S, Brown JP, Sedivy JM, Kinzler KW, and Vogelstein B (1998). Requirement for p53 and p21 to sustain G2 arrest after DNA damage. *Science* **282**, 1497–1501.
[25] Dai MS, Jin Y, Gallegos JR, and Lu H (2006). Balance of Yin and Yang: ubiquitylation-mediated regulation of p53 and c-Myc. *Neoplasia* **8**, 630–644.
[26] Vogelstein B, Lane D, and Levine AJ (2000). Surfing the p53 network. *Nature* **408**, 307–310.
[27] Espinosa JM and Emerson BM (2001). Transcriptional regulation by p53 through intrinsic DNA/chromatin binding and site-directed cofactor recruitment. *Mol Cell* **8**, 57–69.
[28] Espinosa JM, Verdun RE, and Emerson BM (2003). p53 functions through stress- and promoter-specific recruitment of transcription initiation components before and after DNA damage. *Mol Cell* **12**, 1015–1027.
[29] Gomes NP, Bjerke G, Llorente B, Szostek SA, Emerson BM, and Espinosa JM (2006). Gene-specific requirement for P-TEFb activity and RNA polymerase II phosphorylation within the p53 transcriptional program. *Genes Dev* **20**, 601–612.
[30] Teufel DP, Freund SM, Bycroft M, and Fersht AR (2007). Four domains of p300 each bind tightly to a sequence spanning both transactivation subdomains of p53. *Proc Natl Acad Sci USA* **104**, 7009–7014.
[31] Liu WL, Midgley C, Stephen C, Saville M, and Lane DP (2001). Biological significance of a small highly conserved region in the N terminus of the p53 tumour suppressor protein. *J Mol Biol* **313**, 711–731.
[32] Lee H, Mok KH, Muhandiram R, Park KH, Suk JE, Kim DH, Chang J, Sung YC, Choi KY, and Han KH (2000). Local structural elements in the mostly unstructured transcriptional activation domain of human p53. *J Biol Chem* **275**, 29426–29432.
[33] Kaustov L, Yi GS, Ayed A, Bochkareva E, Bochkarev A, and Arrowsmith CH (2006). p53 transcriptional activation domain: a molecular chameleon? *Cell Cycle* **5**, 489–494.
[34] Chi SW, Lee SH, Kim DH, Ahn MJ, Kim JS, Woo JY, Torizawa T, Kainosho M, and Han KH (2005). Structural details on mdm2–p53 interaction. *J Biol Chem* **280**, 38795–38802.
[35] Mapp AK and Ansari AZ (2007). A TAD further: exogenous control of gene activation. *ACS Chem Biol* **2**, 62–75.
[36] Buschmann T, Lin Y, Aithmitti N, Fuchs SY, Lu H, Resnick-Silverman L, Manfredi JJ, Ronai Z, and Wu X (2001). Stabilization and activation of p53 by the coactivator protein TAFII31. *J Biol Chem* **276**, 13852–13857.
[37] Farmer G, Colgan J, Nakatani Y, Manley JL, and Prives C (1996). Functional interaction between p53, the TATA-binding protein (TBP), and TBP-associated factors *in vivo*. *Mol Cell Biol* **16**, 4295–4304.
[38] Leveillard T, Andera L, Bissonnette N, Schaeffer L, Bracco L, Egly JM, and Wasylyk B (1996). Functional interactions between p53 and the TFIIH complex are affected by tumour-associated mutations. *EMBO J* **15**, 1615–1624.
[39] Liu X, Miller CW, Koeffler PH, and Berk AJ (1993). The p53 activation domain binds the TATA box-binding polypeptide in Holo-TFIID, and a neighboring p53 domain inhibits transcription. *Mol Cell Biol* **13**, 3291–3300.
[40] Martin DW, Munoz RM, Subler MA, and Deb S (1993). p53 binds to the TATA-binding protein–TATA complex. *J Biol Chem* **268**, 13062–13067.
[41] Thut CJ, Chen JL, Klemm R, and Tjian R (1995). p53 transcriptional activation mediated by coactivators TAFII40 and TAFII60. *Science* **267**, 100–104.
[42] An W, Kim J, and Roeder RG (2004). Ordered cooperative functions of PRMT1, p300, and CARM1 in transcriptional activation by p53. *Cell* **117**, 735–748.
[43] Avantaggiati ML, Ogryzko V, Gardner K, Giordano A, Levine AS, and Kelly K (1997). Recruitment of p300/CBP in p53-dependent signal pathways. *Cell* **89**, 1175–1184.
[44] Lill NL, Grossman SR, Ginsberg D, DeCaprio J, and Livingston DM (1997). Binding and modulation of p53 by p300/CBP coactivators. *Nature* **387**, 823–827.

[Cell Cycle 6:14, 1730-1740, 15 July 2007]; ©2007 Landes Bioscience

Report

DDB2-Independent Role for p53 in the Recovery from Ultraviolet Light-Induced Replication Arrest

Lawton J. Stubbert[1,2,†]
Jeff D. Hamill[1,†]
Jennifer C. Spronck[1]
Jennifer M. Smith[1,2]
Cecilia Becerril[1]
Bruce C. McKay[1,3,*]

[1]Cancer Therapeutics Program; Ottawa Health Research Institute; [2]Department of Cellular and Molecular Medicine; [3]Departments of Radiology; University of Ottawa; Ottawa, Ontario Canada

[†]These authors contributed equally to this work.

*Correspondence to: Bruce C. McKay; Cancer Therapeutics Program; Ottawa Health Research Institute; 501 Smyth Rd, Box 926; Ottawa, Ontario K1H 8L6 Canada; Tel.: 613.737.7700x70338; Fax: 613.247.3524; Email: bmckay@ohri.ca

Original manuscript submitted: 02/09/07
Revised manuscript submitted: 05/10/07
Manuscript accepted: 05/10/07

Previously published online as a *Cell Cycle* E-publication:
http://www.landesbioscience.com/journals/cc/abstract.php?id=4427

KEY WORDS

cell cycle, DDB2, DNA repair, DNA replication, p53, S phase arrest, translesion synthesis, ultraviolet light

ACKNOWLEDGEMENTS

We would like to thanks Dr. Mats Ljungman (University of Michigan) and Dr. Michael Tainsky (Wayne State University) for fibroblast strains. This work was supported by a grant from the Canadian Institutes of Health Research to B.C.M. J.M.S. was supported with an Ontario Graduate Scholarship and subsequently an Ontario Graduate Scholarship in Science and Technology. J.C.S. was supported with an Ontario Premier's Research Excellence Award to B.C.M. B.C.M. is a Research Scientist of the National Cancer Institute of Canada supported with funds provided by the Canadian Cancer Society.

ABSTRACT

Ultraviolet light (UV light) induces helix distorting DNA lesions that pose a block to replicative DNA polymerases. Recovery from this replication arrest is reportedly impaired in nucleotide excision repair (NER)-deficient xeroderma pigmentosum (XP) fibroblasts and primary fibroblasts lacking functional p53. These independent observations suggested that the involvement of p53 in the recovery from UV-induced replication arrest was related to its role in regulating the global genomic subpathway of NER (GG-NER). Using primary human fibroblasts, we confirm that the recovery from UV-induced replication arrest is impaired in cells lacking functional p53 and in primary XP fibroblasts derived from complementation groups A or C (XP-A and XP-C) that are defective in GG-NER. Surprisingly, DNA synthesis recovered normally in GG-NER-deficient XP complementation group E (XP-E) cells that carry mutations in the p53 regulated DNA repair gene DDB2 and are specifically defective in the repair of cyclobutane pyrimidine dimers (CPD) but not pyrimidine (6-4) pyrimidone photoproducts. Disruption of p53 in these XP-E fibroblasts prevented the recovery from UV-induced replication arrest. Therefore, the roles of p53 and GG-NER in the recovery from UV-induced replication are separable and DDB2-independent. These results further indicate that primary human fibroblasts expressing functional p53 efficiently replicate DNA containing CPD whereas p53-deficient cells do not, consistent with a role for p53 in permitting translesion synthesis of these DNA lesions.

INTRODUCTION

In response to genotoxic agents, several cell cycle checkpoints are activated, blocking cell cycle progression in the G_1, S or G_2 phases of the cell cycle.[1-3] In addition to activated checkpoints, progression of replicative DNA polymerases can be inhibited by UV-induced DNA lesions.[4,5] Immediately after UV exposure, the synthesis of nascent DNA decreases in a dose-dependent manner but nascent DNA synthesis recovers markedly within 6–8 hours following exposure to moderate doses of UV light in normal fibroblasts.[5-11] Recovery from UV-induced replication arrest is thought to require nucleotide excision repair because NER-defective fibroblasts derived from patients with xeroderma pigmentosum (XP) fail to recover nascent DNA synthesis normally.[4,5] Cells lacking functional p53 have a NER defect[10,12,13] and also fail to recover nascent DNA synthesis normally.[9,10] Based on these observations, it was hypothesized that p53 facilitates the recovery from replication arrest by stimulating NER[9,10] but until now, this hypothesis had remained untested.

Here we report that fibroblasts lacking functional p53 and primary XP fibroblasts from complementation groups A and C (XP-A and XP-C) fail to recover from the UV-induced replication arrest. In stark contrast to previous predictions though, nascent DNA synthesis recovers normally in XP complementation group E cells despite the fact that approximately 80% of the CPD remain 24 hours following UV exposure. Furthermore, disruption of p53 in these cells exacerbated their replication arrest and led to a massive accumulation of cells in S phase. These results clearly indicate that the roles of GG-NER and p53 in the recovery from UV-induced replication arrest are separable. Furthermore, these results suggest that the recovery from UV-induced replication arrest involves translesion synthesis in p53 expressing fibroblasts but not in the absence of functional p53.

MATERIALS AND METHODS

Cell culture and UV-irradiation. Normal neonatal foreskin fibroblasts (NF) were obtained from Dr. Mats Ljungman (University of Michigan). Normal fibroblasts (GM38),

XP-A (GM5509), XP-C (GM671), CS-B (GM739) and XP-E (GM1389) fibroblasts were obtained from National Institute of General Medical Sciences Mutant Cell Repository (Camden, NJ). The generation of human papillomavirus-E6-expressing normal fibroblast strains was described previously.[14] Li-Fraumeni syndrome cells (LFS), hemizygous for a frame shift mutation at codon 184 of p53 were obtained from Dr. Michael Tainsky (Wayne State University). Cells were maintained in DMEM supplemented with 10% fetal bovine serum (Wisent, St. Bruno, QC) and 5 μg/ml gentamicin (Sigma-Aldrich Canada Ltd, Oakville, ON).

For UV treatment, growth medium was removed, cells were irradiated immediately at room temperature, fresh prewarmed medium was replaced and cells were returned to the incubator for the indicated period of time. A germicidal bulb (Philips) emitting UV predominately at 254 nm at 1 J/m^2/s, as determined with a hand held UV-radiometer (UVX Radiometer, UVP Inc, Uplands, CA) was used to irradiate cells.

Flow cytometry. Control and UV-irradiated cells were collected at various time points following UV and/or drug treatment. Where indicated, colcemid was added to a final concentration of 1 μM. The harvesting, fixation and staining of cells with propidium iodide (PI) has been described previously.[15] To detect the synthesis of nascent DNA, BrdU (30 μM, Sigma-Aldrich Canada Ltd, Oakville, ON) was added to the medium for between 15 minutes and 24 hours, depending on the experimental design. In pulse chase experiments, BrdU was added for 1 hour, washed twice with PBS and returned to the incubator for the indicated period of time. Detection of BrdU incorporation in single stranded DNA using a primary anti-BrdU antibody (1:100, PharMingen, San Diego, CA) and secondary anti-mouse FITC-conjugated antibody (1:15, Sigma-Aldrich Canada Ltd, Oakville, ON) was performed, as described previously.[15] Detection of UV-induced DNA damage in single stranded DNA was performed similarly except that 1 μg of either anti-thymine dimer antibody (clone KTM53, Kamiya Biomedical Company, Seattle, WA) or Anti-(6-4)PP (clone 64M-2, MBL Internationsal, Woburn, MA) was used instead of anti-BrdU antibody. Stained cells were analyzed via flow cytometry using either a Becton Dickinson LSR FACS station or a Beckman Coulter FACS station. Cell cycle distribution was calculated from the DNA histograms using cell cycle analysis software (ModFit, Verity Software House, Topsham, ME) whereas quantification of BrdU incorporation and UV-induced DNA damage was performed using FCS Express 3 software (DeNovo Software, Thornhill, ON).

Immunoblotting. Cells were harvested, rinsed with PBS, lysed with 1% SDS, sonicated for 10s using a microtip (Branson Sonifier, VWR International Ltd., Mississauga, ON) and protein concentrations determined using the BioRad Protein Assay (BioRad, Mississauga, ON). Whole cell lysates were prepared using LDS NuPAGE sample buffer (Invitrogen Canada Inc., Burlington, ON). Proteins (20 μg per lane) were separated in 10 or 4–12% Bis-Tris NuPAGE precast gels, transferred to nitrocellulose membranes (Hybond-C Extra, Amersham, Baie d'Urfe, QC) and stained with Ponceau S Red (5 mg/ml in 2% glacial acetic acid) to confirm transfer of proteins. Membranes were blocked in PBSMT-A (PBS, 5% nonfat dry milk powder, 0.05% Tween 20) for 1 hr at room temperature, incubated with primary antibody (p53Ab-6 from Oncogene Research Products or β-actin clone AC-74 from Sigma-Aldrich Canada Ltd) diluted in PBSMT-B (PBS, 0.5% nonfat dry milk powder, 0.05% Tween 20) for 1.5 hr at room temperature. Protein bands were visualized using SuperSignal West Pico Chemiluminescent Substrate (Pierce, Rockford, IL) and either Kodak film or a gel documentation system (GeneGnome, Synoptics, Bristol, UK). Membranes were stripped with Restore Western Blot Stripping Buffer (Pierce, Rockford, IL) in order to visualize additional proteins on the same blot.

DNA replication. Cells were seeded at 1 x 10^5 cells/well in six well dishes. Twenty-four hours later, cells were irradiated with 0 or 10 J/m^2 and 2 mL of fresh medium containing 5 μCi/mL [^{3}H]-thymidine were added to cells. Cells were collected at 0, 6 or 12 hours following UV-irradiation. Cell pellets were snap frozen and stored at -80°C until analyzed. Cell pellets were resuspended in 500 μL 1% SDS at room temperature then placed on ice. One mL of 10% trichloroacetic acid (TCA)/0.1 M sodium pyrophosphate (NaPPi) was added and DNA was precipitated by incubating on ice for 30 min. Precipitated DNA was collected on glass fiber filters and washed three times with 2 mL 5% TCA/0.05M NaPPi, 5 mL ddH_2O, 2 mL 100% EtOH. Filters were allowed to dry on vacuum for 1 minute and transfered to scintillation tubes to be counted.

γH2AX immunofluorescence. Cells were seeded into dual chambered slides and the next day sub-confluent monolayers were irradiated as indicated with UV light. Fresh prewarmed media was added to cells and plates were returned to the incubator for 8 hours. Cells were then rinsed with PBS and fixed in 2% formaldehyde in PBS for 20 min at 4°C. Cells were permeabilized in 1:1 ice-cold acetone:methanol. Monolayers were blocked for one hour in PBS supplemented with 10% FBS at 37°C in a humidified incubator. Monolayers were probed with primary anti-γH2AX antibody (Trevigen, Gathersburg, MD) diluted to 1:250 in PBS supplemented with 1% BSA and 0.5% Tween 20 for two hours at 37°C in a humidified incubator. Monolayers were washed three times for five minutes in PBS supplemented with 1% BSA. Monolayers were incubated with secondary goat-anti-rabbit IgG antibody conjugated to Alexa-488 (Invitrogen Canada Inc., Burlington, ON) diluted to 1:2000 in PBS supplemented with 1% BSA for one hour in the dark at 37°C in a humidified incubator. Monolayers were washed three times for five minutes each in PBS supplemented with 1% BSA. Cells were incubated with 0.05 μg/mL Hoechst stain (Sigma) in PBS supplemented with 1% BSA. Monolayers were washed twice for 5 minutes in PBS supplemented with 1% BSA. Chambers were removed and slides were covered with glass coverslips with a drop of fluormount mounting media and sealed with nail polish. Slides were examined using a Ziess Axioscop 2 microscope using the 63X oil immersion objective. A minimum of 100 cells were counted for each treatment and scored for the presence of increased focal staining of γH2AX within nuclei of cells. Counting was performed by an individual without knowledge of the treatment group.

RNA interference. Cells were maintained in antibiotic-free media at least 48 hours prior to transfection. Three days prior to UV-irradiation, cells at 50–80% confluence in 10 cm culture dishes were transfected with SmartPool siRNA duplexes targeting p53 or control duplex (Dharmacon Inc., Lafayette, CO) at 50 nM final concentration using Oligofectamine Reagent and Opti-MEM I (Invitrogen, Burlington, ON) according to manufacturers instructions. Cells were split 1 to 2, 24 hours following transfection. Cells were treated with the indicated doses of UV light and collected at the indicated times for either immunoblot or cell cycle analysis. We routinely found greater than a 4 fold decrease in p53 protein expression in unirradiated samples and greater than 10 fold decrease in expression following UV-irradiation.

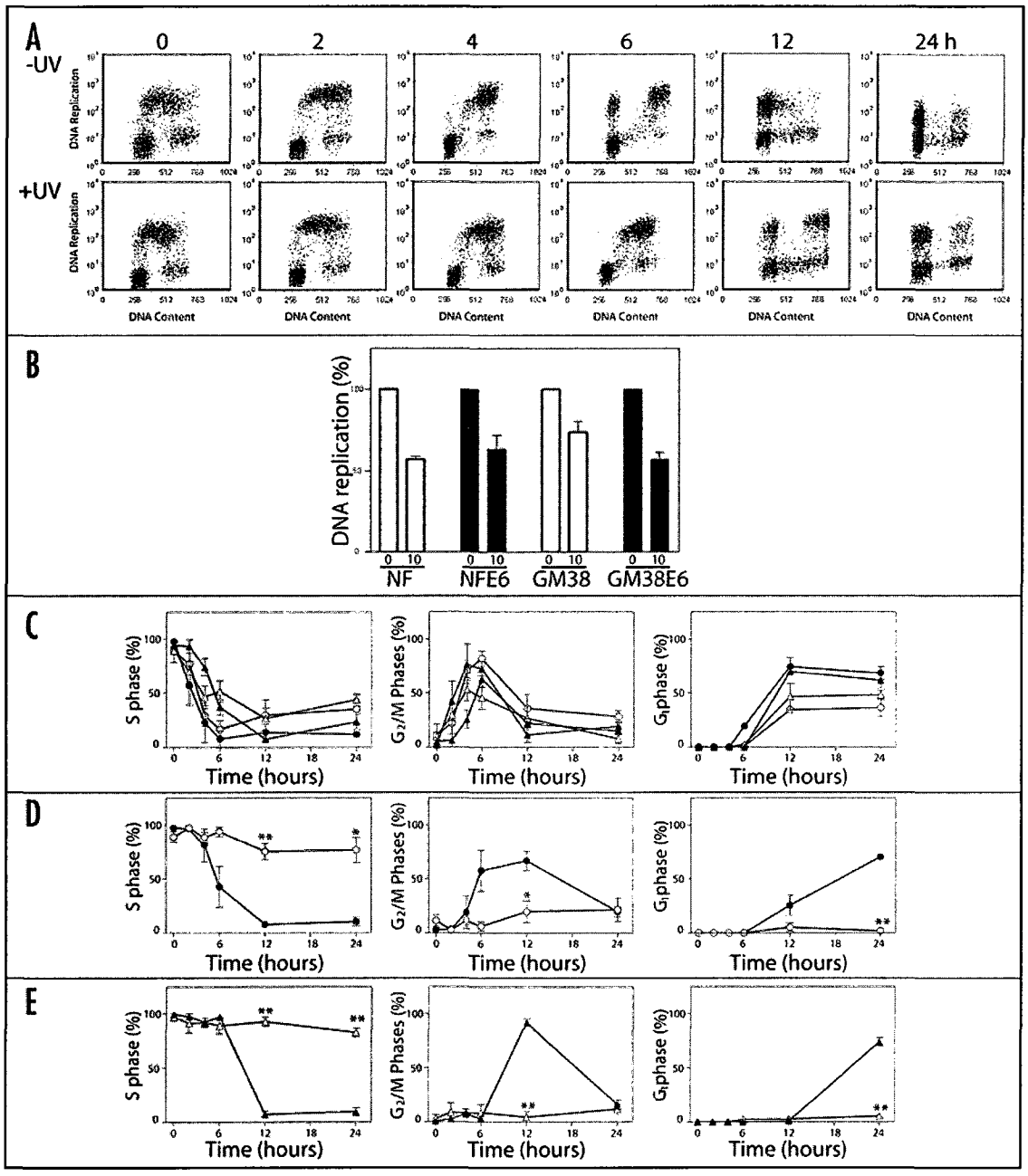

Figure 1. Prolonged ultraviolet light-induced replication arrest in fibroblasts lacking functional p53. Cells were treated with either 0 or 10 J/m^2 of UV light, pulsed with 30 μM BrdU for 1 h, rinsed thoroughly with PBS and returned to the incubator for the indicated time. Two-parameter flow cytometric analysis was performed as described in the materials and methods. (A) Representative dot plots are presented for normal fibroblasts. (B) The relative amount of BrdU incorporated within the first hour following UV exposure compared to unirradiated controls was determined from dot plots like those presented in (A). (C–E) The BrdU-positive cells in (A) were gated and cell cycle distribution was determined based on DNA content for NF (closed circles in C and D), NF-E6 (open circles in C and D), GM38 (closed triangles in C and E) and GM38E6 (open triangles in C and E). Cell cycle distribution is plotted as a function of time following release from BrdU treatment. Cells were exposed to either 0 J/m^2 (C) or 10 J/m^2 (D and E). Each point represents the mean (± SEM) determined from a minimum of three independent experiments. Statistically significant differences between the indicated value and its corresponding control collected at the same time are indicated by either * or ** ($p \leq 0.05$ and $p \leq 0.001$, respectively, student t test, two tailed).

RESULTS

Ultraviolet light induced replication arrest is prolonged in fibroblasts lacking functional p53. In order to study the effects of UV light on the inhibition and recovery of DNA synthesis following UV-irradiation, two parameter flow cytometric BrdU pulse chase experiments were performed. This allowed us to label and follow the fate of cells irradiated in S phase. Cells were pulsed with BrdU for 1 hour immediately following mock- or UV-irradiation and were subsequently incubated for the indicated time in fresh medium without BrdU. Anti-BrdU immunofluorescence was used to quantify replication while PI was used to distinguish cell cycle position based on DNA content (Fig. 1A). UV exposure resulted in a two-fold decrease in the incorporation of BrdU throughout

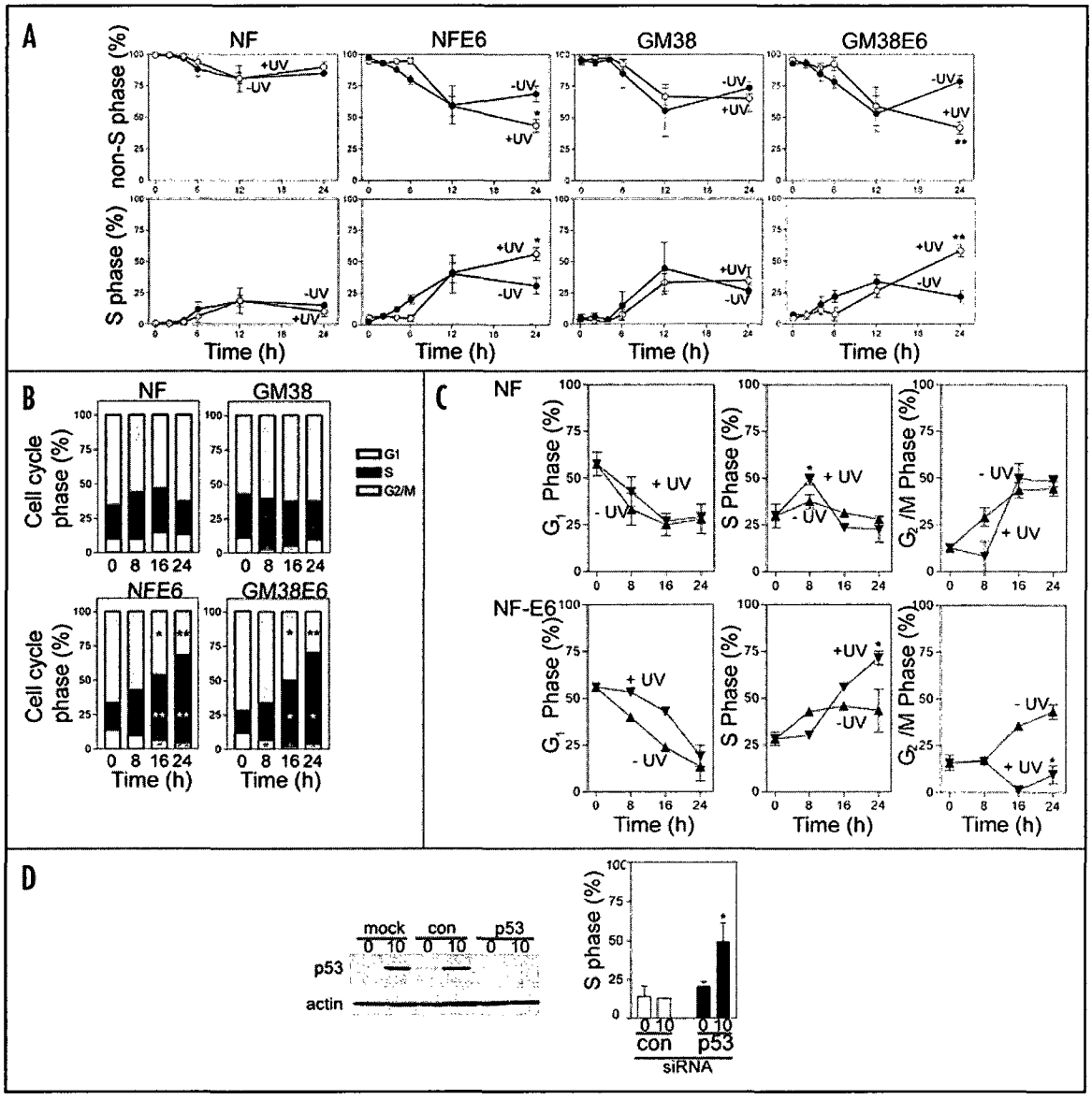

Figure 2. Pronounced S phase arrest in p53-deficient fibroblasts following UV exposure. (A) BrdU pulse chase experiments were performed on the indicated cell line and cell cycle distribution based on DNA content was determined from the BrdU-negative population of cells. (B) One parameter flow cytometric analysis of propidium iodide stained cells was performed and the mean proportion of cells in each phase of the cell cycle was determined from a minimum of three experiments in NF, GM38, NFE6 and GM38E6 fibroblasts. (C) One parameter flow cytometric analysis of propidium iodide stained cells was performed as in (B) except that colcemid was added at the time of irradiation to block entry of cells into the second cell cycle. The mean proportion of cells in the G_1, S and G_2/M phases of the cell cycle was determined from up to ten experiments. (D) GM38 cells were mock transfected or transfected with control siRNA duplex (con) or p53 siRNA duplex 48 hours prior to exposure to 10 J/m^2 of UV light. Lysates were collected 24 hours following UV exposure and subjected to immunoblot and cell cycle analysis based on DNA content. Each value in (A, C and D) represents the mean (± SEM) determined from a minimum of 3 independent experiments. Statistically significant differences between the indicated value and its corresponding control in (A–D) are indicated by either * or ** ($p \leq 0.05$ and $p \leq 0.001$, respectively, student t test, two tailed).

S phase within the first hour following UV exposure, consistent with the direct inhibtion of DNA replication (Fig. 1B). Importantly, the BrdU-positive and BrdU-negative populations of cells remained easily distinguishable (Fig. 1A) following UV exposure allowing us to gate BrdU positive cells separately for cell cycle analysis based on DNA content.

The vast majority of BrdU-positive cells had S phase DNA content at the time of irradiation (Fig. 1C). The BrdU-positive population of unirradiated normal fibroblasts completed S phase within six hours, passed synchronously through G_2 and M phases then entered into the G_1 phase of the subsequent cell cycle within 12 hours (Fig. 1C). A second cycle G_1 phase population was prominent by 24 hours (Fig. 1A). The time required for the BrdU-positive population of normal fibroblasts to exit S phase was extended following exposure to 10 J/m^2 of UV light (Fig. 1A, C and D). UV-irradiated normal fibroblasts passed synchronously through G_2, M and into the G_1 phase of the subsequent cell cycle, with a six hour delay (Fig. 1A, D and E). This short S phase delay is consistent with previous measurements of the inhibition and recovery of nascent DNA synthesis using incorporation of ^{3}[H] thymidine as a measure of DNA replication.[5-11]

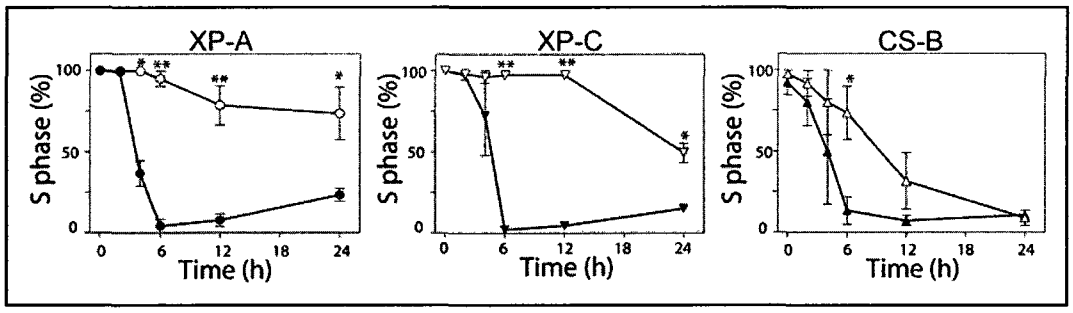

Figure 3. GG-NER contributes to the recovery from UV-induced replication arrest. BrdU pulse chase experiments were performed on XP-A (circles), XP-C (inverted triangles) and CS-B (triangles) fibroblasts and the cell cycle distribution based on DNA content was determined for the BrdU positive population of cells. The proportion of cells in S phase is plotted as a function of time following exposure to either 0 (closed symbols) or 10 J/m^2 (open symbols) of UV light. For representative two parameter flow cytometric data, refer to Supplementary Figures 3 and 4. Each point represents the mean (± SEM) determined from a minimum of three independent experiments. Statistically significant differences between the indicated value and its unirradiated control are indicated by either * or ** ($p \leq 0.05$ and $p \leq 0.001$, respectively, student t test, two tailed).

The unirradiated BrdU positive population of HPV-E6 expressing derivative fibroblast strains exited S phase and progressed through subsequent phases of the cell cycle as rapidly as the parental strains (Fig. 1C). However, in stark contrast to normal fibroblasts, the BrdU positive population of HPV-E6 expressing derivative fibroblasts failed to complete S phase within 24 hours following UV treatment (Figs. 1D and E and Supplementary Fig. 1). Similarly, LFS fibroblasts lacking functional p53 were significantly delayed in S phase compared to the normal diploid human fibroblast strains (Supplementary Fig. 2). Therefore, the wild type p53 expressing strains resumed DNA synthesis with only a brief delay and passed synchronously through G_2 and M phases, entering the subsequent cell cycle, while the p53-deficient strains remained arrested in S phase for an extended period of time.

p53 facilitates the passage of G_1-irradiated fibroblasts through S phase. The effect of UV light on cells irradiated in other phases of the cell cycle was assessed by determining the cell cycle distribution of the BrdU negative population of cells from the experiments described in Figure 1. The majority of BrdU negative cells were in the G_1 phase of the cell cycle at the time of BrdU treatment (Fig. 1A). Analyzing the cell cycle distribution of BrdU-negative cells permitted us to monitor the effect of UV light on S phase entry and progression of primarily G_1-irradiated fibroblasts. A discernible BrdU-negative S phase population was observed in all unirradiated samples within 6 hours and was maximal by 12 hours following BrdU treatment (Figs. 1A and 2A). UV light did not significantly delay the entry of normal fibroblasts into S phase (Figs. 1A and 2A). Therefore, normal fibroblasts entered S phase readily following UV exposure without a prominent first cycle G_1 arrest.

Two obvious differences in cell cycle distribution were observed in the G_1-irradiated HPV-E6-expressing strains. First, the entry of p53-deficient strains into S phase was delayed compared to mock-irradiated controls (Fig. 2A). Second, the HPV-E6 expressing fibroblasts irradiated in the G_1 phase of the cell cycle accumulated in S phase and the non-S phase fraction was significantly depleted by 24 hours (Fig. 2A). These results suggested that p53-deficient fibroblasts underwent a sustained replication arrest following UV exposure regardless of the cell cycle phase at the time of irradiation.

To confirm the results by independent means, cell cycle distribution was determined by one parameter flow cytometric analysis on cells collected 0, 8, 16 and 24 hours following UV exposure. A small increase in the proportion of normal fibroblasts was detected in S phase, 8 and 16 hours following UV exposure but this returned to unirradiated levels within 24 hours (Fig. 2B). In distinct contrast, approximately 70% of HPV-E6 expressing fibroblasts were in S phase 24 hours after UV exposure (Fig. 2B). Consistent with the BrdU pulse chase experiments, HPV-E6 expressing fibroblasts undergo a prolonged replication arrest following UV exposure.

Given the complexity of analyzing the cell cycle distribution in the first and second cell cycles, similar one parameter flow cytometric experiments were performed in the presence of the mitotic inhibitor colcemid. We were thus able to monitor the fraction of cells exiting the G_1 phase, entering S phase and accumulating at the colcemid block in the presence and absence of UV light. Exposure to colcemid alone led to a depletion of cells in G_1 and a corresponding increase in the proportion of cells with 4N DNA content (Fig. 2C). Following UV-irradiation, normal fibroblasts exited G_1 at a similar rate to unirradiated control cells, again indicating that UV light did not induce a pronounced first cycle G_1 arrest (Fig. 2C). Normal fibroblasts accumulated in S phase within eight hours following UV-irradiation and reached the colcemid block within 16 hours (Fig. 2C). In clear contrast, the HPV-E6 expressing cells exited G_1 phase somewhat more slowly, consistent with a previous report,[16] accumulated in S phase, and failed to reach the colcemid block within 24 hours (Fig. 2C).

To provide further evidence that the cell cycle defect in HPV-E6 expressing cells was associated with p53-deficiency and not due to HPV-E6 expression per se, BrdU pulse chase and one parameter flow cytometric analysis were performed in hemizygous LFS fibroblasts carrying a frameshift mutation at codon 184 resulting in premature termination and an unstable p53 protein.[17] These cells underwent a sustained UV-induced replication arrest (Supplementary Fig. 2). Furthermore, targeting p53 by RNA interference led to a significant increase in the proportion of cells in S phase 24 hours following UV exposure, as assessed by one parameter flow cytometry (Fig. 2D). Therefore, all three flow cytometric methods and inactivation of p53 by three separate means yielded similar results. Taken together, normal fibroblasts recovered from UV-induced replication arrest far more efficiently than p53-deficient strains and this supports previous literature.[9,10,15,18,19]

GG-NER contributes to the recovery from replication arrest following UV exposure. UV-induced DNA damage is repaired through NER.[20] It has been reported that NER-defective XP fibroblasts fail to recover nascent DNA synthesis normally so NER is thought to contribute to the efficient recovery from UV-induced replication arrest.[4,5] Therefore, BrdU pulse chase experiments were performed in fibroblasts with a complete defect in NER (XP-A) or specific defects in either GG-NER (XP-C) or TC-NER (CS-B). Unirradiated BrdU-positive XP-A, XP-C and CS-B fibroblasts progressed through S phase within six hours, passing synchronously

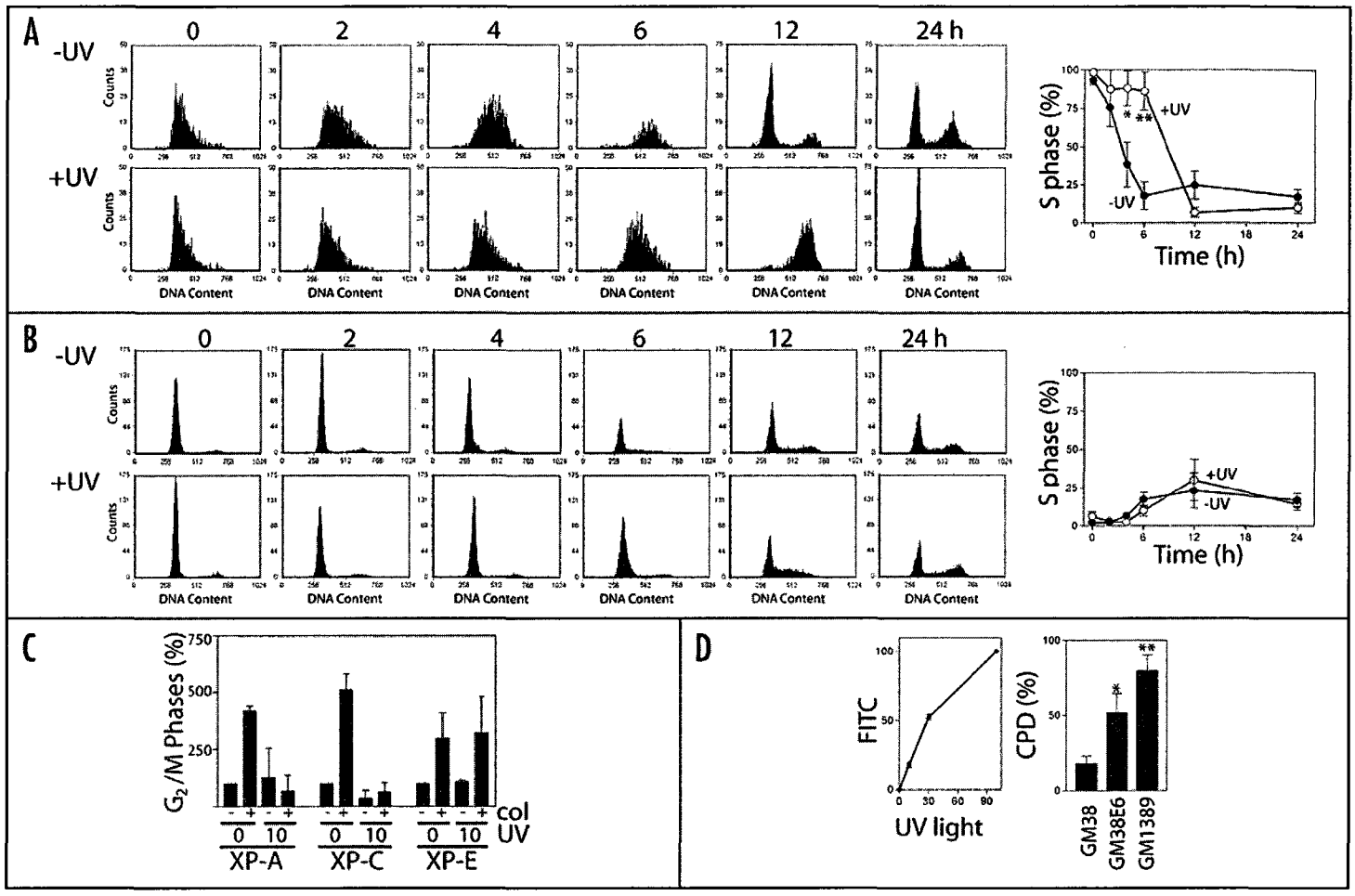

Figure 4. The recovery from UV-induced replication arrest precedes the repair of CPD in XP-E fibroblasts. BrdU pulse chase experiments were performed in XP-E fibroblasts. The BrdU-positive (A) and BrdU-negative population of cells (B) were gated separately and the data are presented as DNA histograms. The proportion of cells in S phase as estimated based on DNA content was determined for the BrdU-positive (right panel in A) and BrdU-negative (right panel in B) from a minimum of four independent experiments. For representative two parameter flow cytometric dot plots, see supplementary figure 5. (C) The proportion of cells with 4N DNA content was assessed 24 hours following mock- or UV-irradiation in the presence or absence of colcemid (col), as indicated. (D) CPD were detected either immediately or 24 hours following exposure of cells to 0, 10, 30 or 100 J/m^2 using an anti-thymine dimer antibody and flow cytometric methods. Fluorescent signal assessed immediately following UV exposure increased in proportion to UV fluence up to 30 J/m^2 (left panel). The proportion of CPD remaining 24 hours following exposure to 10 J/m^2 was determined for GM38, GM38E6 and GM1389 cells (right panel). Each point represents the mean (± SEM) determined from a minimum of 3 independent experiments. Statistically significant differences between the indicated value and its respective control are indicated by either * or ** ($p \leq 0.05$ and $p \leq 0.001$, respectively, student t test, two tailed).

through G_2 and M phases and were able to enter the second cycle G_1 within 12 hours, as observed in normal and HPV-E6 expressing fibroblasts strains (Fig. 3). The effect of UV exposure on the recovery from UV-induced replication arrest varied in a repair-dependent manner. The BrdU-positive population of XP-A and XP-C fibroblasts remained in S phase up to at least 24 hours following UV exposure (Fig. 3, left and centre panels), as expected based on previous literature.[5,7] In contrast, the BrdU positive population of CS-B fibroblasts progressed through S phase following UV exposure (Fig. 3B, right panel). Taken together, these results indicate that it is the GG-NER and not the TC-NER subpathway of NER that contributes to the recovery from UV-induced replication arrest.

Recovery from replication arrest involves p53 but not DDB2 and precedes the repair of cyclobutane pyrimidine dimers. Cells lacking functional p53 have a defect in GG-NER, however this defect is specific for CPD and not pyrimidine (6-4) pyrimidone photoproducts [(6-4) PP], the other major photoproduct induced by UV light.[12,13,21-23] This DNA repair phenotype is identical to that of XP group E cells (XP-E), homozygous for a mutation in the gene encoding DDB2, a p53-regulated DNA repair protein.[10,24] Therefore, to examine how a defect in GG-NER that more closely reflects the defect in p53-deficient cells affects cell cycle progression, BrdU pulse chase experiments were performed using XP-E fibroblasts.

Unirradiated BrdU-positive XP-E fibroblasts were able to complete S phase within 6 hours (Fig. 4A). As with normal fibroblasts, quantitative cell cycle analysis of the BrdU-positive population of XP-E cells indicated that S phase was prolonged by only 6 hours following UV-irradiation (Fig. 4A, right panel). A strikingly normal cell cycle distribution was restored within 24 hours following UV exposure (Fig. 4A, lower right histogram). The progression of XP-E fibroblasts through S phase was readily distinguishable from that of XP-A and XP-C fibroblasts (compare Fig. 3 and 4A, right panel). Similarly, UV light had very little effect on the cell cycle distribution of

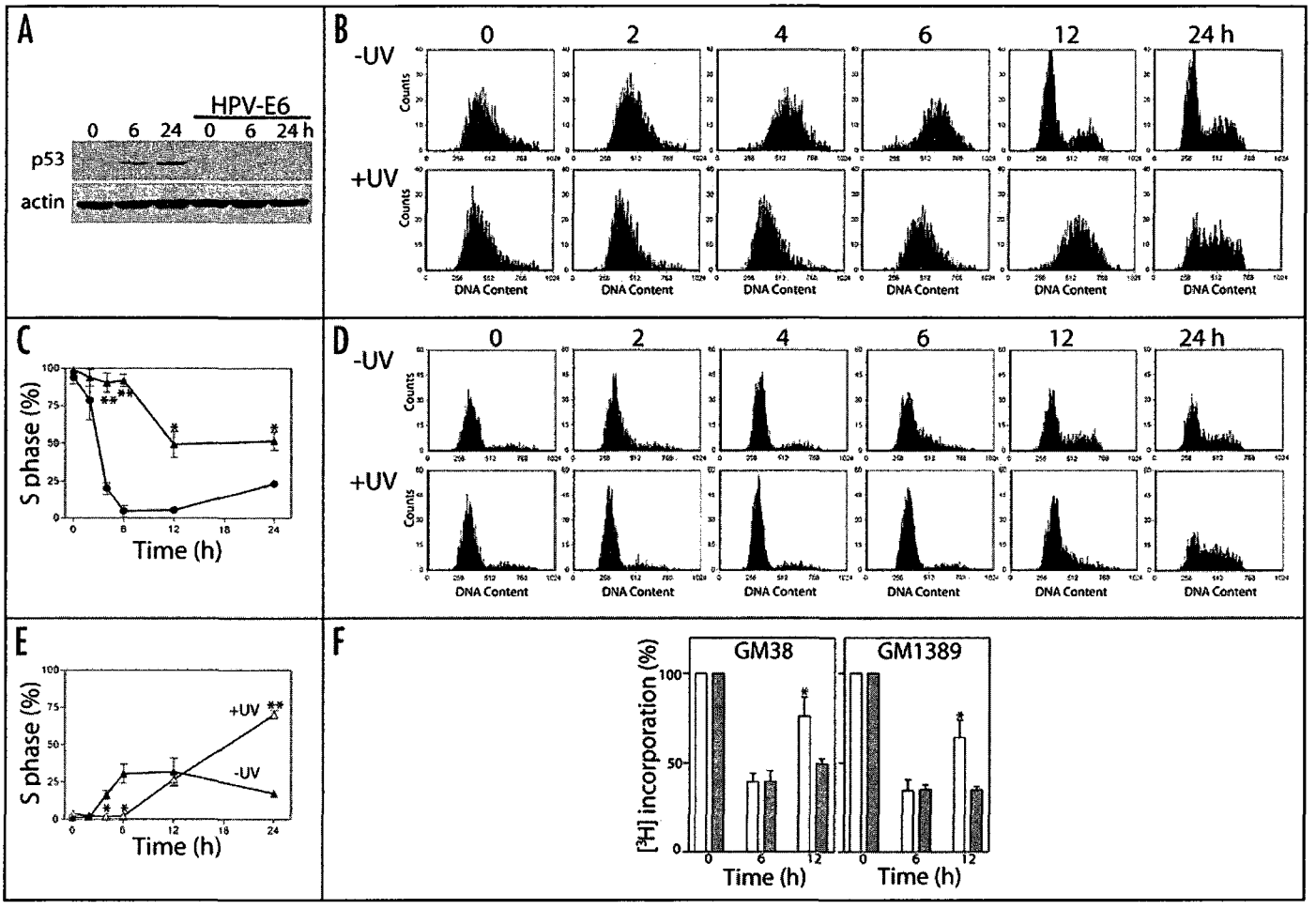

Figure 5. HPV-E6 expression inhibits the recovery from replication arrest in XP-E fibroblasts. (A) Immunoblot analysis comparing the UV-induced accumulation of p53 in XP-E and its isogenic derivative expressing HPV-E6. (B–E) BrdU pulse chase experiments were performed in these HPV-E6 expressing XP-E fibroblasts. The BrdU-positive cells were gated separately and the data are presented as DNA histograms (B) and as the proportion of cells in S phase (C). Similar analysis is presented for the BrdU-negative population of cells (D and E). For representative two parameter flow cytometric data, see supplementary figure 5. (F) The incorporation of [^{3}H] thymidine was assessed over the first 6 and 12 hours following UV exposure. [^{3}H] incorporation is represented as the counts determined from UV treated samples compared to their unirradiated controls collected at the same time. Each point in (C, E and F) represents the mean (± SEM) determined from a minimum of three independent experiments. Statistically significant differences between the indicated value and its corresponding control are indicated by either * or ** ($p \leq 0.05$ and $p \leq 0.001$, respectively, two tailed student t test).

the BrdU-negative population of XP-E cells (Fig. 4B). Therefore, the BrdU negative population of XP-E fibroblasts responded like normal fibroblasts.

To independently assess the effect of UV exposure on S phase progression, the ability of XP-E, XP-A and XP-C fibroblasts to reach G_2/M in the presence of colcemid was assessed, as described in (Fig. 2). Consistent with the BrdU pulse chase experiments, XP-A and XP-C fibroblasts failed to reach the colcemid block following UV-irradiation (Fig. 4C). In contrast, XP-E fibroblasts progressed through S phase and reached the colcemid block following UV-irradiation (Fig. 4C). Therefore, the reported defect in the repair of CPD in XP-E fibroblasts did not prevent these cells from recovering from UV-induced replication arrest.

To ensure that our XP-E fibroblast strain exhibited the reported GG-NER of CPD defect,[24] an anti-CPD monoclonal antibody was used to measure DNA damage and repair in normal, HPV-E6 expressing normal and XP-E fibroblasts using a flow cytometric method. A linear relationship between UV fluence (up to 30 J/m^2 of UV light) and the amount of DNA damage was observed immediately following UV exposure (Fig. 4D). This indicates that fluorescence intensity was proportional to the number of CPDs per cell through this dose range. To measure DNA damage and repair, cells were UV irradiated with either 0 or 10 J/m^2 and samples were collected immediately and 24 hours following UV exposure for flow cytometric analysis of CPDs. Approximately 20, 50 and 80% of CPDs remained in the GM38, GM38-E6 and GM1389 fibroblasts, respectively, twenty-four hours following UV-irradiation (Fig. 4D). This observation is consistent with previous measurements of DNA damage and repair of CPDs in these and similar fibroblast strains.[24] Taken together, the recovery from UV-induced replication arrest occurs normally in GG-NER-deficient XP-E fibroblasts, indicating that this recovery precedes the repair of CPDs.

To further dissociate the roles of p53 and GG-NER in the recovery from UV-induced replication arrest, cell cycle distribution was assessed in HPV-E6 expressing XP-E fibroblasts. As expected, p53 levels increased in the control strain following UV exposure but not in the HPV-E6 expressing XP-E derivative (Fig. 5A). Whereas

the BrdU-positive XP-E fibroblasts were delayed in S phase for approximately 6 hours following UV exposure (recall Fig. 4A), more than 50% of the BrdU-positive XPE-E6 cells remained arrested even 24 hours following UV exposure (Fig. 5B and C). The BrdU-negative population of HPV-E6 expressing XP-E fibroblasts were delayed in their entry into S phase following UV exposure but eventually entered and arrested in S phase (Fig. 5D and E). As another means of visualizing the difference in the recovery between isogenic pairs of fibroblast strains, the incorporation of [^{3}H] thymidine into DNA was used as a quantitative measure of DNA replication over the first 12 hours following UV exposure. The incorporation of [^{3}H] thymidine was reduced in all strains to a similar extent over the first 6 hours following UV exposure (Fig. 5F). However, DNA synthesis recovered significantly within 12 hours in the p53 expressing normal and XP-E strains but not in the p53-deficient strains (Fig. 5F). Therefore, XP-E cells irradiated in S phase resumed DNA synthesis prior to the repair of CPD whereas p53-deficient derivatives arrest in S phase regardless of whether they were irradiated in G_1 or S phase. These results clearly dissociate the roles of p53 and DDB2-dependent GG-NER in the recovery from UV-induced replication arrest.

DISCUSSION

Global genomic nucleotide excision repair and ultraviolet light-induced replication arrest. It has been recognized for over thirty years that UV light inhibits the synthesis of nascent DNA.[4,25-31] In response to low doses of UV light ($\leq$ 1 J/m^2), the firing of replication origins can be inhibited following exposure to UV light.[29,30] In addition, UV lesions induced by higher doses of UV light can stall replication forks directly.[4,5,7,29-31] The extent of the initial block to replication fork progression reflects the probability that replication forks will encounter DNA lesions and is thus dose-dependent. In the present study, we used a dose of UV light (10 J/m^2) that is known to block the progression of replication forks.[4,5,7,29-31] Using BrdU-incorporation as a measure of DNA replication, we found that replication was initially inhibited to a similar extent in all fibroblast strains immediately following UV exposure, regardless of p53 status or NER capacity.

The inhibition and recovery of DNA synthesis following UV exposure has been studied using [^{3}H] thymidine incorporation and velocity sedimentation.[4,5,7] Early work suggested that a single CPD is sufficient to block a replication fork immediately following UV exposure.[8] The recovery from replication arrest is thought to be facilitated by the repair of these replication blocking lesions because UV-irradiation of XP fibroblasts results in a sustained inhibition of [^{3}H] thymidine incorporation.[4,5,7] Our data are again consistent with previous studies since we found that XP-A and XP-C fibroblasts irradiated in S phase remained arrested in that phase of the cell cycle following UV exposure. Importantly, CS-B cells were able to complete S phase, indicating that it is the GG-NER and not the TC-NER subpathway of NER that is required for the recovery from UV-induced replication arrest.

Surprisingly, DDB2-deficient XP-E fibroblasts progressed through S phase as readily as normal cells regardless of whether they were UV-irradiated in the G_1 or S phase of the cell cycle. Consistent with their reported DNA repair defect,[24] we found 80% of the CPD remained 24 hours after UV exposure in these cells. Therefore, XP-E fibroblasts are able to tolerate extensive DNA damage and resume DNA synthesis prior to the repair of CPDs. It is possible that XP-E fibroblasts are able to efficiently synthesize DNA past CPD using one or more of the translesion DNA polymerases.

It seems somewhat paradoxical when considering that GG-NER is required for the recovery from replication arrest yet GG-NER-deficient XP-E fibroblasts appear to tolerate unrepaired CPDs. The severity of the GG-NER defects in XP-A and XP-C fibroblasts is much greater than that described for XP-E. Both XP-A and XP-C fibroblasts are unable to repair the two major UV-induced pyrimidine dimers (CPD and (6-4)PP) from the genome overall while XP-A are further defective in the repair of both predominant UV lesions by transcription-coupled NER.[32-35] In contrast, the GG-NER defect in XP-E fibroblasts is specific to CPD while (6-4)PP are repaired with near normal efficiency[24] (see Supplementary Fig. 6). In general, GG-NER of (6-4)PP is much faster than GG-NER of CPD because (6-4)PP cause a greater structural distortion to the DNA helix and are recognized more readily by DNA damage recognition proteins required for GG-NER.[24,32] Conversely, translesion synthesis (TLS) of CPD is much more efficient than TLS of (6-4)PP[36,37] so (6-4)PP inhibit DNA replication more strongly than CPD.[38] Which is to say that the (6-4)PP pose a greater impediment to translesion polymerases but these lesions are repaired more efficiently by GG-NER. Intriguingly, the short replication arrest in p53 expressing cells corresponds very well temporally with the time required to repair (6-4)PP because the repair of (6-4)PP is essentially complete within 6 hours[24] (see Supplementary Fig. 6) when cells resume DNA synthesis (see Figs. 1 and 4). Taken together, XP-E fibroblasts likely recover from UV-induced replication arrest normally because they retain both the ability to repair (6–4)PP and the ability to replicate DNA templates containing CPD.

p53 and ultraviolet light-induced replication arrest. We found that p53-deficient fibroblasts have a striking defect in the recovery from replication arrest. These results are consistent with previous reports in which nascent DNA synthesis was measured by incubating irradiated cells in medium containing [^{3}H] thymidine for a short period of time, 6-8 hours following UV exposure.[9,10] Under these conditions, p53-deficient strains replicated DNA poorly compared to control strains. Similarly, colorectal cancer cells expressing a temperature sensitive variant of p53 reportedly underwent a pronounced S phase arrest following UV-irradiation at the restrictive temperature but that this S phase arrest could be overcome by restoring functional p53 at the permissive temperature.[18] By monitoring cell cycle position and the recovery from replication arrest simultaneously, the S phase defect in p53-deficient cells following UV-irradiation reported here appears far more pronounced than previously reported. S phase irradiated cells lacking functional p53 remained arrested in S phase even 24 hours following UV exposure. In addition, p53-deficient cells irradiated in G_1 phase entered S phase and underwent a sustained replication arrest. The net effect of the sustained replication arrest in S phase- and G_1 phase-irradiated populations of cells was the massive accumulation of p53-deficient fibroblasts in S phase 24 hours following UV exposure.

Given the GG-NER defect reported in p53 deficient fibroblasts, previous reports assessing the inhibition and recovery of nascent DNA synthesis in p53-deficient fibroblasts suggested that p53 contributed to the recovery of nascent DNA synthesis by regulating NER.[9,10] This was consistent with available data; however the role of p53 in GG-NER was not fully understood at the time. Fibroblasts lacking functional p53 have a repair defect that is virtually indistinguishable from that of XP-E fibroblasts because p53-deficient and XP-E fibroblasts have reduced DDB2 activity.[24,39] Our results indicate that XP-E fibroblasts recovered from the UV-induced replication arrest as

readily as normal fibroblasts despite their repair defect. Furthermore, inactivation of p53 in XP-E cells led to a sustained replication arrest in cells irradiated in either the S or G_1 phase of the cell cycle. Taken together, the S phase defect associated with the absence of p53 in UV treated fibroblasts, is independent of the role of p53 in regulating DDB2 and GG-NER. Perhaps more striking, the recovery from replication arrest appears to involve DNA damage tolerance mechanisms in p53-expressing fibroblasts that are not observed in cells lacking functional p53.

p53 and ultraviolet light-induced G_1 arrest. The p53 protein can induce G_1 arrest by regulating the expression of the cyclin-dependent kinase inhibitor $p21^{WAF1}$.[40-43] A clear p53-dependent G_1 arrest is induced in many cell types in response to agents that induce DNA double strand breaks (DSB).[19,40,41,44,45] This p53-dependent G_1 arrest has been reported in response to UV exposure.[29,46-48] However, there is accumulating evidence that the p53-dependent G_1 checkpoint is inefficient following UV exposure[18,19,44,45,49,50] and that p53-independent G_1 checkpoints also exist.[16,19,45,51,52] Therefore, the role of p53 in mediating a first cycle G_1 arrest in response to UV exposure remains equivocal.

The comprehensive cell cycle analysis presented here clearly indicates that UV treatment of asynchronous repair proficient primary human fibroblasts does not lead to a significant first cycle p53-dependent G_1 arrest, under these conditions. A minor delay in S phase entry was noted but this was more prominent in the HPV-E6 expressing cells, as previously reported.[16] We interpret these results to indicate that the induction of $p21^{WAF1}$ occurs after most cells have passed the restriction point and are either in S phase or irreversibly committed to enter S phase. The integrity of the p53-dependent G_1 arrest in the second cell cycle could not be assessed because cells lacking functional p53 remained arrested in the first cycle S phase. Assessing p53-dependent cell cycle checkpoints at a single time point (18–24 hours) following exposure to UV light could easily be misinterpreted as a bonefide p53-dependent G_1 checkpoint response.

Role of p53 in S phase following UV-irradiation. Resumption of DNA synthesis following replication fork blockage at CPD is thought to involve either translesion synthesis or homologous recombination.[1,3,53-55] DNA polymerase η can readily bypass CPD,[56-58] inserting the correct bases opposite the lesion.[59] Recently, it was reported that p53 regulates the expression of the *POLH* gene encoding DNA polymerase η[60] and DNA polymerase η-deficient XP variant fibroblasts have an S phase defect following UV-irradiation.[61,62] The p53-dependent regulation of bypass polymerases may be more common than currently recognized since the mouse *Dinb* gene encoding DNA polymerase κ also appears to be p53-regulated.[63] Therefore, it is conceivable that p53 expressing cells recover DNA synthesis more efficiently, in part, because of higher levels of TLS polymerases. However, there is presently no evidence that the level of expression of these polymerases is limiting for TLS.

Alternatively when repair and replicative bypass fail, persistently stalled replication forks can be converted to DSB.[31,64-66] Other replication stressors such as hydroxyurea also lead to stalled replication forks that can be converted to DSB.[55,67-70] Intriguingly, UV- and hydroxyurea-induced DSB form predominantly in cells lacking functional p53, suggesting that p53 stabilizes and prevents the conversion of stalled replication forks to DSB.[31,54,55,67,71] The formation of γH2AX foci, frequently used as indicators of DSB, form in response to UV light predominantly as a consequence of replicative stress[64,72] and that this occurs preferentially in cells lacking functional p53 following UV exposure[64,66,73] (Supplementary Fig. 7). It is tempting to speculate that the profound S phase defect in p53-deficient cells is the consequence of secondary DNA damage associated with stalled replication forks. By contrast, cells expressing functional p53 are able to utilize DNA damage tolerance pathways to resume DNA synthesis and complete S phase in the presence of CPD.

S phase defect and sensitivity to ultraviolet light. A striking observation in the present work was the duration of the replication arrest in p53-deficient fibroblasts. Maintaining the stability of stalled replication forks for upwards of 24 hours must constitute a significant challenge to the cell. Given the duration of this block to replication, it is not surprising that DSB form in p53-deficient cells following the collapse of replication forks at sites of DNA damage.[31] DSB are highly cytotoxic lesions so the formation of DSB following UV treatment of p53-deficient cells[31] could have profound effects on the viability of UV treated cells. We and others have reported that p53 protects primary human fibroblasts, some tumour cell lines and primary mouse embryonic fibroblasts against UV-induced apoptosis following exposure to moderate doses of UV light.[14,18,23,49,74,75] Furthermore, the commitment to UV-induced apoptosis appears to require the entry of cells into S phase[15,38,75-77] and UV-induced apoptosis was reportedly preceded by the formation of replication associated DSB[77] (see Supplementary Fig. 7). Taken together, a model is emerging that suggests that the formation of replication associated DSB underlies the sensitivity of p53-deficient fibroblasts to UV-induced apoptosis.

In summary, we clearly demonstrate that fibroblasts expressing functional p53 recover from UV-induced replication arrest prior to the repair of CPD whereas p53-deficient cells have a profound defect in the recovery from this arrest. The role of p53 in promoting recovery from replication arrest is separable from its role in regulating DDB2 and GG-NER of CPD. It remains to be determined whether this defect is linked to impaired TLS, replication fork collapse, DSB formation and sensitivity to UV-induced apoptosis. Deciphering these issues will be important to further our understanding of the role of p53 in tumour suppression.

Note

Supplementary material can be found at:
www.landesbioscience.com/supplement/StubbertCC6-14-sup.pdf

References

1. Osborn AJ, Elledge SJ, Zou L. Checking on the fork: The DNA-replication stress-response pathway. Trends Cell Biol 2002; 12:509-16.
2. Zhou BB, Elledge SJ. The DNA damage response: Putting checkpoints in perspective. Nature 2000; 408:433-9.
3. Cleaver JE, Laposa RR, Limoli CL. DNA replication in the face of (In)surmountable odds. Cell Cycle 2003; 2:310-5.
4. Kaufmann WK, Cleaver JE. Mechanisms of inhibition of DNA replication by ultraviolet light in normal human and xeroderma pigmentosum fibroblasts. J Mol Biol 1981; 149:171-87.
5. Cleaver JE, Kaufmann WK, Kapp LN, Park SD. Replicon size and excision repair as factors in the inhibition and recovery of DNA synthesis from ultraviolet damage. Biochim Biophys Acta 1983; 739:207-15.
6. Cleaver JE, Thomas GH, Park SD. Xeroderma pigmentosum variants have a slow recovery of DNA synthesis after irradiation with ultraviolet light. Biochim Biophys Acta 1979; 564:122-31.
7. Park SD, Cleaver JE. Recovery of DNA synthesis after ultraviolet irradiation of xeroderma pigmentosum cells depends on excision repair and is blocked by caffeine. Nucleic Acids Res 1979; 6:1151-9.
8. Lehmann AR. The relationship between pyrimidine dimers and replicating DNA in UV-irradiated human fibroblasts. Nucleic Acids Res 1979; 7:1901-12.
9. Cistulli CA, Kaufmann WK. p53-dependent signaling sustains DNA replication and enhances clonogenic survival in 254 nm ultraviolet-irradiated human fibroblasts. Cancer Res 1998; 58:1993-2002.
10. Mirzayans R, Enns L, Dietrich K, Barley RDC, Paterson MC. Faulty DNA polymerase delta/epsilon-mediated excision repair in response to gamma radiation or ultraviolet light in p53-deficient fibroblast strains from affected members of a cancer-prone family with Li-Fraumeni syndrome. Carcinogenesis 1996; 17:691-8.

11. Barley RD, Enns L, Paterson MC, Mirzayans R. Aberrant p21WAF1-dependent growth arrest as the possible mechanism of abnormal resistance to ultraviolet light cytotoxicity in Li-Fraumeni syndrome fibroblast strains heterozygous for *TP53* mutations. Oncogene 1998; 17:533-43.
12. Ford JM, Hanawalt PC. Expression of wild-type p53 is required for efficient global genomic nucleotide excision repair in UV-irradiated human fibroblasts. J Biol Chem 1997; 272:28073-80.
13. Ford JM, Hanawalt PC. Li-Fraumeni syndrome fibroblasts homozygous for *p53* mutations are deficient in global DNA repair but exhibit normal transcription-coupled repair and enhanced UV resistance. Proc Natl Acad Sci USA 1995; 92:8876-80.
14. McKay BC, Becerril C, Ljungman M. p53 plays a protective role against UV- and cisplatin-induced apoptosis in transcription-coupled repair proficient fibroblasts. Oncogene 2001; 20:6805-8.
15. McKay BC, Becerril C, Spronck JC, Ljungman M. Ultraviolet light-induced apoptosis is associated with S phase in primary human fibroblasts. DNA Repair 2002; 1:811-20.
16. Loignon M, Drobetsky EA. The initiation of UV-induced G_1 arrest in human cells is independent of the p53/p21/pRb pathway but can be attenuated through expression of the HPV E7 oncoprotein. Carcinogenesis 2002; 23:35-45.
17. Yin Y, Tainsky MA, Bischoff FZ, Strong LC, Wahl GM. Wild-type p53 restores cell cycle control and inhibits gene amplification in cells with mutant *p53* alleles. Cell 1992; 70:937-48.
18. McKay BC, Chen F, Perumalswami CR, Zhang F, Ljungman M. The tumor suppressor *p53* can both stimulate and inhibit ultraviolet light-induced apoptosis. Mol Biol Cell 2000; 11:2543-51.
19. Chang D, Chen F, Zhang F, McKay BC, Ljungman M. Dose-dependent effects of DNA-damaging agents on p53-mediated cell cycle arrest. Cell Growth Differ 1999; 10:155-62.
20. Sengupta S, Harris CC. p53: Traffic cop at the crossroads of DNA repair and recombination. Nat Rev Mol Cell Biol 2005; 6:44-55.
21. Ford JM, Baron EL, Hanawalt PC. Human fibroblasts expressing the human papillomavirus E6 gene are deficient in global genomic nucleotide excision repair and sensitive to ultraviolet irradiation. Cancer Res 1998; 58:599-603.
22. Therrien JP, Drouin R, Baril C, Drobetsky EA. Human cells compromised for p53 function exhibit defective global- and transcription coupled-repair whereas cells compromised for pRb function are defective only in global repair. Proc Natl Acad Sci USA 1999; 96:15038-43.
23. Wani MA, Zhu QZ, El-Mahdy M, Wani AA. Influence of *p53* tumor suppressor protein on bias of DNA repair and apoptotic response in human cells. Carcinogenesis 1999; 20:765-72.
24. Hwang BJ, Ford JM, Hanawalt PC, Chu G. Expression of the p48 xeroderma pigmentosum gene is *p53*-dependent and is involved in global genomic repair. Proc Natl Acad Sci USA 1999; 96:424-8.
25. Lehmann AR, Kirk-Bell S. Effects of caffeine and theophylline on DNA synthesis in unirradiated and UV-irradiated mammalian cells. Mutat Res 1974; 26:73-82.
26. Buhl SN, Setlow RB, Regan JD. Recovery of the ability to synthesize DNA in segments of normal size at long times after ultraviolet irradiation of human cells. Biophys J 1973; 13:1265-75.
27. Buhl SN, Stillman RM, Setlow RB, Regan JD. DNA chain elongation and joining in normal human and xeroderma pigmentosum cells after ultraviolet irradiation. Biophys J 1972; 12:1183-91.
28. Buhl SN, Setlow RB, Regan JD. Steps in DNA chain elongation and joining after ultra-violet irradiation of human cells. Int J Radiat Biol Relat Stud Phys Chem Med 1972; 22:417-24.
29. Chastain IInd PD, Heffernan TP, Nevis KR, Lin L, Kaufmann WK, Kaufman DG, Cordeiro-Stone M. Checkpoint regulation of replication dynamics in UV-irradiated human cells. Cell Cycle 2006; 5:2160-7.
30. Kaufmann WK, Cleaver JE, Painter RB. Ultraviolet radiation inhibits replicon initiation in S phase human cells. Biochim Biophys Acta 1980; 608:191-5.
31. Squires S, Coates JA, Goldberg M, Toji LH, Jackson SP, Clarke DJ, Johnson RT. p53 prevents the accumulation of double-strand DNA breaks at stalled-replication forks induced by UV in human cells. Cell Cycle 2004; 3:1543-57.
32. Friedberg EC, Aguilera A, Gellert M, Hanawalt PC, Hays JB, Lehmann AR, Lindahl T, Lowndes N, Sarasin A, Wood RD. DNA repair: From molecular mechanism to human disease. DNA Repair (Amst) 2006; 5:986-96.
33. van Hoffen A, Venema J, Meschini R, Vanzeeland AA, Mullenders LHF. Transcription-coupled repair removes both cyclobutane pyrimidine dimers and 6-4 photoproducts with equal efficiency and in a sequential way from transcribed DNA in xeroderma pigmentosum group C fibroblasts. EMBO J 1995; 14:360-7.
34. Venema J, Vanhoffen A, Karcagi V, Natarajan AT, Vanzeeland AA, Mullenders LHF. Xeroderma-pigmentosum complementation group-C cells remove pyrimidine dimers selectively from the transcribed strand of active genes. Mol Cell Biol 1991; 11:4128-34.
35. Venema J, van Hoffen A, Natarajan AT, van Zeeland AA, Mullenders LHF. The residual repair capacity of xeroderma pigmentosum complementation group C fibroblasts is highly specific for transcriptionally active DNA. Nuc Acids Res 1990; 18:443-8.
36. Nikolaishvili-Feinberg N, Cordeiro-Stone M. Bypass replication in vitro of UV-induced photoproducts blocking leading or lagging strand synthesis. Biochemistry 2001; 40:15215-23.
37. Cordeiro-Stone M, Nikolaishvili-Feinberg N. Asymmetry of DNA replication and translesion synthesis of UV-induced thymine dimers. Mutat Res 2002; 510:91-106.
38. Orren DK, Petersen LN, Bohr VA. Persistent DNA damage inhibits S-phase and G_2 progression, and results in apoptosis. Mol Biol Cell 1997; 8:1129-42.
39. Hwang BJ, Toering S, Francke U, Chu G. p48 Activates a UV-damaged-DNA binding factor and is defective in xeroderma pigmentosum group E cells that lack binding activity. Mol Cell Biol 1998; 18:4391-9.
40. Kastan M, Onyekwere O, Sidransky D, Vogelstein B, Craig R. Participation of p53 protein in the cellular response to DNA damage. Cancer Res 1991; 51:6304-11.
41. Kuerbitz S, Plunkett B, Walsh V, Kastan M. Wild-type p53 is a cell cycle checkpoint determinant following irradiation. Proc Natl Acad Sci USA 1992; 89:7491-5.
42. El-Deiry W, Tokino T, Velculescu V, Levy D, Parsons R, Trent J, Lin D, Mercer W, Kinzler K, Vogelstein B. WAF1, a potential mediator of *p53* tumor suppression. Cell 1993; 75:817-25.
43. Harper J, Adami G, Wei N, Keyormarsi K, Elledge S. The p21 cdk-interacting protein Cip1 is a potent inhibitor of G_1 cyclin-dependent kinases. Cell 1993; 75:805-16.
44. Lu X, Lane DP. Differential induction of transcriptionally active p53 following UV or ionizing radiation - Defects in chromosome instability syndromes? Cell 1993; 75:765-78.
45. Attardi LD, de Vries A, Jacks T. Activation of the p53-dependent G_1 checkpoint response in mouse embryo fibroblasts depends on the specific DNA damage inducer. Oncogene 2004; 23:973-80.
46. Geyer RK, Nagasawa H, Little JB, Maki CG. Role and regulation of p53 during an ultraviolet radiation-induced G_1 cell cycle arrest. Cell Growth Differ 2000; 11:149-56.
47. van Laar T, Steegenga WT, Jochemsen AG, Terleth C, van der Eb AJ. Bloom's syndrome cells GM1492 lack detectable p53 protein but exhibit normal G_1 cell-cycle arrest after UV irradiation. Oncogene 1994; 9:981-3.
48. Kaufmann WK, Wilson SJ. G_1 arrest and cell-cycle-dependent clastogenesis in UV-irradiated human fibroblasts. Mutat Res 1994; 314:67-76.
49. McKay BC, Ljungman M. Role for p53 in the recovery of transcription and protection against apoptosis induced by ultraviolet light. Neoplasia 1999; 1:276-84.
50. van Laar T, Steegenga WT, Jochemsen AG, Terleth C, van der Eb AJ. GM1492 human diploid skin fibroblasts lack the p53-dependent G_1 cell-cycle checkpoint. Biochem Biophys Res Commun 1995; 217:769-76.
51. Loignon M, Fetni R, Gordon AJE, Drobetsky EA. A p53-independent pathway for induction of p21(waf1cip1) and concomitant G_1 arrest in UV-irradiated human skin fibroblasts. Cancer Res 1997; 57:3390-4.
52. Al-Mohanna MA, Al-Khodairy FM, Krezolek Z, Bertilsson PA, Al-Houssein KA, Aboussekhra A. p53 is dispensable for UV-induced cell cycle arrest at late G_1 in mammalian cells. Carcinogenesis 2001; 22:573-8.
53. Gottifredi V, Prives C. The S phase checkpoint: When the crowd meets at the fork. Semin Cell Dev Biol 2005; 16:355-68.
54. Saintigny Y, Delacote F, Vares G, Petitot F, Lambert S, Averbeck D, Lopez BS. Characterization of homologous recombination induced by replication inhibition in mammalian cells. Embo J 2001; 20:3861-70.
55. Saintigny Y, Lopez BS. inAverbeck D, Lopez BS.

70. Yarbro JW. Mechanism of action of hydroxyurea. Semin Oncol 1992; 19:1-10.
71. Bertrand P, Saintigny Y, Lopez BS. p53's double life: Transactivation-independent repression of homologous recombination. Trends Genet 2004; 20:235-43.
72. Ward IM, Chen J. Histone H2AX is phosphorylated in an ATR-dependent manner in response to replicational stress. J Biol Chem 2001; 276:47759-62.
73. Cleaver JE, Bartholomew J, Char D, Crowley E, Feeney L, Limoli CL. Polymerase eta and p53 jointly regulate cell survival, apoptosis and Mre11 recombination during S phase checkpoint arrest after UV irradiation. DNA Repair (Amst) 2002; 1:41-57.
74. Queille S, Drougard C, Sarasin A, Daya-Grosjean L. Effects of *XPD* mutations on ultraviolet-induced apoptosis in relation to skin cancer-proneness in repair-deficient syndromes. J Invest Dermatol 2001; 117:1162-70.
75. Lackinger D, Kaina B. Primary mouse fibroblasts deficient for c-Fos, p53 or for both proteins are hypersensitive to UV light and alkylating agent-induced chromosomal breakage and apoptosis. Mutat Res 2000; 457:113-23.
76. Dunkern TR, Fritz G, Kaina B. Ultraviolet light-induced DNA damage triggers apoptosis in nucleotide excision repair-deficient cells via Bcl-2 decline and caspase-3/-8 activation. Oncogene 2001; 20:6026-38.
77. Dunkern T, Kaina B. Cell proliferation and DNA breaks are involved in ultraviolet light-induced apoptosis in nucleotide excision repair-deficient chinese hamster cells. Mol Cell Biol 2002; 13:348-61.

Cell Cycle 8:18, 2995-3002; September 15, 2009; © 2009 Landes Bioscience

Ultraviolet light induces the sustained unscheduled expression of cyclin E in the absence of functional p53

Lawton J. Stubbert,[1,2,†] Jennifer C. Spronck,[1,†] Jeff D. Hamill[1] and Bruce C. McKay[1-3,*]

[1]Cancer Therapeutics Program; Ottawa Hospital Research Institute; Ottawa, ON CA; [2]Department of Cellular and Molecular Medicine; and [3]Department of Medicine; University of Ottawa; Ottawa, ON CA

[†]These authors contributed equally to this work.

Key words: cell cycle, cyclin E, DNA damage, p53, UV light

Cell cycle progression is regulated through changes in the activity of cyclin-dependent kinases that are, in turn, regulated by the expression of their respective cyclin partners. In primary cells, cyclin E expression increases through the G_1 phase of the cell cycle and peaks near the G_1/S boundary. The unscheduled expression of cyclin E in primary human fibroblasts leads to chromosomal instability that is greatly increased by loss of the p53 tumour suppressor. Intriguingly, ultraviolet light (UV), the most prevalent environmental carcinogen, is similarly known to induce chromosomal instability more dramatically in the absence of p53. Here we report that UV light transiently increased the expression of cyclin E in normal human fibroblasts. Strikingly, cyclin E levels remained elevated for an extended period of time in the absence of functional p53. UV-induced cyclin E expression was not restricted to the G_1/S boundary but remained elevated throughout S phase and this correlated with a massive accumulation of p53-deficient fibroblasts in this phase of the cell cycle. Forced expression of cyclin E alone was insufficient to cause a similar S phase arrest but forced expression of cyclin E led to an increase in the proportion of UV-irradiated cells in S phase. The present work suggests that p53 affects S phase progression following UV exposure by preventing the sustained unscheduled expression of cyclin E and that this may limit the clastogenic and carcinogenic effects of UV light.

Introduction

The ultraviolet (UV) light component of sunlight is considered to be the most prevalent environmental carcinogen.[1-3] UV light is a genotoxic agent that induces DNA lesions primarily at dipyrimidine sites.[4,5] Replicative bypass of these lesions gives rise to the characteristic "UV signature" mutations characteristic of sunlight exposure: typically C to T and CC to TT transitions.[6,7] In addition to point mutations, replication of UV-damaged DNA can lead to the accumulation of DNA double strand breaks (DSB) and sister chromatid exchanges.[8-12] The p53 tumour suppressor decreases the susceptibility of cells to UV-induced point mutations, replication-associated DSB and UV-induced recombination.[10-13] Therefore, p53 plays an important role in regulating genomic stability and protecting against skin carcinogenesis following UV exposure.[14,15]

Cyclin E is considered a G_1 cyclin.[16] Transcription of the *CCNE1* gene encoding cyclin E is positively regulated by the E2F family of transcription factors as cells progress through the late G_1 phase of the cell cycle.[17,18] In other phases of the cell cycle, specific E2Fs repress transcription from the *CCNE1* locus.[19,20] Furthermore, cyclin E protein levels are negatively regulated by proteasome-mediated degradation by the SCF^{Fbw7} ubiquitin ligase complex as cells enter S phase.[21,22] Through a combination of transcriptional and post-translational regulation, cyclin E levels are thought to peak in normal cells at or near the G_1/S boundary and are actively repressed elsewhere in the cell cycle.

In partial contrast to the situation in primary cells, cyclin E is deregulated in a variety of cancers. It was previously thought that cyclin E was essential and rate limiting for the G_1 to S phase transition.[16] However, cyclin E nullizygous mouse cells retain the ability to proliferate.[23] In fact, cyclin E ablation in mouse embryonic fibroblasts decreases their susceptibility to oncogenic transformation, suggesting that cyclin E is an oncogene.[23] Consistent with this observation, the unscheduled expression of cyclin E in tumour cells is associated with genomic instability.[24-28] The FBW7 component of the SCF^{Fbw7} complex is a tumour suppressor and this is at least partly due to its role in targeting cyclin E for proteasome-mediated degradation.[21,26-33] Taken together, the unscheduled expression of cyclin E appears to contribute to genomic instability and oncogenic transformation.

Here we report that UV light, a potent skin carcinogen, increased the expression of cyclin E at both the mRNA and protein level. The induction of cyclin E occurred in a p53-independent manner, however cyclin E levels remained elevated much longer in cells lacking functional p53. The sustained induction of cyclin E was not restricted to the G_1/S boundary but was prominent throughout S phase. The unscheduled expression of cyclin E was associated with the accumulation of cells in S phase and

*Correspondence to: Bruce C. McKay; Email: bmckay@ohri.ca
Submitted: 04/17/09; Revised: 07/04/09; Accepted: 07/25/09
Previously published online: www.landesbioscience.com/journals/cc/article/9614

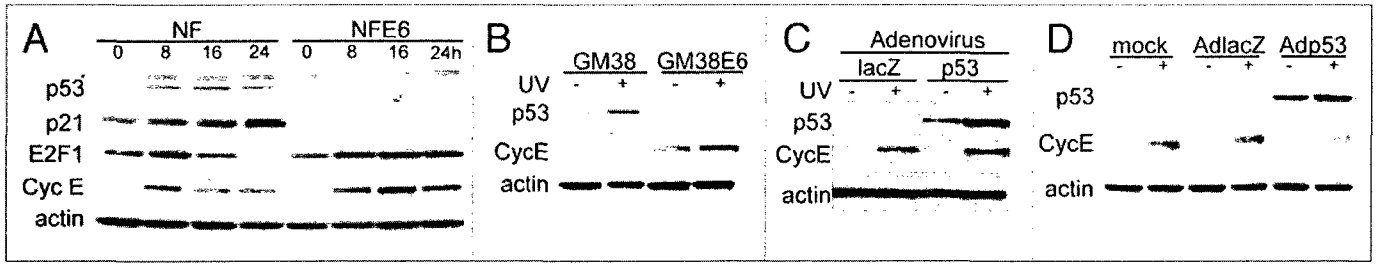

Figure 1. Cyclin E is induced in response to UV light. Immunoblot analysis of total cellular protein was performed using antibodies raised against the indicated proteins. (A) NF and NFE6 samples were collected at the indicated times following exposure to 10 J/m² of UV light. *denotes a non-specific band recognized by the anti-p53 antibody. (B) Immunoblot analysis was performed using protein samples collected from GM38 and GM38E6 cells 24 hours following UV exposure. (C and D) LFS cells were infected with a recombinant adenovirus expressing either lacZ or p53, 24 hours prior to UV exposure. Cell lysates were collected either 6 (C) or 24 (D) hours following UV-irradiation. - and + in (B–D) correspond to 0 or 10 J/m², respectively.

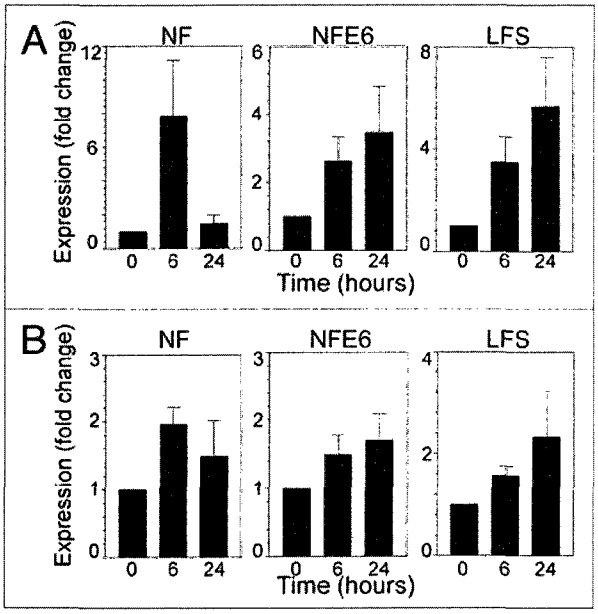

Figure 2. Transcriptional upregulation of cyclin E following UV-irradiation. Real-time reverse transcriptase polymerase chain reaction was used to monitor changes in CCNE1 (A) and E2F1 (B) transcript levels at 6 and 24 hours following UV exposure in the indicated cell lines. Each value represents the mean (±SEM) determined from either 3 or 4 independent experiments.

forced expression of cyclin E in combination with UV light led to an S phase arrest even in the presence of p53. These observations highlight the importance of regulating cyclin E expression for S phase progression following UV exposure.

Results

Cyclin E is induced in a p53-independent manner following UV-irradiation. Normal fibroblasts were exposed to 10 J/m² of UV light and cell lysates were collected at various times following UV exposure for immunoblot analysis. We have previously reported that this dose of UV light in these specific strains induced apoptosis in less than 10% of UV exposed cells so this dose of UV light is not highly cytotoxic.[34,37-39] Under these conditions, UV light led to an increase in the expression of the p53-regulated protein $p21^{WAF1}$ and cyclin E (E2F1-regulated) within 8 hours (**Fig. 1A**). However, the time course for cyclin E induction was clearly distinguishable from that of $p21^{WAF1}$. Whereas $p21^{WAF1}$ levels increased over the 24 hour period, cyclin E expression peaked at 8 hours and subsequently decreased (**Fig. 1A**).

Cyclin E expression was similarly assessed in isogenic fibroblasts in which p53 expression (and hence $p21^{WAF1}$) was decreased by HPV-E6 expression (**Fig. 1A**). The expression of cyclin E again increased within 8 hours in the absence of p53 but cyclin E expression remained elevated even 24 hours following UV exposure in the HPV-E6 expressing fibroblasts (**Fig. 1A**). An inverse correlation between cyclin E and both p53 and $p21^{WAF1}$ induction was observed 24 hours following UV exposure in both isogenic pairs of normal and HPV-E6 expressing fibroblasts strains (**Fig. 1A and B**). These results indicate that cyclin E was induced in a p53-independent manner but that the duration of increased cyclin E expression was affected by HPV-E6 expression.

To ensure that prolonged cyclin E expression following UV exposure was related to the loss of p53 and not to HPV-E6 expression per se, cyclin E expression was assessed in LFS fibroblasts that do not express detectable p53.[40] Cyclin E levels were elevated 6 and 24 hours following UV exposure in these p53-deficient cells (**Fig. 1C and D**). Expression of p53 in LFS cells using a recombinant adenovirus did not prevent the UV-induced accumulation of p53 at 6 hours (**Fig. 1C**) but reduced cyclin E levels 24 hours following UV exposure (**Fig. 1D**). Taken together, these results indicate that cyclin E is induced in response to UV treatment in a p53-independent manner but that p53 limits the duration of cyclin E induction.

Cyclin E is induced at the transcriptional level. The regulation of cyclin E involves both transcriptional and post-transcriptional mechanisms.[16] Therefore, *CCNE1* transcript levels were assessed using real-time reverse transcriptase polymerase chain reaction 0, 6 and 24 hours following UV exposure. CCNE1 mRNA levels were increased at 6 hours but not 24 hours following UV-irradiation in normal diploid fibroblasts expressing p53 (**Fig. 2A**). A similar transient increase in CCNE1 mRNA levels was observed in a series of microarray experiments, under similar conditions in an unrelated normal fibroblast strain.[41] In contrast to the pattern observed in normal fibroblasts, *CCNE1* mRNA levels were elevated at both 6 and 24 hours following UV exposure in HPV-E6 expressing normal and LFS fibroblasts (**Fig. 2A**). Therefore,

CCNE1 mRNA correlated with cyclin E protein expression following UV exposure.

Transcription of the *CCNE1* gene is positively regulated by the E2F1 transcription factor[18] and E2F1 is known to be UV-inducible.[42] Consistent with the pattern of cyclin E protein expression, E2F1 protein levels peaked at 8 hours following UV exposure and subsequently decreased in p53-expressing fibroblasts but remained elevated in the absence of functional p53 (**Fig. 1A**). Although the pattern of *E2F1* mRNA expression mirrored that of *CCNE1*, the fold increase in *E2F1* mRNA was rather modest in comparison (**Fig. 2B**). Taken together, cyclin E is induced at the transcript level in a p53-independent manner that correlates with increased E2F1 protein levels but that p53 limits the duration of the UV-induced accumulation of cyclin E and its transcriptional regulator E2F1.

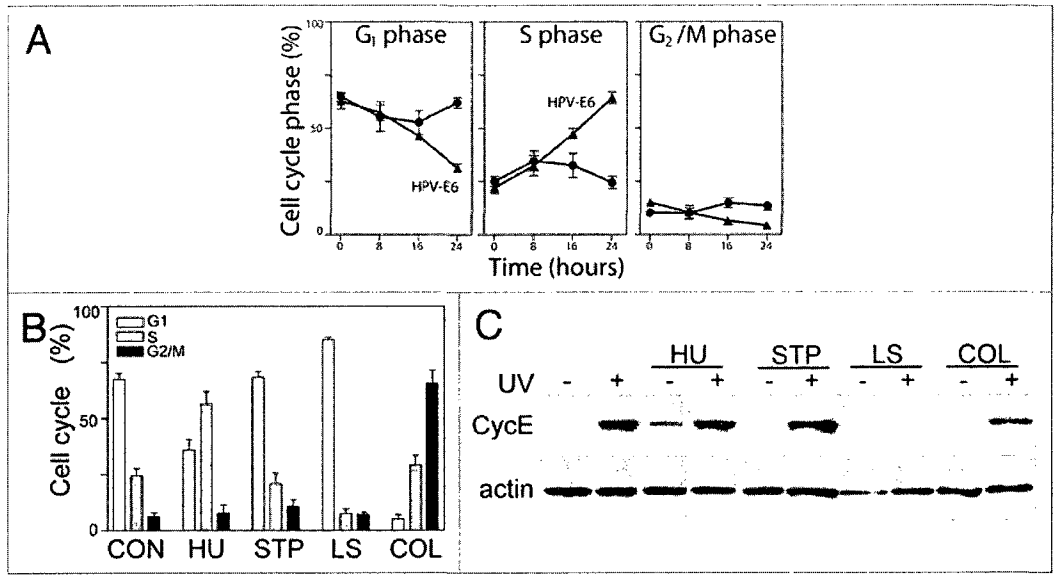

Figure 3. Correlation between cyclin E expression and cell cycle phase following UV exposure. (A) The cell cycle distribution of GM38 (circles) and GM38E6 (triangles) fibroblasts was determined at various times following exposure to either 0 or 10 J/m^2 of UV light. (B) The cell cycle distribution of LFS cells incubated for 16 hours in hydroxyurea (HU), staurosporine (STP) or colcemid (COL) was determined. LS indicates that cells were cultured under low serum conditions (0.5% FBS) for 3 days. (C) Cells treated as described in (B) were UV treated (0 or 10 J/m^2) and cell lysates were collected for immunoblot analysis 6 hours later. Each value in (A and B) represents the mean (±SEM) determined from a minimum of 3 independent experiments.

Unscheduled expression of cyclin E. Cyclin E is considered a G_1 cyclin with its expression peaking near the G_1/S boundary.[43-45] To determine how cyclin E was expressed through the cell cycle, flow cytometric analysis was first performed at various times following UV-irradiation. In normal fibroblasts, the proportion of UV treated cells in G_1 phase decreased while the S phase fraction increased marginally at 8 and 16 hours following UV exposure (**Fig. 3A**). A normal cell cycle distribution was restored within 24 hours (**Fig. 3A**). In sharp contrast, the proportion of HPV-E6 expressing fibroblasts in S phase accumulated markedly while the proportion of cells in G_1 phase plummeted during the observed period of up to 24 hours following UV exposure (**Fig. 3A**).[12] Therefore, the sustained induction of cyclin E coincided with conditions that led to a massive S phase arrest with a concomitant depletion of the G_1 population (**Fig. 3A**), suggesting that cyclin E induction was unlikely to be specific to the G_1 to S phase transition.

A variety of drugs were then used to manipulate the cell cycle to determine if cyclin E could be induced in an unscheduled manner. Staurosporine is a kinase inhibitor that inhibits cell cycle progression in G_1 prior to the peak in cyclin E expression.[46,47] Hydroxyurea (HU) is a ribonucleotide reductase inhibitor that selectively blocks cell cycle progression in S phase.[48] Colcemid is a microtubule inhibitor that blocks cells in M phase.[49] Staurosporine treatment of p53-deficient LFS cells did not significantly affect cell cycle distribution and failed to block the UV-induced accumulation of cyclin E (**Fig. 3B and C**). Treatment of LFS cells with HU for 24 hours resulted in the accumulation of more than 50% of the cells in S phase with a concomitant decrease in the proportion of cells in G_1 (**Fig. 3B**). UV exposure of HU arrested cells led to a significant increase in cyclin E expression despite the pronounced S phase arrest (**Fig. 3C**). Most striking, cyclin E was induced in response to UV light in colcemid-treated (M phase arrested) cells despite the complete depletion of the G_1 population within 24 hours (**Fig. 3B and C**). Of the conditions tested, only exit from the cell cycle by prolonged culture (3 days) in 0.5% serum blocked the induction of cyclin E (**Figs. 3B and C, lane 8**). These results suggest that cyclin E can be induced in an unscheduled manner following UV exposure.

To more directly assess cyclin E expression as a function of cell cycle phase following UV-irradiation, cyclin E expression and DNA content were simultaneously assessed on a per cell basis using two-parameter flow cytometry 16 hours following UV exposure. In normal diploid fibroblasts, cyclin E expression peaked near the G_1/S boundary with cyclin E levels appearing lowest in the small S phase population (**Fig. 4A**). A small proportion of cells with 4N DNA content appeared to be cyclin E positive. Exposure of normal cells to UV light led to an increase in the proportion of cells in late S and G_2/M phase (**Fig. 4A**). This relatively small population of cells had increased cyclin E expression compared to untreated controls in the same phase of the cell cycle (**Fig. 4A**). Therefore, UV light induced the unscheduled expression of cyclin E in small proportion of normal fibroblasts with 4N DNA content.

The pattern of cyclin E expression was near normal in the HPV-E6 expressing cells prior to UV exposure (**Fig. 4B**). Again, cyclin E expression was lowest in early S phase (**Fig. 4B**). Consistent with **Figure 3**, the most prominent change in cell cycle distribution following UV exposure was the accumulation of HPV-E6

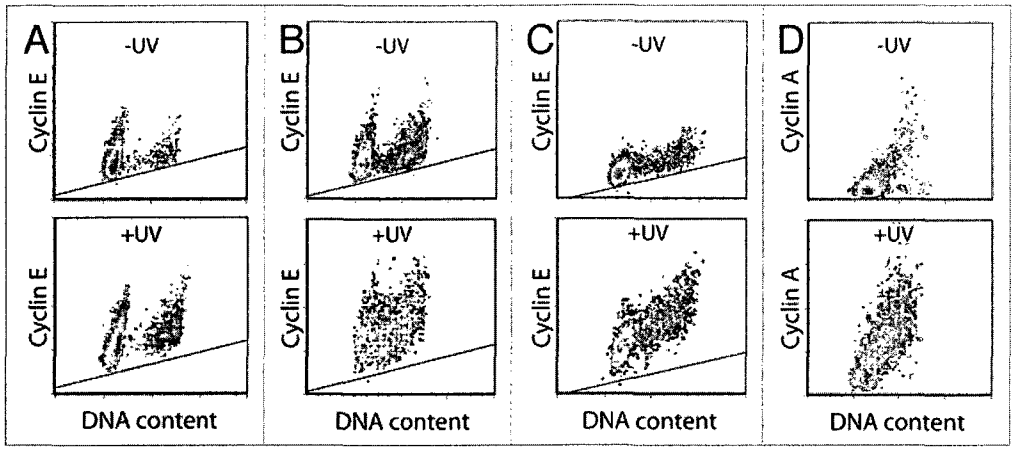

Figure 4. Ultraviolet light induces the unscheduled expression of cyclin E. GM38 (A), GM38E6 (B) and LFS (C) fibroblasts were exposed to 0 or 10 J/m² of UV light and were collected 16 hours later for two-parameter flow cytometric analysis. Cyclin E expression was assessed as a function of DNA content. (D) Similarly, Cyclin A expression was assessed in LFS cells as a function of DNA content, 24 hours following exposure to 0 or 10 J/m² of UV light. The lines in (A–C) approximate the lower limit of cyclin E expression in unirradiated controls (upper). They serve to facilitate the comparison in cyclin E expression between treatments.

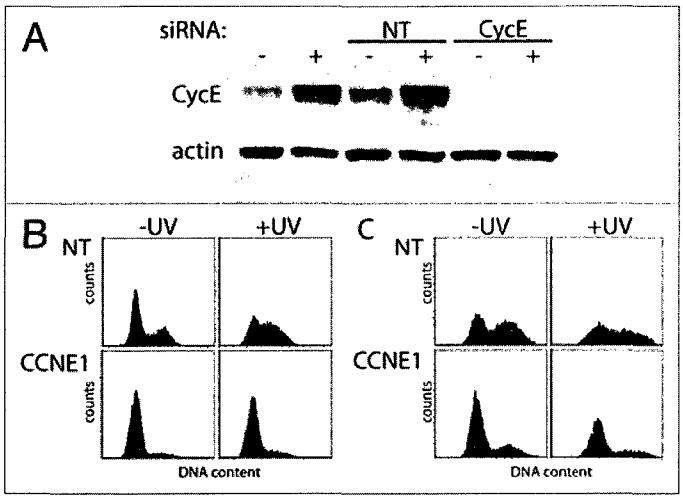

Figure 5. RNA interference against CCNE1 prevents the sustained accumulation of cells in S phase following UV exposure. (A) LFS cells were transfected with either siRNAs against the CCNE1 transcript or non-targeting control siRNAs (NT) 72 hours prior to UV exposure (0 or 10 J/m²). Cell lysates were collected 24 hours following UV exposure for immunoblot analysis of cyclin E expression. GM38E6 (B) and LFS (C) cells were treated as described in (A) except that samples were collected 24 hours following UV exposure for flow cytometric analysis of DNA content. Similar results were obtained in 3 independent experiments.

expressing cells in S phase (**Fig. 4B**).[12] UV light led to a significant increase in cyclin E expression in S phase (**Fig. 4B**). In unirradiated LFS cells, cyclin E was expressed more evenly throughout the cell cycle (**Fig. 4C**). Following UV exposure, cyclin E expression increased throughout S phase such that the highest expressing cells had 4N DNA content (**Fig. 4C**). This unscheduled pattern of expression was similar to the normal cell cycle-dependent pattern of cyclin A expression (**Fig. 4D**).[50] Taken together, our results indicate that the exposure of fibroblasts to UV light resulted in the unscheduled expression of cyclin E and that this was far more dramatic in p53-deficient fibroblast strains.

Cyclin E and ultraviolet light-induced S phase arrest. As indicated above, UV light induced the unscheduled expression of cyclin E and this correlated with the accumulation of cells in S phase. Overexpression of cyclin E but not cyclin A or cyclin D1 can lead to an S phase arrest.[28,51] In an initial attempt to determine whether cyclin E contributed to the observed S phase arrest following UV exposure, RNA interference was used to decrease the expression of cyclin E (**Fig. 5A**). Decreased cyclin E expression led to an increase in the proportion of cells in G_1 with a concomitant decrease in S phase (**Fig. 5B and C**), consistent with its role in promoting G_1 to S phase transition.[16] HPV-E6 expressing and LFS fibroblasts transfected with control siRNAs accumulated in S phase following UV exposure, as expected (**Fig. 5B and C**). In contrast, cells transfected with *CCNE1* siRNA did not, suggesting that cyclin E is required to establish this prolonged arrest. As indicated above, the siRNAs against CCNE1 decreased the proportion of cells in S phase. This change in cell cycle distribution complicated the interpretation of these RNA interference experiments.

To clarify the issue, an alternate strategy was used to manipulate cyclin E expression. Infection of normal human fibroblasts with an adenovirus expressing *CCNE1* led to a significant increase in cyclin E protein levels that was not greatly affected by UV exposure (**Fig. 6A**). Forced expression of cyclin E led to a significant increase in the proportion of cells in S phase (**Fig. 6B and C**). Remarkably, the cyclin E overexpressing fibroblasts accumulated in S phase following UV exposure despite the presence of wildtype p53 in these cells (**Fig. 6B and C**). Taken together, unscheduled expression of cyclin E contributed to the accumulation of cells in S phase following UV-irradiation.

Discussion

Ultraviolet light and cyclin E. Cyclin E expression is thought to be rate limiting for G_1 to S phase transition.[18,21] The peak expression of cyclin E is coincident with this transition and is achieved through a combination of transcriptional and post-transcriptional mechanisms.[18,21] Cell cycle-dependent transcription of the *CCNE1* gene is driven, in large part, by activator E2F proteins, like E2F1. Here, we found that UV light induced the expression of *CCNE1* mRNA and cyclin E protein and this was not inhibited by the PI3 kinase inhibitors wortmannin or caffeine (**Suppl. Fig. 1**). The induction of cyclin E was not dependent on p53 but correlated with increased expression of E2F1. This transcription factor is

UV-induced[42,52-54] so our results are consistent with a role for E2F1 in regulating cyclin E expression at the transcriptional level following UV exposure.

We found that cyclin E (mRNA and protein) remained elevated for an extended period of time following UV exposure, in the absence of functional p53. Importantly, the sustained UV-induced accumulation of cyclin E in p53-deficient fibroblasts was not restricted to the late G_1 phase and early S phase of the cell cycle. Two parameter flow cytometric analysis indicated that cyclin E levels increased throughout the S and G_2 phases following UV exposure in LFS cells but not when cyclin E was overexpressed from a recombinant adenovirus (**Suppl. Fig. 2**). In fact, forced expression of cyclin E was highest in G_1 phase despite the fact that expression was driven by a constitutively active promoter derived from human cytomegalovirus. Therefore, increased mRNA expression is insufficient to recapitulate the unscheduled expression observed in UV-irradiated cells.

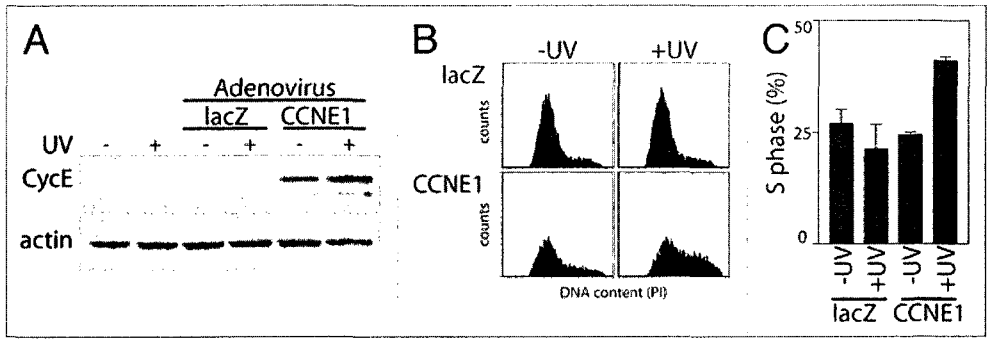

Figure 6. Forced expression of cyclin E leads to a UV-induced S phase arrest in p53 expressing fibroblasts. Cyclin E was overexpressed in primary human fibroblasts using a recombinant adenovirus construct. (A) GM38 cells were UV-irradiated (0 or 10 J/m^2) 24 hours following infection with the indicated recombinant adenovirus construct and protein extracts were collected 24 hours following UV exposure for immunoblot analysis of cyclin E expression. (B) GM38 cells were treated as in (A) except that cells were collected for flow cytometric analysis based on DNA content. Similar results were obtained in 3 independent experiments and the mean (±SEM) S phase population is plotted in (C).

Post-transcriptional regulation of cyclin E. The expression of cyclin E is normally held in check through proteasome-mediated degradation involving the SCF^{Fbw7}-ubiquitin ligase complex.[21,55-58] Unscheduled expression of cyclin E occurs in cells that have lost or carry mutations in *FBW7*.[26,28] Therefore, the pattern of cyclin E expression noted here is consistent with increased stability of cyclin E protein. Intriguingly, transcription of the *CCNA2* gene encoding cyclin A is also positively regulated by E2F1,[59] but unlike cyclin E, cyclin A is targeted for proteasome-mediated degradation much later in the cell cycle by a distinct ubiquitin ligase complex: the anaphase promoting complex.[60,61] The cell cycle-dependent pattern of cyclins E and A are normally quite distinct, peaking near the G_1/S and G_2/M boundaries, respectively.[50,60,61] In the present work, the cell cycle-dependent pattern of cyclin E expression resembled that of cyclin A (recall **Fig. 4C and D**) in LFS cells exposed to UV light. These results suggest that the prolonged accumulation of cyclin E involves decreased protein turnover in addition to increased transcription of the *CCNE1* gene.

There are three isoforms of Fbw7 that are identical in the C-terminal half of the protein but have distinct N-terminal regions due to alternative splicing of 5' exons.[62,63] Notably, they are expressed from 3 separate promoters and these isoforms respond differentially to UV light.[58,62,63] Specifically, α and γ isoforms were reportedly downregulated in response to UV exposure whereas the β isoform was reported to be induced in a p53-dependent manner.[58,62] Using primers specific for isoforms α, β and γ, as well as an isoform-independent pair of primers, we used real time reverse transcriptase PCR to confirm this previous work. As expected, we found that p53 greatly affects the expression of various transcripts encoding these isoforms of Fbw7 following UV exposure (**Suppl. Fig. 3**). In primary human fibroblasts, total Fbw7 and Fbw7β were induced in response to UV exposure while the expression of the other isoforms was decreased. In the HPV-E6 expressing subline, the expression of all isoforms was reduced following UV exposure initially (**Suppl. Fig. 3**). It is possible that decreased expression of Fbw7 in p53-deficient fibroblasts contributes to increased cyclin E expression through transcriptional derepression, as reported for c-Jun.[62]

Unscheduled cyclin E expression, UV light and genomic instability. The cell cycle-dependent expression of cyclin E is important to maintain genomic stability. Forced expression of cyclin E induced micronuclei and karyotypic changes in primary human fibroblasts within one passage following transduction.[64-66] Decreased cyclin E turnover due to either Fbw7 depletion by shRNA or a mutation in codon 380 of cyclin E (encoding the cyclin E-T380A variant) led to a transient increase in chromosomal instability.[64,66] Under these conditions, p53 was activated and limited the proliferation of cyclin E overexpressing cells.[66] Disruption of p53 with HPV-E6 expression or shRNAs against p53 resulted in the sustained unscheduled expression of cyclin E, a sustained S phase delay, prolonged chromosomal instability and aneuploidy.[64-66] Taken together, unscheduled expression of cyclin E results in S phase defects and genomic instability that is prolonged and exacerbated in the absence of functional p53.

UV light slows the progression of cells through S phase.[67,68] The synthesis of nascent DNA decreases in a dose-dependent manner immediately following UV exposure but replication is restored within 6–8 hours following exposure to moderate doses of UV light.[12,68-74] Fibroblasts lacking functional p53 fail to recover DNA synthesis normally following UV exposure and accumulate DNA double strand breaks, as evidenced by the formation of γH2AX foci.[12,72] In the present work, the sustained UV-induced S phase arrest observed in p53-deficient cells was associated with the unscheduled expression of cyclin E and the forced expression of cyclin E prolonged the UV-induced S phase arrest in cells expressing wildtype p53. Unscheduled expression of cyclin E leads to chromosomal instability and is strongly associated with cancer[21,26,28-31,33,51,75] and UV light is mutagenic, clastogenic and carcinogenic.[72,76-78] Taken together, the present work suggests that unscheduled expression of cyclin E contributes to S phase defects

in UV-exposed cells lacking functional p53 and may contribute to genomic instability associated with exposure to UV light.

In summary, our data indicate that UV light induces the unscheduled expression of cyclin E and that this is exacerbated by the loss of functional p53. The unscheduled expression of cyclin E appeared to delay S phase progression and led to a massive S phase arrest in the absence of functional p53. The present work suggests that UV-induced clastogenesis and carcinogenesis may be at least partly related to the unscheduled expression of cyclin E. The present work has important implications for cutaneous malignancies.

Materials and Methods

Cell culture, viruses and UV-irradiation. Normal neonatal foreskin fibroblasts (NF) were obtained from Dr. Mats Ljungman (University of Michigan). Normal fibroblasts (GM38) were obtained from Coriell Repositories (Camden, NJ). These primary human fibroblasts were used between passage 10 and 20. Human papilloma virus-E6-expressing strains were described previously.[34] Li-Fraumeni syndrome cells (LFS), hemizygous for a frame shift mutation at codon 184 of p53 were obtained from Dr. Michael Tainsky (Wayne State University). Cells were maintained in DMEM supplemented with 10% fetal bovine serum (Wisent, St. Bruno, QC) and gentamicin (5 μg/ml, Sigma-Aldrich Canada Ltd., Oakville, ON), except that GM38 and GM38E6 were cultured in the presence of 15% fetal bovine serum, as recommended by the supplier. Adenoviruses expressing lacZ, p53 and cyclin E were obtained from Drs. Graham (McMaster University) and Nevins (Duke University).

For UV treatment, growth medium was removed, cells were irradiated immediately at room temperature, fresh pre-warmed medium was replaced and cells were returned to the incubator for the indicated period of time. A germicidal bulb (Philips) emitting UV light predominately at 254 nm was used to irradiate cells at a dose rate of 1 J/m^2/s, as estimated with a UV-radiometer (UVX Radiometer, UVP Inc., Uplands, CA).

Adenovirus infections. Virus was propagated and titred using standard methods.[35] Cells were grown to approximately 70% confluency for viral infection. In each experiment, one plate of cells was used to accurately estimate the number of cells per plate using a cell counter (Vi-Cell XR, Beckman Coulter). Unless otherwise stated, infections were performed at a multiplicity of infection of 25 plaque-forming units (pfu) per cell. To infect cells, medium was removed and replaced with 1 mL of serum free medium containing the required amount of virus. Virus was allowed to adsorb for 1 hour at 37°C in the virus suspension, while dishes were rocked every 15 minutes to ensure even distribution of virus. Fresh pre-warmed medium was added and cells were returned to the incubator for the indicated period of time. Mock infected cultures were incubated in 1 mL of serum free medium alone for 1 hour at 37°C.

Flow cytometry. Control and UV-irradiated cells were collected at the indicated times following UV and/or drug treatment, washed twice with PBS, fixed with 70% ethanol and stored at -20°C for a minimum of 30 minutes. Where indicated, cells were incubated for 16 hours with 1 μM of hydroxyurea, 2 nM staurosporine, 500 μM mimosine or 1 μM of colcemid. Where indicated cells were cultured in 0.5% fetal bovine serum for a minimum of three days prior to UV-irradiation. For cell cycle analysis, fixed cells were washed twice with PBS and then incubated in phosphate buffered saline (PBS, Hyclone) with RNase A (40 μg/ml, Sigma-Aldrich Canada Ltd., Oakville, ON) and propidium iodide (PI, 18 μg/ml, Sigma-Aldrich Canada Ltd., Oakville, ON) for a minimum of 30 minutes.

To detect cyclins A and E, fixed cells were washed twice with PBS and resuspended in 100 μL of 0.25% Triton X-100 (Sigma-Aldrich) in PBS and incubated on ice for 15 minutes. Cells were rinsed once in PBS, resuspended in 0.5% Tween 20 (Sigma-Aldrich) and collected by centrifugation. Cells were resuspended in 1% bovine serum albumin (BSA) in PBS with 0.75 μg of primary antibody (either rabbit polyclonal anti-cyclin E or anti-cyclin A, Santa Cruz Biotechnology, Santa Cruz, CA) and incubated at room temperature for 3 hours. Cells were rinsed with 1 mL of 1% BSA in PBS, resuspended in 100 μl of 1% BSA in PBS containing 1:30 dilution of ALEXA 488 conjugated goat anti-rabbit IgG (Molecular Probes, Eugene, OR) and incubated in the dark at room temperature for 30 minutes. Cells were again rinsed with 1 mL of 1% BSA in PBS, collected by centrifugation and resuspended in PBS with PI and RNase A. Controls for antibody specificity included the absence of primary antibody as well as overexpression of cyclin E using a recombinant adenovirus.[36]

Red and green fluorescence was measured using either a Becton Dickinson LSR FACS station or a Beckman Coulter FACS station. Flow cytometric data was analyzed using FCS Express 3 software (De Novo Software, Thornhill, ON, CAN) and cell cycle distribution (G_1, S and G_2M) was calculated from the DNA histograms using Modfit cell cycle analysis software (Verity Software House, Topsham, ME).

Western blotting. Cells were harvested, rinsed with PBS, lysed with either 1% SDS or RIPA buffer, sonicated for 10 s using a microtip (Branson Sonifier, VWR International Ltd., Mississauga, ON) and protein concentrations determined using the BioRad Protein Assay (BioRad, Mississagua, ON). Whole cell lysates were prepared in LDS NuPAGE sample buffer (Invitrogen, Burlington, ON). Proteins (20 μg per lane) were separated using 10 or 12% Bis-Tris NuPAGE pre-cast gels (Invitrogen, Burlington, ON). Proteins were then transferred to Hybond-C Extra nitrocellulose membranes (Amersham, Baie d'Urfé, QC). Membranes were stained with Ponceau S Red (5 mg/ml Ponceau S Red, 2% glacial acetic acid) to confirm transfer of proteins. Membranes were blocked for 1 hour at room temperature in PBSMT-A (PBS, 5% nonfat dry milk powder, 0.05% Tween 20). Membranes were incubated with primary antibody for 1.5 hours at room temperature in PBSMT-B (PBS, 0.5% nonfat dry milk powder, 0.05% Tween 20). The primary antibodies used were raised against p53 (Ab-6, 1:250, Oncogene Research Products, Cambridge, MA), p21^{WAF1} (Ab-1, 1:250, Oncogene Research Products, Cambridge, MA), cyclin E (C-19, 1:200, Santa Cruz Biotechnology, Santa Cruz, CA) and β-actin (clone AC-74, 1:15,000, Sigma-Aldrich Canada Ltd., Oakville, ON). Either Kodak film (X-OMAT LS, Kodak, Rochester, NY) or a gel documentation system (Gene Gnome, Synoptics, Bristol, UK) in combination with SuperSignal West Pico Chemiluminescent Substrate (Pierce, Rockford, IL) was used to visualize protein bands. Membranes were stripped with Restore western Blot Stripping Buffer (Pierce, Rockford, IL) in order to

detect additional proteins on the same blot.

RT-PCR. Cells at approximately 70% confluence were irradiated with the indicated doses of UV light and cells were harvested at the indicated times following treatment. Total RNA was isolated using the RNeasy RNA isolation kit (Qiagen, Mississauga, ON) according to manufacturer's specifications. Five micrograms of total RNA was reverse-transcribed using First Strand cDNA synthesis kit (Fermentas Life Sciences, Burlington, ON). Quantitative reverse transcriptase polymerase chain reaction (RT-PCR) was performed using the SYBR green fluorescent DNA stain (Molecular Probes, Eugene, OR) and a LightCycler 2 quantitative PCR machine with LightCycler software version 3 (Roche Diagnostics, Laval, QC). The primers used were *ACTB* (ggg cat ggg tca gaa gga t and gtg gcc atc tct tgc tcg a), *CCNE1* (CAC ACA ACA TAC AGA CCC ACA G and AGC ACC TTC CAT AGC AGC ATC), E2F1 (ACT GAC TCT GCC ACC ATA G and GCT CAC ACA GAT TCA CCC), FBW7 (TTG GTC AGC AGT CAC AGG and AAA CAG GTC ACA GCA CTC), FBW7 isoform 1 (AGG ATG AGG AGG AGG AGG AG and GTT GGT GTT GCT GAA CAT GG), FBW7 isoform 2 (ACT GAG CTG CAT TTG CCT TT and GAA AAA GAG CGG ACC TCA GA) and FBW7 isoform 3 (CTC CCT TTT TGT CGA AGA CG and GTT GGT GTT GCT GAA CAT GG). The primers were synthesized by Sigma-Genosys Canada (Oakville, ON). Transcript levels were normalized to the abundance of ACTB transcript determined from the same cDNA sample.

RNA interference. Cells were maintained in antibiotic free medium for two days prior to transfection. Cells at approximately 70% confluence in 10 cm dishes were transfected with 50 nM of either non-targeting control or SmartPool siRNA duplexes targeting CCNE1 (Dharmacon Inc., Lafayette, CO) three days prior to UV exposure using Oligofectamine Reagent and Opti-MEM I (Invitrogen, Burlington, ON). To prevent cultures from reaching confluence, cells were split 1:2, 24 hours following transfection. Cells were treated with the indicated doses of UV light 2 days later and collected at the indicated times following UV exposure for immunoblot and cell cycle analysis.

Acknowledgements

We would like to thank Drs. J. Nevins, F. Graham and M. Tainsky for providing virsuses and cell lines. This work was supported by the Canadian Institutes of Health Research to B.C.M. and the National Cancer Institute of Canada with Funds from the Terry Fox Run to B.C.M.. J.C.S and L.J.S. were supported by an Ontario Premier's Research Excellence Award to B.C.M. L.J.S. is presently supported with an Ontario Graduate Scholarship in Science and Technology. B.C.M. was supported through a Biomedical Research Scientist Award from the Canadian Cancer Society.

Note

Supplementary materials can be found at:
www.landesbioscience.com/supplement/StubbertCC8-18-Sup.pdf

References

1. Ehrhart JC, Gosselet FP, Culerrier RM, Sarasin A. UVB-induced mutations in human key gatekeeper genes governing signalling pathways and consequences for skin tumourigenesis. Photochem Photobiol Sci 2003; 2:825-34.
2. Cleaver JE, Crowley E. UV damage, DNA repair and skin carcinogenesis. Front Biosci 2002; 7:1024-43.
3. van Steeg H, Kraemer KH. Xeroderma pigmentosum and the role of UV-induced DNA damage in skin cancer. Mol Med Today 1999; 5:86-94.
4. Hanawalt PC, Spivak G. Transcription-coupled DNA repair: two decades of progress and surprises. Nat Rev Mol Cell Biol 2008; 9:958-70.
5. Tornaletti S, Hanawalt P. Effect of DNA lesions on transcription elongation. Biochimie 1999; 81:139-46.
6. Drobetsky EA, Moustacchi E, Glickman BW, Sage E. The mutational specificity of simulated sunlight at the aprt locus in rodent cells. Carcinogenesis 1994; 15:1577-83.
7. Giglia-Mari G, Sarasin A. TP53 mutations in human skin cancers. Hum Mutat 2003; 21:217-28.
8. Kaufmann WK, Wilson SJ. G_1 arrest and cell cycle-dependent clastrogenesis in UV-irradiated human fibroblasts. Mutat Res 1994; 314:67-76.
9. Limoli CL, Giedzinski E, Bonner WM, Cleaver JE. UV-induced replication arrest in the xeroderma pigmentosum variant leads to DNA double-strand breaks, gammaH2AX formation and Mre11 relocalization. Proc Natl Acad Sci USA 2002; 99:233-8.
10. Limoli CL, Giedzinski E, Morgan WF, Cleaver JE. Inaugural article: polymerase eta deficiency in the xeroderma pigmentosum variant uncovers an overlap between the S phase checkpoint and double-strand break repair. Proc Natl Acad Sci USA 2000; 97:7939-46.
11. Cleaver JE, Afzal V, Feeney L, McDowell M, Sadinski W, Volpe JPG, et al. Increased ultraviolet sensitivity and chromosomal instability related to p53 function in the xeroderma pigmentosum variant. Cancer Res 1999; 59:1102-8.
12. Stubbert LJ, Hamill JD, Spronck JC, Smith JM, Becerril C, McKay BC. DDB2-independent role for p53 in the recovery from ultraviolet light-induced replication arrest. Cell Cycle 2007; 6:1730-40.
13. Havre PA, Yuan J, Hedrick L, Cho KR, Glazer PM. p53 inactivation by HPV16 E6 results in increased mutagenesis in human cells. Cancer Res 1995; 55:4420-4.
14. Brash DE. Sunlight and the onset of skin cancer. Trends Genet 1997; 13:410-4.
15. Jonason AS, Kuala S, Restifo RJ, Spinelli HM, Persing JA, Leffell OJ, et al. Frequent clones of p53-mutated keratinocytes in normal human skin. Proc Natl Acad Sci USA 1996; 93:14025-9.
16. Moroy T, Geisen C, Cyclin E. Int J Biochem Cell Biol 2004; 36:1424-39.
17. Lew DJ, Dulic V, Reed SI. Isolation of three novel human cyclins by rescue of G_1 cyclin (Cln) function in yeast. Cell 1991; 66:1197-206.
18. Ohtani K, DeGregori J, Nevins J. Regulation of the cyclin E gene by transcription factor E2F1. Proc Natl Acad Sci USA 1995; 92:12146-50.
19. Blais A, Dynlacht BD. E2F-associated chromatin modifiers and cell cycle control. Curr Opin Cell Biol 2007; 19:658-62.
20. Cobrinik D. Pocket proteins and cell cycle control. Oncogene 2005; 24:2796-809.
21. Strohmaier H, Spruck CH, Kaiser P, Won KA, Sangfelt O, Reed SI. Human F-box protein hCdc4 targets cyclin E for proteolysis and is mutated in a breast cancer cell line. Nature 2001; 413:316-22.
22. Koepp DM, Schaefer LK, Ye X, Keyomarsi K, Chu C, Harper JW, Elledge SJ. Phosphorylation-dependent ubiquitination of cyclin E by the SCF^{Fbw7} ubiquitin ligase. Science 2001; 294:173-7.
23. Geng Y, Yu Q, Sicinska E, Das M, Schneider JE, Bhattacharya S, et al. Cyclin E ablation in the mouse. Cell 2003; 114:431-43.
24. Perez-Losada J, Mao JH, Balmain A. Control of genomic instability and epithelial tumor development by the p53-Fbxw7/Cdc4 pathway. Cancer Res 2005; 65:6488-92.
25. Rajagopalan H, Jallepalli PV, Rago C, Velculescu VE, Kinzler KW, Vogelstein B, Lengauer C. Inactivation of hCDC4 can cause chromosomal instability. Nature 2004; 428:77-81.
26. Willmarth NE, Albertson DG, Ethier SP. Chromosomal instability and lack of cyclin E regulation in hCdc4 mutant human breast cancer cells. Breast Cancer Res 2004; 6:531-9.
27. Rajagopalan H, Lengauer C. hCDC4 and genetic instability in cancer. Cell Cycle 2004; 3:693-4.
28. Hubalek MM, Widschwendter A, Erdel M, Gschwendtner A, Fiegl HM, Muller HM, et al. Cyclin E dysregulation and chromosomal instability in endometrial cancer. Oncogene 2004; 23:4187-92.
29. Ekholm-Reed S, Spruck CH, Sangfelt O, van Drogen F, Mueller-Holzner E, Widschwendter M, et al. Mutation of hCDC4 leads to cell cycle deregulation of cyclin E in cancer. Cancer Res 2004; 64:795-800.
30. Cassia R, Moreno-Bueno G, Rodriguez-Perales S, Hardisson D, Cigudosa JC, Palacios J. Cyclin E gene (CCNE) amplification and hCDC4 mutations in endometrial carcinoma. J Pathol 2003; 201:589-95.
31. Spruck CH, Strohmaier H, Sangfelt O, Muller HM, Hubalek M, Muller-Holzner E, et al. hCDC4 gene mutations in endometrial cancer. Cancer Res 2002; 62:4535-9.
32. Akhoondi S, Sun D, von der Lehr N, Apostolidou S, Klotz K, Maljukova A, et al. FBXW7/hCDC4 is a general tumor suppressor in human cancer. Cancer Res 2007; 67:9006-12.

33. Mao JH, Perez-Losada J, Wu D, Delrosario R, Tsunematsu R, Nakayama KI, et al. Fbxw7/Cdc4 is a p53-dependent, haploinsufficient tumour suppressor gene. Nature 2004; 432:775-9.
34. McKay BC, Becerril C, Ljungman M. p53 plays a protective role against UV- and cisplatin-induced apoptosis in transcription-coupled repair proficient fibroblasts. Oncogene 2001; 20:6805-8.
35. Hitt M, Bett AJ, Addison CJ, Prevec L, Graham FL. Techniques for human adenovirus vector construction and characterization. Adolph KW, ed., (Academic Press, Orlando, Fl). Meth Mol Genet 1995; 13-30.
36. Leone G, DeGregori J, Jakoi L, Cook JG, Nevins JR. Collaborative role for E2F transcriptional activity and G_1 cyclin-dependent kinase activity in the induction of S phase. Proc Natl Acad Sci USA 1999; 96:6626-31.
37. Stubbert LJ, Smith JM, Hamill JD, Arcand TL, McKay BC. The anti-apoptotic role for p53 following exposure to ultraviolet light does not involve DDB2. Mutat Res 2009; 663:69-76.
38. McKay BC, Becerril C, Spronck JC, Ljungman M. Ultraviolet light-induced apoptosis is associated with S phase in primary human fibroblasts. DNA Repair 2002; 1:811-20.
39. McKay BC, Ljungman M. Role for p53 in the recovery of transcription and protection against apoptosis induced by ultraviolet light. Neoplasia 1999; 1:276-84.
40. Yin Y, Tainsky MA, Bischoff FZ, Strong LC, Wahl GM. Wild-type p53 restores cell cycle control and inhibits gene amplification in cells with mutant p53 alleles. Cell 1992; 70:937-48.
41. Gentile M, Latonen L, Laiho M. Cell cycle arrest and apoptosis provoked by UV radiation-induced DNA damage are transcriptionally highly divergent responses. Nucleic Acids Res 2003; 31:4779-90.
42. Blattner C, Sparks A, Lane D. Transcription factor E2F-1 is upregulated in response to DNA damage in a manner analogous to that of p53. Mol Cell Biol 1999; 19:3704-13.
43. Ohtsubo M, Roberts JM. Cyclin-dependent regulation of G_1 in mammalian fibroblasts. Science 1993; 259:1908-12.
44. Tsai LH, Lees E, Faha B, Harlow E, Riabowol K. The cdk2 kinase is required for the G_1-to-S transition in mammalian cells. Oncogene 1993; 8:1593-602.
45. Gong J, Ardelt B, Traganos F, Darzynkiewicz Z. Unscheduled expression of cyclin B1 and cyclin E in several leukemic and solid tumor cell lines. Cancer Res 1994; 54:4285-8.
46. Bruno S, Ardelt B, Skierski JS, Traganos F, Darzynkiewicz Z. Different effects of staurosporine, an inhibitor of protein kinases, on the cell cycle and chromatin structure of normal and leukemic lymphocytes. Cancer Res 1992; 52:470-3.
47. Gong J, Traganos F, Darzynkiewicz Z. Staurosporine blocks cell progression through G_1 between the cyclin D and cyclin E restriction points. Cancer Res 1994; 54:3136-9.
48. Yarbro JW. Mechanism of action of hydroxyurea. Semin Oncol 1992; 19:1-10.
49. Rieder CL, Palazzo RE. Colcemid and the mitotic cycle. J Cell Sci 1992; 102:387-92.
50. Gong J, Traganos F, Darzynkiewicz Z. Discrimination of G_2 and mitotic cells by flow cytometry based on different expression of cyclins A and B1. Exp Cell Res 1995; 220:226-31.
51. Spruck CH, Won KA, Reed SI. Deregulated cyclin E induces chromosome instability. Nature 1999; 401:297-300.
52. Hofferer M, Wirbelauer C, Humar B, Krek W. Increased levels of E2F-1-dependent DNA binding activity after UV- or gamma-irradiation. Nucleic Acids Res 1999; 27:491-5.
53. Lin WC, Lin FT, Nevins JR. Selective induction of E2F1 in response to DNA damage, mediated by ATM-dependent phosphorylation. Genes Dev 2001; 15:1833-44.
54. O'Connor DJ, Lu X. Stress signals induce transcriptionally inactive E2F-1 independently of p53 and Rb. Oncogene 2000; 19:2369-76.
55. Won KA, Reed SI. Activation of cyclin E/CDK2 is coupled to site-specific autophosphorylation and ubiquitin-dependent degradation of cyclin E. EMBO J 1996; 15:4182-93.
56. Clurman BE, Sheaff RJ, Thress K, Groudine M, Roberts JM. Turnover of cyclin E by the ubiquitin-proteasome pathway is regulated by cdk2 binding and cyclin phosphorylation. Gene Dev 1996; 10:1979-90.
57. Nakayama K, Nagahama H, Minamishima YA, Matsumoto M, Nakamichi I, Kitagawa K, et al. Targeted disruption of Skp2 results in accumulation of cyclin E and p27(Kip1), polyploidy and centrosome overduplication. EMBO J 2000; 19:2069-81.
58. Kimura T, Gotoh M, Nakamura Y, Arakawa H. hCDC4b, a regulator of cyclin E, as a direct transcriptional target of p53. Cancer Sci 2003; 94:431-6.
59. DeGregori J, Kowalik T, Nevins J. Cellular targets for activation by the E2F1 transcription factor include DNA synthesis- and G_1-S-regulatory genes. Mol Cell Biol 1995; 15:4215-24.
60. Fung TK, Poon RY. A roller coaster ride with the mitotic cyclins. Semin Cell Dev Biol 2005; 16:335-42.
61. van Leuken R, Clijsters L, Wolthuis R. To cell cycle, swing the APC/C. Biochim Biophys Acta 2008; 1786:49-59.
62. Anzi S, Finkin S, Shaulian E. Transcriptional repression of c-Jun's E3 ubiquitin ligases contributes to c-Jun induction by UV. Cell Signal 2008; 20:862-71.
63. Welcker M, Orian A, Grim JA, Eisenman RN, Clurman BE. A nucleolar isoform of the Fbw7 ubiquitin ligase regulates c-Myc and cell size. Curr Biol 2004; 14:1852-7.
64. Minella AC, Grim JE, Welcker M, Clurman BE. p53 and SCF^{Fbw7} cooperatively restrain cyclin E-associated genome instability. Oncogene 2007; 26:6948-53.
65. Minella AC, Clurman BE. Mechanisms of tumor suppression by the SCF(Fbw7). Cell Cycle 2005; 4: 1356 - 1359
66. Minella AC, Swanger J, Bryant E, Welcker M, Hwang H, Clurman BE. p53 and p21 form an inducible barrier that protects cells against cyclin E-cdk2 deregulation. Curr Biol 2002; 12:1817-27.
67. Kaufmann WK, Cleaver JE. Mechanisms of inhibition of DNA replication by ultraviolet light in normal human and xeroderma pigmentosum fibroblasts. J Mol Biol 1981; 149:171-87.
68. Cleaver JE, Kaufmann WK, Kapp LN, Park SD. Replicon size and excision repair as factors in the inhibition and recovery of DNA synthesis from ultraviolet damage. Biochim Biophys Acta 1983; 739:207-15.
69. Cleaver JE, Thomas GH, Park SD. Xeroderma pigmentosum variants have a slow recovery of DNA synthesis after irradiation with ultraviolet light. Biochim Biophys Acta 1979; 564:122-31.
70. Park SD, Cleaver JE. Recovery of DNA synthesis after ultraviolet irradiation of xeroderma pigmentosum cells depends on excision repair and is blocked by caffeine. Nucleic Acids Res 1979; 6:1151-9.
71. Lehmann AR. The relationship between pyrimidine dimers and replicating DNA in UV-irradiated human fibroblasts. Nucleic Acids Res 1979; 7:1901-12.
72. Cistulli CA, Kaufmann WK. p53-dependent signaling sustains DNA replication and enhances clonogenic survival in 254 nm ultraviolet-irradiated human fibroblasts. Cancer Res 1998; 58:1993-2002.
73. Mirzayans R, Enns L, Dietrich K, Barley RDC, Paterson MC. Faulty DNA polymerase delta/epsilon-mediated excision repair in response to gamma radiation or ultraviolet light in p53-deficient fibroblast strains from affected members of a cancer-prone family with Li-Fraumeni syndrome. Carcinogenesis 1996; 17:691-8.
74. Barley RD, Enns L, Paterson MC, Mirzayans R. Aberrant $p21^{WAF1}$-dependent growth arrest as the possible mechanism of abnormal resistance to ultraviolet light cytotoxicity in Li-Fraumeni syndrome fibroblast strains heterozygous for TP53 mutations. Oncogene 1998; 17:533-43.
75. Calhoun ES, Jones JB, Ashfaq R, Adsay V, Baker SJ, Valentine V, et al. BRAF and FBXW7 (CDC4, FBW7, AGO, SEL10) mutations in distinct subsets of pancreatic cancer: potential therapeutic targets. Am J Pathol 2003; 163:1255-60.
76. Cordeiro-Stone M, Frank A, Bryant M, Oguejiofor I, Hatch SB, McDaniel LD, et al. DNA damage responses protect xeroderma pigmentosum variant from UVC-induced clastogenesis. Carcinogenesis 2002; 23:959-65.
77. Bullock SK, Kaufmann WK, Cordeiro-Stone M. Enhanced S phase delay and inhibition of replication of an undamaged shuttle vector in UVC-irradiated xeroderma pigmentosum variant. Carcinogenesis 2001; 22:233-41.
78. Kaufmann WK. Cell cycle checkpoints and DNA repair preserve the stability of the human genome. Cancer Metastasis Rev 1995; 14:31-41.